

ABSTRACT

Title of Document: Living Coordinative Chain Transfer
Polymerization of 1-Alkenes
Wei Zhang, Doctor of Philosophy, 2008

Directed By: Professor Lawrence R. Sita
Department of Chemistry and Biochemistry

A novel polymerization method, living coordinative chain transfer polymerization (CCTP), was recently developed with monocyclopentadienyl monoamidinate (CpAm) Group 4 metal complexes, which were previously applied for the traditional living coordination polymerization (TLCP) and stereomodulated degenerative transfer living (SDTL) coordination polymerization. In addition to a CpAm precatalyst and a cocatalyst, a chain transfer agent (CTA) was also added to the CCTP system. The CTA undergoes a rapid and reversible chain transfer with the Group 4 metal catalyst, which results in chain growth on an inexpensive main group metal alkyl. This new CCTP technique provides a practical solution towards the intrinsic problem, one chain per catalytic center, for a TLCP polymerization process.

The first example of living CCTP was provided with ZnEt_2 via $(\eta^5\text{-C}_5\text{Me}_5)\text{HfMe}_2[\text{N}(\text{Et})\text{C}(\text{Me})\text{N}(\text{Et})]$ (**35**) activated by $[\text{PhNHMe}_2][\text{B}(\text{C}_6\text{F}_5)_4]$ (**01**). It was very efficient for the polymerization of ethene, propene, higher α -olefins and

α,ω -nonconjugated dienes, and copolymerization of these monomers. The (co)polymers obtained possess very narrow polydispersity (PDI 1.03-1.10) and tunable molecular weights by several factors including a wide range of equivalents of ZnEt_2 . The living property of this CCTP system was further confirmed by kinetic studies and end group functionalization. The quantitative chain extension on zinc was clearly shown by *in situ* NMR spectroscopy. The coordinative chain shuttling polymerization (CCSP) was also studied while binary precatalysts, binary cocatalysts, or binary chain transfer agents were applied.

The TLCP, SDTL and CCTP of propene *via* some new CpAm complexes other than **35** were also studied, including the zirconium analogue of **35**, ($\eta^5\text{-C}_5\text{Me}_5$) $\text{ZrMe}_2[\text{N}(\text{Et})\text{C}(\text{Me})\text{N}(\text{Et})]$ (**36**), and a series of binuclear complexes which have the common structure of $[(\eta^5\text{-C}_5\text{Me}_5)\text{ZrMe}_2]_2[\text{N}(\text{tBu})\text{C}(\text{Me})\text{N}(\text{CH}_2)_x\text{NC}(\text{Me})\text{N}(\text{tBu})]$ (**26**, $x = 8$; **27**, $x = 6$; **28**, $x = 4$). The formamidinate precatalyst (**12**) was also covered in this study. Under both SDTL and CCTP conditions, the binuclear catalysts showed a tether-length dependent chain transfer process as observed by the polymerization results especially by the tacticity of resulting polypropene (PP). Using CCSP process, multi-stereoblock PP was successfully prepared *via* **12** and **27**. The structures and properties of these new complexes and (co)polymers were fully characterized by X-ray crystallography, elemental analysis, GPC, DSC, GC and high field ^1H and ^{13}C NMR spectroscopy.

LIVING COORDINATIVE CHAIN TRANSFER
POLYMERIZATION OF 1-ALKENES

By

Wei Zhang

Dissertation submitted to the Faculty of the Graduate School of the
University of Maryland, College Park, in partial fulfillment
of the requirements for the degree of
Doctor of Philosophy
2008

Advisory Committee:
Professor Lawrence R Sita, Chair
Professor Bryan W. Eichhorn
Professor Jeffery T. Davis
Professor Andrei Vedernikov
Professor Kyu-Yong Choi

© Copyright by
Wei Zhang
2008

Acknowledgements

First of all, I would like to thank my advisor, Dr. Lawrence R. Sita for his continuous support of both my research and personal life. His profound knowledge in the area of organometallics and polymer science helped me build up the foundation of a chemist. His enthusiasm in chemistry constantly encouraged me. The skills that I learned while in his research group will benefit my chemical career forever.

Secondly, I will extend my gratitude to my committee, Dr. Davis, Dr. Vedernikov, Dr. Eichhorn and Dr. Choi, for their great help both in my classes and on my research. Without their support, this work would not have been possible.

I also want to thank all the previous and present members in the Sita group who worked with me for their help and friendship. Special thanks to Dr. Yonghui Zhang, Dr. Philip Fontaine, Emily Trunkely and Jia Wei for useful discussion and the time we have experienced in the laboratory.

Moreover, I thank my wife, Jinshan Wang and my daughters, Jialei and Jiahan for their invaluable love and confidence. Also thanks to my parents-in-law, Mingsheng Wang and Wenxiu Zhang, for their love and indispensable support to my family. And to my parents, Zhicheng Zhang and Shufen He, for their understanding of my staying here over many years without going home.

Finally, I am thankful to the Ann G. Wylie Dissertation Fellowship from the Graduate School at the University of Maryland to support my thesis writing.

Table of Contents

Acknowledgements	ii
Table of Contents	iii
List of Abbreviations	vii
List of Tables	viii
List of Figures	ix
List of Schemes	xv
List of Preparation for Selected Compounds	xvi
Chapter 1: Introduction	1
1.1 A Brief History of Coordination Polymerization	1
1.1.1 Heterogeneous Ziegler-Natta polymerization	1
1.1.2 Homogeneous metallocene and post-metallocene catalysis	3
1.2 A General View of Living Polymerization Processes	5
1.2.1 Discovery of living anionic polymerization and its characters	5
1.2.2 Development of cationic and radical living polymerizations	6
1.2.3 Living coordination polymerization based on homogeneity	8
1.2.4 An example of traditional living coordination polymerization (TLCP)	10
1.2.5 Stereomodulated degenerative transfer living coordination polymerization	11
1.3 Coordinative Chain Transfer Polymerization (CCTP)	13
1.3.1 CCTP of ethene	13
1.3.2 CCSP random copolymerization of ethene and 1-octene	15
1.3.3 Challenges in the area of CCTP	17
Chapter 2: Polymerization of Propene <i>via</i> Novel CpAm Group 4 Metal Complexes	18
2.1 Background	18
2.1.1 Development of the CpAm group 4 metal catalyst family	18
2.1.2 Polymerization of propene <i>via</i> precatalyst 04	20

2.2 A Tether-Length Dependent Series of Group 4 Bimetallic Initiators for SDTL Coordination Polymerization of Propene	23
2.2.1 Introduction	23
2.2.2 Synthesis of binuclear initiators	24
2.2.3 TLCP and SDTL polymerization of propene <i>via</i> binuclear initiators	27
2.2.4 Kinetic study for the SDTL polymerization of propene <i>via</i> 28	29
2.2.5 Pentad analysis for the polymerization of propene <i>via</i> binuclear initiators	31
2.3 Development of CpAm Group 4 Metal Initiators with High Activity for Propene Polymerization	35
2.3.1 Introduction	35
2.3.2 Synthesis of new CpAm complexes	36
2.3.3 TLCP polymerization of propene by diethyl amidinate catalysts	39
2.3.4 TLCP polymerization of propene by formamidinate catalysts	44
2.4 Conclusions	47
Chapter 3: Truly Living CCTP of Propene with ZnEt ₂ Catalyzed by Highly Active CpAm Complexes — Production of Amorphous Polypropene with Extremely Narrow PDI	
3.1 Background	49
3.1.1 Chain transfer process in coordination polymerization, general view	49
3.1.2 Examples of reversible polypropene chain transfer to aluminum	50
3.2 Living CCTP of Propene with ZnEt ₂ by 35	51
3.2.1 Description and general procedures	51
3.2.2 A series of propene polymerization under CCTP conditions	52
3.2.3 Linear increase of molecular weight with time during CCTP of propene	55
3.2.4 Quantitative control of PP's molecular weight by the amount of ZnEt ₂	57
3.2.5 Characterization of polypropene <i>via</i> CCTP	58
3.2.6 An example of scaled up CCTP experiment of propene	61
3.2.7 Iodine terminated atactic polypropene by CCTP	61
3.3 CCTP of Propene with ZnEt ₂ <i>via</i> 35 and 36 by Different Cocatalysts	63
3.4 CCTP of Propene <i>via</i> 35 with Combination of ZnEt ₂ and AlEt ₃	65
3.5 Conclusions	67

Chapter 4: Catalyzed Polyethene Chain Growth on Zinc by the CpAm Hafnium Complex — Polymerization and Mechanistic Investigation	68
4.1 Living Polymerization of Ethene under CCTP Conditions <i>via</i> 35	68
4.1.1 Background and procedures	68
4.1.2 A series of CCTP polymerization of ethene <i>via</i> 35	69
4.1.3 Dependence of the t_p -normalized M_n on the amount of CTA	70
4.2 NMR Analysis and in situ Mechanistic Study	71
4.2.1 NMR spectra of linear PE and 2-methyl PE	71
4.2.2 Direct observation of quantitative chain growth on zinc by NMR study	72
4.3 Alkane Distribution in the PE Product Characterized by GC	75
4.3.1 GC analysis of polyethene aliquots quenched at different t_p	75
4.3.2 Poisson distribution of PE aliquots showed the living character	77
4.4 End Group Functionalized Linear PE	78
4.5 Conclusions	82
Chapter 5: Living CCTP of Higher α -olefins and 1,5-hexadiene, and Random CCTP Copolymerization of these Monomers with Propene or Ethene	83
5.1 Living CCTP of Higher α -olefins and 1,5-hexadiene	83
5.1.1 Background and description	83
5.1.2 Living property shown by the kinetic study for the CCTP of 1-hexene	84
5.1.3 Polymer structural elucidation by NMR spectroscopy	86
5.2 CCTP Random Copolymerization of Propene with Higher α -olefins or 1,5-HD	89
5.2.1 Description of CCTP copolymerization of propene with higher α -olefins and 1,5-hexadiene	89
5.2.2 An example of propene copolymer structure illustrated by ^{13}C NMR	90
5.3 CCTP Random Copolymerization of Ethene with Higher α -olefins or 1,5-HD	91
5.3.1 Description of CCTP copolymerization of ethene with higher α -olefins and 1,5-hexadiene	91
5.3.2 Detailed structural analysis of PE copolymers by NMR spectroscopy	92
5.4 CCSP Copolymerization of Ethene and 1-octene with Dual Precatalysts	95
5.5 CCSP Random Copolymerization in a Dual Cocatalyst System	98
5.5.1 CCSP copolymerization of ethene and 1-hexene with two cocatalysts	98

5.5.2 CCSP copolymerization of ethene and 1,5-HD with dual cocatalysts	101
5.6 Conclusions	104
Chapter 6: Multi-stereoblock Polypropene by CCSP with ZnEt ₂ between CpAm Group 4 Metal Catalysts	105
6.1 Background	105
6.1.1 Well-defined stereoblock PP <i>via</i> TLCP technique	105
6.1.2 Stereoblock PP obtained through chain transfer process	106
6.2 Stereoregular PP by CCTP <i>via</i> Binuclear Catalysts	108
6.3 Pure Atactic PP by CCTP <i>via</i> 12	111
6.4 Coordinative Chain Shuttling Polymerization between 12 and 27	113
6.5 Modulation of Isotactic Block Content during the CCSP Process	116
6.6 Preparation of an <i>iso-a-iso</i> triblock PP and microstructure comparison	119
6.7 Conclusions	121
Chapter 7: Conclusions	123
Appendix I: Experimentals	126
Appendix II: NMR spectra for selected (co)polymers	143
References:	155

List of Abbreviations

TLCP	traditional living coordination polymerization
SDTL	stereomodulated degenerative transfer living
CCTP	coordinative chain transfer polymerization
CCSP	coordinative chain shuttling polymerization
CTA	chain transfer agent(s)
Cp	cyclopentadienyl: $\eta^5\text{-C}_5\text{H}_5$
Cp*	pentamethylcyclopentadienyl: $\eta^5\text{-C}_5\text{Me}_5$
CpAm	monocyclopentadienyl monoamidinate
PE	polyethene or polyethylene
PP	polypropene or polypropylene
PH	poly(1-hexene)
PO	poly(1-octene)
PMCP	poly(methylene-1,3-cyclopentane)
M_n	number average molecular weight
M_w	weight average molecular weight
PDI	polydispersity index: M_w / M_n
GPC	gel permeation chromatography, or size exclusion chromatography
DSC	differential scanning calorimetry
GC	gas chromatography

List of Tables

<i>Table 1:</i> Propene polymerization conditions and GPC analysis <i>via</i> binuclear initiators	27
<i>Table 2:</i> Pentad distribution of PP obtained <i>via</i> binuclear initiators.....	32
<i>Table 3:</i> TLCP polymerization of propene <i>via</i> CpAm catalysts	40
<i>Table 4:</i> Experimental conditions, GPC analysis and triad contents for propene polymerization <i>via</i> formamidinate initiators	45
<i>Table 5:</i> Living CCTP of propene with ZnEt ₂ <i>via</i> 35 according to Scheme 15	54
<i>Table 6:</i> CCTP of propene <i>via</i> 35 and 36 activated by different cocatalysts	64
<i>Table 7:</i> CCTP of propene <i>via</i> 35 with combination of ZnEt ₂ and AlEt ₃	66
<i>Table 8:</i> Living CCTP of ethene with ZnR ₂ <i>via</i> 35 activated by 03	69
<i>Table 9:</i> Living CCTP of higher α -olefins and 1,5-hexadiene.....	84
<i>Table 10:</i> Living random CCTP copolymerization of propene with higher α -olefins and 1,5- hexadiene.....	89
<i>Table 11:</i> CCTP copolymerization of ethene with higher α -olefins and 1,5-HD	91
<i>Table 12:</i> CCSP copolymerization of ethene and 1-octene <i>via</i> 35 and 48	96
<i>Table 13:</i> CCSP random copolymerization of ethene and 1-hexene with ZnEt ₂ <i>via</i> 35 activated by different amount of 01 and 03	99
<i>Table 14:</i> CCSP of ethene and 1,5-hexadiene <i>via</i> 35 activated by 01 and 03	103
<i>Table 15:</i> CCTP of propene <i>via</i> a series of CpAm zirconium precatalysts.....	108
<i>Table 16:</i> CCSP of propene with ZnEt ₂ <i>via</i> precatalyst 12 and 27	114
<i>Table 17:</i> CCSP of propene <i>via</i> 12 and 27 beyond homogeneity	118

List of Figures

<i>Figure 1:</i> Typical microstructures of polypropene	3
<i>Figure 2:</i> Examples of catalyst precursors for living coordination polymerization	9
<i>Figure 3:</i> Examples of precatalysts employed for the CCTP of ethene.....	15
<i>Figure 4:</i> Precatalysts used to make multiblock PE-co-PO by Dow Chemical	16
<i>Figure 5:</i> Schematic diagram of PP microstructure on a pentad level.....	20
<i>Figure 6:</i> $^{13}\text{C}\{^1\text{H}\}$ NMR (125 MHz, 1,1,2,2- $\text{C}_2\text{D}_2\text{Cl}_4$, 70 °C) of methyl region of PP with different activation percentage of 04 by 01	21
<i>Figure 7:</i> Molecular structures (30% thermal ellipsoids) of 26 . Hydrogen atoms have been removed for the sake of clarity.....	26
<i>Figure 8:</i> Molecular structures (30% thermal ellipsoids) of 27 . Hydrogen atoms have been removed for the sake of clarity.....	26
<i>Figure 9:</i> Molecular structures (30% thermal ellipsoids) of 28 . Hydrogen atoms have been removed for the sake of clarity.....	26
<i>Figure 10:</i> $^{13}\text{C}\{^1\text{H}\}$ NMR (125 MHz, 1,1,2,2- $\text{C}_2\text{D}_2\text{Cl}_4$, 70 °C) of methyl region of PP materials (top to bottom: <i>via</i> 28 , 27 , 26 and 04 ; left to right: 100%, 70% and 50% activation).....	28
<i>Figure 11:</i> Kinetics of 50% activated SDTL polymerization of propene <i>via</i> 28	30
<i>Figure 12:</i> Kinetics of 75% activated SDTL polymerization of propene <i>via</i> 28	31
<i>Figure 13:</i> Pentad analysis of PP obtained <i>via</i> 26	33
<i>Figure 14:</i> Pentad analysis of PP <i>via</i> binuclear initiators at 70% activation	33
<i>Figure 15:</i> Dependence of pentad content on the level of activation and tether length in the binuclear initiators for PP obtained <i>via</i> 04 , 26 , 27 and 28	34
<i>Figure 16:</i> Molecular structures (30% thermal ellipsoids) of 35 (right) and 36 (left). Hydrogen atoms have been removed for the sake of clarity.	37

<i>Figure 17:</i> Molecular structure (30% thermal ellipsoids) of 48 (left), 49 (middle) and 50 (right). Hydrogen atoms have been removed for the sake of clarity, except the distal H in 50	37
<i>Figure 18:</i> Kinetics of propene polymerization via 36	42
<i>Figure 19:</i> Kinetics of propene polymerization via 35	43
<i>Figure 20:</i> ^{13}C $\{^1\text{H}\}$ NMR (125 MHz, 1,1,2,2- $\text{C}_2\text{D}_2\text{Cl}_4$, 70 °C) of the methyl region of PP via 12 , 50% (top) and 100% (bottom) activation.....	46
<i>Figure 21:</i> Full ^{13}C $\{^1\text{H}\}$ NMR spectra (125 MHz, 1,1,2,2- $\text{C}_2\text{D}_2\text{Cl}_4$, 70 °C) of PP via 04 (top, Entry 2.13) and 12 (bottom, Entry 2.37)	46
<i>Figure 22:</i> GPC curves of PP from Entry 3.01 (middle) and two PS standards with PDI of 1.05 (left and right).....	53
<i>Figure 23:</i> GPC curves for PP by living CCTP from Entries 3.04-3.11 (left to right)	55
<i>Figure 24:</i> Kinetic study of propene polymerization under CCTP by 35	56
<i>Figure 25:</i> ^1H NMR (125 MHz, 1,1,2,2- $\text{C}_2\text{D}_2\text{Cl}_4$, 70 °C) of PP from Entry 3.03	56
<i>Figure 26:</i> Quantitative control of polymer's molecular weight by the amount of chain transfer agent (data from Entries 3.04-3.09)	58
<i>Figure 27:</i> DSC traces (2 nd heating cycle, 10 °C /min) for the polypropene materials from Entries 3.04-3.09 in Table 5 and 2.2.3 in Table 3	59
<i>Figure 28:</i> Typical ^{13}C $\{^1\text{H}\}$ NMR (125 MHz, 1,1,2,2- $\text{C}_2\text{D}_2\text{Cl}_4$, 70 °C) of methyl region of polypropene via 35	60
<i>Figure 29:</i> Powder X-ray diffraction study for PP material of Entry 2.2.3	60
<i>Figure 30:</i> ^{13}C NMR (150 MHz, 1,1,2,2- $\text{C}_2\text{D}_2\text{Cl}_4$, 90 °C) spectra of iodo-PP (top) and regular PP (bottom) by CCTP via 35 (methylene region was not shown)	62
<i>Figure 31:</i> Plot of t_p -normalized M_n as a function of total alkyls on both active and surrogate metals	71
<i>Figure 32:</i> ^{13}C $\{^1\text{H}\}$ NMR (150 MHz, 1,1,2,2- $\text{C}_2\text{D}_2\text{Cl}_4$, 90 °C) spectra of isolated PE (Entry 4.05, top) and 2-methyl PE (Entry 4.06, bottom) by CCTP via 35	72
<i>Figure 33:</i> ^{13}C $\{^1\text{H}\}$ NMR (150 MHz, Tol- d_8 , 20 °C) spectra of a mixture of 35 ⁺ and Zn^iPr_2 without ethene (top) and after 15 min introduction of ethene (bottom).....	73

<i>Figure 34:</i> ^1H NMR (600 MHz, Tol- d_8 , 20 °C) spectra of a mixture of 35^+ and Zn^iPr_2 in the absence of ethene (top) and after 15 min introduction of ethene (bottom).	74
<i>Figure 35:</i> GC chromatograms of PE aliquots at (top to bottom) 25, 30, 35 and 40 min.....	76
<i>Figure 36:</i> Distribution of <i>n</i> -alkanes in PE aliquots quenched at different times by GC analysis (dotted lines are showing the best Poisson distribution fitting).....	77
<i>Figure 37:</i> ^1H (600 MHz, top) and ^{13}C (150 MHz, 1,1,2,2- $\text{C}_2\text{D}_2\text{Cl}_4$, 90 °C, bottom) NMR spectra of Et-PE-I, the water peak was marked by an asterisk *.....	79
<i>Figure 38:</i> ^1H NMR (600 MHz, top) and ^{13}C $\{^1\text{H}\}$ NMR (150 MHz, 1,1,2,2- $\text{C}_2\text{D}_2\text{Cl}_4$, 90 °C, bottom) spectra of ^iPr -PE-I.....	80
<i>Figure 39:</i> Kinetic analysis of the living CCTP of 1-hexene with ZnEt_2	85
<i>Figure 40:</i> ^{13}C $\{^1\text{H}\}$ NMR (150 MHz, CDCl_3 , 20 °C) spectrum of poly-1-octene from Entry 5.05 of Table 9.	87
<i>Figure 41:</i> ^{13}C $\{^1\text{H}\}$ NMR (150 MHz, 1,1,2,2- $\text{C}_2\text{D}_2\text{Cl}_4$, 90 °C) spectrum of PMCP from Entry 5.06 of Table 9. The spectrum on the top left shows resonances arising from 1,2-insertion of 1,5-hexadiene.	87
<i>Figure 42:</i> ^1H NMR (600 MHz, 1,1,2,2- $\text{C}_2\text{D}_2\text{Cl}_4$, 90 °C) spectrum of PMCP from Entry 5.06 of Table 9. The spectrum on the top left shows resonances arising from 1,2-insertion of 1,5-hexadiene.	88
<i>Figure 43:</i> ^{13}C $\{^1\text{H}\}$ NMR (150 MHz, 1,1,2,2- $\text{C}_2\text{D}_2\text{Cl}_4$, 90 °C) spectrum of poly(propene-co-1-dodecene) from Entry 5.09 in Table 10. Peaks marked by asterisks are from <i>n</i> -pentane.	90
<i>Figure 44:</i> Illustrative structures of poly(ethene-co-1-hexene) from Entry 5.11 (top), poly(ethene-co-1-octene) from Entry 5.13 (middle) and PE-co-PMCP from Entry 5.16 of Table 11 (bottom).	93
<i>Figure 45:</i> ^{13}C $\{^1\text{H}\}$ NMR (150 MHz, 1,1,2,2- $\text{C}_2\text{D}_2\text{Cl}_4$, 90 °C) of poly(ethene-co-1-hexene) from Entry 5.11 of Table 11. Resonances for trace hexane are marked with asterisks (*).	94
<i>Figure 46:</i> ^{13}C NMR (150 MHz, 1,1,2,2- $\text{C}_2\text{D}_2\text{Cl}_4$, 90 °C) spectrum of poly(ethene-co-1-octene) from Entry 5.13 in Table 11.	94

<i>Figure 47:</i> ^{13}C $\{^1\text{H}\}$ NMR (150 MHz, 1,1,2,2- $\text{C}_2\text{D}_2\text{Cl}_4$, 90 °C) of poly(ethene- <i>co</i> -PMCP) from Entry 5.16 of Table 11.....	95
<i>Figure 48:</i> ^1H NMR (600 MHz, 1,1,2,2- $\text{C}_2\text{D}_2\text{Cl}_4$, 90 °C) spectra of PE- <i>co</i> -PO obtained from CCSP <i>via</i> varied ratios of 35 and 48 activated by 01 (top to bottom: Entries 5.18-5.21). Peaks at 1.30 ppm were normalized to the same height.	97
<i>Figure 49:</i> ^{13}C $\{^1\text{H}\}$ NMR (150 MHz, 1,1,2,2- $\text{C}_2\text{D}_2\text{Cl}_4$, 90 °C) spectra of PE- <i>co</i> -PO obtained from CCSP <i>via</i> varied ratios of 35 and 48 activated by 01 (top to bottom: Entries 5.18-5.21).	98
<i>Figure 50:</i> ^1H NMR (600 MHz, 1,1,2,2- $\text{C}_2\text{D}_2\text{Cl}_4$, 90 °C) spectra of PE- <i>co</i> -PH obtained from CCSP <i>via</i> 35 activated by varied ratios of 01 and 03 (top to bottom: Entries 5.22-5.25).	100
<i>Figure 51:</i> ^{13}C $\{^1\text{H}\}$ NMR (150 MHz, 1,1,2,2- $\text{C}_2\text{D}_2\text{Cl}_4$, 90 °C) spectra of PE- <i>co</i> -PH obtained from CCSP <i>via</i> 35 activated by varied ratios of 01 and 03 (top to bottom: Entries 5.22-5.25). The peak marked by * was from acetone.	101
<i>Figure 52:</i> ^1H NMR (600 MHz, 1,1,2,2- $\text{C}_2\text{D}_2\text{Cl}_4$, 90 °C) spectra of PE- <i>co</i> -PMCP obtained from CCSP <i>via</i> 35 activated by varied ratios of 01 and 03 (top to bottom: Entries 5.26-5.28 and 5.16).	102
<i>Figure 53:</i> Partial ^{13}C $\{^1\text{H}\}$ NMR (150 MHz, 1,1,2,2- $\text{C}_2\text{D}_2\text{Cl}_4$, 90 °C) spectra of PE- <i>co</i> -PMCP obtained from CCSP <i>via</i> 35 activated by varied ratios of 01 and 03 (top to bottom: Entries 5.26-5.28 and 5.16).	103
<i>Figure 54:</i> ^{13}C $\{^1\text{H}\}$ NMR (125 MHz, 1,1,2,2- $\text{C}_2\text{D}_2\text{Cl}_4$, 70 °C) spectra of methyl region of PP obtained under CCTP by five CpAm zirconium precatalysts (top to bottom: <i>via</i> 12 , 04 and 26-28).	109
<i>Figure 55:</i> Kinetic study for the polymerization of propene under CCTP <i>via</i> 12	113
<i>Figure 56:</i> ^{13}C NMR (150 MHz, 1,1,2,2- $\text{C}_2\text{D}_2\text{Cl}_4$, 90 °C) spectra of methyl region of multi-stereoblock PP samples from Entries 6.09 (top), 6.10 (middle), and 6.10e (bottom)...	115
<i>Figure 57:</i> ^{13}C $\{^1\text{H}\}$ NMR (150 MHz, 1,1,2,2- $\text{C}_2\text{D}_2\text{Cl}_4$, 90 °C) spectra of methyl region of multi-stereoblock PP obtained using different ratios of 12 and 27 , top (Entry 6.08), middle (Entry 6.10), bottom (Entry 6.13).	117
<i>Figure 58:</i> GPC curves for a homogenous PP sample (left) and a PP mixture (right) before (top) and after (bottom) extraction with diethyl ether	119

<i>Figure 59:</i> ^{13}C NMR (150 MHz, 1,1,2,2- $\text{C}_2\text{D}_2\text{Cl}_4$, 90 °C) spectra of methyl region of a multi-stereoblock PP from Entry 6.09 (bottom), a well-defined <i>iso-a-iso</i> triblock PP (middle) and its corresponding <i>iso-a</i> diblock PP (top).....	121
<i>Figure 60:</i> ^1H NMR (600 MHz, 1,1,2,2- $\text{C}_2\text{D}_2\text{Cl}_4$, 90 °C) spectrum of iodo-PP by CCTP via 35 (section 3.2.7).....	143
<i>Figure 61:</i> ^1H NMR (600 MHz, 1,1,2,2- $\text{C}_2\text{D}_2\text{Cl}_4$, 90 °C) spectra of isolated PE (Entry 4.05, top) and 2-methyl PE (Entry 4.06, bottom) by CCTP via 35	143
<i>Figure 62:</i> Partial ^{13}C $\{^1\text{H}\}$ NMR (150 MHz, 1,1,2,2- $\text{C}_2\text{D}_2\text{Cl}_4$, 90 °C) spectra of Et-PE-I (top) and ^iPr -PE-I (bottom) obtained by CCTP via 35 (Section 4.4).....	144
<i>Figure 63:</i> ^{13}C $\{^1\text{H}\}$ NMR (100 MHz, CDCl_3 , 20 °C) spectrum of poly-1-butene from Entry 5.01 in Table 9. The three peaks marked by * are from <i>n</i> -pentane.	145
<i>Figure 64:</i> ^1H NMR (400 MHz, CDCl_3 , 20 °C) spectrum of poly-1-butene from Entry 5.01 in Table 9. The peak marked by * is from water.....	145
<i>Figure 65:</i> ^{13}C $\{^1\text{H}\}$ NMR (150 MHz, CDCl_3 , 20 °C) spectrum of poly-1-pentene from Entry 5.02 in Table 9.....	146
<i>Figure 66:</i> ^1H NMR (600 MHz, CDCl_3 , 20 °C) spectrum of poly-1-pentene from Entry 5.02 in Table 9.....	146
<i>Figure 67:</i> ^{13}C $\{^1\text{H}\}$ NMR (100 MHz, CDCl_3 , 20 °C) spectrum of poly-1-hexene from Entry 5.03 in Table 9. The three resonances marked by asterisks (*) are from a trace amount of <i>n</i> -pentane.....	147
<i>Figure 68:</i> ^1H NMR (400 MHz, CDCl_3 , 20 °C) spectrum of poly-1-hexene from Entry 5.03 in Table 9.....	147
<i>Figure 69:</i> ^1H NMR (600 MHz, CDCl_3 , 20 °C) spectrum of poly-1-octene from Entry 5.05 in Table 9. The resonance marked by an asterisk (*) is from H_2O	148
<i>Figure 70:</i> ^1H NMR (600 MHz, 1,1,2,2- $\text{C}_2\text{D}_2\text{Cl}_4$, 90 °C) spectrum of poly(propene- <i>co</i> -1-hexene) from Entry 5.07 in Table 10.	148
<i>Figure 71:</i> ^{13}C $\{^1\text{H}\}$ NMR (150 MHz, 1,1,2,2- $\text{C}_2\text{D}_2\text{Cl}_4$, 90 °C) spectrum of poly(propene- <i>co</i> -1-hexene) from Entry 5.07 in Table 10.	149
<i>Figure 72:</i> ^1H NMR (600 MHz, 1,1,2,2- $\text{C}_2\text{D}_2\text{Cl}_4$, 90 °C) spectrum of poly(propene- <i>co</i> -1-octene) from Entry 5.08 in Table 10.	149

<i>Figure 73:</i> ^{13}C $\{^1\text{H}\}$ NMR (150 MHz, 1,1,2,2- $\text{C}_2\text{D}_2\text{Cl}_4$, 90 °C) spectrum of poly(propene- <i>co</i> -1-octene) from Entry 5.08 in Table 10. Peaks marked by asterisks * are from <i>n</i> -pentane.	150
<i>Figure 74:</i> ^1H NMR (600 MHz, 1,1,2,2- $\text{C}_2\text{D}_2\text{Cl}_4$, 90 °C) spectrum of poly(propene- <i>co</i> -1-dodecene) from Entry 5.09 in Table 10.....	150
<i>Figure 75:</i> ^1H NMR (600 MHz, 1,1,2,2- $\text{C}_2\text{D}_2\text{Cl}_4$, 90 °C) spectrum of PP- <i>co</i> -PMCP from Entry 5.10 in Table 10.....	151
<i>Figure 76:</i> ^{13}C $\{^1\text{H}\}$ NMR (150 MHz, 1,1,2,2- $\text{C}_2\text{D}_2\text{Cl}_4$, 90 °C) spectrum of PP- <i>co</i> -PMCP from Entry 5.10 in Table 10. Peaks marked by * are from <i>n</i> -pentane.	151
<i>Figure 77:</i> ^1H NMR (600 MHz, 1,1,2,2- $\text{C}_2\text{D}_2\text{Cl}_4$, 90 °C) spectrum of poly(ethene- <i>co</i> -1-hexene) from Entry 5.11 in Table 11. The resonance marked by an asterisk (*) is from H_2O	152
<i>Figure 78:</i> ^1H NMR (600 MHz, 1,1,2,2- $\text{C}_2\text{D}_2\text{Cl}_4$, 90 °C) spectrum of poly(ethene- <i>co</i> -1-octene) from Entry 5.13 in Table 11. The resonance marked by an asterisk (*) is from H_2O	152
<i>Figure 79:</i> ^1H NMR (600 MHz, 1,1,2,2- $\text{C}_2\text{D}_2\text{Cl}_4$, 90 °C) spectrum of PE- <i>co</i> -PMCP from Entry 5.16 in Table 11. The resonance marked by an asterisk (*) is from water. .	153
<i>Figure 80:</i> ^{13}C $\{^1\text{H}\}$ NMR (150 MHz, 1,1,2,2- $\text{C}_2\text{D}_2\text{Cl}_4$, 90 °C) spectra of methyl region of multi-stereoblock PP sample from Entry 6.06 of Table 16.....	153
<i>Figure 81:</i> ^{13}C $\{^1\text{H}\}$ NMR (150 MHz, 1,1,2,2- $\text{C}_2\text{D}_2\text{Cl}_4$, 90 °C) spectra of methyl region of multi-stereoblock PP sample from Entry 6.11 of Table 16.....	154
<i>Figure 82:</i> ^{13}C $\{^1\text{H}\}$ NMR (150 MHz, 1,1,2,2- $\text{C}_2\text{D}_2\text{Cl}_4$, 90 °C) spectra of methyl region of multi-stereoblock PP sample from Entry 6.12 of Table 16.....	154

List of Schemes

<i>Scheme 1:</i> Cossee mechanism for Ziegler-Natta polymerization	2
<i>Scheme 2:</i> Mechanism for the activation of a metallocene with MAO.....	4
<i>Scheme 3:</i> The mechanism for RAFT polymerization of methyl methacrylate.....	8
<i>Scheme 4:</i> Activation of 04 by 01 and formation of 04 ⁺	11
<i>Scheme 5:</i> The mechanism of SCTL polymerization	12
<i>Scheme 6:</i> Mechanism of coordinative chain transfer polymerization	13
<i>Scheme 7:</i> The mechanism of CCSP.....	16
<i>Scheme 8:</i> CpAm Zr and Hf Complexes.....	19
<i>Scheme 9:</i> Synthesis of diureas	24
<i>Scheme 10:</i> Synthesis of biscarbodiimides	24
<i>Scheme 11:</i> Synthesis of binuclear CpAm zirconium precatalysts	25
<i>Scheme 12:</i> Synthesis of new CpAm complexes	36
<i>Scheme 13:</i> Synthesis of 49 and 50 from CpAm zirconium dichloride.....	38
<i>Scheme 14:</i> Synthesis routes for compounds 52 , 53 and 51	38
<i>Scheme 15:</i> CCTP of propene with ZnEt ₂ via 35	52
<i>Scheme 16:</i> Illustrative structures of iodo-PP and regular PP by CCTP via 35	62
<i>Scheme 17:</i> Mechanism of M _B assisted chain transfer between M _A and M _C	65
<i>Scheme 18:</i> Proposed synthetic route for poly-1-alkenes with unsaturated bonds on both ends by the living CCTP technique	81

List of Preparation for Selected Compounds

<i>Syn 1:</i> Preparation of ^t Bu-NH-CO-NH-(CH ₂) ₈ -NH-CO-NH- ^t Bu (29).....	127
<i>Syn 2:</i> Preparation of ^t Bu-N=C=N-(CH ₂) ₈ -N=C=N- ^t Bu (32).....	127
<i>Syn 3:</i> Prep of [(η ⁵ -C ₅ Me ₅)ZrMe ₂] ₂ [N(^t Bu)C(Me)N(CH ₂) ₈ NC(Me)N(^t Bu)](26).....	128
<i>Syn 4:</i> Preparation of ^t Bu-NH-CO-NH-(CH ₂) ₆ -NH-CO-NH- ^t Bu (30).....	129
<i>Syn 5:</i> Preparation of ^t Bu-N=C=N-(CH ₂) ₆ -N=C=N- ^t Bu (33).....	129
<i>Syn 6:</i> Prep of [(η ⁵ -C ₅ Me ₅)ZrMe ₂] ₂ [N(^t Bu)C(Me)N(CH ₂) ₆ NC(Me)N(^t Bu)] (27).....	130
<i>Syn 7:</i> Preparation of ^t Bu-NH-CO-NH-(CH ₂) ₄ -NH-CO-NH- ^t Bu (31).....	130
<i>Syn 8:</i> Preparation of ^t Bu-N=C=N-(CH ₂) ₄ -N=C=N- ^t Bu (34).....	131
<i>Syn 9:</i> Prep of [(η ⁵ -C ₅ Me ₅)ZrMe ₂] ₂ [N(^t Bu)C(Me)N(CH ₂) ₄ NC(Me)N(^t Bu)] (28).....	131
<i>Syn 10:</i> Preparation of Et-NH-CO-NH-Et (40).....	132
<i>Syn 11:</i> Preparation of Et-N=C=N-Et (41).....	132
<i>Syn 12:</i> Preparation of (η ⁵ -C ₅ Me ₅)HfMe ₂ [N(Et)C(Me)N(Et)] (35).....	133
<i>Syn 13:</i> Preparation of (η ⁵ -C ₅ Me ₅)ZrMe ₂ [N(Et)C(Me)N(Et)] (36).....	134
<i>Syn 14:</i> Preparation of ⁱ Pr-NH-CO-NH-Et (42).....	134
<i>Syn 15:</i> Preparation of ⁱ Pr-N=C=N-Et (43).....	135
<i>Syn 16:</i> Preparation of (η ⁵ -C ₅ Me ₅)ZrMe ₂ [N(ⁱ Pr)C(Me)N(Et)] (37).....	135
<i>Syn 17:</i> Preparation of ^t BuCH ₂ -NH-CO-NH-Et (44).....	136
<i>Syn 18:</i> Preparation of ^t BuCH ₂ -N=C=N-Et (45).....	136
<i>Syn 19:</i> Preparation of (η ⁵ -C ₅ Me ₅)ZrMe ₂ [N(CH ₂ ^t Bu)C(Me)N(Et)] (38).....	137
<i>Syn 20:</i> Preparation of CH ₃ CH ₂ C(CH ₃) ₂ -NH-CO-NH-Et (46).....	138
<i>Syn 21:</i> Preparation of CH ₃ CH ₂ C(CH ₃) ₂ -N=C=N-Et (47).....	138
<i>Syn 22:</i> Preparation of (η ⁵ -C ₅ Me ₅)ZrMe ₂ [N(ⁱ Pr)C(Me)N(Et)] (39).....	139
<i>Syn 23:</i> Preparation of (1,3- ^t Bu ₂ -η ⁵ -C ₅ H ₃)ZrMe ₂ [N(Et)C(Me)N(^t Bu)] (48).....	139

<i>Syn 24:</i> Preparation of $(\eta^5\text{-C}_5\text{Me}_5)\text{ZrMe}_2[\text{N}(\text{iPr})\text{C}(\text{NMe}_2)\text{N}(\text{iPr})]$ (49).....	140
<i>Syn 25:</i> Preparation of $\text{Et-N}=\text{CH-N}(\text{Et})\text{-SiEt}_3$ (52).....	141
<i>Syn 26:</i> Preparation of $\text{Et-N}=\text{CH-NH-Et}$ (53).....	141
<i>Syn 27:</i> Preparation of $(\eta^5\text{-C}_5\text{Me}_5)\text{ZrCl}_2[\text{N}(\text{Et})\text{C}(\text{H})\text{N}(\text{Et})]$ (51)	141
<i>Syn 28:</i> Preparation of $(\eta^5\text{-C}_5\text{Me}_5)\text{ZrMe}_2[\text{N}(\text{Et})\text{C}(\text{H})\text{N}(\text{Et})]$ (50).....	142

Chapter 1: Introduction

1.1 A Brief History of Coordination Polymerization

1.1.1 Heterogeneous Ziegler-Natta polymerization

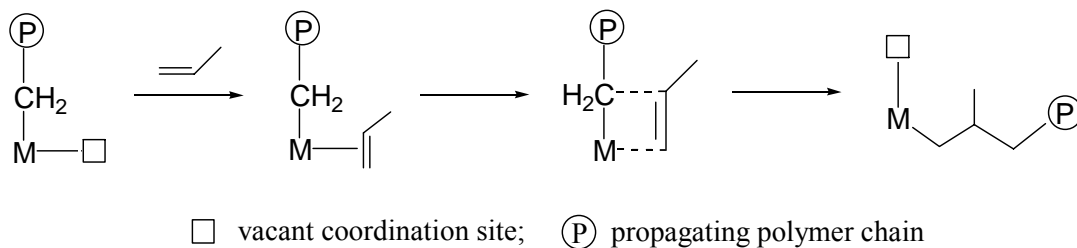
Chain growth polymerization processes can be divided into three categories according to the nature of the active species: free radical polymerization, ionic polymerization, and coordination polymerization. Coordination polymerization is also known as Ziegler-Natta polymerization to memorialize the revolutionary work by the 1963 chemistry Nobel laureates, Karl Ziegler¹ and Giulio Natta². In this dissertation, though there is no clear difference between the terms of Ziegler-Natta polymerization and coordination polymerization, the former is usually referred to a heterogeneous system such as that discovered by Ziegler and the MgCl₂-supported system,³ and coordination polymerization is used to represent a homogeneous single-site metallocene or post-metallocene system which will be discussed later.

Ziegler-Natta polymerization is one of the most successful applications of transition metal catalysis. In 2005, 65 million tons of polyethene (PE) and 40 million tons of polypropene (PP) were produced worldwide, and the production has been increasing at the annual rate of 6% and 8% respectively.⁴ For the nomenclature of monomers widely employed in the area of coordination polymerization I will adopt the IUPAC names in this thesis, for example, ethene and propene instead of the terms of ethylene and propylene which are also commonly used. 1-alkenes include ethene, propene and beyond; α -olefins will exclude ethene; higher α -olefins are referred to as 1-butene (1-but), 1-pentene (1-pen), 1-hexene (1-hex), 1-octene (1-oct) and so on.

By definition, a Ziegler-Natta catalyst refers to the combination of two components: a transition metal complex of Group IV to VIII known as a precatalyst and a main group metal alkyl or alkyl halide named as a cocatalyst. Normally the cocatalyst also functions as an activator and that is the case for the systems studied in this thesis. An early example of a Ziegler-Natta catalyst was composed by TiCl_4 and AlEt_2Cl and the effective species was believed to be TiCl_3 introduced by a reduction process. With this binary system, Karl Ziegler synthesized high density polyethene (HDPE) under mild pressure and Giulio Natta made isotactic polypropene which was also crystalline for the first time.^{1,2}

The mechanism for Ziegler-Natta polymerization of alkenes was not very clear until now. A widely accepted pathway was proposed by Cossee and coworkers.^{5, 6} The Cossee mechanism involves the complexation of a monomer to the active transition metal center through a vacant coordination site followed by migratory insertion of the complexed monomer to the bond between the transition metal and α -carbon on the alkyl or polymeryl group (Scheme 1). A new vacant site is produced which was originally occupied by the polymer chain and the Cossee process can be repeated.^{7, 8}

Scheme 1: Cossee mechanism for Ziegler-Natta polymerization



In addition to the linear structure of the resulting polymers, another very important feature of Ziegler-Natta polymerization is the stereoregularity of the polyolefins obtained. Four typical tacticities used to describe PP microstructure are illustrated in Figure 1. The physical properties of a polyolefin material are greatly reliant on its microstructure. For example, isotactic PP and syndiotactic PP are crystalline; however atactic PP is amorphous.

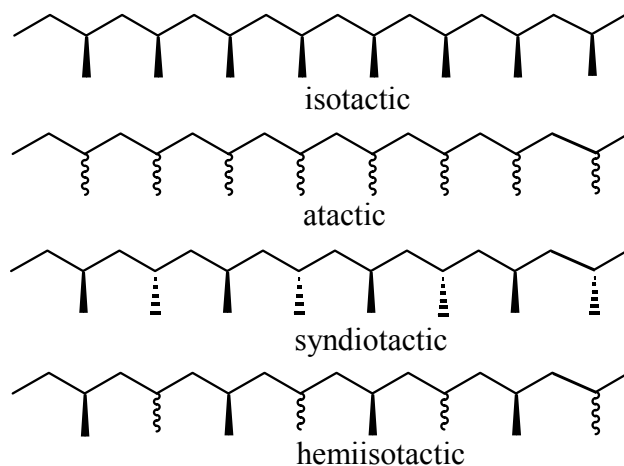
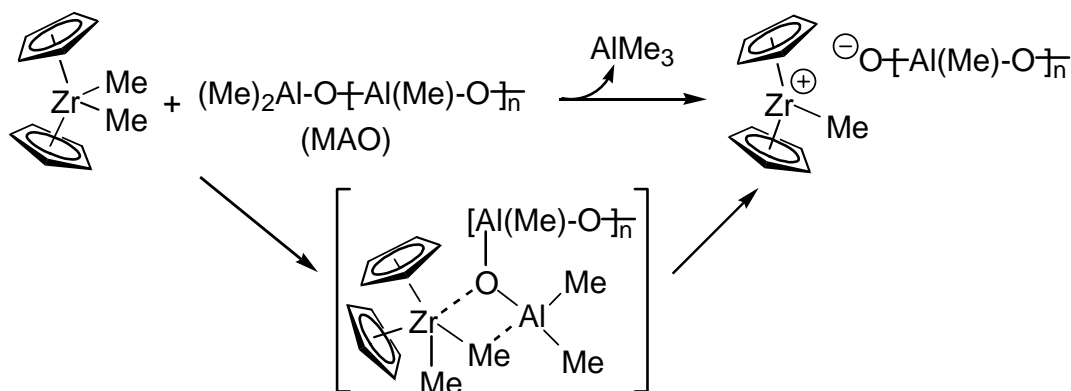


Figure 1: Typical microstructures of polypropylene

1.1.2 Homogeneous metallocene and post-metallocene catalysis

Metallocenes are transition metal complexes containing two cyclopentadienyl (Cp), or its derivative, anions. Alkene polymerization catalyzed by homogeneous metallocenes has been studied since 1957.^{9, 10} However only very low activity was achieved until the invention of methylaluminoxane (MAO) by Sinn and Kaminsky in 1980.¹¹ It was proposed that metallocenes were methylated by MAO through a Cl-CH₃ exchange process, and the active cationic species was produced through a mechanism as shown in Scheme 2. The combination of metallocenes with MAO widely opened the area of homogeneous single-site coordination polymerization.^{7, 12}

Scheme 2: Mechanism for the activation of a metallocene with MAO



Besides MAO, some perfluorinated borates were also introduced as cocatalysts, such as $[\text{PhNHMe}_2][\text{B}(\text{C}_6\text{F}_5)_4]$ (**01**), $[\text{Ph}_3\text{C}][\text{B}(\text{C}_6\text{F}_5)_4]$ (**02**) and $\text{B}(\text{C}_6\text{F}_5)_3$ (**03**).¹³⁻¹⁵ Soluble cationic metallocene catalysts were formed with these borates, and some well-defined living coordination polymerization systems were developed.^{16, 17} The cocatalysts adopted for the research in this thesis belong to this type. In this dissertation, the cationic species, which is active towards polymerization reactions, is referred to as a catalyst no matter what type of alkyl or polymeryl groups it bears, not an initiator even if the alkyl group is methyl, because of the catalytic enchainment of monomer(s) and living characteristics. The neutral precursor of a catalyst is referred to as a precatalyst.

While innumerable metallocenes were developed and tested for the coordination polymerization of 1-alkenes, a variety of polymers with different composition, architecture and tacticity were obtained. The relationship between the structure of a metallocene and the tacticity of a polymer was systematically described by Ewen in 1984,¹⁸ and even now it is still an important rule regarding catalyst design.

Post-metallocenes are another type of homogeneous single-site catalysts which can also be activated by the above cocatalysts. One example was given by Brookhart and coworkers in 1995. Nickel complexes bearing diimine ligands were used to catalyze the polymerization of ethene and α -olefins.¹⁹ In the past two decades post-metallocene catalysis demonstrated diverse applications in the area of homogeneous coordination polymerization.²⁰ Some examples will be given later in the topic of living coordination polymerization.

1.2 A General View of Living Polymerization Processes

1.2.1 Discovery of living anionic polymerization and its characters

The first living anionic polymerization system was discovered by Michael Szwarc in 1956.^{21, 22} He polymerized styrene in THF by naphthyl sodium under an inert atmosphere and the active living anion persisted until being quenched by water. Fifty years after this innovative discovery, living polymerization has become one of the most important concepts in polymer science. Numerous well-defined block copolymers were made by living techniques in both academic laboratories and industrial plants.^{23, 24}

There are many features in a living polymerization system. First, there are no, or only negligible, termination events during the polymerization process, and consequently all the active centers stay stable and living. Other features include: 1, the initiation process is fast relative to propagation to make sure all the polymer chains start to grow at the same time; 2, no chain transfer or other process, such as β -hydride elimination, are responsible for the cessation of polymer chains; 3, number

averaged molecular weight (M_n) can be calculated stoichiometrically; 4, resulting polymers possess narrow molecular weight distribution, presented by the polydispersity index (PDI); 5, polymerization can be resumed by adding more monomers and block copolymer can be obtained by sequential monomer addition; 6, end group functionalization can be realized and controlled.^{25, 26}

It is not easy to find an ideal system which meets all the criteria mentioned above. However there are many polymerization systems which show some of these features and have been claimed to be living systems. Sometimes a process might proceed in a controlled fashion even if it obviously deviates from a living system, and the terms of controlled or quasi-living polymerization are commonly used.²⁷

1.2.2 Development of cationic and radical living polymerizations

More than ten years after the first example of living polymerization was discovered, the living cationic ring opening polymerization of THF was realized in 1974. Later on, this system was applied to the polymerization of other heterocyclic monomers and well-defined block copolymers were finally achieved.^{28, 29} In the living cationic polymerization system the well separated ion pairs, whose cation were highly active, experienced a rapid dynamic exchange with the aggregates of macroesters, which were the dormant species.³⁰

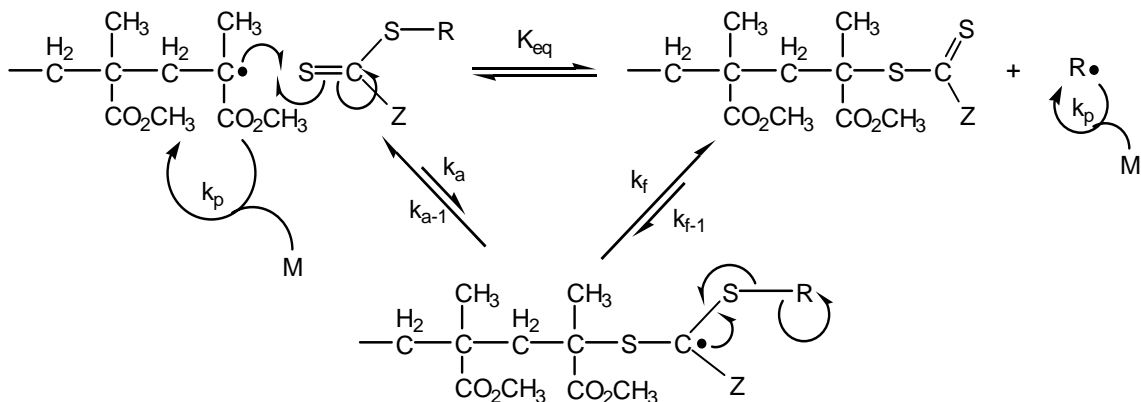
Radical species usually produce polymer chains in a very short time (≈ 1 s) and then terminate in some way. Because of this it was quite challenging to get a living radical polymerization system. However, several methods were developed in the past 15 years and living/controlled radical polymerization was also achieved. In such a

system, the active radical species was either stabilized by an external compound, such as a stable radical or a cobalt complex, or was in equilibrium with a dormant species under degenerative transfer conditions.³¹

In 1993, a TEMPO (2,2,6,6-tetramethyl-1-piperidynyl-N-oxy) mediated radical polymerization of styrene was reported by Georges and coworkers which was regarded as the first controlled free radical polymerization (CFRP).³² Later on, more stable nitroxide radicals and other types of organic mediators³³ as well as metal complexes^{34, 35} were applied in the polymerization system with a similar mechanism. In 1995, Matyjaszewski and Wang³⁶ and Sawamoto and coworkers³⁷ independently reported the atom transfer radical polymerization (ATRP), which was one of the most widely studied living techniques. In an ATRP system, a transition metal (e.g. Cu, Ru or Fe) complex is involved in a reversible end-capping process with a propagating polymer chain, which bears the active radical, through an oxidation–reduction mechanism.³¹

Reversible addition–fragmentation chain transfer (RAFT) is another important living radical polymerization technique and was initially reported by Chiefari, et al in 1998.³⁸ RAFT falls in the category of degenerative chain transfer polymerization, in which the dormant species was originally a thiocarbonylthio compound, such as dithioesters, xanthates and dithiocarbamates.³⁹ The RAFT mechanism is illustrated by Scheme 3, in which the thiocarbonylthio compound may have different Z and/or R groups from the big family of RAFT chain transfer agents.⁴⁰

Scheme 3: The mechanism for RAFT polymerization of methyl methacrylate



Living ring opening metathesis polymerization (ROMP) is another polymerization technique based on a different mechanism, which is a unique C=C double bond exchange process mediated by metal complexes called olefin metathesis.⁴¹ The Nobel Prize in chemistry 2005 was awarded to Yves Chauvin, Robert H. Grubbs and Richard R. Schrock for the development of this metathesis process. In addition to the living polymerizations mentioned above, there are some other types of living techniques^{40, 42, 43} developed recently, which will not be discussed here due to the limited investigation. In the following sections, the focus will be on the living technique with a coordination mechanism⁴⁴ instead of ionic (anionic or cationic), radical (CFRP, ATRP or RAFT) and metathesis (ROMP) polymerization.

1.2.3 Living coordination polymerization based on homogeneity

In the homogeneous metallocene and post-metallocene based polymerization systems, the propagating polymer chains might undergo some side reactions such as decomposition and β -H elimination. To obtain a living coordination polymerization,

stable catalysts are needed and the reactions are usually carried out at a relative low temperature. Since the first example reported by Doi in 1979,⁴⁵ a number of catalytic systems (e.g. those developed by McConville,^{16, 46} Schrock,^{17, 47} Fujita /Coates,⁴⁸⁻⁵⁰ Sita,^{51, 52} Ikeda^{53, 54} and Kol,^{55, 56} see Figure 2 for structures) were claimed as controlled/living polymerization and showed living characters.⁴⁴ In this thesis, TLCP is used to represent such a traditional living coordination polymerization in order to differentiate it from two other processes: stereomodulated degenerative transfer living (SDTL) coordination polymerization, and coordinative chain transfer polymerization (CCTP).

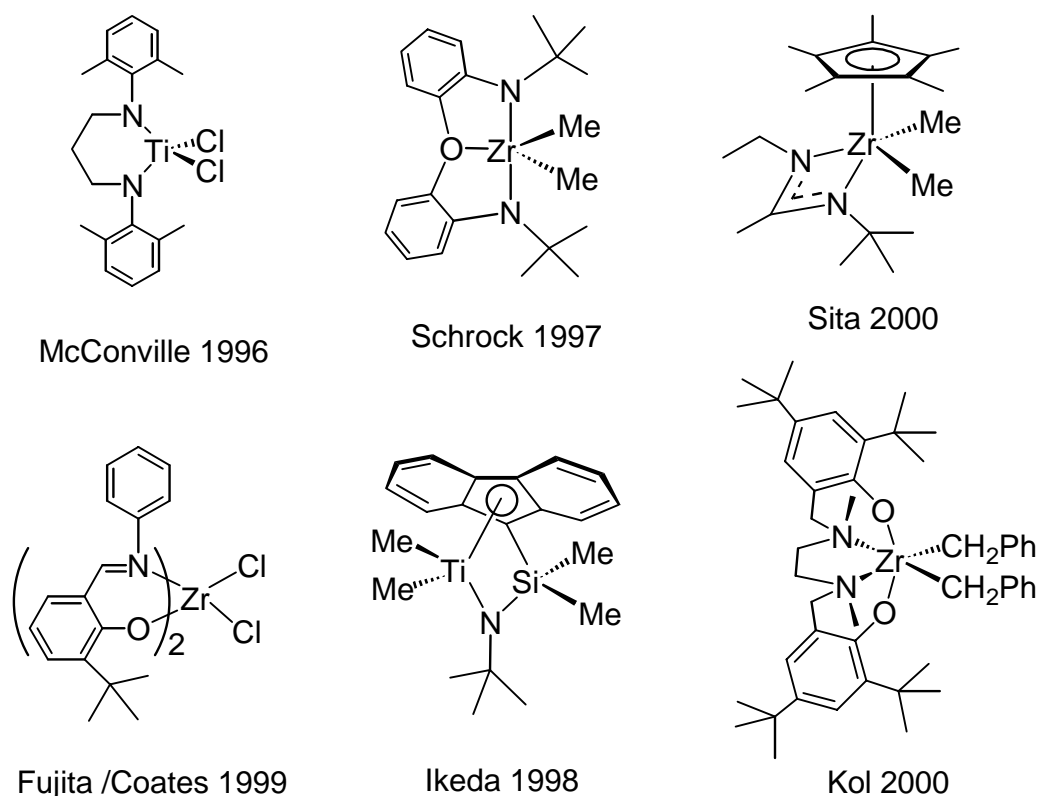


Figure 2: Examples of catalyst precursors for living coordination polymerization

With those catalysts used for TLCP, plenty of polyolefin structures were prepared including many fundamentally novel ones. The monocyclopentadienyl

monoamidinate (CpAm) zirconium complex $(\eta^5\text{-C}_5\text{Me}_5)\text{ZrMe}_2[\text{N}(\text{Et})\text{C}(\text{Me})\text{N}(\text{tBu})]$ (**04**) will be taken as an example to describe the process of a living coordination polymerization, mainly because of the diverse polymers obtained by it. In this thesis, CpAm refers the ligand combination of any monocyclopentadienyl ring, including pentamethylcyclopentadienyl (Cp*) and 1,3-di-*tert*-butylcyclopentadienyl, and any amidinate component, such as acetamidinate, formamidinate and *tert*-butylamidinate.

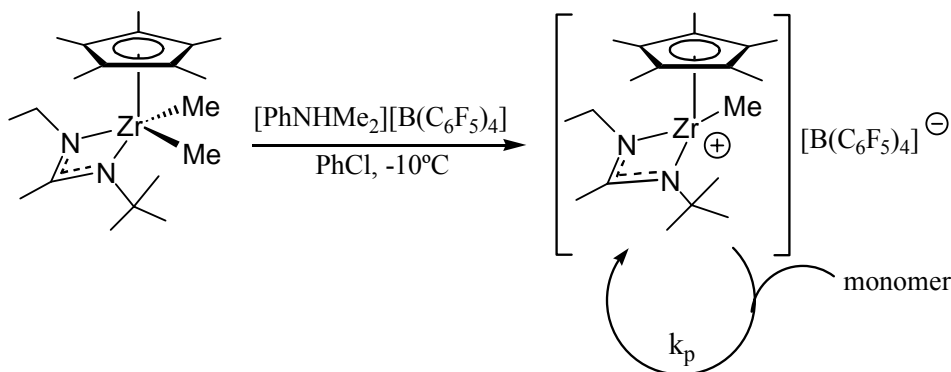
1.2.4 An example of traditional living coordination polymerization (TLCP)

In 2000, Sita and coworkers reported the synthesis and polymerization behavior of a new family of homogeneous post-metallocene catalysts with the half-sandwich CpAm structure. Upon being activated by the perfluorinated borate **01**, by a demethylation process as shown in Scheme 4, **04** turned into a cationic species which is active towards the polymerization of many alkenes. The living stereospecific polymerization of 1-hexene was first reported with **04** and isotactic poly-1-hexene (PH) was obtained.⁵¹ Later on, the homopolymerization of 1,5-hexadiene and the block copolymerization of 1-hexene and 1,5-hexadiene (1,5-HD) were also achieved.⁵⁷ Isotactic PH and the block copolymer of 1-hexene and 1-octene (iso~PH-*b*-iso~PO, *b* indicates a block structure) were also made by a lightly-crosslinked poly(styrene-divinylbenzene) supported CpAm zirconium catalyst derived from **04**.⁵⁸ The living polymerization of propene by $(\eta^5\text{-C}_5\text{Me}_5)\text{ZrMe}[\text{N}(\text{Et})\text{C}(\text{Me})\text{N}(\text{tBu})]^+$ (**04**⁺) derived from **04** and **01** will be discussed in the next chapter.

In this thesis, the neutral numbers, such as **04**, represent the neutral precatalysts, and the positive sign, such as **04**⁺, refers to the cation derived from the precatalyst with one methyl group being detached. The cationic species are the only species

which are active towards a polymerization process; the neutral precatalysts are not. But for the convenience of statements, I tend to say “polymerization by/using/via a precatalyst”, which does not mean the precatalyst is active. The real active center is the cation or ion pair derived from the precatalyst upon being activated by a cocatalyst.

Scheme 4: Activation of **04** by **01** and formation of **04**⁺

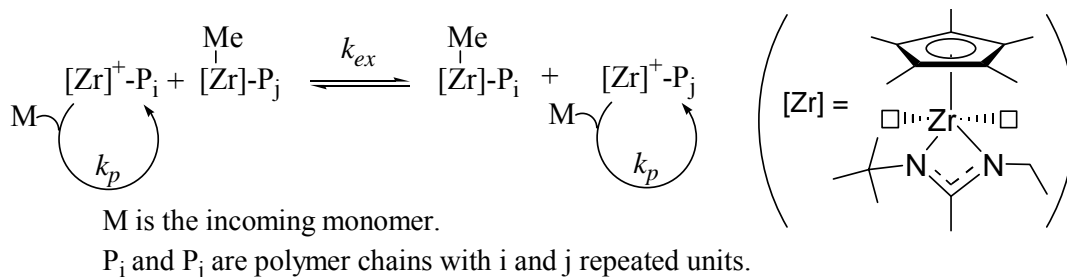


1.2.5 Stereomodulated degenerative transfer living coordination polymerization

A special and very important feature of the catalytic system with **04** as the precatalyst is that the tacticity of the resulting polyolefins can be easily adjusted using a substoichiometric amount of cocatalyst **01**, which induces stereomodulated degenerative transfer living (SDTL) coordination polymerization.⁵⁹ Its mechanism falls in the category of degenerative group transfer polymerization, as summarized in Scheme 5. When the number of moles of **01** is less than that of **04**, the active cationic species **04**⁺ are present along with the neutral species **04**, which are dormant and inactive toward polymerization of α -olefins. The active species and dormant species are in equilibrium and the rate of methyl group exchange is much faster than the propagation rate ($k_{\text{ex}} \gg k_p$), which is directly associated with a low PDI.⁶⁰ The

methyl group exchange between neutral and cationic zirconium centers was believed to occur *via* a methyl-bridged binuclear intermediate.⁶¹

Scheme 5: The mechanism of SDTL polymerization



In this partially activated system, the neutral and cationic species are different not only in terms of their dormant or active states, but also in their configuration stability regarding the amidinate ring-flipping, which causes the metal-centered epimerization.⁵⁹ In the neutral complex, the amidinate ring-flipping is fast and the site stereoselectivity changes between the *re* and *si* faces. After the dormant species turn to active centers, this change results in the loss of stereospecificity in the polymer product since the epimerization rate is faster than that of methyl group exchange ($k_{\text{epi}} \gg k_{\text{ex}}$).

The polymerization system with **04** meets all the criteria for a SDTL process. The polymer produced has a narrow polydispersity and the amount of polymer chains is stoichiometrically equal to the amount of total zirconium centers. The stereoregularity can be continuously adjusted from isotactic (TLCP) to purely atactic (SDTL) by changing the activation percentage. In addition to the atactic polyolefins obtained under SDTL conditions, stereoblock copolymers were also successfully prepared by switching SDTL process to TLCP polymerization and/or vice versa.⁶² The chloride mediated SDTL was also reported as an efficient alternative to the

transfer with the catalytically active species, $[M_A]^+ - P_A$, which is usually derived from a transition metal precatalyst and a cocatalyst. If this chain transfer process, presumably *via* a binuclear intermediate,⁶⁶ is very fast and quantitative, all the alkyl/polymeryl groups will be in a degenerative state and grow simultaneously. We named the chain transfer agent (CTA) as a surrogate, not a dormant species, because it never turned to an active center, even though the alkyl groups on it were also being extended. The CCTP was also called (M_A) catalyzed chain growth (on M_B), which was considered as a degenerative chain transfer polymerization process.⁶⁷

Bearing this in mind, researchers started to explore numerous coordination polymerization systems and CCTP was proven to happen in some cases. One example I would like to describe here was reported by Gibson and coworkers in 2002.⁶⁸ They studied the CCTP of ethene with $ZnEt_2$ *via* an iron complex (Figure 3) activated by MAO. This system requires high equivalents (≥ 500) of $ZnEt_2$. The PE obtained showed a Poisson distribution of alkanes. Later on, more main group metal alkyls were tested as chain transfer agents for the iron system. $GaMe_3$ and Zn^iPr_2 were found to be effective CTA similar to $ZnEt_2$ and other alkyls studied displayed somewhat inferior behavior.⁶⁹ Also, the CCTP of ethene with $ZnEt_2$ was investigated for a series of metallocene and post-metallocene catalysts and a Fujita catalyst showed effective chain transfer with zinc.⁷⁰

Other CCTP systems of ethene include the yttrium system activated by **01**, or other borates, with Al^iBu_3 or other aluminum alkyls as CTA developed by Kempe and coworkers in 2006;⁷¹ the samarium system with $^nBu-Mg-Et$ as both an activator and CTA studied by Mortreux, et al in 1996;⁷² the system of $CrCp^*(PMe_3)Me_2$

activated by **03** with AlMe_3 or AlEt_3 reported by Bazan and coworkers in 2001,⁷³ and a neutral chromium catalyst undergoing chain transfer with AlEt_3 designed by Gabbai and coworkers in 2004.^{74, 75} The structures of these precatalysts employed for CCTP of ethene are listed in Figure 3.

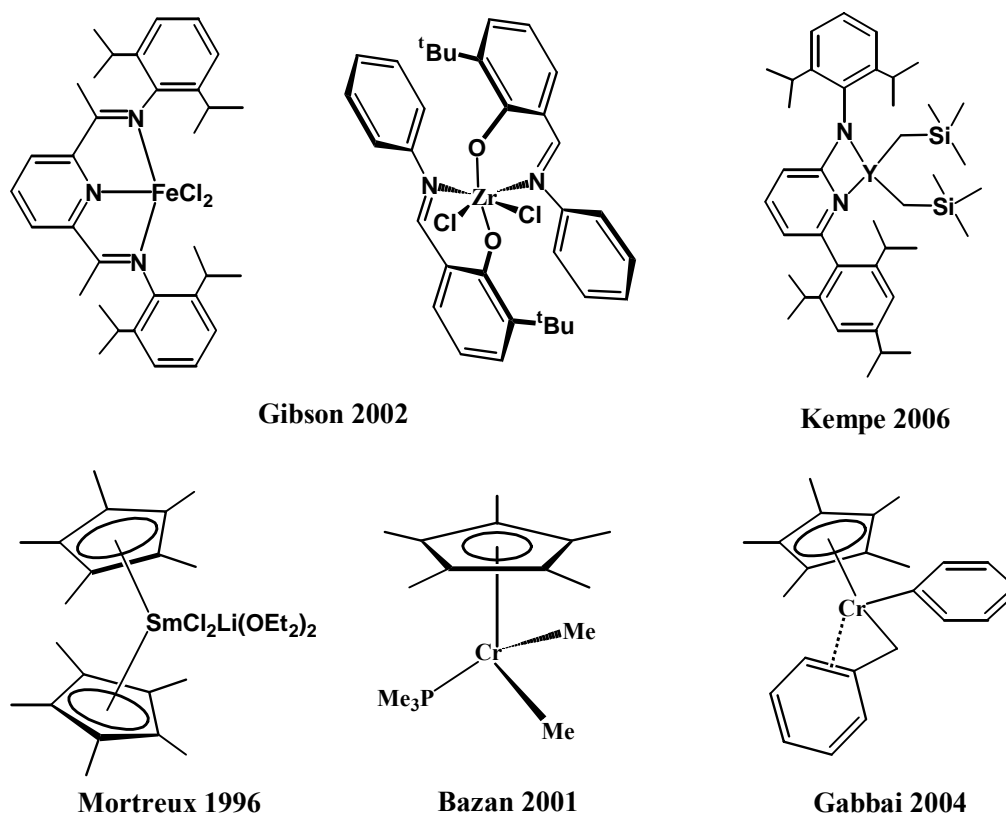


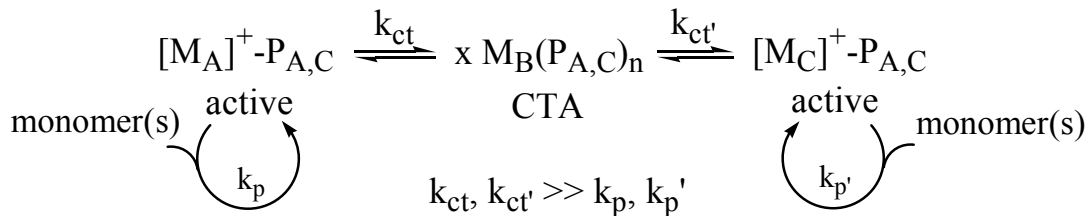
Figure 3: Examples of precatalysts employed for the CCTP of ethene

1.3.2 CCSP random copolymerization of ethene and 1-octene

A new strategy in the area of CCTP was proposed and realized by the researchers at the Dow Chemical Company, namely coordinative chain shuttling polymerization (CCSP). In the CCSP system, two catalysts were employed at the same time which both underwent chain transfer with the same chain transfer agent during the random copolymerization of ethene and 1-octene. In this thesis, CCSP refers to any CCTP

process involving two components having the same function, including dual precatalysts, dual cocatalysts or dual chain transfer agents. When different (co)polymer structures were produced by these two catalysts, the final product would have a multiblock backbone caused by the chain transfer processes (Scheme 7).⁷⁶

Scheme 7: The mechanism of CCSP



The two precatalysts (Figure 4) were selected by a high throughput screening protocol, and both underwent effective chain transfer with $ZnEt_2$ after being activated by MAO under identical conditions. The copolymer incorporation rate by the zirconium catalyst was low and resulted in hard chain segments; the hafnium catalyst incorporated more 1-octene into the PE backbone and provided a soft constituent. Every polymer chain had the chance to grow on both catalysts due to chain transfer processes, and a multiblock structure of hard and soft segments was formed.

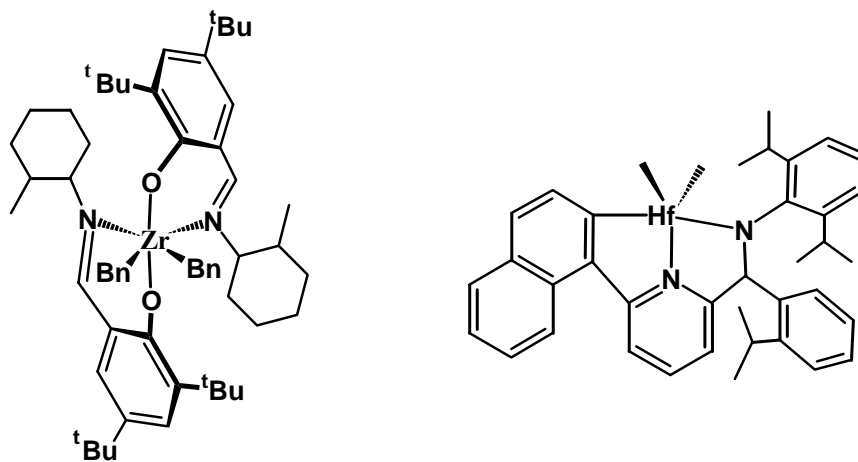


Figure 4: Precatalysts used to make multiblock PE-co-PO by Dow Chemical

1.3.3 Challenges in the area of CCTP

CCTP provided a practical solution to the “one chain per catalyst” restriction of TLCP polymerization. Examples mentioned above demonstrate the feasibility and potential of CCTP technique, though there are still many issues to be explored. To date before this work, there was only one monomer that was successfully polymerized by CCTP, which was ethene. And the molecular weight of PE reached up to 4 kDa. The CCTP and CCSP of propene were also tried, but for most cases a polymer mixture was obtained. Research about this topic will be discussed later in Chapters 3 and 6. The CCTP of higher α -olefins, dienes or cyclic alkenes has not been reported.

In addition to the narrow window of monomers applied, there are some other challenges to CCTP: the effective combinations of precatalyst, cocatalyst and chain transfer agent are only a few, and more systems need to be developed for better performance such as high temperature tolerance; multiblock copolymers already showed good elastomeric properties and more examples of this type are desired including stereoblock copolymers obtained from one monomer; controllable functionalization of end groups, and block copolymers by conjunction of living CCTP with other types of living polymerization techniques. The research in this thesis made several breakthroughs for some of these challenges. It was also realized that CCTP was just in its preliminary stage of development. More accomplishments and progress will happen in the future for this new polymerization method.

Chapter 2: Polymerization of Propene *via* Novel CpAm Group 4

Metal Complexes

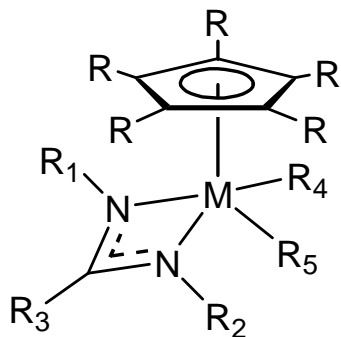
2.1 Background

2.1.1 Development of the CpAm group 4 metal catalyst family

The polymerization behavior of 1-hexene *via* **04** (M = Zr, R = R₃ = R₄ = R₅ = Me, R₁ = ^tBu, R₂ = Et in Scheme 8) was already discussed in Chapter 1. A symmetric complex, **05** (M = Zr, R = R₃ = R₄ = R₅ = Me, R₁ = R₂ = Cy), was also reported at the same time as **04**, and was used as a precatalyst for the polymerization of 1-hexene to produce atactic polymers.⁵¹ Later on, a series of CpAm zirconium complexes (**06** – **11**) were synthesized by modifying R₂ in Scheme 8, and their ability, together with the cocatalyst **01**, to initiate the polymerization of 1-hexene was studied in detail, in order to illustrate the ligand effects derived from steric factors on the polymerization activity and polymer microstructure.⁷⁷ In 2004, the goldilocks effect of the distal substituent (R₃ in Scheme 8) was discussed based on the polymerization results *via* four zirconium complexes with different amidinate components (**04**, **12** – **14**).⁷⁸

In addition, several precatalysts with dramatically enhanced activities (**15** – **17**) were synthesized successfully by replacing the Cp* ring to a Cp ring.⁷⁹ By these catalysts, even vinylcyclohexane (VCH) was polymerized in a living fashion and isotactic PVCH was obtained through a chain end control mechanism. A triblock copolymer of PH-*b*-PVCH-*b*-PH was also obtained with a PDI value of 1.08.

Scheme 8: CpAm Zr and Hf Complexes



04, 05 (M = Zr, R = R₃ = R₄ = R₅ = Me)

R₁ = ^tBu, R₂ = Et (**04**), R₁ = R₂ = Cy (**05**);

06–11 (M = Zr, R = R₃ = R₄ = R₅ = Me, R₁ = ^tBu)

R₂ = ⁱBu (**06**), R₂ = CH₂^tBu (**07**), R₂ = Bn (**08**), R₂ = CH₂(2-ClC₆H₄) (**09**), R₂ = CH₂(3-MeC₆H₄) (**10**), R₂ = CH₂(2,4,6-Me₃C₆H₂) (**11**)

12–14 (M = Zr, R = R₄ = R₅ = Me, R₁ = ^tBu, R₂ = Et)

R₃ = H (**12**), R₃ = Ph (**13**), R₃ = ^tBu (**14**)

15–17 (M = Zr, R = H, R₃ = R₄ = R₅ = Me)

R₁ = R₂ = ⁱPr (**15**), R₁ = R₂ = Cy (**16**), R₁ = ^tBu, R₂ = Cy (**17**)

18–25 (R = R₃ = R₄ = Me, R₁ = ^tBu, R₂ = Et)

M = Zr, R₅ = Et (**18**), M = Zr, R₅ = ⁿPr (**19**), M = Zr, R₅ = ⁱPr (**20**), M = Zr, R₅ = ⁿBu (**21**), M = Zr, R₅ = ⁱBu (**22**), M = Zr, R₅ = 2-EtBu (**23**), M = Hf, R₅ = ⁱBu (**24**), M = Hf, R₅ = ^tBu (**25**)

Another change made on the ligand set was achieved by attaching different alkyl groups onto the metal center directly (**18 – 25**). Instead of focusing on activities, this

series of complexes were used to model the cationic metal center for the living propagation of polymer chains and their stabilities were discussed.⁸⁰

Continuing effort was taken in this thesis (Section 2.2 & 2.3) to develop more precatalysts of CpAm group 4 metal complexes for coordination polymerization. A series of binuclear CpAm zirconium precatalysts⁸¹ and several highly active CpAm zirconium and hafnium complexes were made and their catalytic behavior for the polymerization of propene was thoroughly studied.

2.1.2 Polymerization of propene *via* precatalyst 04

Polypropene deserves more attention to some extent than polyethylene due to the tacticity issue and its physical properties determined by varieties of microstructures. Figure 5 shows the ten different configurations on a pentad level, in which *m* represents the *meso* stereochemical relationship between two adjacent stereocenters on a polymer backbone and *r* represents the *racemic* dyads. An effective tool to illustrate these microstructures for a real sample is the high resolution ¹³C NMR spectroscopy technique.⁸²

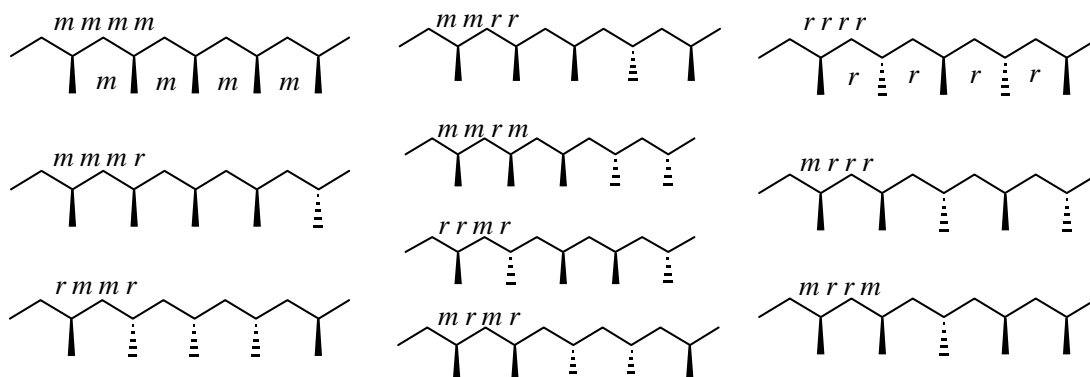


Figure 5: Schematic diagram of PP microstructure on a pentad level

The polymerization of propene was conducted under both TLCP and SDTL conditions with precatalyst **04**.⁶² When fully activated by **01**, **04** provided polypropylene with an *mmmm* pentad content of 0.71 (top spectrum in Figure 6), and the corresponding σ value is 0.92. Here, σ is a parameter commonly used to indicate the stereoselectivity of a monomer insertion into a catalytic center under enantiomorphic site control. It is defined as the probability of each monomer adding to the R site on a *re* face, same as that to the S site on a *si* face.

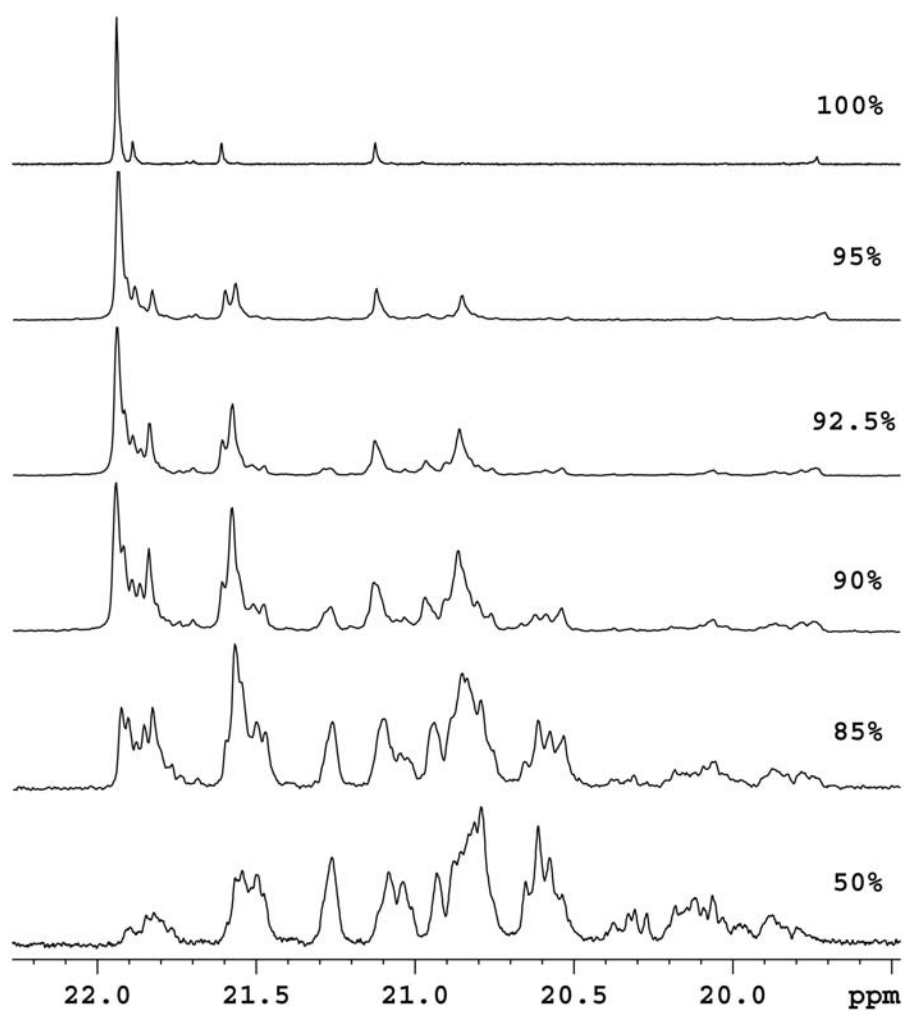


Figure 6: $^{13}\text{C}\{^1\text{H}\}$ NMR (125 MHz, $1,1,2,2\text{-C}_2\text{D}_2\text{Cl}_4$, 70 °C) of methyl region of PP with different activation percentage of **04** by **01**.⁸³

Under SDTL conditions, the tacticity of the resulting PP measured by the *mmmm* pentad content or *mm* triad content was consecutively modulated by the relative ratio of the cocatalyst to the precatalyst, e.g. activation percentage.⁸³ All the microstructures shown in Figure 6, and in fact an infinite number of microstructures, were obtained by only one complex **04**. In addition to the microstructural control, **04** was also used to prepare some fundamentally new forms of polymers, including stereogradient PP⁸³ and well-defined stereoblock PP⁶². A diblock *a-iso* PP, a triblock *a-iso-a* PP and a tetrablock *a-iso-a-iso* PP copolymers were synthesized and well characterized.⁶² In this thesis, another type of well-defined stereoblock PP, *iso-a-iso* PP was obtained with isotactic PP blocks on both ends (Chapter 6).

2.2 A Tether-Length Dependent Series of Group 4 Bimetallic Initiators for SCTL

Coordination Polymerization of Propene

2.2.1 Introduction

Binuclear species of metallocene or post-metallocene based catalysts were observed⁸⁴ or even isolated and characterized.⁵² Compared with the corresponding mononuclear compounds, they usually display lower activity towards the polymerization of alkenes or have no activity at all. Marks and coworkers made some physically linked binuclear precatalysts and cocatalysts by which they observed an increase in the branching content and molecular weight of PE during ethene homopolymerization, and also an increase in the enchainment level of 1-hexene or 1-pentene during their copolymerization with ethene.⁸⁵⁻⁸⁷ Branched PE was also obtained *via* a heterobinuclear catalysts.⁸⁸ The copolymerization of styrene and ethene with some bimetallic catalysts was also reported by Marks^{89, 90} and Noh⁹¹⁻⁹⁴ separately. When we moved this area to the polymerization of propene, it turned out much less fruitful due to the low activity. As far as I know, only one bimetallic species was reported to be active for the polymerization of propene⁹⁵, and in most cases only oligomerization of propene was achieved.⁹⁶⁻⁹⁹ In all these references, no proximity effect or its possible influence on stereochemistry was studied for propene.

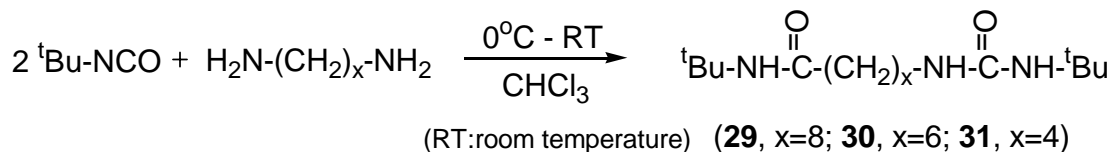
In light of the above work, a series of binuclear CpAm zirconium catalysts were made with the expectation of possessing some new catalytic behavior for the polymerization of propene. Possible proximity effects due to the physically tethered zirconium centers, which are cationic under TLCP conditions, might influence the

activity, stereochemistry, living character, molecular weight and molecular weight distribution during a polymerization process. Under SDTL conditions, the linked neutral and cationic zirconium centers might provide additional control factors to the polymerization, methyl group exchange and metal-centered epimerization by both inter- and intra-molecular processes. In addition to obtaining new polymer products, this series of bimetallic catalysts can also highlight the mechanistic study of the methyl group exchange process and the amidinate ring-flipping process within the SDTL coordination polymerization system.⁸¹

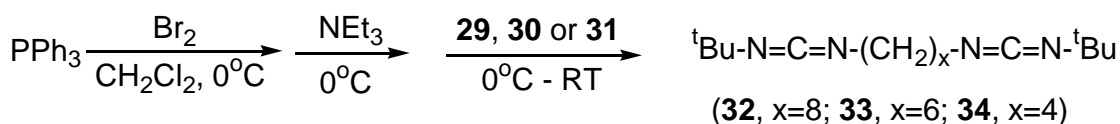
2.2.2 Synthesis of binuclear initiators

To synthesize the binuclear zirconium initiators, which have the common structure of $[(\eta^5\text{-C}_5\text{Me}_5)\text{ZrMe}_2]_2[\text{N}(\text{tBu})\text{C}(\text{Me})\text{N}(\text{CH}_2)_x\text{NC}(\text{Me})\text{N}(\text{tBu})]$ (**26**, $x = 8$; **27**, $x = 6$; **28**, $x = 4$), the corresponding diurea $\text{tBu-NH-CO-NH-(CH}_2)_x\text{-NH-CO-NH-tBu}$ (**29**, $x = 8$; **30**, $x = 6$; **31**, $x = 4$) and biscarbodiimide $\text{tBu-N=C=N-(CH}_2)_x\text{-N=C=N-tBu}$ (**32**, $x = 8$; **33**, $x = 6$; **34**, $x = 4$) were prepared first as the ligand precursors. Following are the synthesis processes:

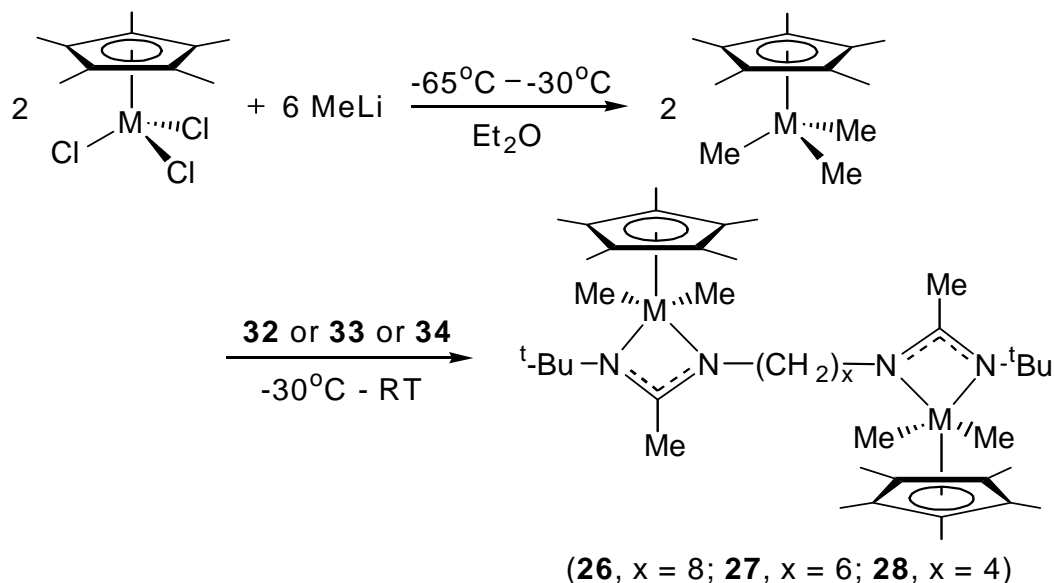
Scheme 9: Synthesis of diureas



Scheme 10: Synthesis of biscarbodiimides



Scheme 11: Synthesis of binuclear CpAm zirconium precatalysts



In Scheme 9, the diureas were easily obtained as white powders from the starting materials, tert-butyl isocyanate and diamines. The reaction went almost to 100% conversion in chloroform. In Scheme 10, a three-step reaction was adopted, but in a one-pot process. About 25% excess amount of triphenylphosphine, bromine and triethylamine were added relative to the moles of diureas. For this reaction, methylene chloride was used as the solvent throughout. The biscarbodiimide products were purified by distillation *in vacuo* at the end.¹⁰⁰

Another one-pot reaction was performed according to Scheme 11 under an inert atmosphere of nitrogen.⁷⁹ The synthesis of these binuclear zirconium complexes is successful, providing a yield as high as 79%. The structures of these diureas, biscarbodiimides and binuclear zirconium complexes were characterized by elemental analysis, ¹H NMR spectroscopy and X-ray crystallography techniques. The single crystal X-ray structures of compound **26**, **27** and **28** are shown in Figures 7, 8 and 9

separately. Experimental details for the synthesis of all these compounds are provided in Appendix I.

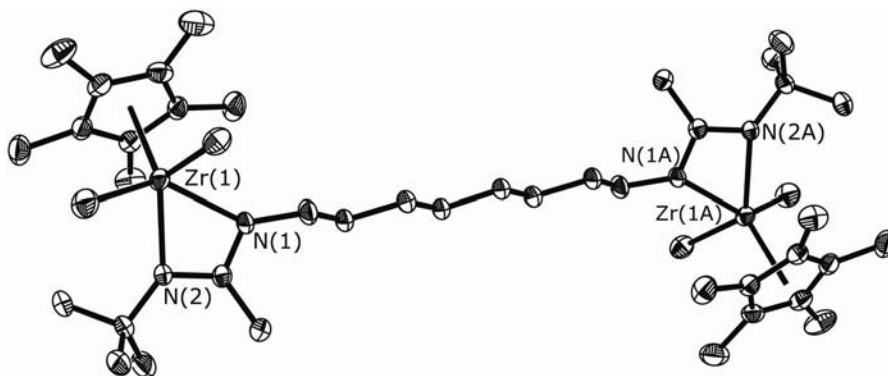


Figure 7: Molecular structures (30% thermal ellipsoids) of **26**. Hydrogen atoms have been removed for the sake of clarity.

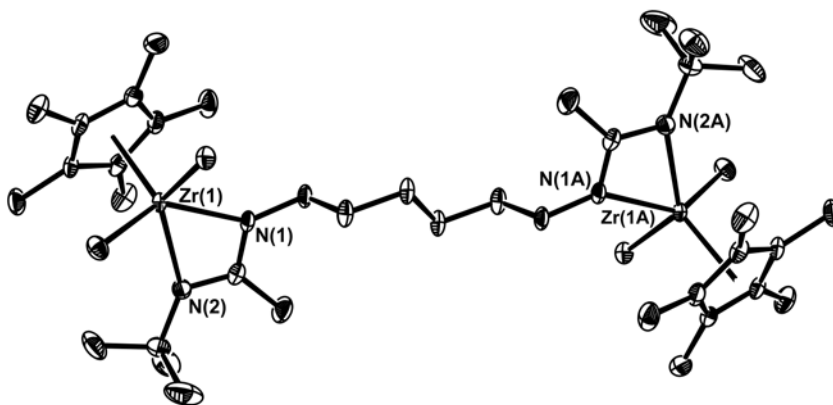


Figure 8: Molecular structures (30% thermal ellipsoids) of **27**. Hydrogen atoms have been removed for the sake of clarity.

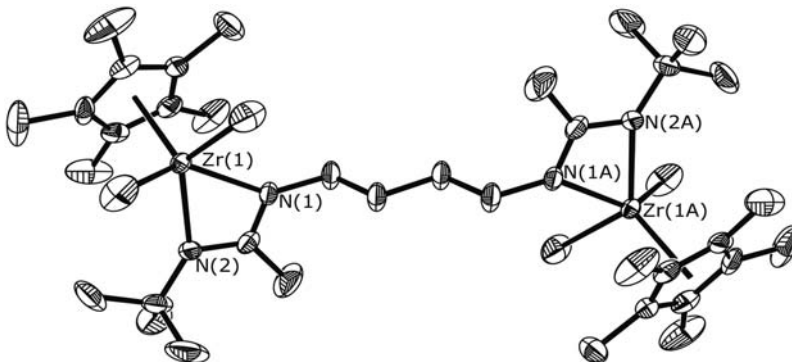


Figure 9: Molecular structures (30% thermal ellipsoids) of **28**. Hydrogen atoms have been removed for the sake of clarity.

2.2.3 TLCP and SCTL polymerization of propene *via* binuclear initiators

The following description provides a typical procedure for polymerization reactions. This procedure was performed exactly unless otherwise noted. To a solution of 12.5 μmol **26**, **27**, **28** or 25.0 μmol **04** in 0.5 mL of chlorobenzene at -10 $^{\circ}\text{C}$ was added a desired amount of cocatalyst **01** in 0.5 mL of chlorobenzene. This solution was then rapidly added to a 250 mL Schlenk flask charged with 19 mL of chlorobenzene at -10 $^{\circ}\text{C}$, which was previously pressurized to 5 psi with propene and stirred for over 10 min. The flask was then repressurized and the pressure was maintained for a certain reaction time while stirring before quenching with 0.5 mL of methanol. The volatiles were then removed *in vacuo* and the crude polymeric material was purified through precipitation of a hot toluene solution into a large volume of acidic methanol. The final pure polypropene was collected and dried overnight at 60 $^{\circ}\text{C}$ (0.01 mmHg). The detailed experimental conditions, GPC analysis and ^{13}C $\{^1\text{H}\}$ NMR spectra are provided in Table 1 and Figure 10.

Table 1: Propene polymerization conditions and GPC analysis *via* binuclear initiators

Entry	Precat	Activation percentage	Cocat 01 (mg)	t_p (h)	Yield (mg)	M_n (kDa)	M_w (kDa)	PDI
2.01	28 9.9 mg	100%	21.0	2	290	--	--	--
2.02		90%	18.0	3	370	--	--	--
2.03		70%	14.0	4	350	36.5	46.3	1.27
2.04		50%	10.0	6	350	30.5	37.5	1.23
2.05	27 10.3 mg	100%	21.0	3	280	--	--	--
2.06		90%	18.0	4	200	--	--	--
2.07		70%	14.0	5	480	42.0	52.6	1.25
2.08		50%	10.0	6	340	33.0	42.2	1.28

2.09	26 10.6 mg	100%	21.0	3	210	--	--	--
2.10		90%	18.0	3	290	--	--	--
2.11		70%	14.0	5	450	37.0	43.6	1.18
2.12		50%	10.0	7	410	36.9	44.7	1.21
2.13	04 9.9 mg	100%	21.0	3	350	--	--	--
2.14		90%	18.0	3	360	--	--	--
2.15		70%	14.0	5	560	41.2	48.7	1.19
2.16		50%	10.0	6	470	34.2	39.0	1.14

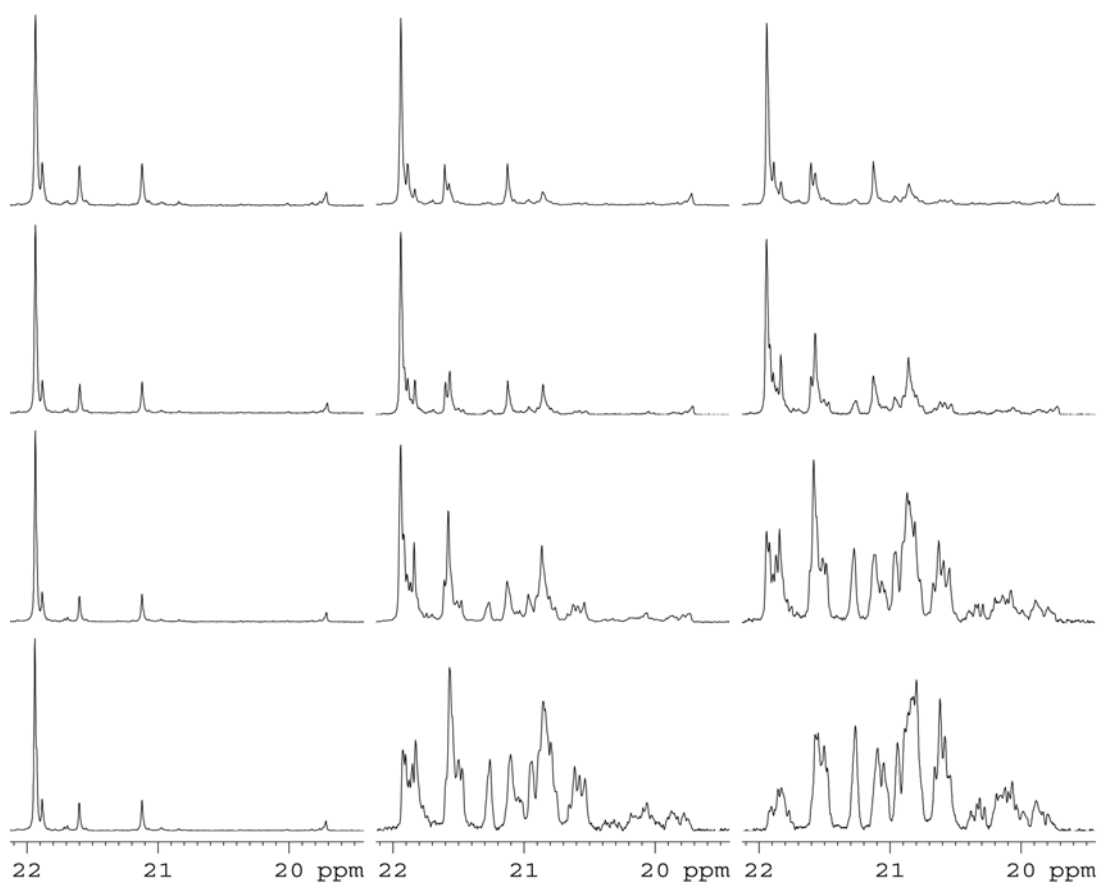


Figure 10: $^{13}\text{C} \{^1\text{H}\}$ NMR (125 MHz, 1,1,2,2- $\text{C}_2\text{D}_2\text{Cl}_4$, 70 °C) of methyl region of PP materials (top to bottom: via **28**, **27**, **26** and **04**; left to right: 100%, 70% and 50% activation)

Under TLCP conditions, the binuclear initiators were also very isoselective for the polymerization of propene and the stereoerror pattern (left column in Figure 10) followed the enantiomorphic site control mechanism ($mmmm:mmrr:mrrm = 2:2:1$). This result was not surprising when we noticed that there was no obvious geometry deviation in the solid state X-ray structures of the binuclear precatalysts from the mononuclear counterpart **04**. The small influence on the stereoselectivity indicated by the σ values (0.92 for **04**, 0.92 for **26**, 0.91 for **27** and 0.89 for **28**) due to the close tether length was reasonably attributed to the steric effect of one zirconium site to the other in one molecule.

At SDTL conditions, controllable tacticity of the resulting PP was also achieved for the binuclear precatalysts. However less change in tacticity of polypropene was observed in the case of binuclear precatalysts than that *via* the mononuclear precatalyst **04**, and the polymer tacticity was highly dependent on the length of the binuclear linkage. This trend can be seen in Figure 10 and the following pentad analysis (section 2.2.5). The PDI shown in Table 1 was as low as 1.1-1.3, which indicated the living character in the polymerization system. The living character can also be seen from the kinetic studies below.

2.2.4 Kinetic study for the SDTL polymerization of propene *via* **28**

50% activation: the polymerization was carried out in the same manner as the procedure described above (section 2.2.3), using 29.8 mg (37.5 μ mol) of **28**, 30.1 mg (37.5 μ mol) of **01** and 30 mL of chlorobenzene. The reaction was allowed to proceed for 3 h before aliquots were quenched every 45 min with methanol over 4.5 h. PP

samples were filtered through silica gel and GPC data was collected as shown in Figure 11.

75% activation: the kinetic experiment was carried out in the same manner as 50% activation, except 45.1 mg (56.3 μmol) of **01** was used and the reaction was allowed to proceed for 1.5 h before aliquots were quenched every 30 min over 3 h. GPC data were collected and shown in Figure 12.

In both cases, the number average molecular weight (M_n) of PP increased linearly with the reaction time. Together with the relative low polydispersity, this feature showed that the polymerization of propene proceeded in a living fashion with negligible termination.

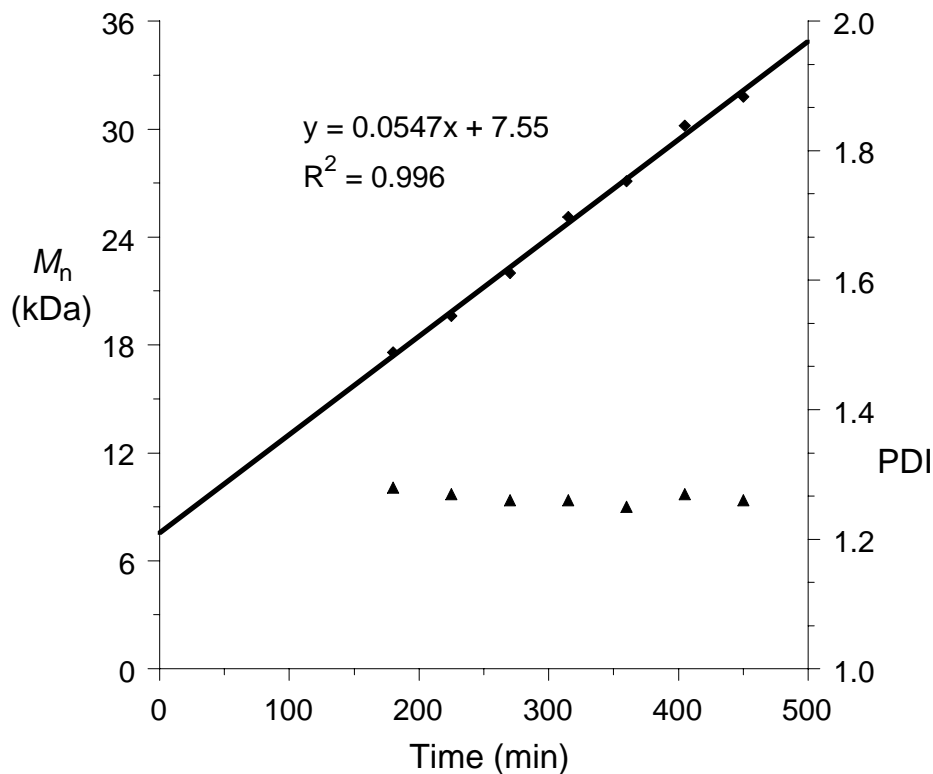


Figure 11: Kinetics of 50% activated SDTL polymerization of propene via **28**

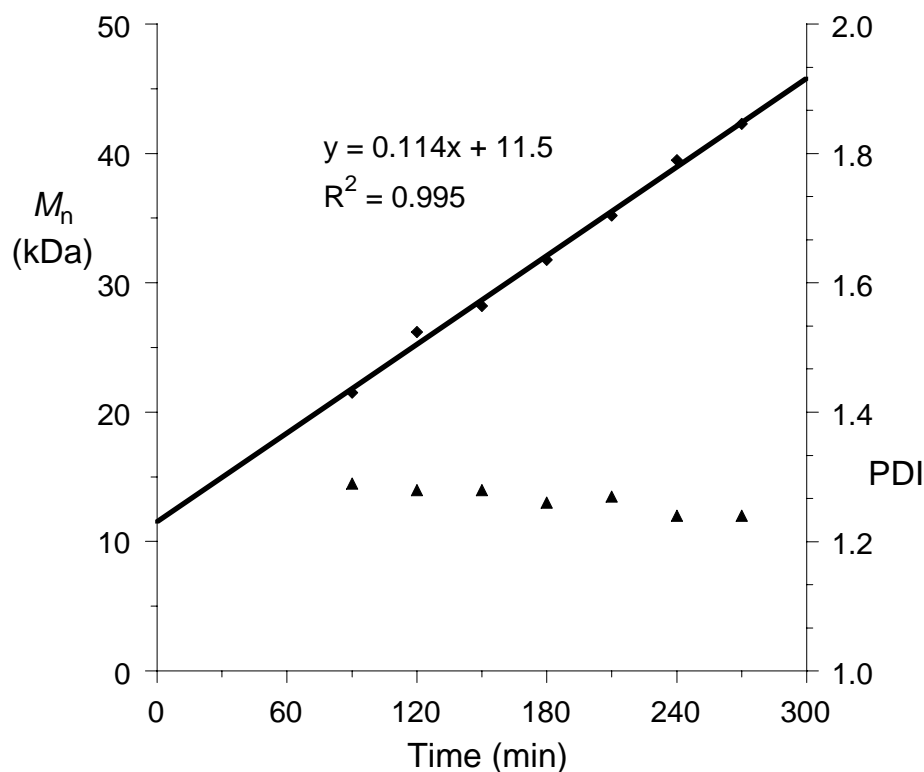


Figure 12: Kinetics of 75% activated SDTL polymerization of propene *via* **28**

2.2.5 Pentad analysis for the polymerization of propene *via* binuclear initiators

This analysis was performed based on the ^{13}C $\{^1\text{H}\}$ NMR spectra of the PP materials.⁸² The data are provided in Table 2, in which the total pentad content is 100% for each entry. Figure 13 illustrates that the tacticity of PP changes gradually with the activation percentage, a key feature of SDTL polymerization *via* CpAm zirconium initiators due to the fast methyl group exchange and facial metal-centered epimerization processes. The narrow PDI provided a direct clue for the methyl group exchange process and the latter was illustrated by the variable temperature ^1H NMR (500MHz, toluene- d_8 , 183-298 K) spectroscopy. All the neutral binuclear precatalysts showed about the same coalescence temperature tracked by the two methyl group bonded to zirconium ($T_c = 203$ K, which is much lower than the polymerization

temperature of 263 K). That is to say, the epimerization process happened frequently on the neutral zirconium centers during the polymerization.

Table 2: Pentad distribution of PP obtained via binuclear initiators

Entry	<i>mmmm</i>	<i>mmmr</i>	<i>rmmr</i>	<i>mmrr</i>	<i>mmrm</i> + <i>rmrr</i>	<i>rmmr</i>	<i>rrrr</i>	<i>rrrm</i>	<i>mrrm</i>
2.01	0.617	0.131	0.010	0.133	0.031	0.004	0.007	0.010	0.058
2.02	0.611	0.129	0.009	0.131	0.032	0.007	0.009	0.011	0.062
2.03	0.555	0.157	0.012	0.118	0.085	0.013	0.002	0.011	0.048
2.04	0.449	0.163	0.024	0.109	0.128	0.037	0.012	0.026	0.051
2.05	0.671	0.111	0.009	0.110	0.026	0.005	0.008	0.009	0.050
2.06	0.692	0.108	0.005	0.112	0.022	0.002	0.003	0.006	0.051
2.07	0.500	0.169	0.018	0.089	0.136	0.028	0.004	0.017	0.040
2.08	0.360	0.182	0.031	0.088	0.192	0.057	0.014	0.037	0.040
2.09	0.703	0.104	0.006	0.106	0.024	0.003	0.005	0.006	0.043
2.10	0.614	0.104	0.002	0.125	0.062	0.004	0.026	0.013	0.050
2.11	0.344	0.199	0.031	0.081	0.215	0.062	0.007	0.027	0.034
2.12	0.159	0.181	0.054	0.091	0.266	0.116	0.027	0.063	0.043
2.13	0.713	0.101	0.009	0.103	0.021	0.003	0.005	0.003	0.044
2.14	0.647	0.135	0.006	0.101	0.064	0.005	0.000	0.005	0.038
2.15	0.164	0.205	0.053	0.095	0.279	0.105	0.012	0.047	0.039
2.16	0.052	0.126	0.070	0.103	0.274	0.159	0.052	0.103	0.061

Figure 14 shows that the tacticity change is highly dependent on the linkage length in the binuclear precatalysts. At 70% activation, mononuclear initiator **04** provides quite atactic polypropene, however PP *via* binuclear initiator **28** is much more isotactic. The tacticities of PP materials from **27** and **26** are right between those from **28** and **04**. That is to say, from full activation to partial activation, tacticity

change is very dramatic *via* **04** and quite smooth by **28**. Complexes **27** and **26** provide medium influence on polymer microstructure by activation percentage.

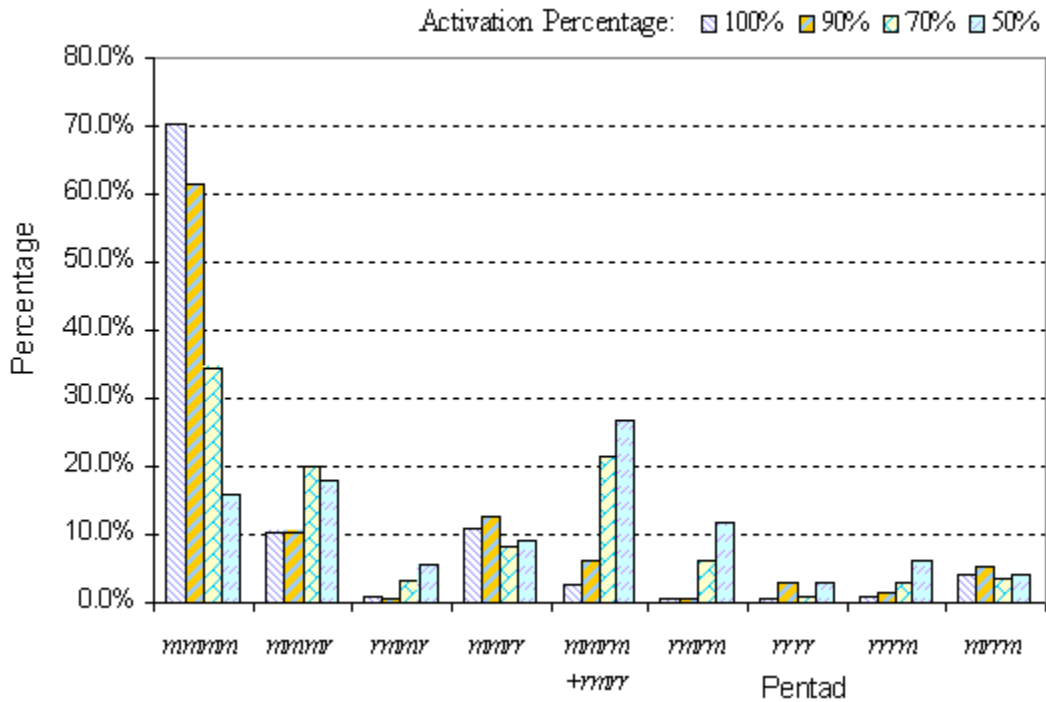


Figure 13: Pentad analysis of PP obtained *via* **26**

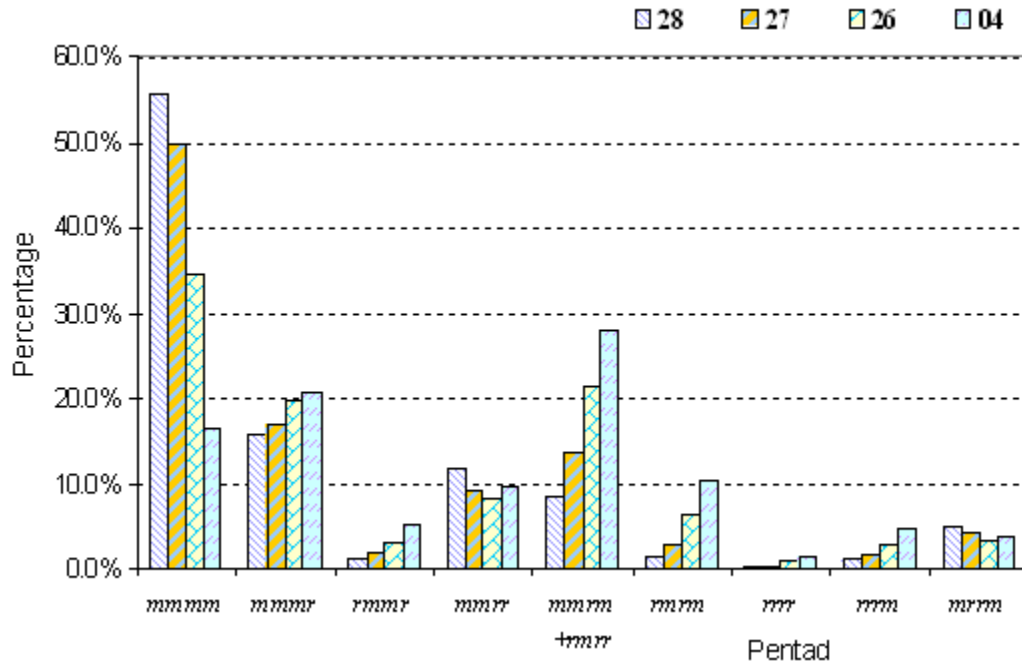


Figure 14: Pentad analysis of PP *via* binuclear initiators at 70% activation

These two trends can be seen clearly in Figure 15. For selected pentads, the tacticity varies not only with the activation percentage, but also with the identity of the binuclear initiators possessing different tether lengths between two zirconium centers. It is noticeable that under SDTL conditions, even **28** with a linkage of $-(\text{CH}_2)_8-$ does not behave like the mononuclear initiator **04** which has an infinite tether length.

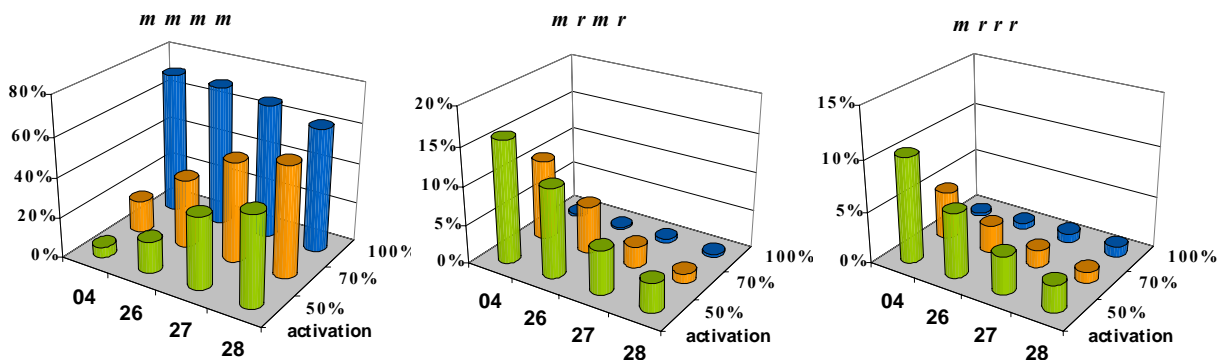


Figure 15: Dependence of pentad content on the level of activation and tether length in the binuclear initiators for PP obtained via **04**, **26**, **27** and **28**

For the less sensitivity to stereoerror occurrence of binuclear catalysts under SDTL conditions, which was indicated by the decrease in the frequency of *mr* triad incorporation with the decreased tether length (*mrmr* and *mrrr* in Figure 15), we attributed to the proximity effect largely steric in nature that governs the rate of metal-centered epimerization. This is much more likely when we are considering additional steric effects from the long propagating polymer chains and the bulky counterion $[\text{B}(\text{C}_6\text{F}_5)_4]^-$ close to the active centers. More experimental phenomena and models are needed in order to elucidate the real factors that dominate the stereoselectivity.

2.3 Development of CpAm Group 4 Metal Initiators with High Activity for Propene

Polymerization

2.3.1 Introduction

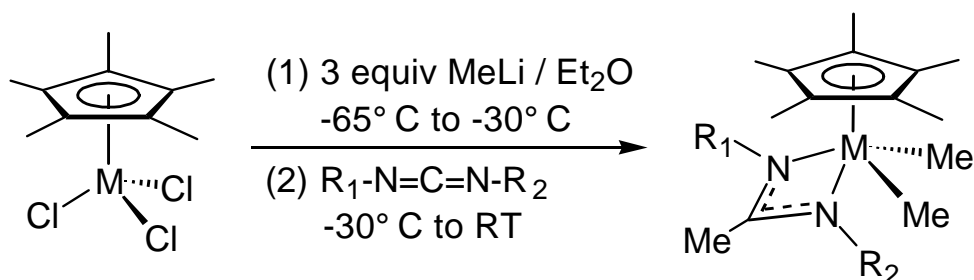
Ligand manipulation provides an effective way to make a large family of complexes. As shown in Scheme 8, we can modify R on the cyclopentadienyl ring, R₁ and R₂ originally from the carbodiimide employed, R₃ on the distal position, R₄ and R₅ attached to the metal center, and the transition metal. With different ligand sets, the CpAm complexes will display different polymerization behaviors, such as activity, stereospecificity, regioselectivity, living characters, monomer selection, stability and impurity tolerance. Some CpAm complexes were already summarized in section 2.1. This thesis continued to add more new CpAm group 4 complexes to the area of post-metallocene catalysis, including the binuclear initiators studied in section 2.2.

The TLCP polymerization of propene was delivered with these new precatalysts recently developed, and several precatalysts reported previously. Complexes **35** and **36** (in Scheme 12) showed much higher activity compared with **04** towards propene polymerization attributed to the small size of the ligand set. The catalytic behavior of these two complexes under TLCP conditions will be discussed thoroughly in this chapter, considering that polymerization activity is always an important issue with obvious reasons such as time, energy, apparatus efficiency, catalyst stability, labor and safety. The formamidinate precatalyst **12** is another important example due to the unique microstructure of PP obtained with it.

2.3.2 Synthesis of new CpAm complexes

The synthesis strategy shown in Scheme 11 was also very efficient to make the structures described in Scheme 12. The detailed procedures to make these new precatalysts are summarized in Appendix I. The solid state single crystal X-ray structures of **35** and **36** are shown in Figure 16. The carbodiimide ligands and their corresponding ureas were prepared according to similar processes shown in Schemes 9 and 10. These ureas and carbodiimides are Et-NH-CO-NH-Et (**40**), Et-N=C=N-Et (**41**), ⁱPr-NH-CO-NH-Et (**42**), ⁱPr-N=C=N-Et (**43**), ^tBu-CH₂-NH-CO-NH-Et (**44**), ^tBu-CH₂-N=C=N-Et (**45**), CH₃CH₂C(CH₃)₂-NH-CO-NH-Et (**46**) and CH₃CH₂C(CH₃)₂-N=C=N-Et (**47**). Details for synthesis are also provided in Appendix I.

Scheme 12: Synthesis of new CpAm complexes



35 M = Hf, R₁ = Et, R₂ = Et

36 M = Zr, R₁ = Et, R₂ = Et

37 M = Zr, R₁ = Et, R₂ = ⁱPr

38 M = Zr, R₁ = Et, R₂ = CH₂^tBu

39 M = Zr, R₁ = Et, R₂ = C(CH₃)₂CH₂CH₃

In addition to the above five new complexes, three more CpAm precatalysts were also prepared and studied for the polymerization of propene. They are (1,3-^tBu₂-η⁵-C₅H₃)ZrMe₂[N(Et)C(Me)N(^tBu)] (**48**), (η⁵-C₅Me₅)ZrMe₂[N(ⁱPr)C(NMe₂)N(ⁱPr)] (**49**)

and $(\eta^5\text{-C}_5\text{Me}_5)\text{ZrMe}_2[\text{N}(\text{Et})\text{C}(\text{H})\text{N}(\text{Et})]$ (**50**). Their single crystal X-ray structures are shown in Figure 17.

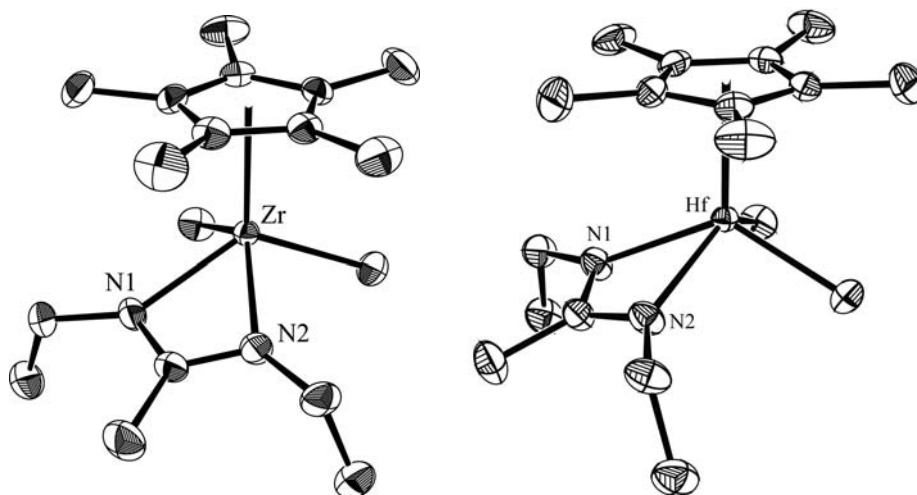


Figure 16: Molecular structures (30% thermal ellipsoids) of **35** (right) and **36** (left). Hydrogen atoms have been removed for the sake of clarity.

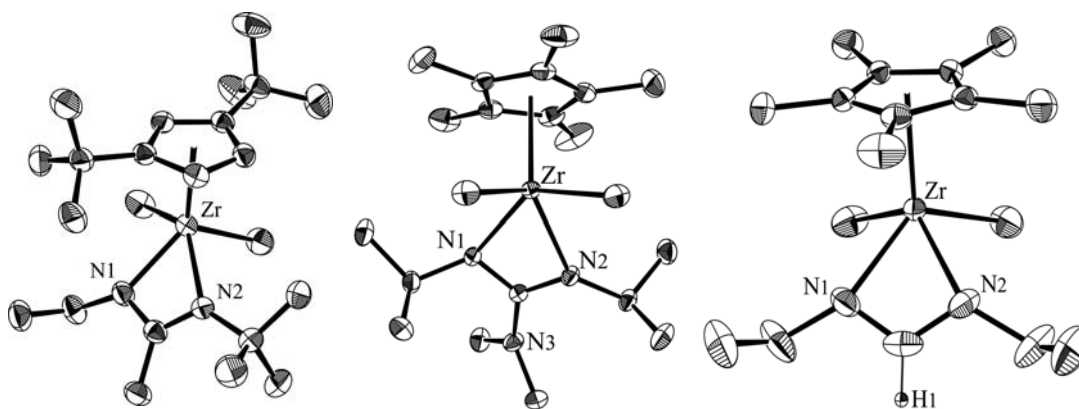


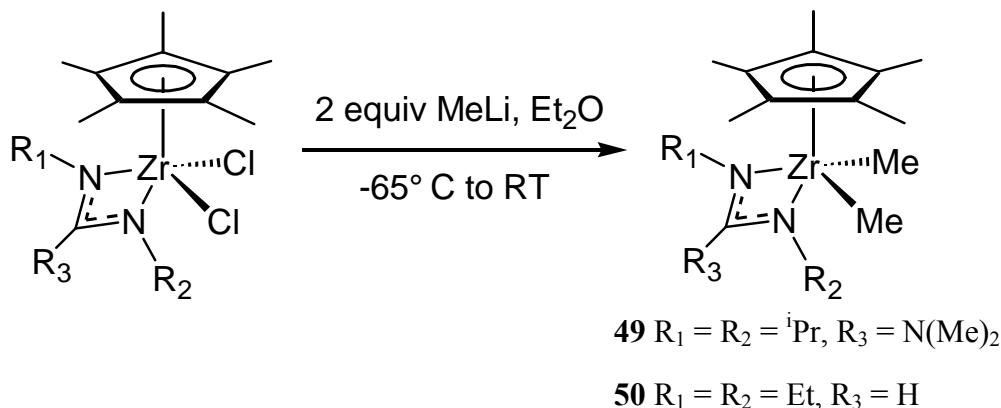
Figure 17: Molecular structure (30% thermal ellipsoids) of **48** (left), **49** (middle) and **50** (right). Hydrogen atoms have been removed for the sake of clarity, except the distal H in **50**.

Complex **48** was synthesized using the one-pot process as described in Scheme 12 from $(1,3\text{-}^t\text{Bu}_2\text{-}\eta^5\text{-C}_5\text{H}_3)\text{ZrCl}_3$, which was prepared according to the literature.^{101,}

¹⁰² **49** was made through a methylation reaction (see Scheme 13) from $(\eta^5\text{-}$

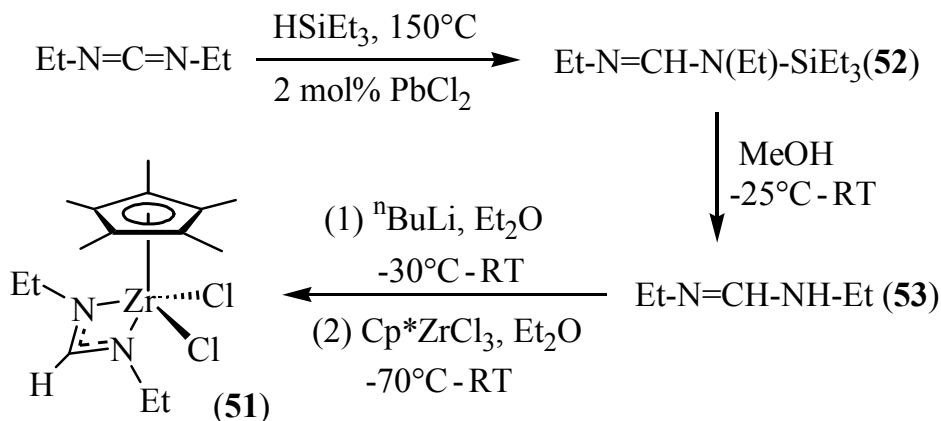
$C_5Me_5ZrCl_2[N(iPr)C(NMe_2)N(iPr)]$, which was also prepared by reported procedures.¹⁰³ The experimental details are summarized in Appendix I.

Scheme 13: Synthesis of **49** and **50** from CpAm zirconium dichloride



The formamidinate complex **50** was also prepared from the corresponding dichloride, $(\eta^5-C_5Me_5)ZrCl_2[N(Et)C(H)N(Et)]$ (**51**), which was synthesized using the following reactions illustrated in Scheme 14.⁷⁸ The purity of **51** was not ideal and the yield of **50** was quite low (16%), mainly due to the low stability and high sensitivity caused by the small ligand set. To get a higher yield, the experimental conditions need to be optimized. Detailed procedures to make **50**, **51** and the involved ligand compounds **52** and **53** are also described in Appendix I.

Scheme 14: Synthesis routes for compounds **52**, **53** and **51**



2.3.3 TLCP polymerization of propene by diethyl amidinate catalysts

Among the CpAm complexes described above, **38** and **39** were designed to obtain higher stereoselectivity for the polymerization of propene than **04**. However the precatalyst **38** showed the reverse of this goal and provided atactic polypropene. The PP by **39** had the same isotacticity as that by **04**, and the activity of **39** was much lower. **48** and **49** showed almost no activity towards the polymerization of propene. None of these four complexes has an advantage over **04** and deserves more effort for the polymerization of propene, at least under current experimental conditions. **48** was used for the copolymerization of ethene and 1-octene under CCTP conditions, that will be discussed in Chapter 5.

Polymerization of propene *via* **37** showed a higher rate than that *via* **04** (Entries 2.17 and 2.18 in Table 3). This showed **37** had the advantage over **04** according to activity though the PP produced was atactic. But later on, two more active catalysts, **35** and **36**, were developed and took the place of **37**. This section is going to focus on the propene polymerization results using **35** and **36**. It is kind of surprising that **35** has similar activity as **36** (Entries 2.20 and 2.21) when you notice that polymerization of propene *via* **54** (Entry 2.19) is much slower than that *via* **04**. **54** is the hafnium complex, $(\eta^5\text{-C}_5\text{Me}_5)\text{HfMe}_2[\text{N}(\text{tBu})\text{C}(\text{Me})\text{N}(\text{Et})]$,¹⁰⁴ which has the same ligand set as **04**.

Ultrahigh molecular weight (UHMW) PP materials were obtained using **36** and **35** (Entries 2.22 and 2.23) by the virtue of their high activity. The weight average molecular weight (M_w) was 1.17 and 2.02 million Da respectively. Another

experiment to show the high activity of **36** was done for the polymerization of vinylcyclohexane (VCH). In 10mL PhCl at -10°C, using 25 μmol of **36** activated by **01**, 0.24 g PVCH was obtained in 2 h (200eq of VCH was added). ¹³C NMR shows the product is isotactic, which is presumably attributed to a chain end control mechanism.⁷⁹

Table 3: TLCP polymerization of propene *via* CpAm catalysts

Entry	pre-cat		PhCl (mL)	t _p (h)	Yield (g)	M _n (kDa)	PDI
	identity	(μmol)					
2.17	37	20	25	2	2.36	154	1.50
2.18 ⁸³	04	25	10	2	0.50	--	--
2.19	54	25	10	16	0.15	--	--
2.20	36	10	10	0.5	1.55	156	1.36
2.21	35	10	10	0.5	1.04	137	1.12
2.22	36	10	100	2.5	3.58	618	1.90
2.23	35	10	100	15	8.22	830	2.43

Conditions: fully activated by the cocatalyst **01**, T_p: -10 °C

To study the solvent effect on the polymerization of propene *via* **35** and **36**, methylene chloride (CH₂Cl₂) and toluene (Tol) were also used as the polymerization media in addition to chlorobenzene (PhCl). CH₂Cl₂ led to a lower activity for **36** (Entry 2.24) compared to PhCl and no activity when using **35** under the same experimental conditions. Toluene is also an effective medium for the polymerization reactions. It gave a slightly lower activity for catalyst **35** (Entry 2.25) compared to PhCl, but no influence on the result when using **36** (Entry 2.26). The non-polar

solvent heptane was also tried and no polymer was produced in it due to its poor solubility for the catalytic species.

Table 4: TLCP of propene *via* diethyl amidinate catalysts

Entry	pre-cat	co-cat	solvent	Yield (g)	M_n (kDa)	PDI
2.24	36	01	CH ₂ Cl ₂	0.32	63.6	1.09
2.25	35	01	Tol	0.59	122	1.16
2.26	36	01	Tol	1.65	169	1.59
2.21	35	01	PhCl	1.04	137	1.12
2.20	36	01	PhCl	1.55	156	1.36
2.27	35	02	PhCl	0.87	147	1.11
2.28	36	02	PhCl	1.45	179	1.34
2.29	35	03	PhCl	0.30	53.9	1.05
2.30	36	03	PhCl	1.53	181	1.30

Conditions: 10 μ mol of precat, 10 μ mol of cocat, 10 mL of solvent, Tp: -10 °C, tp: 30min

The cocatalyst effect was also investigated by using two more activators, [Ph₃C][B(C₆F₅)₄] (**02**) and B(C₆F₅)₃ (**03**), for the polymerization of propene *via* **35** and **36**. The results were compared with those by [PhNMe₂H][B(C₆F₅)₄] (**01**) as shown in Table 4. These three cocatalysts gave almost the same results when using catalyst **36** (Entries 2.28 and 2.30). But for catalyst **35**, **03** showed a lower activity than **01** and **02** (Entries 2.27 and 2.29). Another compound, Ga(C₆F₅)₃, was also tried as a cocatalyst under the same conditions and had no activity for the polymerization of propene.

The polydispersity indexes in Table 4 are quite low in most cases, which indicate the living character of the polymerization system *via* **35** and **36**. However the PDI was not always very low especially when using **36**. To describe such a system accurately, the kinetic study was performed for both catalysts. The experiments were delivered following the procedures described in Section 2.2.3. For **36**, the conditions were the same as Entry 2.22 in Table 3, and aliquots were taken out and quenched with methanol every 10 min over a period of 1 h. PP samples were purified by precipitation into acidic methanol and dried *in vacuo*. The GPC analysis was performed and the results are shown below.

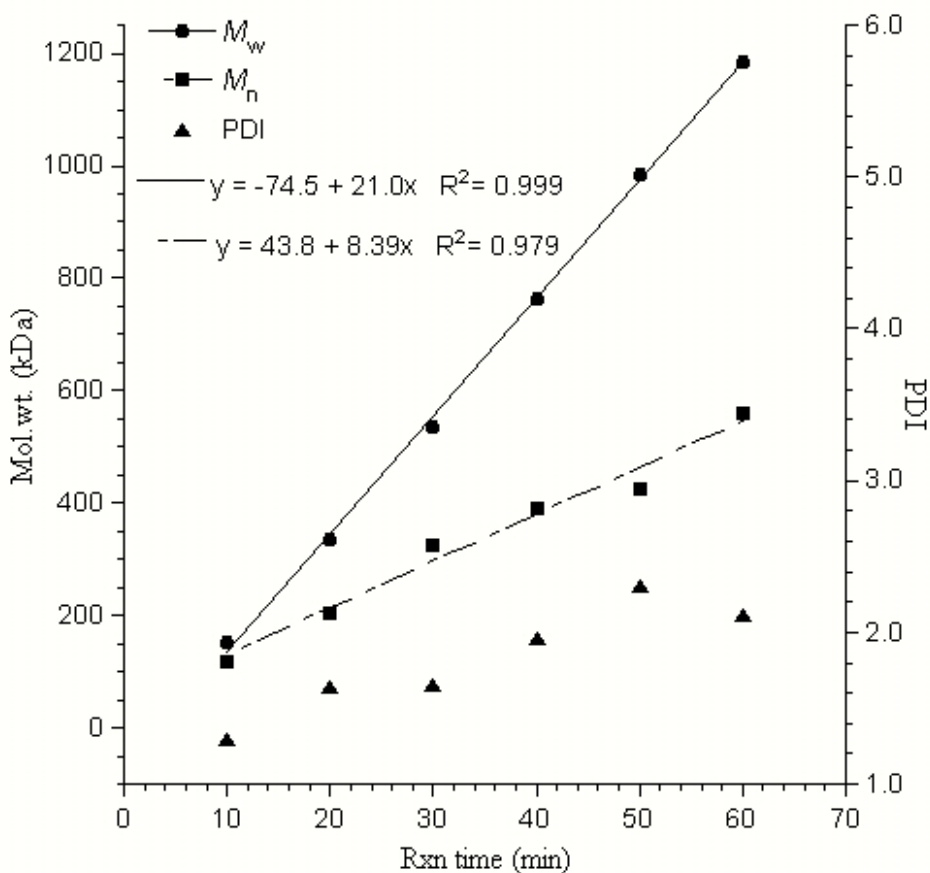


Figure 18: Kinetics of propene polymerization *via* **36**

For **35**, the experimental conditions were the same as Entry 2.23 in Table 3, and aliquots were taken out and quenched with methanol every 30 min over a period of 3 h. PP samples were purified by precipitation into acidic methanol and dried *in vacuo* before GPC analysis. The results are shown in Figure 19.

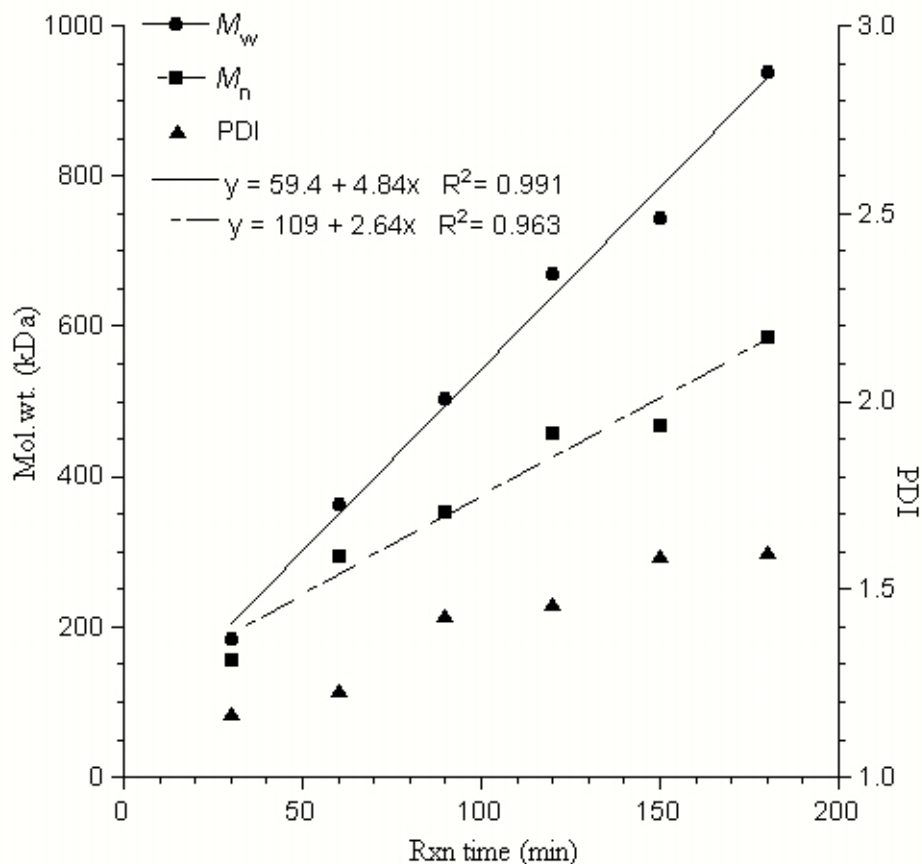


Figure 19: Kinetics of propene polymerization via **35**

The kinetic data showed that the weight average molecular weight (M_w) of PP increased linearly with the polymerization time for both **36** and **35**, at least during the experimental period. The relationship between the number average molecular weight (M_n) and reaction time was not linear associated with the somewhat high values of PDI. So even though the polymerization process was not a strictly living system, it still proceeded in a highly controllable fashion.

2.3.4 TLCP polymerization of propene by formamidinate catalysts

The formamidinate complex $(\eta^5\text{-C}_5\text{Me}_5)\text{ZrMe}_2[\text{N}(\text{tBu})\text{C}(\text{H})\text{N}(\text{Et})]$ (**12**) was synthesized and used to initiate 1-hexene's polymerization under full activation conditions.⁷⁸ The PH produced was not as isotactic as that *via* **04**. This was explained by the fact that the cation $(\eta^5\text{-C}_5\text{Me}_5)\text{ZrMe}[\text{N}(\text{tBu})\text{C}(\text{H})\text{N}(\text{Et})]^+$ (**12**⁺) undergoes metal-centered epimerization through the amidinate ring-flipping process which is absent in the structurally stable cation $(\eta^5\text{-C}_5\text{Me}_5)\text{ZrMe}[\text{N}(\text{tBu})\text{C}(\text{Me})\text{N}(\text{Et})]^+$ (**04**⁺). Another formamidinate $(\eta^5\text{-C}_5\text{Me}_5)\text{ZrMe}_2[\text{N}(\text{iPr})\text{C}(\text{H})\text{N}(\text{iPr})]$ (**55**) was also reported and atactic PH was obtained with it.

Propene was successfully polymerized with precatalyst **12** under both TLCP and SDTL conditions. Experiments were performed in the same way as those with binuclear initiators (section 2.2.3), and details were summarized in Table 4. The similar loss of stereoregularity was observed with PP under TLCP conditions (Entry 2.31 in Table 4). The value of *mmmm* pentad decreased to 30.8% from 71.3% as observed when using precatalyst **04**. The PP obtained with 50% activation of **12** (SDTL conditions) is slightly syndio-rich (Entry 2.32 in Table 4). Its *rr* triad content is 37.2%. PP *via* **55** under full activation condition is also syndio-rich with an *rr* content of 41.4% (Entry 2.33 in Table 4). The higher yield showed that **55** is more active than **12** for the polymerization of propene. To get even higher activity, one more formamidinate precatalyst $(\eta^5\text{-C}_5\text{Me}_5)\text{ZrMe}_2[\text{N}(\text{Et})\text{C}(\text{H})\text{N}(\text{Et})]$ (**50**) was also prepared and used to initiate the propene polymerization. However the yield was not high and the polymerization didn't proceed in a controllable fashion, most likely due

to the low stability and decomposition of this zirconium catalyst with such a small ligand set. The ^{13}C $\{^1\text{H}\}$ NMR spectra of PP from Entries 2.31 and 2.32 *via* **12** are shown in Figure 20.

Table 4: Experimental conditions, GPC analysis and triad contents for propene polymerization *via* formamidinate initiators

Entry	12 (μmol)	01 (μmol)	PhCl (mL)	T_p ($^{\circ}\text{C}$)	t_p (min)	Yield	M_n (kDa)	PDI	mm%	mr%	rr%
2.31	50	50	20	-10	130	3.00	113	1.17	47.3	34.1	18.6
2.32	52	26	50	-10	120	1.14	35.1	1.07	15.1	47.7	37.2
2.33	25 ^b	25	20	-10	75	3.12	142	1.43	8.5	50.1	41.4
2.34	50	50	20	-20	120	2.91	88.0	1.16	51.8	29.2	19.0
2.35	50	50	20	0	110	2.88	93.9	1.17	51.8	32.7	15.5
2.36 ^a	50	50	20	0	110	2.35	90.1	1.16	49.4	31.5	19.1
2.37	25	25 ^c	20	-10	120	0.80	92.1	1.24	51.7	30.1	17.3
2.38	25	25 ^c	20	-10	120	0.82	102	1.15	50.3	31.5	18.2

Notes: a, conditions: under a constant propene pressure of 5psi, except Entry 2.36 which was under 10psi; b, **55** was used instead of **12**; c, **02** (Entry 2.37) and **03** (Entry 2.38) were used instead of **01**.

It was already mentioned that the cation **12**⁺ was configurationally unstable as studied by variable temperature NMR.⁷⁸ An attempt to influence the ring-flipping process and thus get different polymerization results, specifically different microstructures of PP, was carried out by changing temperature (Entries 2.34 and 2.35 in Table 4), pressure (Entry 2.36) and cocatalyst (Entries 2.37 and 2.38) during the polymerization reaction. However, the data obtained didn't show any significant difference in the tacticity of PP. A possible reason might be that the epimerization

rate didn't change appreciably with temperature or pressure, or it was dwarfed by the concomitant polymerization rate change and the relative rate ratio was stable.

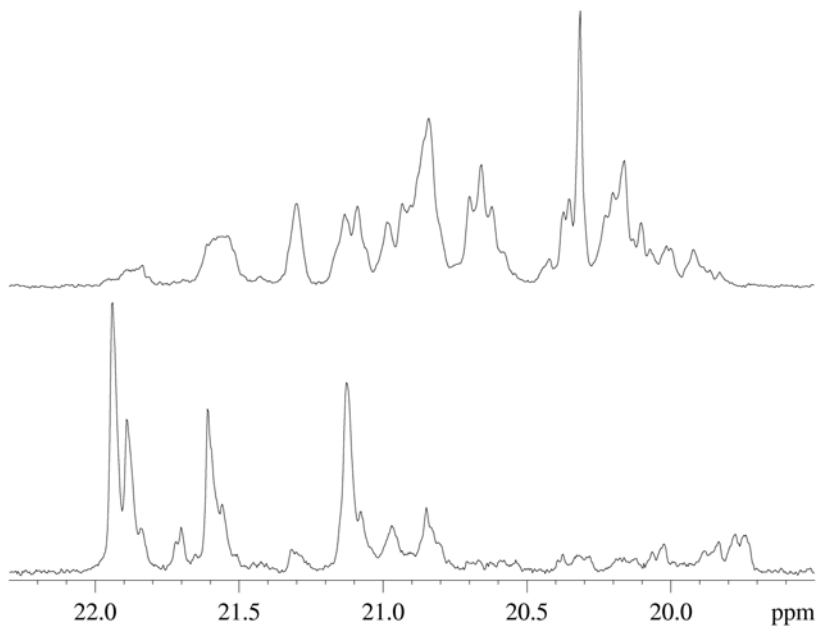


Figure 20: ^{13}C $\{^1\text{H}\}$ NMR (125 MHz, 1,1,2,2- $\text{C}_2\text{D}_2\text{Cl}_4$, 70 °C) of the methyl region of PP via **12**, 50% (top) and 100% (bottom) activation

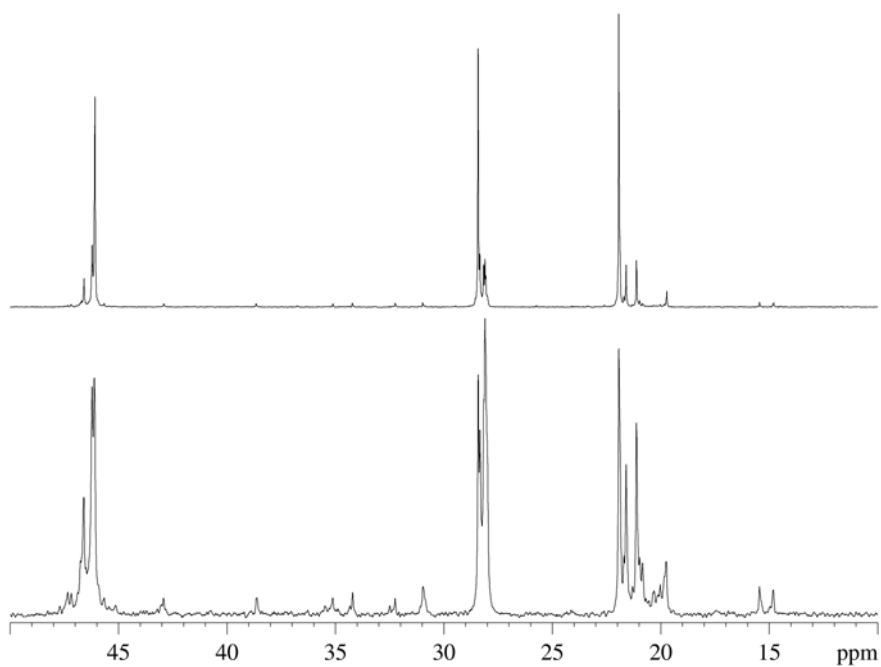


Figure 21: Full ^{13}C $\{^1\text{H}\}$ NMR spectra (125 MHz, 1,1,2,2- $\text{C}_2\text{D}_2\text{Cl}_4$, 70 °C) of PP via **04** (top, Entry 2.13) and **12** (bottom, Entry 2.37)

The more interesting aspect about the propene polymerization *via* **12** was the unique microstructure of PP obtained and its potential applications. In Figure 21, both stereoerrors and regioerrors were observed by $^{13}\text{C} \{^1\text{H}\}$ NMR spectroscopy for the bottom spectrum *via* **12**. The regioerrors were mainly shown in the range of 30-45 ppm and negligible in the top spectrum from **04**. This is an additional factor for PP microstructure and might give rise of some useful physical properties for the PP materials such as elasticity.^{105, 106}

2.4 Conclusions

A series of bimetallic CpAm zirconium complexes were prepared and fully characterized with ^1H NMR, elemental analysis and single crystal X-ray diffraction. These complexes turned out to be active for the polymerization of propene under both TLCP and SDTL conditions, with comparable activities to the structurally related mononuclear complex **04**. Upon being fully activated, isotactic polypropene was obtained from **26-28**. The stereoerror increased slightly as the tether length between the two zirconium centers decreased. Under partial activation conditions, atactic PP was prepared as expected from the SDTL mechanism, and the tacticity was found to be dependent not only on the activation percentage, but also on the linkage length within a binuclear molecule due to the proximity effect which was presumably steric in nature.

Among the new CpAm group 4 metal complexes recently prepared, the diethyl amidinate precatalysts **35** and **36** were found to be very active towards the polymerization of propene attributed to their small ligand set. They were activated with different cocatalysts and the propene polymerization by them was performed in

different solvents. High molecular weight PP was easily made from these two catalysts. Other less active or inactive complexes have potential to initiate the polymerization of ethene in a controllable fashion. The polypropene obtained from the formamidinate **12** showed both stereoerrors and regioerrors, which are important microstructure factors in determining the physical properties of a PP material.

Chapter 3: Truly Living CCTP of Propene with ZnEt_2 Catalyzed by Highly Active CpAm Complexes — Production of Amorphous Polypropene with Extremely Narrow PDI

3.1 Background

3.1.1 Chain transfer process in coordination polymerization, general view

Chain transfer is one of the most common concepts in polymer chemistry as chain initiation, propagation and termination. During the development of any type of polymerization process, chemists always tried to find whether there was any chain transfer reactions, how to control or avoid it, and how to make use of it. In the area of coordination polymerization, back to fifty years ago, Ziegler and co-workers documented polymer chain growing on an aluminum compound.¹⁰⁷ Polypropene chain transfer to aluminum was observed frequently, especially when methylaluminoxane (MAO) was used as the activator.¹⁰⁸⁻¹¹⁴ More often than not, the chain transfer process was irreversible and resulted in relatively low molecular weight polymer and broader polydispersity.

Chain transfer could happen not only to the cocatalyst, but also to any chemical species in the reaction container, including monomers, solvents, byproducts, intermediates, other polymer chains, and the added chain transfer agents (CTA). When the chain transfer process is not reversible, it functions as a termination event. For metallocene or post-metallocene systems, another important process which will also result in termination of a chain growth is β -hydride elimination. This happens

quite often because most transition metal complexes are not stable when carrying beta hydrogen(s). We benefit a lot from the CpAm group 4 metal complexes because this structure is not sensitive to such a process.⁸⁰

These chain transfer or termination processes mentioned above are very common and that's why a living coordination polymerization system is hard to develop and deserves more attention. Some systems have been claimed as living when these processes only happen to a very small extent.⁴⁴ In the CpAm group 4 metal system studied in this thesis, these irreversible processes are absent and will not be discussed further.

3.1.2 Examples of reversible polypropene chain transfer to aluminum

To realize the catalyzed chain growth of propene on inexpensive metals and also make novel PP structures, researchers explored the area of CCTP quite a lot even though the results were not so encouraging. Reversible chain transfer processes were observed and new PP materials were even isolated from the polymer products. The latter will be discussed further in Chapter 6.

In 2002, Rieger and coworkers investigated the reversible chain transfer to aluminum during propene polymerization by three novel oxygen-substituted asymmetric zirconocene complexes.¹¹⁵ The transfer process was proposed as the origin of stereoerror in the resulting polypropene. In a later report, the stereoerror derived from chain transfer showed influences on crystallizing behavior and mechanical properties of the PP materials obtained *via* dual site zirconocenes activated by MAO.¹¹⁶

In 2006, Shiono reported that monomodal polypropene was obtained with the titanium catalyst [^tBuNSiMe₂(3,6-^tBu₂Flu)]TiMe₂ activated by MMAO (modified MAO), and chain transfer was observed in the presence of specific amount of triisobutylaluminum.¹¹⁷ In 2007, Busico and Stevens reported a polypropene chain shuttling process between enantiomorphous species of a (pyridyl-amide)HfMe₂ complex with AlMe₃. Conjunctions in the stereoblock isotactic PP were detected by ¹³C NMR.¹¹⁸ At the same time, the authors pointed out that CCTP had a wide scope, but only a fairly narrow operation window currently, and most time the combination of precatalyst/cocatalyst/CSA displayed monomer dependence.

In this thesis, some CpAm group 4 metal complexes, in fact a big family, were added to expand the operation window of CCTP. These catalysts showed highly efficient reversible chain transfer with ZnEt₂, and polymers of very narrow polydispersity were produced using ethene, propene, higher α-olefins and other type of alkenes.

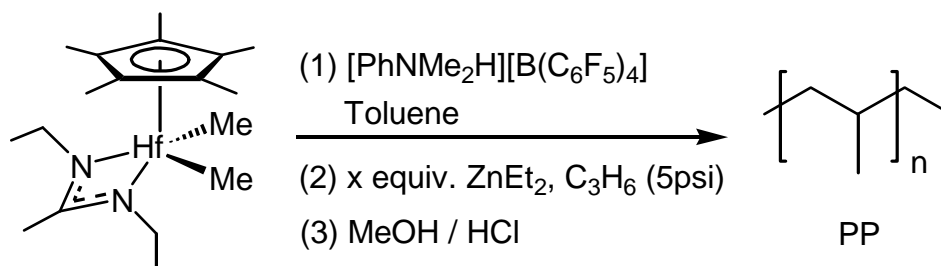
3.2 Living CCTP of Propene with ZnEt₂ by 35

3.2.1 Description and general procedures

(η⁵-C₅Me₅)HfMe₂[N(Et)C(Me)N(Et)] (**35**) was selected as the precatalyst to deliver the CCTP polymerization because of its high activity and relative thermostability. ZnEt₂ was chosen in light of that it worked very well as chain transfer agent during catalyzed chain growth of ethene,⁶⁸⁻⁷⁰ and chain transfer to zinc was also observed during the coordination polymerization of propene.¹¹⁹⁻¹²¹ This

chapter will focus on the CCTP homopolymerization of propene. The process is depicted below.

Scheme 15: CCTP of propene with ZnEt₂ via 35



The following description for Entry 3.07 of Table 5 represents a typical procedure for coordinative chain transfer polymerization reactions. This procedure was performed exactly unless otherwise noted. In a 250-mL Schlenk flask, to a solution of the cocatalyst **01** (16.0 mg, 20 μ mol) in 20 mL toluene at 0 °C were added **35** (9.1 mg, 20 μ mol) and ZnEt₂ solution (1.1 M in toluene, 329 mg, 20eq). The flask was then pressurized to 5 psi with propene and the pressure was maintained for 2 h with stirring before quenching with 1.0 mL of methanol. The toluene solution was precipitated into 600 mL of acidic methanol to isolate the polypropene. The final product was collected and dried overnight *in vacuo*. Yield: 4.18g. GPC: M_w = 9.06 kDa; M_n = 8.75 kDa; PDI = 1.04.

3.2.2 A series of propene polymerization under CCTP conditions

To start, we delivered the CCTP of propene *via 35* in toluene at -10 °C with 20 eq of ZnEt₂ (Entry 3.01 in Table 5). From the amount of catalyst added, the yield and the molecular weight of PP obtained, we know that chain transfer took place. For the polydispersity, it was surprising that the value was only 1.03. This indicated, together

with the monodisperse GPC curve, the chain transfer process between Zr and Zn was very efficient and reversible. The GPC curve for Entry 3.01 is shown in Figure 22 and compared with two commercial polystyrene (PS) standards which were obtained from living ionic polymerization.

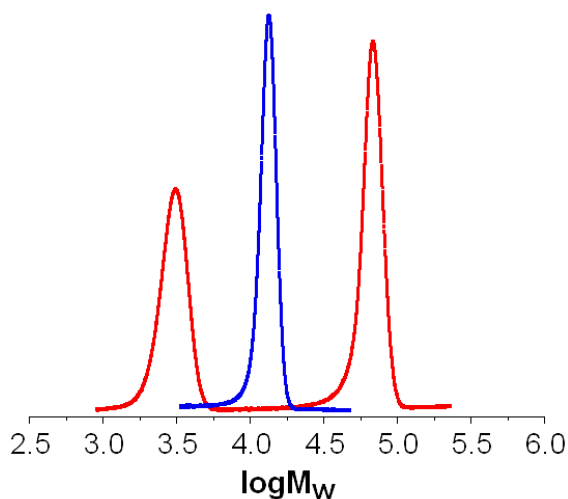


Figure 22: GPC curves of PP from Entry 3.01 (middle) and two PS standards with PDI of 1.05 (left and right)

Then the CCTP polymerization was accomplished at different temperatures, -20 °C, 0 °C and 20 °C, as listed in Table 5. Satisfactorily, even at room temperature (Entry 3.03), a PDI of 1.05 was obtained indicating the living character of the polymerization process. The relative lower yield at higher temperature was reasonably explained by the fact that propene had a lower solubility in toluene under the same pressure at higher temperature, which resulted in a slower reaction rate.

Another series of CCTP polymerizations was performed by varying the amount of added chain transfer agent (CTA) ZnEt₂, from 5eq to 200eq. It was noticeable that for such a broad range of ZnEt₂, the CCTP reactions worked just as what was expected. The molecular weight distribution kept narrow and the yield was fairly

stable. The GPC curves of these PP samples are shown in Figure 23. Other features of this system will be discussed further in the following sections.

*Table 5: Living CCTP of propene with ZnEt₂ via **35** according to Scheme 15*

Entry	35, 01 (μmol)	ZnEt ₂ (equiv.)	T _p ($^{\circ}\text{C}$)	Yield (g)	M _n (kDa)	PDI
3.01	20	20	-10	6.02	12.6	1.03
3.02	20	20	-20	7.92	15.9	1.03
3.03	20	20	20	1.63	3.63	1.05
3.04	20	200	0	4.99	1.45	1.08
3.05	20	100	0	4.93	2.28	1.06
3.06	20	50	0	4.94	4.18	1.04
3.07	20	20	0	4.18	8.75	1.04
3.08	20	10	0	4.78	18.7	1.04
3.09	20	5	0	4.85	33.3	1.09
3.10	10	10	0	10.1	71.9	1.09
3.11	10	5	0	9.64	111	1.15

Conditions: ZnEt₂ added as 1.1 M solution in Tol, total volume of Tol = 20 mL and t_p = 2 h, except Entries 3.10 and 3.11 (50 mL, 14h), at a constant propene pressure (5 psi).

From the polymerizations mentioned above, we got a molecular weight range of 1 to 33 kDa for the PP obtained. It was curious whether we could make the molecular weight higher. Indeed Entries 3.10 and 3.11 showed that this was achieved successfully. Thus a CCTP reaction was able to provide a polymer with a M_n over 100kDa and very narrow PDI (GPC curves also shown in Figure 23). In fact, this number could go higher and the polydispersity might be narrower if the viscosity had not been a problem. Of course there is no limitation for PP of low molecular weight. The polymerization can be quenched at any stage as needed.

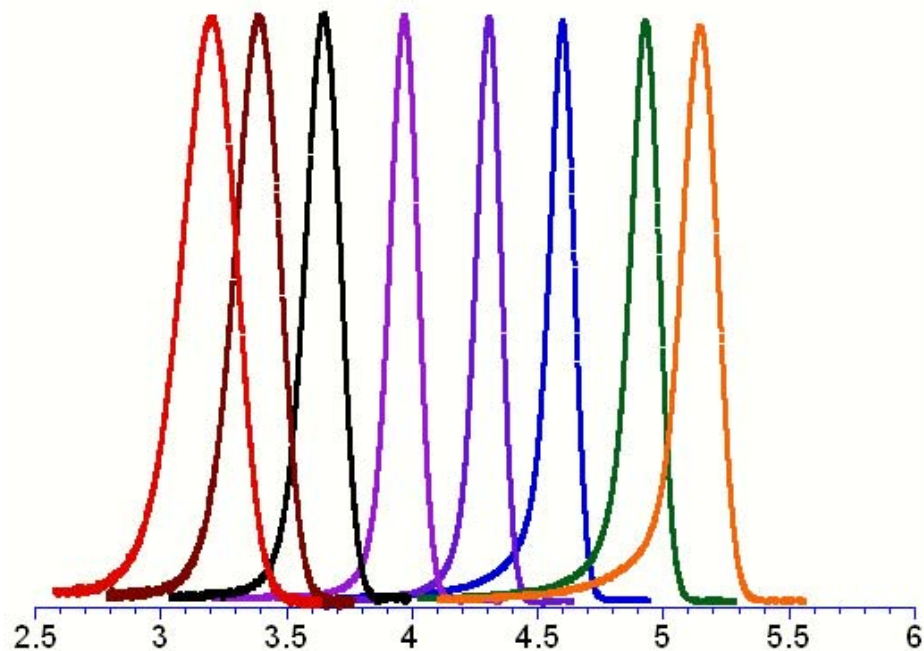


Figure 23: GPC curves for PP by living CCTP from Entries 3.04-3.11 (left to right)

3.2.3 Linear increase of molecular weight with time during CCTP of propene

The increase in the molecular weight of PP obtained under CCTP was monitored along with polymerization time. The kinetic experiment was performed in the same way as described in Section 3.2.1, except 22.8 mg of **35** (50 μmol), 40.0 mg of **01** (50 μmol), 0.82 g of ZnEt_2 solution (20 eq., 1.1 M in Tol) were used in 50 mL of toluene. Aliquots were taken every 30 min over a period of 3 h and quenched with methanol. The aliquots were also purified by precipitation into acidic methanol and dried *in vacuo* before GPC analysis. Figure 24 clearly showed that both M_w and M_n were linearly increasing with the polymerization time, at least during the reaction time explored. This is a direct evidence of the living character for a polymerization system when the monomer concentration was kept constant. Again, the PDI values for the entire aliquots were staying very low (1.04-1.06).

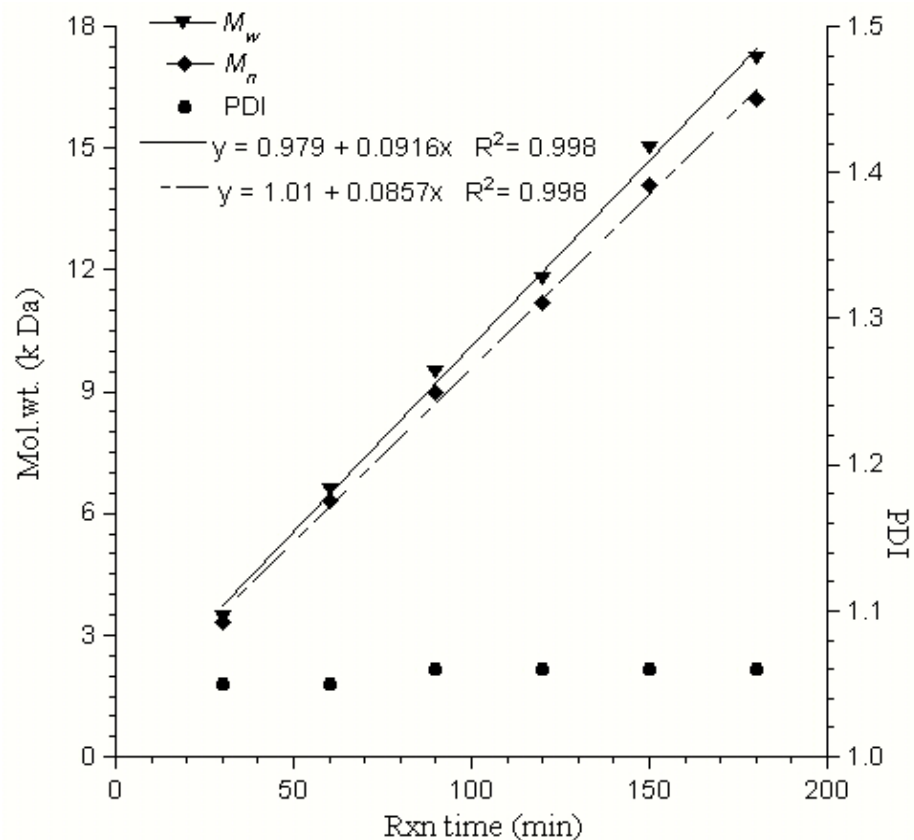


Figure 24: Kinetic study of propene polymerization under CCTP by **35**

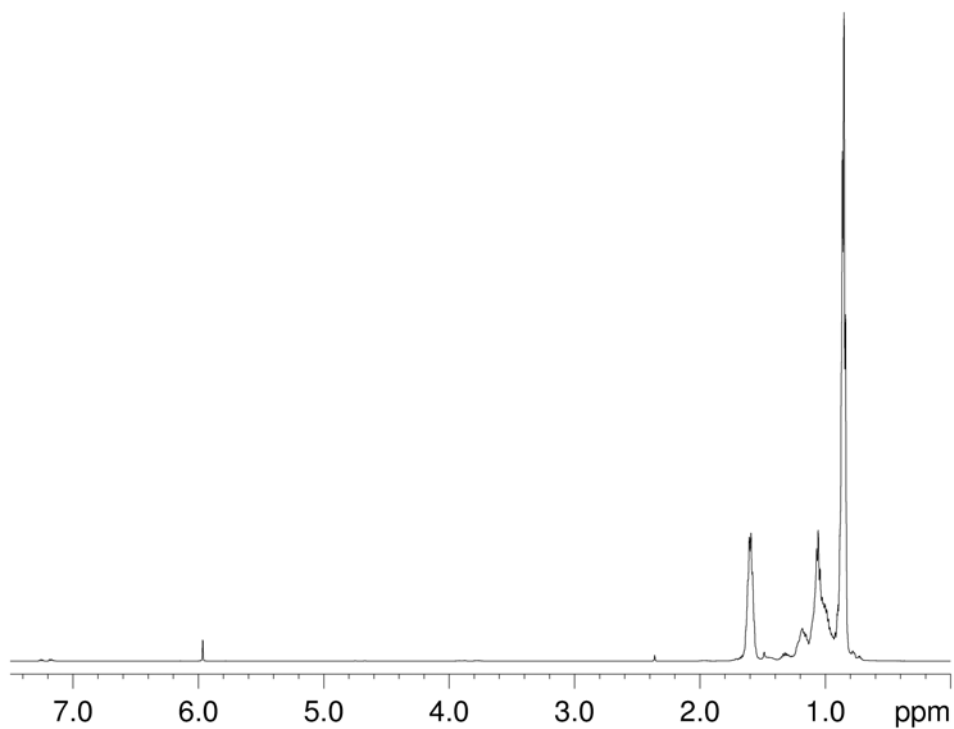


Figure 25: ^1H NMR (125 MHz, $1,1,2,2\text{-C}_2\text{D}_2\text{Cl}_4$, 70°C) of PP from Entry 3.03

The strict linear relationship between molecular weight and reaction time, together with the narrow polydispersity for all the PP samples obtained, and the fact that vinyl group resonances were absent in the region of 4.5 to 5.0 ppm in the ^1H NMR spectrum of PP produced even at 20 °C (Figure 25), proved a truly living coordinative chain transfer polymerization system *via* **35** with ZnEt_2 .

3.2.4 Quantitative control of PP's molecular weight by the amount of ZnEt_2

ZnEt_2 was used as a chain transfer agent for the catalyzed chain growth of polyethene.⁷⁰ Unlike trialkyl aluminum, ZnEt_2 showed little influence on the activity of the catalyst involved. The same conclusion was reached from the stable yield of PP in Table 5 when the same amount of catalyst was used under the same conditions except equivalents of ZnEt_2 . Another observation in the literature was that for some catalysts, the chain transfer process worked efficiently only with a high amount of ZnEt_2 (≥ 1700 eq) as indicated by the PDI index. However, this was not what we observed. For our CpAm hafnium system, we delivered the CCTP polymerization successfully using as low as 5 equivalents of ZnEt_2 .

One more behavior about ZnEt_2 investigated was the extension percentage of carbon zinc bonds based on the numbers of moles of added ZnEt_2 , molecular weight and yield of the polyethene. We didn't do this type of calculation due to the lack of the absolute molecular weight for the PP materials obtained (this work is under way), and even so, it was difficult to measure these numbers needed for calculation accurately on a quantitative level due to the experimental errors. The quantitative way to check the extension ratio of carbon zinc bond will be discussed in the next chapter. Here we studied the relationship between the molecular weight of PP and the amount

of total metals added while other experimental conditions were kept the same. The linear relationship in Figure 26 showed the extension ratio didn't change from 5 to 200 equivalents of added ZnEt_2 . With more chain transfer agent, more polymer chains were produced. The molecular weight of PP can be controlled quantitatively over such a wide range of ZnEt_2 .

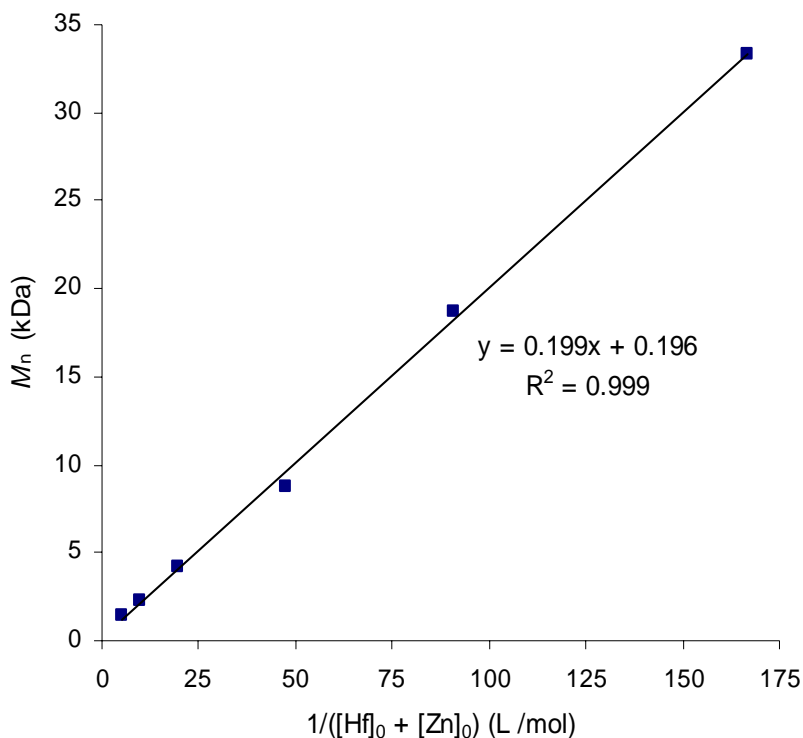


Figure 26: Quantitative control of polymer's molecular weight by the amount of chain transfer agent (data from Entries 3.04-3.09)

3.2.5 Characterization of polypropene via CCTP

Besides the GPC and ^1H NMR shown above, ^{13}C $\{^1\text{H}\}$ NMR, DSC and powder X-ray diffraction were also used to characterize the PP materials obtained from CCTP or TLCP techniques. ^{13}C $\{^1\text{H}\}$ NMR spectroscopy was used to illustrate the tacticity of the PP materials. The spectrum in Figure 28 was quantitatively representative for all the PP samples obtained under both CCTP (Table 5) and TLCP conditions (Table

4) *via* **35**. This spectrum for the methyl region of PP showed an atactic structure, or slightly syndiotactic rich (cf: $mm\% = 9.5\%$; $mr\% = 49.2\%$; $rr\% = 41.3\%$). This was in accordance with the result of powder X-ray diffraction (Figure 29) and DSC analyses. The latter showed that the glass transition temperature decreased with lowered molecular weight of the amorphous PP materials, and no melting point was detected (Figure 27).

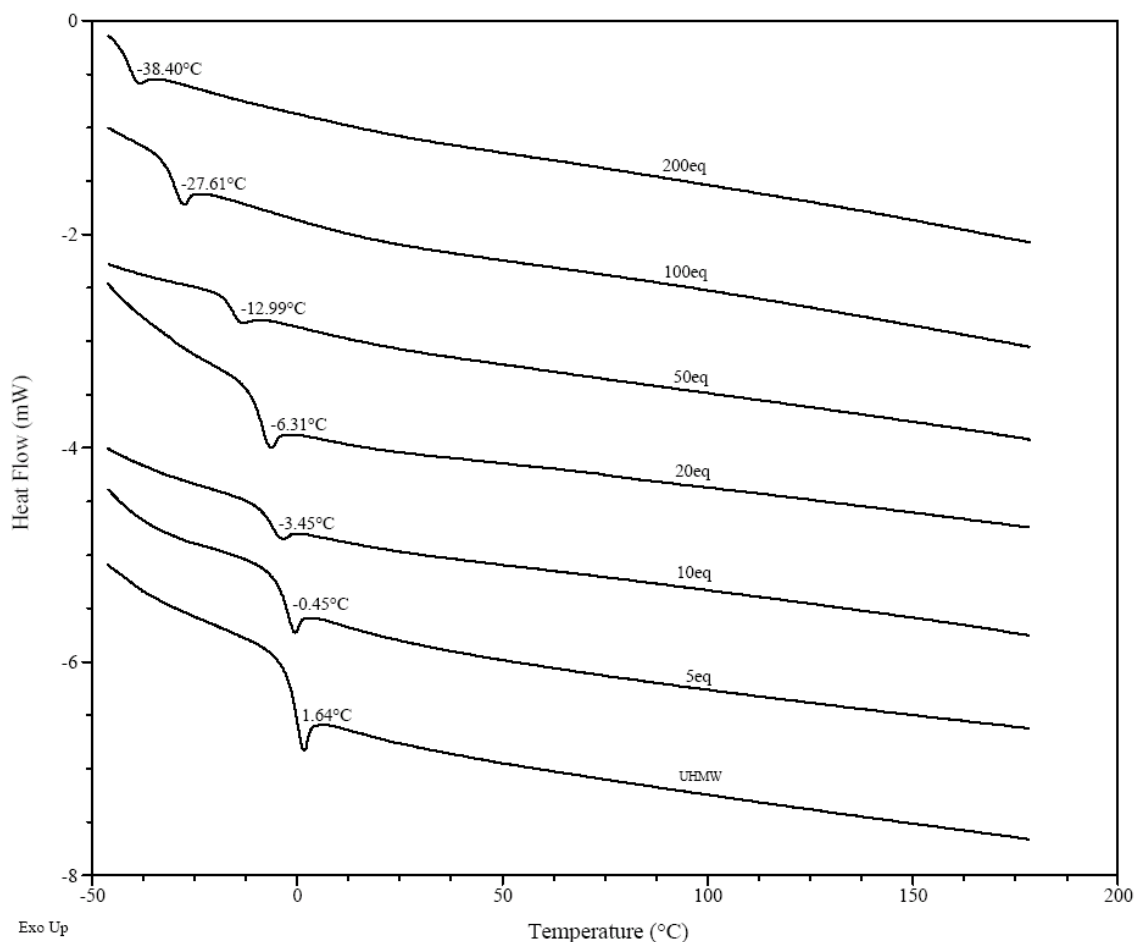


Figure 27: DSC traces (2nd heating cycle, 10 °C /min) for the polypropene materials from Entries 3.04-3.09 in Table 5 and 2.2.3 in Table 3

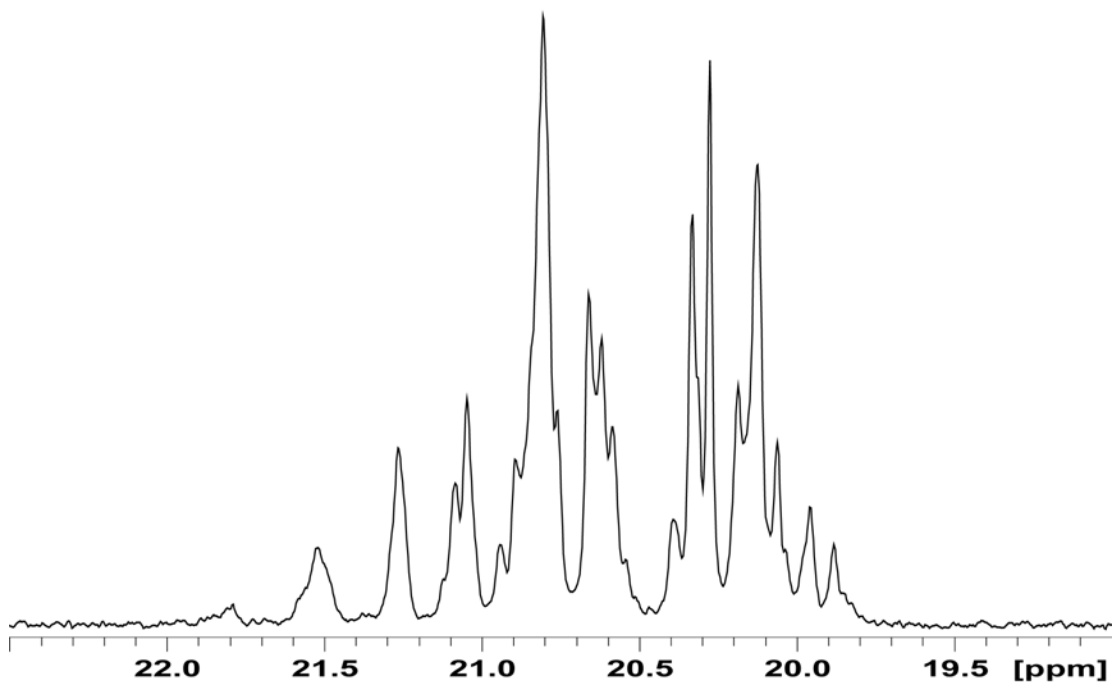


Figure 28: Typical ^{13}C $\{^1\text{H}\}$ NMR (125 MHz, 1,1,2,2- $\text{C}_2\text{D}_2\text{Cl}_4$, 70 $^\circ\text{C}$) of methyl region of polypropene *via* 35

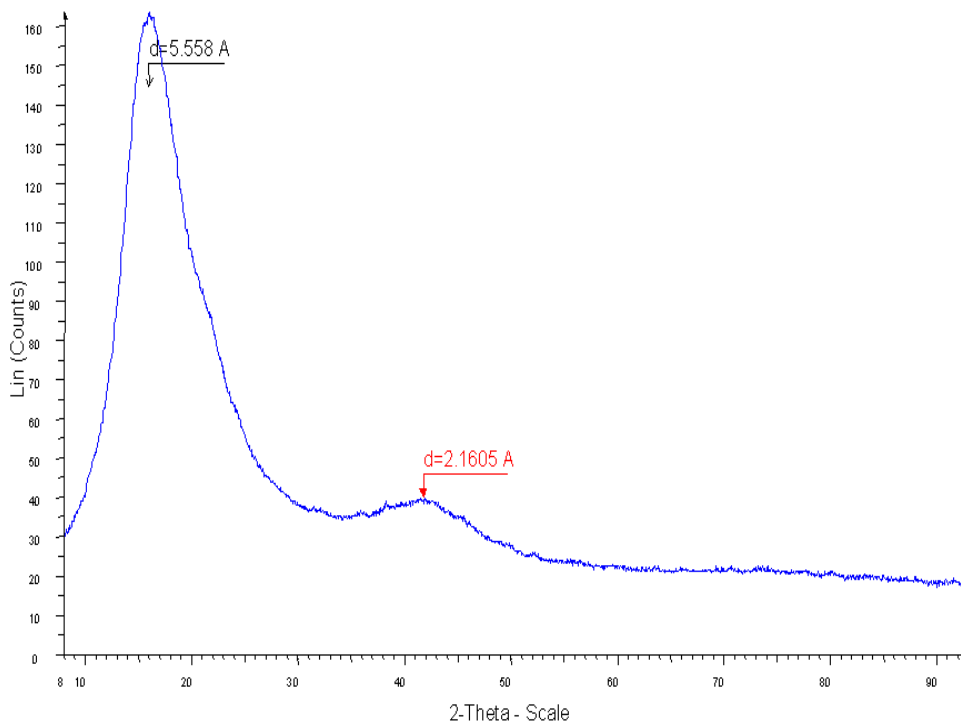


Figure 29: Powder X-ray diffraction study for PP material of Entry 2.2.3

3.2.6 An example of scaled up CCTP experiment of propene

Scale up is a necessary process during the development of laboratory work to industrial production. Sometimes this process determines whether a product will be commercial. Herein, to demonstrate the feasibility of large scale production of PP materials *via* the CCTP technique using **35**, 90g of polymer was successfully prepared in a half-liter glassware as described in the following. In a 500 mL Schlenk flask, to a solution of the cocatalyst [PhNHMe₂][B(C₆F₅)₄] (**01**) (0.16 g, 0.20 mmol) in 240 mL toluene at 0 °C were added **35** (0.092 g, 0.20 mmol) and ZnEt₂ (4.9 g, 200 eq, 1.1 M in Tol). The flask was then pressurized to 5 psi with propene and the pressure was maintained for 8 h while stirring before quenching with 2 mL of methanol. The toluene solution was washed with acidic water (5% HCl, 250mL × 2) and filtered through silica gel. The final product was collected after toluene was removed by vacuum (0.1 mmHg, 15h). Yield: 90g. GPC: $M_w = 2.25$ kDa; $M_n = 2.12$ kDa; PDI = 1.06.

It is noticeable that only 92 mg of precatalyst was used to produce 90g of polypropene with M_n value of 2.12 kDa. If the same amount of product was made by TLCP polymerization method, about 19.4g of **35** would be needed to add into the polymerization vessel theoretically.

3.2.7 Iodine terminated atactic polypropene by CCTP

Facile chain end functionalization is also an important feature of a living polymerization system. Here we realized the incorporation of a halogen group into the polypropene chain end. Iodinated polyethene will be discussed in the next chapter.

Scheme 16: Illustrative structures of iodo-PP and regular PP by CCTP via 35

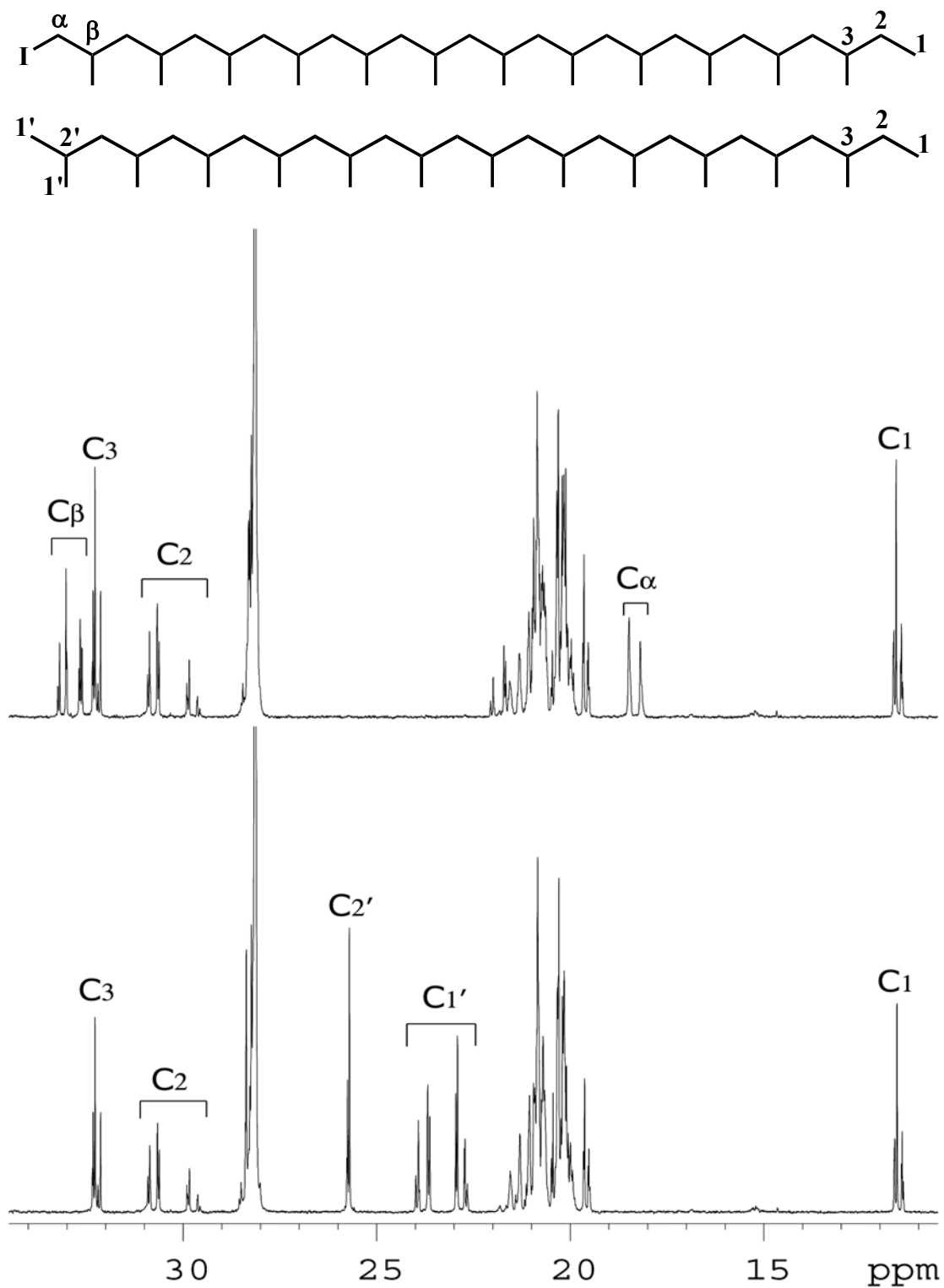


Figure 30: ^{13}C NMR (150 MHz, 1,1,2,2- $\text{C}_2\text{D}_2\text{Cl}_4$, 90 $^\circ\text{C}$) spectra of iodo-PP (top) and regular PP (bottom) by CCTP via 35 (methylene region was not shown)

The iodination experiment was delivered in the same way as Entry 3.04 in Table 5 except that a saturated iodine solution in toluene was used to quench the metal species at the end of polymerization. Addition of iodine stopped when the color of iodine stayed in the toluene solution. For both Entry 3.04 and the iodine termination reaction, extraction of the resultant toluene solution with 5% HCl aqueous solution was adopted to isolate the final product. Yield of the iodinated product (iodo-PP): 5.48g. GPC: $M_w = 1.08$ kDa; $M_n = 1.00$ kDa; PDI = 1.08. ^{13}C NMR spectra and illustrative structures of both iodinated PP and regular PP are shown in Figure 30 and Scheme 16.

It can be clearly seen that peaks for the 2-butyl group in the initiation end (C1, C2 and C3) were shown in both ^{13}C NMR spectra. However, peaks from the isobutyl group in the termination end (C1' and C2') of regular PP ¹¹⁵ only appeared in the bottom spectrum and were completely absent in the top one. In their place were peaks belonging to α - and β - carbons in the iodinated PP sample. It is safe to draw the conclusion that all the polypropene chains on zinc were quantitatively functionalized with iodine. The iodination of the chain end was also confirmed by ^1H NMR spectroscopy (see Appendix II).

3.3 CCTP of Propene with ZnEt_2 via **35** and **36** by Different Cocatalysts

36, the zirconium counterpart of **35**, was also investigated as a precatalyst for the CTPP polymerization of propene with ZnEt_2 . It turned out that **36** was also an effective catalyst and its activity for propene polymerization was slightly lower compared with **35** under CCTP conditions (Entry 3.12 in Table 6). Most features of the living hafnium system were maintained when the zirconium complex **36** was

used: molecular weight of polypropene was lowered by the addition of ZnEt₂; the polydispersity was also very narrow (1.04-1.09); at lower temperature, higher yield was obtained due to the increased concentration of the gas monomer (Entry 3.13). Quite high molecular weight PP was also produced by **36** with narrow polydispersity (Entry 3.14). However in the case of employing 200 equivalents of ZnEt₂, unlike the hafnium catalyst, **36** gave a negative result for the polymerization of propene.

Table 6: CCTP of propene via **35** and **36** activated by different cocatalysts

Entry	precat & cocat			ZnEt ₂ (equiv.)	Tol (mL)	T _p °C	t _p (h)	Yield (g)	M _n (kDa)	PDI
	Identity	(μmol)								
3.12	36	01	20	20	20	0	1	2.08	4.59	1.05
3.13	36	01	20	20	20	-10	1	3.72	7.63	1.04
3.14	36	01	10	5	40	0	7	4.43	61.7	1.09
3.15	36	02	20	20	20	0	1	2.22	4.89	1.05
3.16	36	03	20	20	20	0	2	2.29	4.87	1.05
3.07	35	01	20	20	20	0	2	4.18	8.75	1.04
3.17	35	02	20	20	20	0	2	4.77	9.91	1.04
3.18	35	03	20	20	20	0	8	0.28	1.37	1.06

Note: polymerization performed under a constant pressure of propene (5psi)

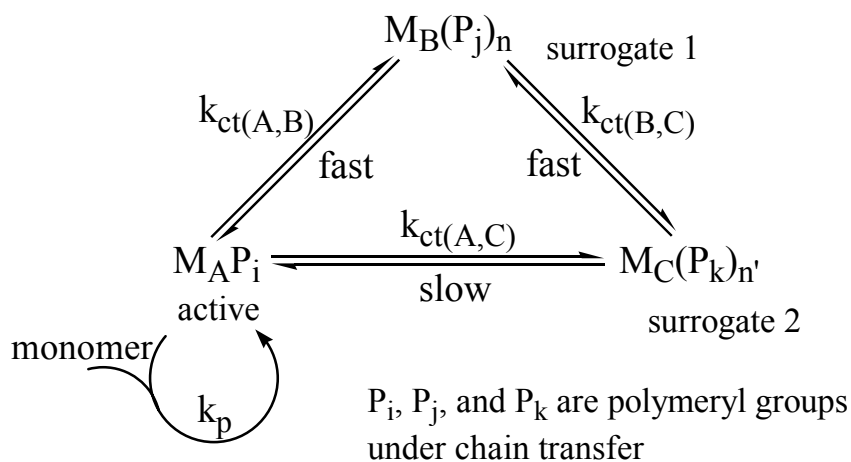
Cocatalyst [Ph₃C][B(C₆F₅)₄] (**02**) and B(C₆F₅)₃ (**03**) were also used to activate **35** and **36** under CCTP conditions for the polymerization of propene. **02** provided the same results for both **35** and **36** (Entries 3.15 and 3.17) as those when [PhNMe₂H][B(C₆F₅)₄] (**01**) was used. However, **03** rendered a slightly lower activity for **36** (Entry 3.16) and a much lower activity for **35** (Entry 3.18). It can be seen that

for both traditional coordination polymerization (see Table 4 in Section 2.3.3) and CCTP conditions, the tris(perfluorophenyl) borane **03** was a mild activator compared with the trityl and anilinium tetra(perfluorophenyl) borate **01** and **02**.

3.4 CCTP of Propene via **35** with Combination of $ZnEt_2$ and $AlEt_3$

As a chain transfer agent, $AlEt_3$ has a lower price than $ZnEt_2$ and higher alkyl group content (number of alkyl groups per unit mass). After $ZnEt_2$ was studied, we were curious if $AlEt_3$ was also an efficient CTA for the CCTP of propene via **35**. Under the same conditions, the polymerization results with $AlEt_3$ were not as ideal as those with $ZnEt_2$. No matter whether **01** (Entry 3.19 in Table 7) or **02** (Entry 3.20) used as the cocatalyst, the polymerization rate via **35** was depressed a little bit by $AlEt_3$, and the molecular weight distribution of PP was broader (PDI 1.19 and 1.16).

Scheme 17: Mechanism of M_B assisted chain transfer between M_A and M_C



To overcome this problem, we proposed the concept of assisted chain transfer for the first time (Scheme 17). This strategy adopted the combination of an efficient CTA (M_B) with another inefficient or ineffective CTA (M_C) in a CCTP system. Between M_C and the catalyst M_A , usually a transition metal complex, chain transfer was not

fast enough to provide the same opportunity for all the polymer chains to grow equally. But the fast chain transfer processes between M_B and M_A or M_C can do so. Then as a whole result, all the polymer chains are involved in a reversible, fast and efficient chain transfer process and growing in the same rate. Herein we used **35**, $ZnEt_2$ and $AlEt_3$ as M_A , M_B and M_C separately. Polymerization results are shown in Table 7 (Entries 3.21-3.24).

Table 7: CCTP of propene via **35** with combination of $ZnEt_2$ and $AlEt_3$

Entry	$ZnEt_2$	$AlEt_3$	Et_{total}		Yield (g)	M_n (kDa)	PDI	PP (mmol)	ratio
	(equiv.)	(equiv.)	(equiv.)	(mmol)					
3.07	20	0	40	0.8	4.18	8.75	1.04	0.478	0.598
3.08	10	0	20	0.4	4.78	18.7	1.04	0.256	0.640
3.19	0	20	60	1.2	3.86	5.21	1.19	0.741	0.618
3.20	0	20	60	1.2	4.08	5.30	1.16	0.770	0.642
3.21	10	10	50	1.0	4.37	7.31	1.02	0.598	0.598
3.22	10	20	80	1.6	3.06	3.38	1.04	0.905	0.566
3.23	20	10	70	1.4	4.77	5.81	1.03	0.821	0.586
3.24	5	20	70	1.4	3.15	3.67	1.04	0.858	0.613

Notes: conditions: 20 μ mol of **35** and 20 μ mol of **01** (except **02** used for Entry 3.20) were added into 20 mL of toluene at $-0^\circ C$, under a constant propene pressure of 5psi, t_p 2h. In the cases where $AlEt_3$ was used, the polymer product also contained a tiny amount of high molecular weight product.

For the ratios of $ZnEt_2$ versus $AlEt_3$ tested in the Table above (1:1, 1:2, 2:1 and 1:4), the yield might be slightly affected by the addition of $AlEt_3$, however the polydispersity stayed extremely narrow (1.02-1.04) all the time. This confirmed that

very effective assisted chain transfer happened for the CCTP polymerization of propene *via* **35**. Indeed, we calculated the relative ratio of moles of the PP product and the total ethyl group added (Et_{total}), and the values kept stable as shown by the right column in Table 7. This result told us that all the alkyl groups on both Zn and Al are involved in the propagation process.

As a potential strategy, we could take advantage of both chain transfer agents by assisted chain transfer polymerization. When only a small amount of the efficient CTA was added, a catalyzed CCTP process might be realized. The window of chain transfer agents will be greatly expanded and we can make use of some main group alkyls which are inefficient or not chain transfer agents at all.

3.5 Conclusions

The CpAm hafnium system provided the first example of a truly living coordinative chain transfer polymerization process. In this system, the polymerization activity was only controlled by the amount of the catalyst **35**⁺. The equivalents of ZnEt_2 added will determine the moles of the resulted polypropene. The living character of this process was confirmed by the extremely narrow polydispersity, kinetic study and ¹H NMR spectroscopy results. The CCTP technique provided the correct way to produce a significant amount of polymer materials for any further study and application. This system also showed precatalyst and cocatalyst tolerance and the propensity of quantitative chain end functionalization and large-scale production. The realization of assisted chain transfer process in this CCTP system illustrates a promising area in future studies.

Chapter 4: Catalyzed Polyethene Chain Growth on Zinc by the CpAm Hafnium Complex — Polymerization and Mechanistic Investigation

4.1 Living Polymerization of Ethene under CCTP Conditions via 35

4.1.1 Background and procedures

The coordinative chain transfer polymerization (also named as catalyzed chain growth) of ethene was realized using several transition metal complexes as summarized in Chapter 1. Narrow molecular weight distribution (PDI \sim 1.1) was obtained in some cases even though the polymerization process was not living. Functionalized end group terminated polyethene was also reported utilizing CCTP technique.^{71, 122}

As described in the last chapter, we successfully realized the living CCTP polymerization of propene with ZnEt_2 via an active CpAm hafnium catalyst. In this chapter, our interests will focus on the polymerization behavior for ethene of the CpAm hafnium system. Mechanistic considerations of the CCTP process will also be examined through the polymerization of ethene.

Ethene usually has a much higher activity than propene. To achieve a controllable process, the mild cocatalyst $\text{B}(\text{C}_6\text{F}_5)_3$ (**03**) was used to lower the polymerization activity of **35**⁺ for ethene. For the same reason, less catalyst was loaded and more solvent was added. Also, the reaction temperature was set at 25 °C to lower the concentration of the gas monomer. The polymerization was delivered in the

same manner as that for propene (see Section 2.3.1). Experimental details are summarized in Table 8.

4.1.2 A series of CCTP polymerization of ethene *via* **35**

To begin, ethene was polymerized by CCTP technique *via* **35** with 20 equivalents of ZnEt₂, and the polymerization was delivered for a period of 8 min without precipitation of polyethene. With more equivalents of ZnEt₂, the time window of homogeneity was expanded, and the yield of polyethene was also higher (Entries 4.01-4.05 in Table 8).

Table 8: Living CCTP of ethene with ZnR₂ *via* **35** activated by **03**

Entry ^a	ZnEt ₂	t _p	Yield	M _n ^c	PDI ^d	T _m ^e
	(equiv.)	(min)	(g)	(Da)		(°C)
4.01	20	8	0.21	665	1.03	80
4.02	50	18	0.34	527	1.07	67
4.03	100	32	0.72	526	1.06	66
4.04	150	48	0.92	499	1.07	63
4.05	200	63	1.17	466	1.07	61
4.06	50 ^b	21	0.24	449	1.06	56

Notes: a, conditions: 10 μmol of **35** and **03** were added in 40 mL of toluene at 25 °C, under a constant pressure of ethene (5psi); b, 1.0 M ZnⁱPr₂ solution was added instead of 1.1 M ZnEt₂ in toluene for Entry 4.06; c, determined by ¹H NMR end group analysis; d, determined by GPC; e, measured by DSC.

The molecular weight of PE obtained, as calculated from ¹H NMR end group analysis, didn't change much for the range of 20 to 200 equivalents of ZnEt₂, and dropped only a little bit with a higher yield. The molecular weight reduction was

reasonable because the starting point of precipitation depends on both the concentration and molecular weight of PE. Correspondingly, the melting point of PE, as determined by DSC, also decreased slightly for PE of lower molecular weight. The polydispersity, which was measured by GPC, kept narrow for all the experiments (≤ 1.07), indicating the living character of the CCTP system.

For Entry 4.06, the CCTP polymerization was performed with Zn^iPr_2 as the chain transfer agent. It was surprising that the polymerization rate only dropped slightly compared with the case using ZnEt_2 , bearing in mind that no polymer was obtained for the propene polymerization when Zn^iPr_2 was used under CCTP conditions. The successful realization of employing Zn^iPr_2 as a CTA allowed us to track the initiation polymer end and investigate the polymerization mechanism for future studies.

4.1.3 Dependence of the t_p -normalized M_n on the amount of CTA

The CCTP polymerization of ethene was quenched at the onset of turbidity in the reaction solution. To standardize the time difference, a t_p -normalized M_n was used for studying the relationship between the molecular weight of PE and the amount of ZnEt_2 . As shown by Figure 31, the value of M_n/t_p was inversely proportional to the total alkyl groups on both hafnium and zinc. This was just what we expected for a CCTP process in which termination events were absent and the metal alkyls were quantitatively extended by catalytic monomer insertion. This was also a proof that the molecular weight of the resulted polymer could be adjusted by the addition of different equivalents of chain transfer agent.

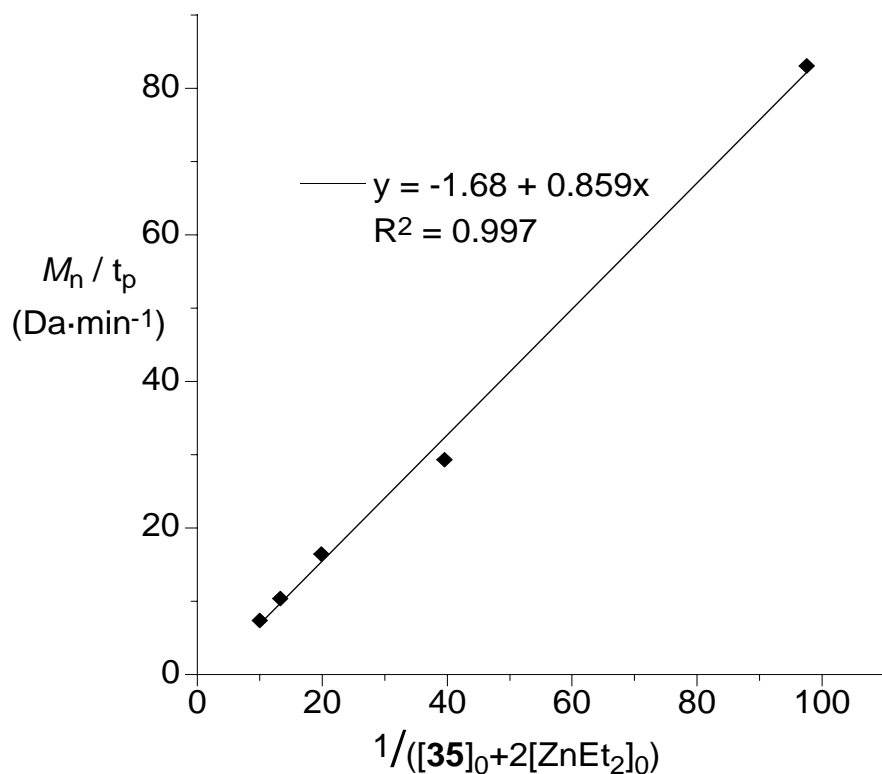


Figure 31: Plot of t_p -normalized M_n as a function of total alkyls on both active and surrogate metals

4.2 NMR Analysis and in situ Mechanistic Study

4.2.1 NMR spectra of linear PE and 2-methyl PE

The isolated PE materials were subject to ^1H and ^{13}C NMR spectroscopy. As shown in Figure 32, the PE by CCTP of ethene with ZnEt_2 via **35** possesses a purely linear structure of a long chain n -alkane. It is more interesting that the bottom spectrum for the PE by CCTP with Zn^iPr_2 showed both a linear n -alkyl end group and a 2-methyl alkyl end group. All the peaks in the ^{13}C NMR spectrum were definitely assigned. The isopropyl group was successfully incorporated onto the linear PE chain end, and the incorporation was quantitative which can be tracked from the integration values of signals in the NMR spectrum. The results from ^{13}C NMR were also

confirmed by ^1H NMR (see Appendix II). The chain ends of PE materials were clearly shown by both types of spectra. This information was also used to determine the absolute M_n of PE as presented in Table 8.

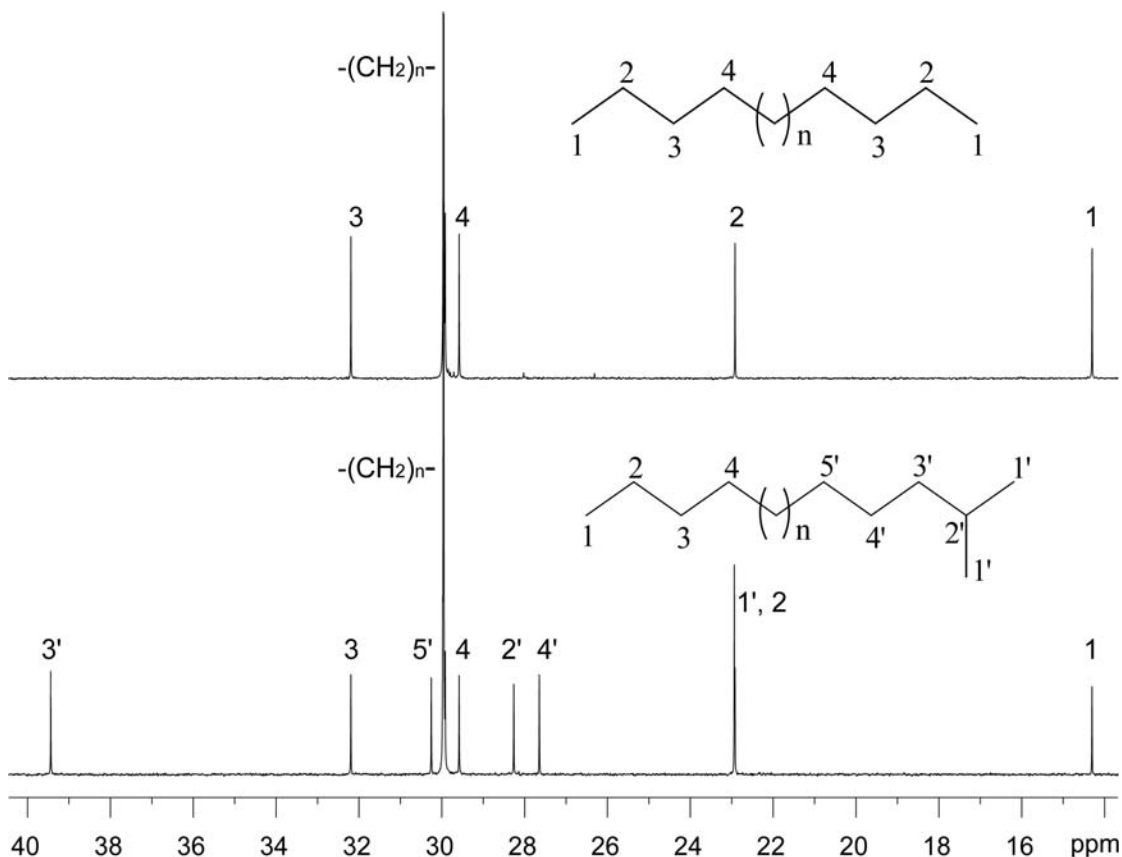


Figure 32: ^{13}C $\{^1\text{H}\}$ NMR (150 MHz, $1,1,2,2\text{-C}_2\text{D}_2\text{Cl}_4$, 90°C) spectra of isolated PE (Entry 4.05, top) and 2-methyl PE (Entry 4.06, bottom) by CCTP *via* **35**

4.2.2 Direct observation of quantitative chain growth on zinc by NMR study

After the isolated polymer was characterized by NMR spectroscopy, we were thinking about direct observation of growing polymer chains on the chain transfer agent. This goal was accomplished by the *in situ* NMR study of the CCTP of ethene with Zn^iPr_2 *via* **35** in toluene- d_8 . The experiment was delivered as the following: in a 100 mL Schlenk flask, to a solution of **03** (1.8 mg, $3.3\ \mu\text{mol}$) in 5.3 mL toluene- d_8 at

20 °C were added **35** (1.5 mg, 3.0 μmol) and Zn^iPr_2 (147 mg 1.0 M solution in Tol, 50 eq). After an NMR sample was taken out, the flask was pressurized to slightly above 1 atm with ethene and the pressure was maintained for 15 min with stirring. The pressure was released before another NMR sample was taken out of the reaction solution. Both ^1H NMR and ^{13}C $\{^1\text{H}\}$ NMR spectra were recorded for these two samples, as shown in Figures 33 and 34.

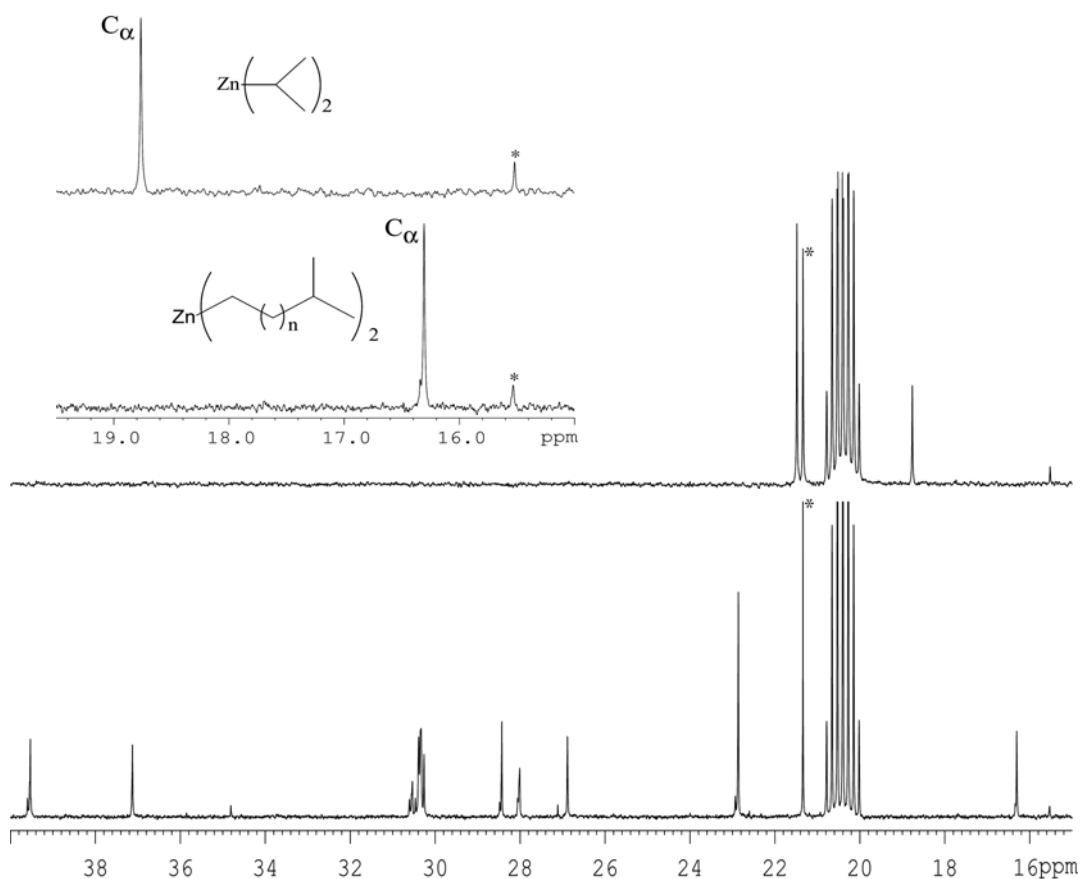


Figure 33: ^{13}C $\{^1\text{H}\}$ NMR (150 MHz, Tol- d_8 , 20 °C) spectra of a mixture of **35**⁺ and Zn^iPr_2 without ethene (top) and after 15 min introduction of ethene (bottom). The septet is the H,D residual isotopomer solvent peak and the singlet marked by * at 21.34 ppm indicates the natural abundance toluene peak from the Zn^iPr_2 solutions. The enlarged partial spectra on the top left showed the Zn- C_α region, and the resonance for a trace amount of Et_2O at 15.54 ppm is marked by * as a reference.

In the ^{13}C $\{^1\text{H}\}$ NMR spectrum for the mixture of 35^+ and Zn^iPr_2 (Figure 33), the isopropyl groups of the latter exhibited resonances at 18.77 and 21.48 ppm for the C_α and C_β carbons, respectively, in the absence of ethene. A short time after introduction of ethene (~ 15 min), a new spectrum revealed that these resonances completely disappeared and only those for the resulting dipolymeryl zinc were observed. The terminal isopropyl end-groups on these polymeryl fragments had resonances at 28.43 and 22.86 ppm for the original C_α and C_β carbons, which are in accordance with the peak assignments of the isopropyl end group in a 2-methyl PE (see Figure 32, bottom). The new C_α carbons on zinc for these polymeryl groups had a chemical shift at 16.31 ppm.

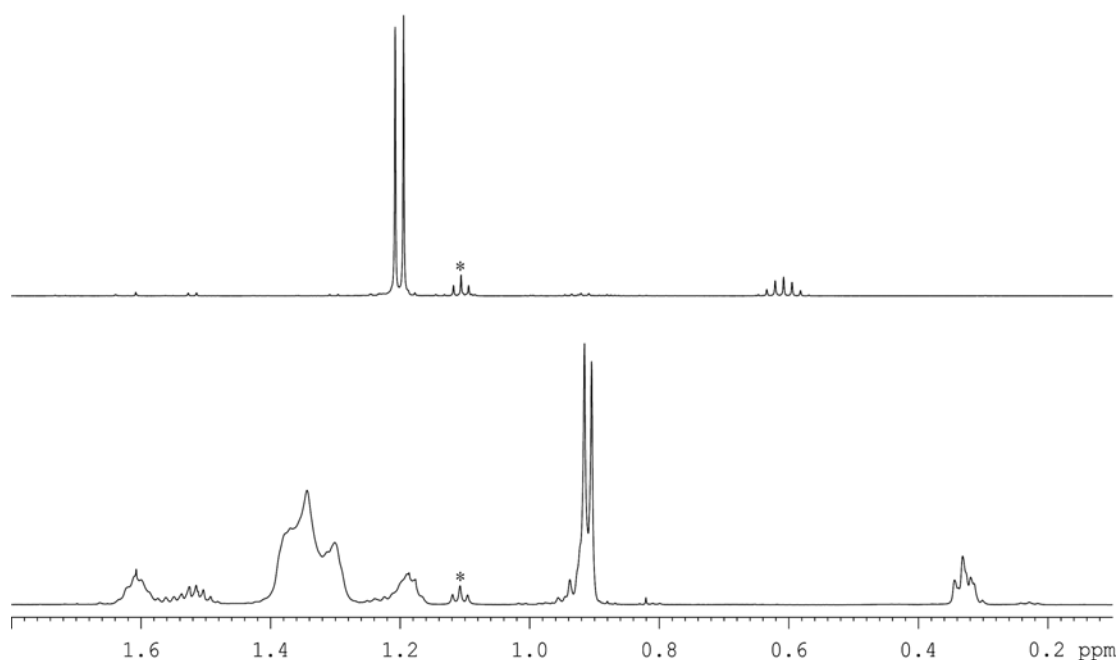


Figure 34: ^1H NMR (600 MHz, $\text{Tol-}d_8$, 20 $^\circ\text{C}$) spectra of a mixture of 35^+ and Zn^iPr_2 in the absence of ethene (top) and after 15 min introduction of ethene (bottom). The resonance for a trace amount of Et_2O is marked with an asterisk (*).

The quantitative and complete changes in the ^{13}C NMR spectra were also confirmed by ^1H NMR spectra, in which the doublet for $-\text{CH}_3$ in the isopropyl groups shifted from 1.20 to 0.91 ppm and the septet for the CH in isopropyl groups shifted from 0.61 to 1.51 ppm after the polymerization of ethene (Figure 34). The hydrogen on the new α -carbons showed a separate triplet at 0.33 ppm. By tracking the isopropyl groups and new α -atoms using NMR spectroscopy, we observed the chain growth on zinc directly. It is safe to draw the conclusion now that both alkyl groups on zinc are fully involved in the efficient, rapid and reversible chain transfer process in the CCTP system *via* **35**.

4.3 Alkane Distribution in the PE Product Characterized by GC

4.3.1 GC analysis of polyethene aliquots quenched at different t_p

Gas chromatography is a powerful tool to identify and quantitatively analyze polyethene oligomers.^{70, 75} To follow the alkane distribution in the PE products during the polymerization process and thus to get mechanistic information, we delivered the following kinetic experiment: in a 250-mL Schlenk flask, to a solution of the cocatalyst **03** (5.1 mg, 10 μmol) in 39 mL toluene at 25 $^\circ\text{C}$ were added **35** (4.6 mg, 10 μmol) and a ZnEt_2 solution (1.24 g, 150 eq, 1.1 M in Tol). The flask was then pressurized to slightly greater than 1 atm with ethene and the pressure was maintained while stirring. Timed aliquots were taken at 25, 30, 35 and 40 min. The samples were quenched with silica gel, filtered, concentrated if need be and analyzed by gas chromatography. The raw GC chromatograms are presented in Figure 35.

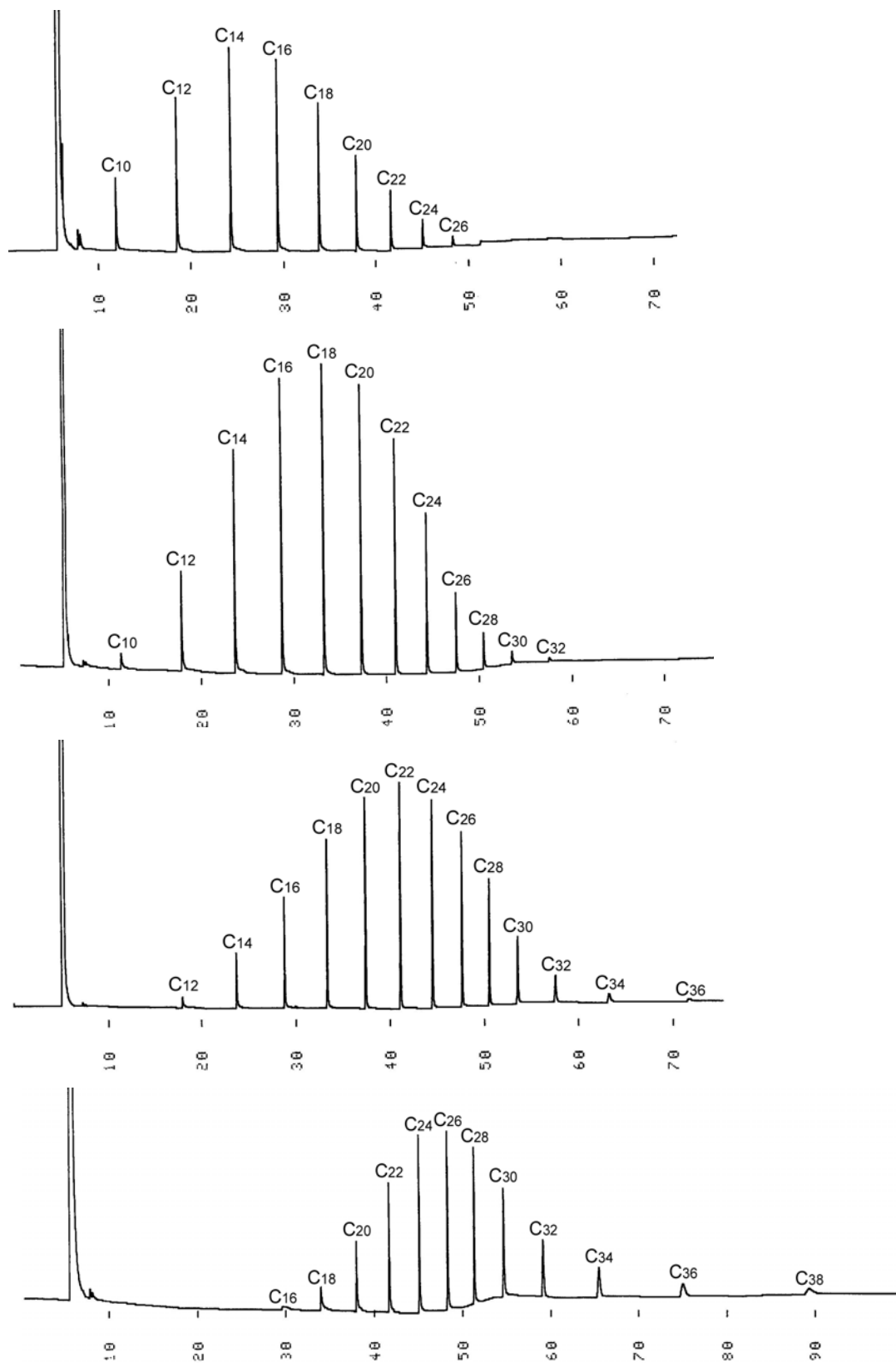


Figure 35: GC chromatograms of PE aliquots at (top to bottom) 25, 30, 35 and 40 min

4.3.2 Poisson distribution of PE aliquots showed the living character

The area value of each peak in the GC chromatograms was plotted against its corresponding carbon number, which was identified by four *n*-alkane standards of known carbon number (C_{12} , C_{20} , C_{21} and C_{30}). As shown below, for all these aliquots obtained at different polymerization time (t_p), the occurrence of linear alkanes in the PE samples fitted the Poisson distribution very well. The highest peak value moved over time, but the distribution curve didn't change. This is an important feature of a living ethene polymerization process.

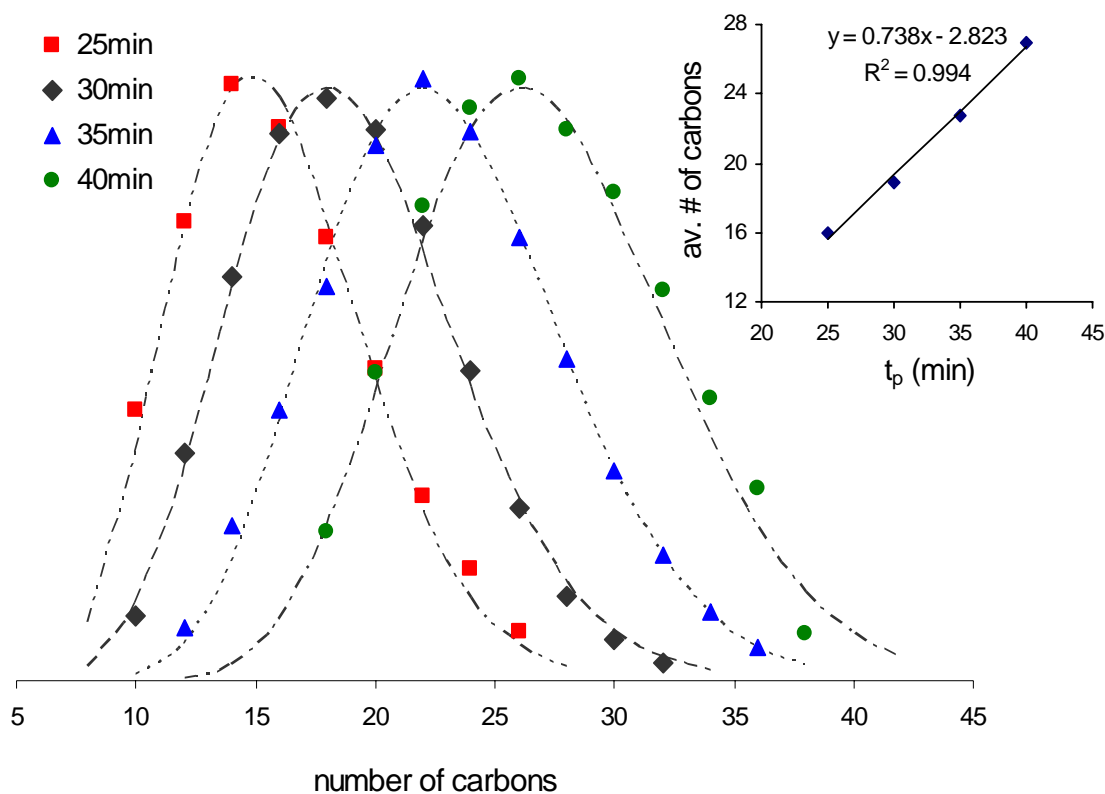


Figure 36: Distribution of *n*-alkanes in PE aliquots quenched at different times by GC analysis (dotted lines are showing the best Poisson distribution fitting). Curve on top right shows the linear relationship between average carbon numbers and polymerization time.

The living character was also confirmed by the linear relationship between the GC peak area-averaged carbon number of the PE samples and polymerization time, which was illustrated in Figure 36. Thus the living CCTP system for propene with ZnEt_2 via **35** was also applied to ethene, and the living character was maintained and confirmed by GPC, GC and kinetic studies. The following end group functionalization was an additional proof for the living property in the CpAm hafnium system.

4.4 End Group Functionalized Linear PE

Living polymerization provided a good chance to realize end group functionalization. The resulting materials might have some special applications. More important, these functionalized polymers can be used as the starting material for post-polymerization reactions and/or further polymerizations. For example, a hydroxy-terminated polyethene (PE-OH) macroinitiator was prepared and used to synthesize a block copolymer by combining CCTP with ring opening polymerization.¹²³

Herein two near perfect iodo-PE samples were prepared using the living CCTP technique. First, the CCTP of ethene with ZnR_2 (100eq ZnEt_2 or 60eq Zn^iPr_2) via 10 μmol of **35** activated by **01** was delivered in 40 mL toluene at 25 °C in the same fashion as described in Section 4.1.1. At the onset of turbidity, the saturated iodine solution in toluene was added to quench the polymerization reaction. The titration stopped when the purple color of I_2 persisted. Upon standard isolation procedures, e.g. precipitation into acidic methanol and filtration, white powder product was obtained. For the ZnEt_2 case, 0.86g of Et-PE-I was obtained, M_n 884 Da, PDI 1.09. For the Zn^iPr_2 case, 0.60g of ^iPr -PE-I was obtained with M_n 1.06 kDa, PDI 1.06. The

illustrative structures, ^1H NMR and ^{13}C $\{^1\text{H}\}$ NMR spectra of both samples are shown in Figures 37 and 38. Detailed peak assignments were also carried out as labeled therein.

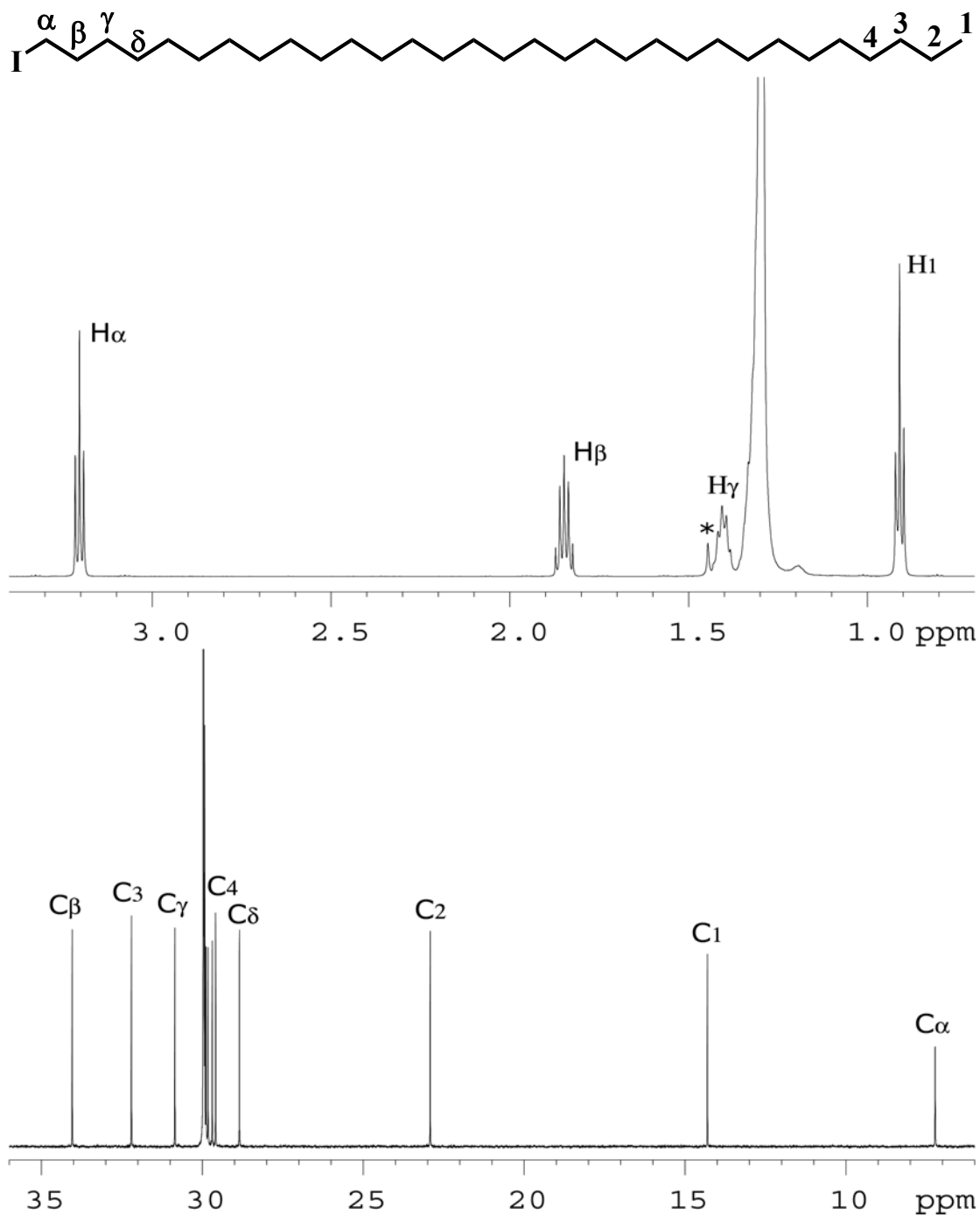


Figure 37: ^1H (600 MHz, top) and ^{13}C (150 MHz, 1,1,2,2- $\text{C}_2\text{D}_2\text{Cl}_4$, 90 $^\circ\text{C}$, bottom) NMR spectra of Et-PE-I, the water peak was marked by an asterisk *.

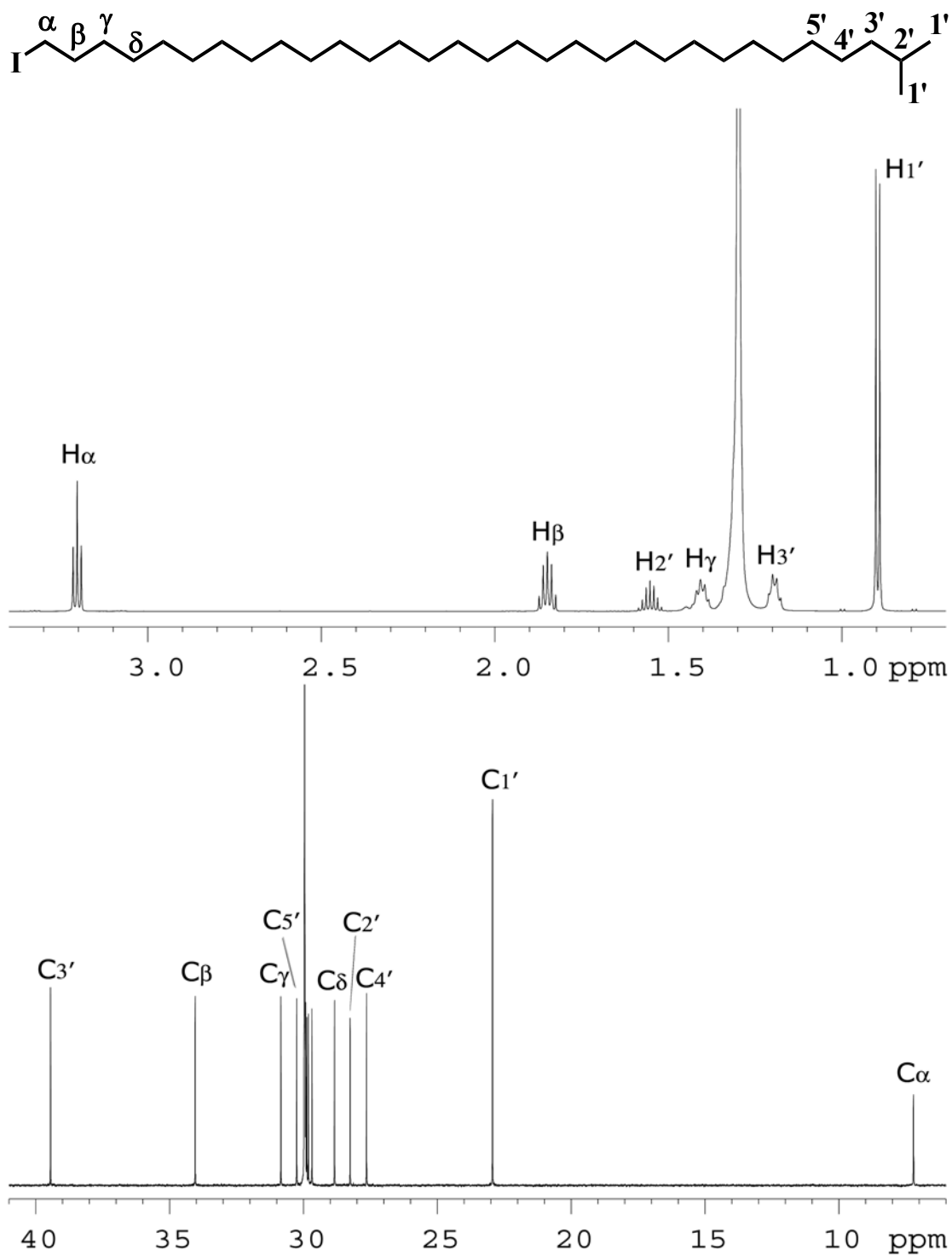
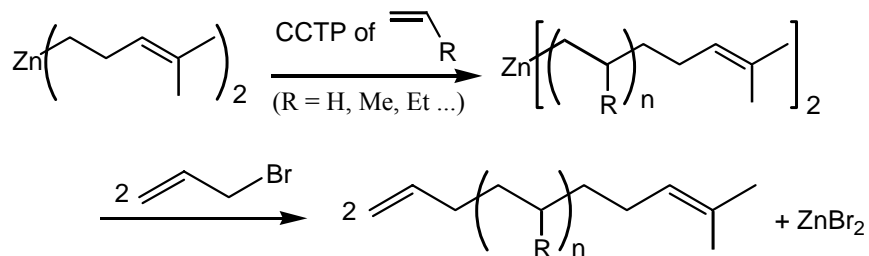


Figure 38: ^1H NMR (600 MHz, top) and ^{13}C $\{^1\text{H}\}$ NMR (150 MHz, 1,1,2,2- $\text{C}_2\text{D}_2\text{Cl}_4$, 90 $^\circ\text{C}$, bottom) spectra of ^1Pr -PE-I.

From Figure 37 we can see that iodine was successfully incorporated into the linear PE chain end, and this process was quantitative based on the NMR peak integration. The quantitative process of incorporation of iodine was more obvious in Figure 38, which showed that eventually both ends of the PE chain were fully capped with modification groups, one end with isopropyl and the other end with iodine. The expanded partial region of both ^{13}C NMR spectra (30.5-29.5 ppm) is attached in Appendix II, with tentative assignments for the highly resolved methylene peaks.

This termination process provided pure polymer products by the virtue of living CCTP technique. No further separation procedure is necessary to get rid of unfunctionalized polymers, which is an attractive aspect for practical production. Furthermore, the iodinated polyethene is just an example of end group modification. Using the same methodology, we should also be able to make a series of polymers capped with different functional groups by quenching the polymerization with different reagents, such as oxygen¹²⁴, ketone^{125, 126}, carbon monoxide, etc. The application of these materials will also open the door to a new area for engineering.

Scheme 18: Proposed synthetic route for poly-1-alkenes with unsaturated bonds on both ends by the living CCTP technique



The end group functionalization can be performed not only through the termination process, but also from the initiation point, as shown by I-PE-ⁱPr. It is

quite straightforward to apply other zinc alkyls¹²⁷ as chain transfer agents and incorporate different alkyl groups to the polymer chain end, and such alkyl groups can also bear different functional groups providing they don't negatively influence the catalytic system. It is also very promising to work out functionalized polymers with desired groups on both ends, as long as we combine the quantitative chain transfer and termination processes compatible in the same CCTP system.¹¹⁹⁻¹²¹ Scheme 18 shows a strategy for this purpose, which is very feasible considering that it was already accomplished, even though not ideally, in an irreversible chain transfer process for the polymerization of propene.¹¹⁹

4.5 Conclusions

The living CCTP of ethene with ZnR_2 ($R = Et$ or iPr) via **35** was successfully accomplished. The polyethene obtained possessed a narrow molecular weight distribution and a purely linear structure, which were clearly shown by GPC chromatography and NMR spectroscopy. The *n*-alkane distribution in the PE product followed the Poisson distribution during the whole process of polymerization. The molecular weight increased linearly with reaction time, and could be adjusted by the equivalents of added chain transfer agent. The complete chain extension on the Zn-C bond and the quantitative termination by iodine were confirmed by mechanistic studies and chain end functionalization experiments.

Chapter 5: Living CCTP of Higher α -olefins and 1,5-hexadiene, and Random CCTP Copolymerization of these Monomers with Propene or Ethene

5.1 Living CCTP of Higher α -olefins and 1,5-hexadiene

5.1.1 Background and description

In addition to ethene and propene, chain transfer to aluminum was also reported during the coordination polymerization of 1-butene,¹⁰⁸ 1-hexene,¹²⁸ allylbenzene,¹²⁹ 1,5-hexadiene (1,5-HD)¹³⁰ and styrene.¹³¹ However no example in literature was regarded as a reversible process. In the area of CCTP, as far as I know, there was no report concerning higher α -olefins beyond propene or any other type of olefins. The challenge is most likely due to the monomer dependence displayed by coordination polymerization.^{118, 132}

The living CCTP system *via* **35** developed by us is very efficient for the polymerization of both ethene and propene. This triggered us to explore its catalytic behavior for other olefins. The latest results showed that the living CCTP polymerization of higher α -olefins and α,ω -nonconjugated dienes was also successful by the CpAm hafnium system. The unprecedented achievement opened a wide window of monomers employed in the area of CCTP.

The polymerization experiment was delivered as following: to a toluene solution of the cocatalyst **01** at a desired temperature were added the precatalyst **35**, ZnEt₂ and the liquid monomer. The reaction mixture was stirred for a specific time before

quenching with 0.5 mL of methanol. The toluene solution was precipitated into 600 mL of acidic methanol to isolate the polymer. The final product was collected and dried overnight *in vacuo* before GPC and NMR analyses. Details of the amount of reagents, reaction temperature, and polymerization time are provided in Table 9.

Table 9: Living CCTP of higher α -olefins and 1,5-hexadiene

Entry	ZnEt ₂	Monomer			T _p	t _p	Yield	M _n	PDI
	(equiv.)	Identity	(g)	(equiv.)	(°C)	(h)	(g)	(kDa)	
5.01	10	1-But	1.00	1780	-10	3	0.33	2.60	1.05
5.02	10	1-Pen	1.22	1740	-10	15	0.57	4.40	1.05
5.03	10	1-Hex	1.40	1670	-10	15	1.05	6.65	1.06
5.04	20	1-Hex	1.40	1670	-10	15	1.08	3.83	1.05
5.05	20	1-Oct	1.12	1000	-10	18	0.82	3.37	1.06
5.06	10	1,5-HD	1.15	1400	0	15	0.77	8.02	1.04

Conditions: 10 μ mol of **01** and 10 μ mol of **35** were used in 10 mL of toluene.

The data in Table 9 clearly showed the success of living CCTP of these monomers for the first time. As expected, the number of polymer chains (estimated by the ratio of yield/ M_n) was determined by the total amount of alkyl groups on both zinc and hafnium, and it can be freely adjusted by the equivalents of ZnEt₂ added (Entries 5.03 and 5.04). The very narrow polydispersity of the polymer samples obtained (PDI: 1.04-1.06), together with the monomodal and symmetric nature of all GPC curves, displayed the living character of the polymerization process *via* **35**.

5.1.2 Living property shown by the kinetic study for the CCTP of 1-hexene

In addition to the extremely narrow molecular weight distribution, the living character was further confirmed by the kinetics of 1-hexene's CCTP. The experiment

was performed as following: in a 250-mL Schlenk flask, to a solution of **01** (20.0 mg, 25.0 μmol) in 25 mL of toluene at 0 °C were added **35** (11.4 mg, 25.0 μmol), and ZnEt_2 (206 mg, 10 eq) as a 1.1 M solution in toluene and 1-hexene (2.10 g, 1000 eq) with stirring. Aliquots were taken at 0, 1h, 2h, 3.5h, 5h, 7h and 11h, and quenched with silica gel. The relative concentration of 1-hexene in the toluene solution was determined by gas chromatography. The values are 100, 70.6, 55.1, 38.5, 26.4, 15.4 and 4.9 respectively. Conversions are 0, 29.4%, 44.9%, 61.5%, 73.6%, 84.6% and 95.1% respectively.

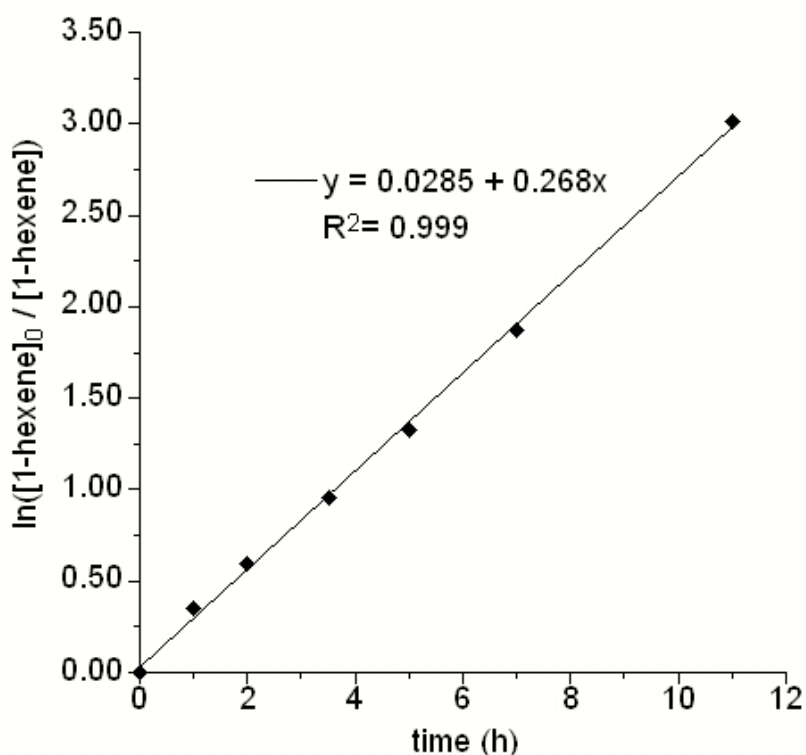


Figure 39: Kinetic analysis of the living CCTP of 1-hexene with ZnEt_2

As shown in Figure 39, the polymerization was a first order reaction with respect to the monomer. That is to say, the amount of catalyst didn't change during the polymerization process, at least for the time period studied. This demonstrated that

the polymerization proceeded in a living fashion. The kinetic model can be seen from the following equations:

$$R_p = -\frac{d[M]}{dt} = k_p[Hf][M] \Rightarrow -\frac{d[M]}{[M]} = k_p[Hf]dt \Rightarrow \ln \frac{[M]_0}{[M]} = k_p[Hf] \cdot t$$

Here R_p is the polymerization rate, and the monomer M is 1-hexene. When $[Hf]$ is a constant, we got the kinetic equation: $\ln \frac{[M]_0}{[M]} = k_p' \cdot t$

As a comparison, I need point out that for the kinetic study of propene CCTP polymerization (Figure 24), the monomer concentration was constant due to the maintained pressure of propene. So the polymerization rate was also a constant, and the yield, which in turn determined the molecular weight, was proportional to the reaction time when a stable catalyst was employed and the moles of polymer produced didn't change.

5.1.3 Polymer structural elucidation by NMR spectroscopy

High field NMR spectroscopy was used to elucidate the structures of newly synthesized polymers using CCTP technique. All the expected peaks were shown in the spectra obtained.¹³³ For example, in the ^{13}C NMR spectrum of poly-1-octene, eight separate signals were seen, and the polymer possessed an atactic structure (Figure 40). Other ^1H and ^{13}C NMR spectra of poly(higher α -olefin)s are attached in Appendix II.

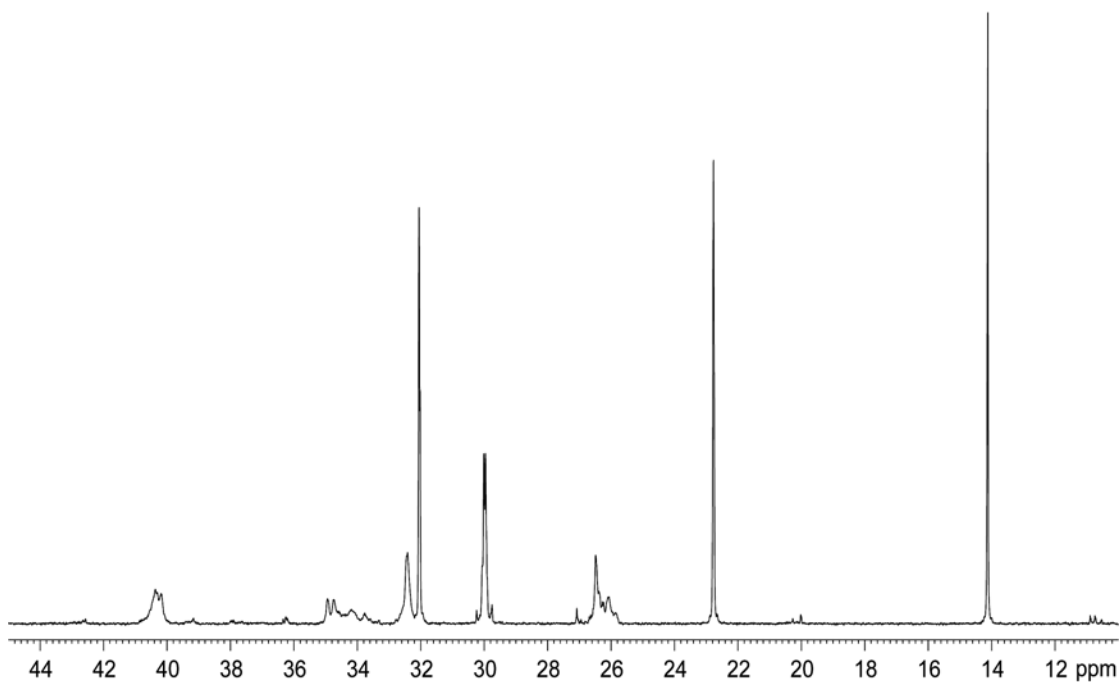


Figure 40: ^{13}C $\{^1\text{H}\}$ NMR (150 MHz, CDCl_3 , 20 $^\circ\text{C}$) spectrum of poly-1-octene from Entry 5.05 of Table 9.

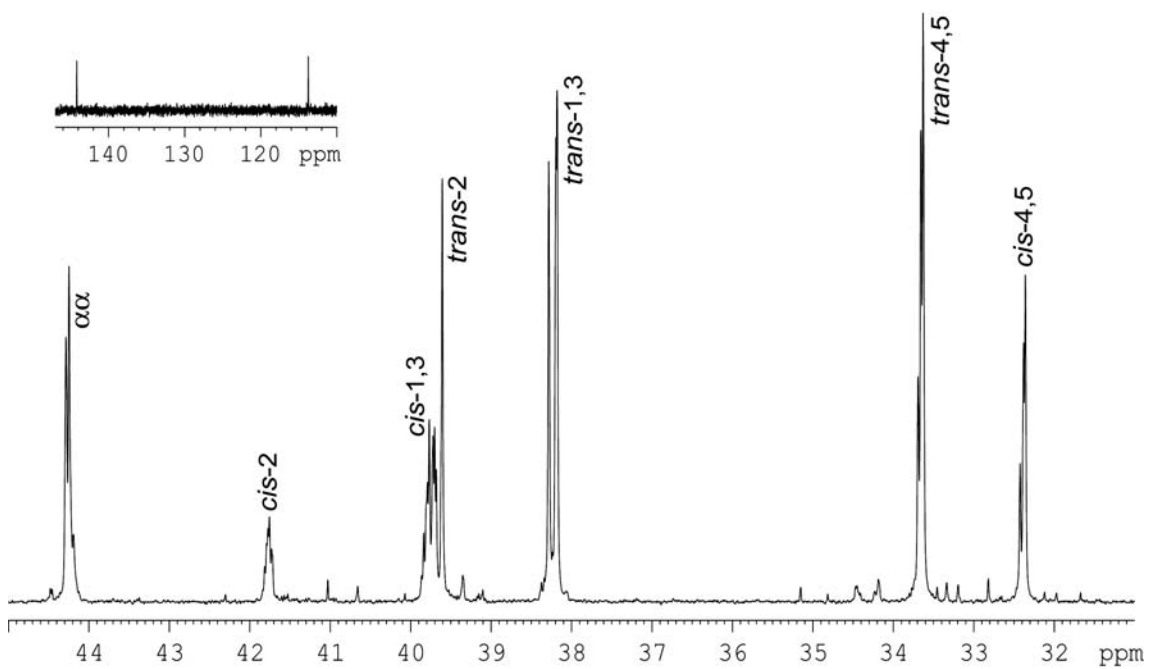


Figure 41: ^{13}C $\{^1\text{H}\}$ NMR (150 MHz, $1,1,2,2\text{-C}_2\text{D}_2\text{Cl}_4$, 90 $^\circ\text{C}$) spectrum of PMCP from Entry 5.06 of Table 9. The spectrum on the top left shows resonances arising from 1,2-insertion of 1,5-hexadiene.

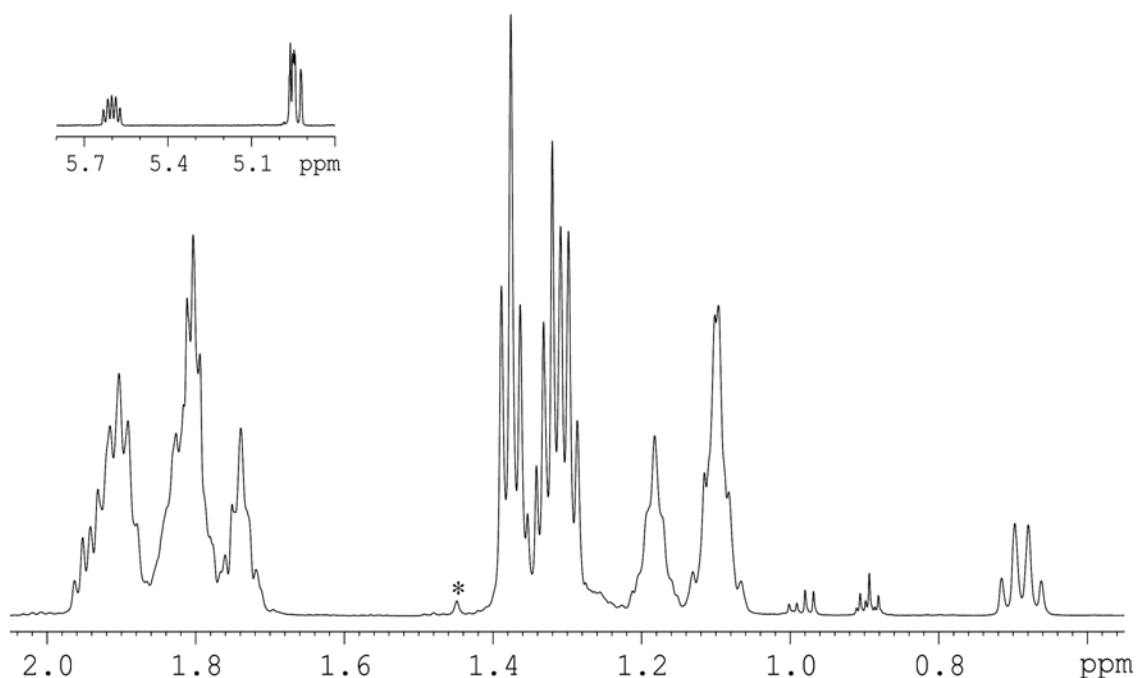


Figure 42: ¹H NMR (600 MHz, 1,1,2,2-C₂D₂Cl₄, 90 °C) spectrum of PMCP from Entry 5.06 of Table 9. The spectrum on the top left shows resonances arising from 1,2-insertion of 1,5-hexadiene. The resonance marked by an asterisk (*) is from a trace amount of water.

Figures 41 and 42 showed the ¹H and ¹³C NMR spectra of poly(methylene-1,3-cyclopentane) (PMCP) obtained from 1,5-hexadiene (1,5-HD).^{57, 134-136} We can see that the propagation of 1,5-HD proceeded almost exclusively by a cyclopolymerization process to provide PMCP with a 2:1 of *trans*: *cis* ratio, and there was only a tiny amount of pendant vinyl groups due to the non-cyclized 1,2-insertion of 1,5-HD.

5.2 CCTP Random Copolymerization of Propene with Higher α -olefins or 1,5-HD

5.2.1 Description of CCTP copolymerization of propene with higher α -olefins and 1,5-hexadiene

With the success of CCTP polymerization of both propene and higher α -olefins, it is not too surprising to accomplish the random CCTP copolymerization of propene with higher α -olefins. The experiments were delivered in the same fashion as the homopolymerization of higher α -olefins (Section 5.1.1), except 5 psi of propene was charged after addition of the comonomer and the propene pressure was maintained until the reaction mixture was quenched with a small amount of methanol. The experimental details are provided in Table 10.

Table 10: Living random CCTP copolymerization of propene with higher α -olefins and 1,5-hexadiene

Entry	ZnEt ₂	Comonomer			t _p	Yield	M _n	PDI	co-%
	(equiv.)	Identity	(g)	(equiv.)	(h)	(g)	(kDa)		
5.07	20	1-Hex	0.84	500	3	3.25	6.90	1.09	16.4
5.08	20	1-Oct	0.56	250	3	3.50	7.65	1.08	10.1
5.09	20	1-Dod	1.68	500	3	3.53	8.07	1.09	10.7
5.10	20	1,5-HD	1.64	1000	3	3.34	7.24	1.08	--

Conditions: 20 μ mol of **01** and 20 μ mol of **35** were used, total volume of toluene was 20 mL, and temperature was set up at 20°C; the copolymer incorporation content co-% (molar percentage) was calculated based on NMR analysis.

We can see, for all the propene copolymers including that with 1,5-hexadiene, the molecular weights are dictated by the amount of chain transfer agent added as

expected by the mechanism of an efficient CCTP process. Again, the polydispersity was very narrow for all the samples ($PDI \leq 1.1$), which indicates the living character of the CpAm hafnium system *via* **35**.

5.2.2 An example of propene copolymer structure illustrated by ^{13}C NMR

The structural information of these propene copolymers was provided by NMR spectroscopy. Figure 43 shows the ^{13}C NMR spectrum of poly(propene-*co*-1-dodecene), in which the peak assignments were also carried out.^{137, 138} Other NMR spectra of these propene copolymers are included in Appendix II.

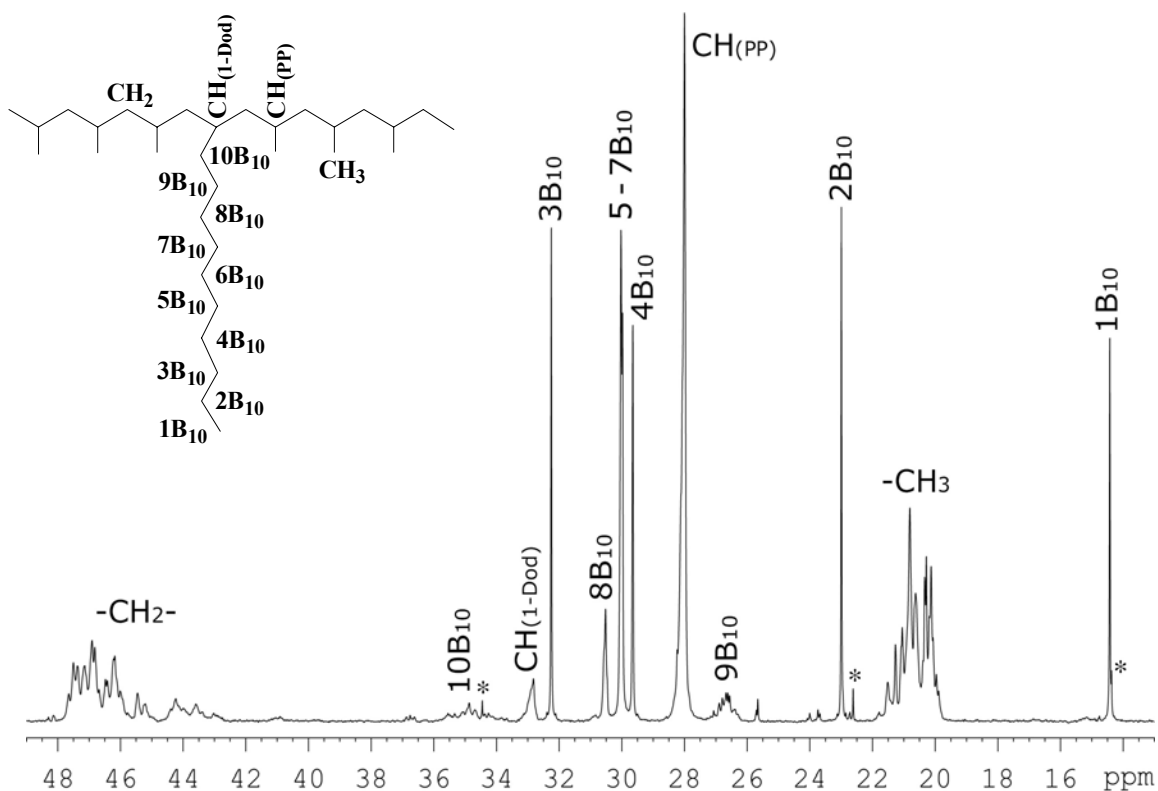


Figure 43: ^{13}C $\{^1\text{H}\}$ NMR (150 MHz, 1,1,2,2- $\text{C}_2\text{D}_2\text{Cl}_4$, 90 °C) spectrum of poly(propene-*co*-1-dodecene) from Entry 5.09 in Table 10. Peaks marked by asterisks are from *n*-pentane.

5.3 CCTP Random Copolymerization of Ethene with Higher α -olefins or 1,5-HD

5.3.1 Description of CCTP copolymerization of ethene with higher α -olefins and 1,5-hexadiene

The copolymerization of ethene with higher α -olefins and 1,5-HD was also successfully realized by the CCTP system with ZnEt_2 via **35**. This was somewhat surprising when we noticed that the polymerization activity of ethene was much higher than that of higher α -olefins or α,ω -nonconjugated dienes. The presence of ethene helped the enchainment of other olefins. The copolymerization reactions were also performed in the same fashion as the homopolymerization of higher α -olefins (Section 5.1.1), except ethene was charged under a positive pressure right after addition of the comonomer and the pressure was maintained until the reaction mixture was quenched with methanol. Details are provided in Table 11.

Table 11: CCTP copolymerization of ethene with higher α -olefins and 1,5-HD

Entry	ZnEt_2 (equiv.)	Comonomer			Tol (mL)	t_p (min)	Yield (g)	PE %mol	M_n (kDa)	PDI
		identity	(g)	(equiv.)						
5.11	20	1-Hex	1.26	1500	40	60	2.79	84	13.0	1.16
5.12	50	1-Hex	1.26	1500	40	60	2.56	82	5.91	1.24
5.13	20	1-Oct	1.68	1500	40	60	2.47	80	10.4	1.14
5.14	20	1-Oct	1.12	1000	25	60	2.60	88	12.1	1.15
5.15	20	1-Oct	1.12	1000	40	30	1.60	91	8.87	1.25
5.16	20	1,5-HD	1.23	1500	40	60	2.45	85	14.8	1.06
5.17	50	1,5-HD	1.23	1500	40	60	2.34	84	6.22	1.11

Notes: 10 μmol of **01** and 10 μmol of **35** were used at 25 $^\circ\text{C}$; PE %mol was determined by NMR. Products also contained a tiny amount of insoluble polymer.

From the amount of catalyst and chain transfer agent added, the molecular weight and yield of PE copolymers obtained, again, we can conclude that the efficient reversible chain transfer process was going on for the random CCTP copolymerization of ethene with 1-hexene, 1-octene and 1,5-hexadiene *via* **35**. The narrow molecular weight distribution once again indicated the living property of the catalytic system. The PDI value was slightly higher (~ 1.2) in several cases, suggesting that chain transfer process in the ethene copolymerization was not as rapid as that in other CCTP process previously described. The molecular weight of the resulting copolymer depended on several factors, such as time (Entry 5.13 vs. 5.15), concentration (Entry 5.13 vs. 5.14), and finally the equivalents of ZnEt_2 (Entry 5.11 vs. 5.12, and 5.16 vs. 5.17) as expected from the mechanism of CCTP. However the equivalents of ZnEt_2 had no influence on the comonomer content enchainned.

DSC analyses displayed different thermal behaviors for all the PE copolymer from the corresponding homopolymers. In fact, the PE-*co*-PMCP products possessed unique melting points (T_m 87 °C for Entry 5.16, 76 °C for 5.17), showing the homogeneity of the copolymers.

5.3.2 Detailed structural analysis of PE copolymers by NMR spectroscopy

High field ^1H and ^{13}C NMR spectroscopy was used as a powerful tool to illustrate the structures of polymer products. The illustrative structures of PE-*co*-PH, PE-*co*-PO and PE-*co*-PMCP are shown in Figure 44, and their ^{13}C NMR spectra are shown in Figures 45-47 with detailed assignments for all the defined peaks.¹³⁹ The ^1H NMR spectra are attached in Appendix II. For these PE copolymers, the comonomer units were almost exclusively separated by the ethene units. The copolymer chains

only contained a tiny amount of block component (as shown by $\alpha\alpha$ for the consecutive comonomer diads, H-H, O-O or HD-HD) and alternating structure (as shown by $\beta\beta$ and $\alpha\gamma$ for the alternative triads H-E-H, O- E-O or HD- E-HD). This indicated that the comonomer tended to be polymerized following ethene instead of itself. The previously inserted ethene unit facilitated the coordination and/or insertion of other olefins presumably because of the steric effect. In the ^1H NMR spectrum of PE-*co*-PMCP, no signal was detected in the vinyl region, which suggested that 1,5-HD underwent exclusive cyclopolymerization without any double bond left. The cyclopentane ring formed also exhibited more *trans* configuration than *cis* (Figure 47).

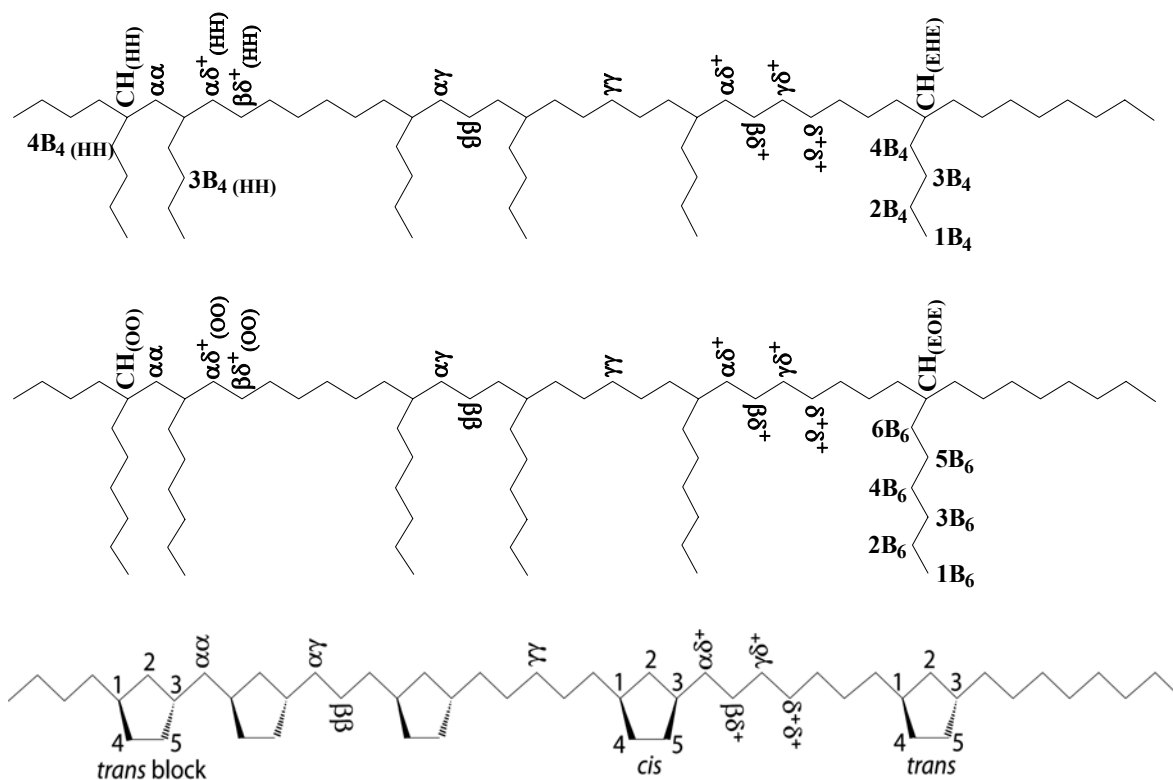


Figure 44: Illustrative structures of poly(ethene-*co*-1-hexene) from Entry 5.11 (top), poly(ethene-*co*-1-octene) from Entry 5.13 (middle) and PE-*co*-PMCP from Entry 5.16 of Table 11 (bottom).

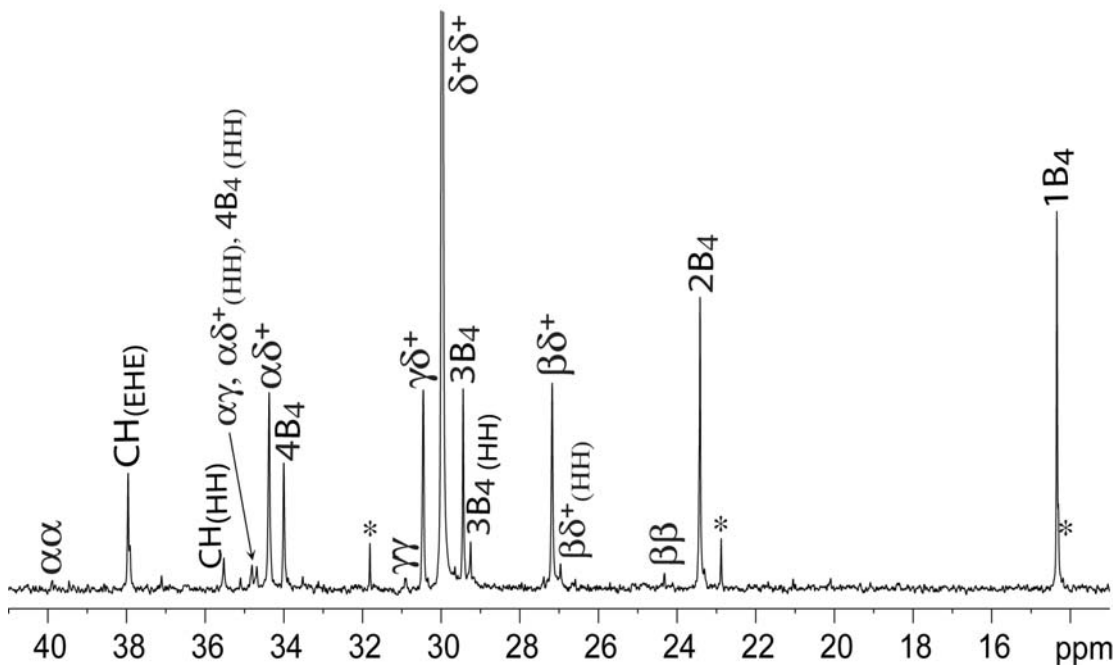


Figure 45: ^{13}C $\{^1\text{H}\}$ NMR (150 MHz, 1,1,2,2- $\text{C}_2\text{D}_2\text{Cl}_4$, 90 °C) of poly(ethene-co-1-hexene) from Entry 5.11 of Table 11. Resonances for trace hexane are marked with asterisks (*).

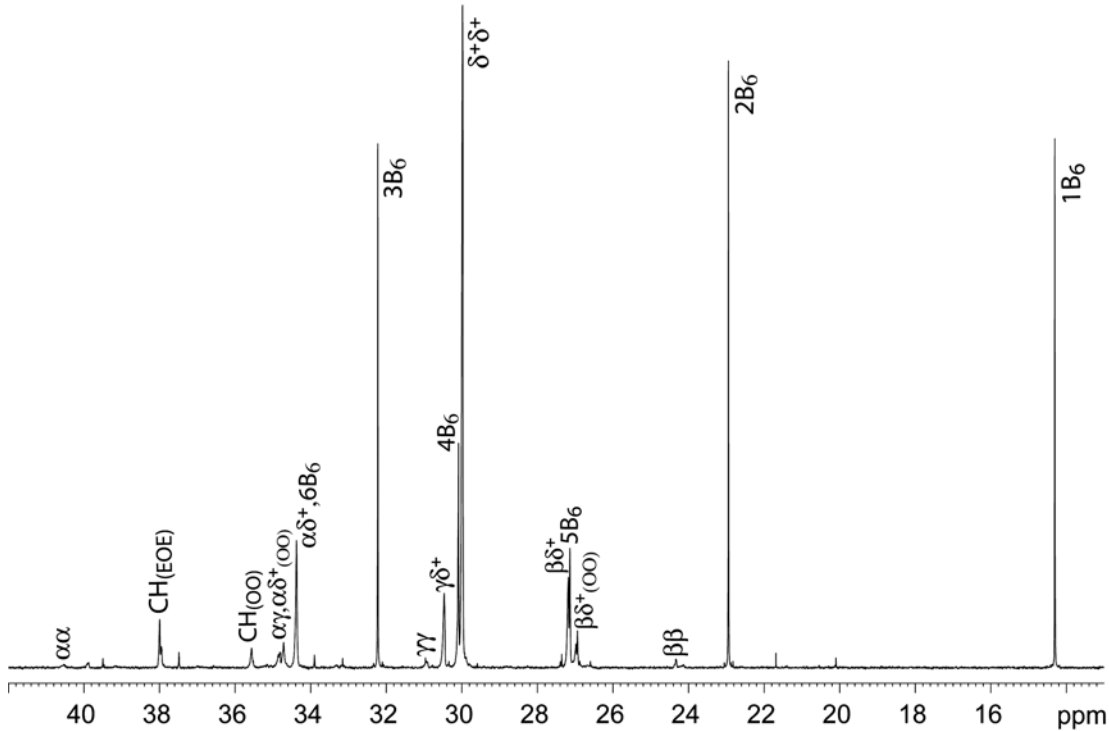


Figure 46: ^{13}C NMR (150 MHz, 1,1,2,2- $\text{C}_2\text{D}_2\text{Cl}_4$, 90 °C) spectrum of poly(ethene-co-1-octene) from Entry 5.13 in Table 11.

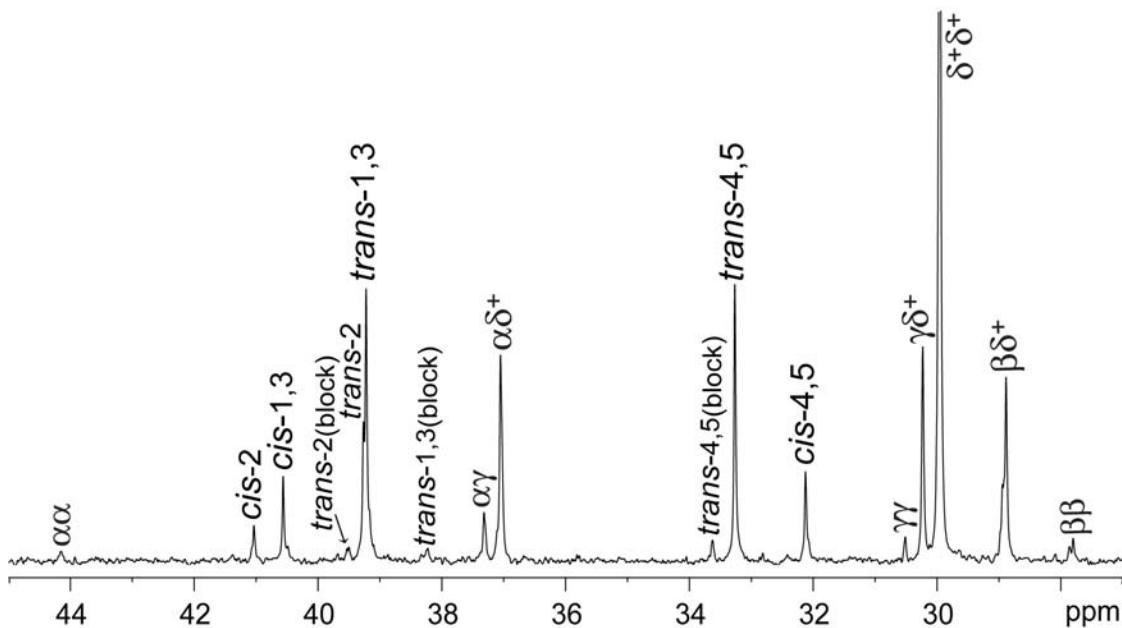


Figure 47: ^{13}C $\{^1\text{H}\}$ NMR (150 MHz, 1,1,2,2- $\text{C}_2\text{D}_2\text{Cl}_4$, 90 $^\circ\text{C}$) of poly(ethene-co-PMCP) from Entry 5.16 of Table 11.

5.4 CCSP Copolymerization of Ethene and 1-octene with Dual Precatalysts

Different catalysts displayed different homopolymerization behaviors for the same monomer, and/or different copolymerization behaviors for the same set of monomers. The resultant (co)polymers showed different mechanical properties associated with their structures. If we can combine two catalysts into one catalytic system and produce a monomodal polymer through a chain transfer process, the desired characters derived from both catalysts might be combined together within one polymer molecule. Stereoblock polypropene was produced from a mixture of catalysts with different stereoselectivity. This topic will be discussed in the next chapter in detail. Dow Chemical made multiblock copolymer of ethene and 1-octene as described in Chapter 1.¹⁴⁰ Herein the CCSP random copolymerization of ethene and 1-octene was realized using two recently developed CpAm precatalysts and the

comonomer incorporation rate was adjusted by the relative ratio of these two precatalysts.

The random CCTP copolymerization of ethene with 1-octene *via* **35** was already discussed in Section 5.3.1. To realize the CCSP by two different precatalysts, the CpAm zirconium complex (1,3-^tBu₂-η⁵-C₅H₃)ZrMe₂[N(Et)C(Me)N(^tBu)] (**48**) was selected to provide a lower comonomer incorporation rate. **48** was also found to be an effective precatalyst for the living CCTP of ethene when being activated by [PhNHMe₂][B(C₆F₅)₄] (**48**). But this combination **48** of **48** and was not active towards the polymerization of propene or higher α-olefins. For the ethene copolymerization, **48** incorporated a small amount of 1-octene into the polyethene chain, and the comonomer content was much lower than that *via* **35** (Entry 5.18 vs. 5.21 in Table 12).

Table 12: CCSP copolymerization of ethene and 1-octene *via* **35** and **48**

Entry	35	48	t _p (min)	Yield (g)	M _n (kDa)	PDI	co-%
	(μmol)	(μmol)					
5.18	20	0	60	4.29	8.53	1.21	18.5%
5.19	4	16	60	3.03	6.54	1.24	15.2%
5.20	2	18	60	2.66	5.80	1.29	13.4%
5.21	0	20	30	0.79	--	--	2.4%

Conditions: 20 μmol of **01**, 2.24 g (1000 eq) of 1-octene, and 20 equivalents of ZnEt₂ were used; total volume of toluene, 40 mL; T_p, 20 °C. Comonomer content co-% was determined by NMR.

The CCSP random copolymerization *via* **35** and **48** was delivered in the same manner as the CCTP random copolymerization *via* **35** with the only difference being that **48** was added immediately after the addition of **35**. The experimental details are

summarized in Table 12. We can see that the comonomer content decreased with more **48** used. This trend is also illustrated by the ^1H and ^{13}C NMR spectra of the copolymers obtained. In Figure 48, the intensity of the triplet (0.91 ppm) for the methyl group in the pendant side chain (from 1-octene) changed gradually relative to the polyethylene backbone peak at 1.30 ppm. Figure 49 clearly shows that the intensity of all the three peaks for 1B₆, 2B₆ and 3B₆ changed gradually relative to the biggest peak for $\delta^+\delta^+$ carbons (see Figures 44 and 46 for peak assignments).

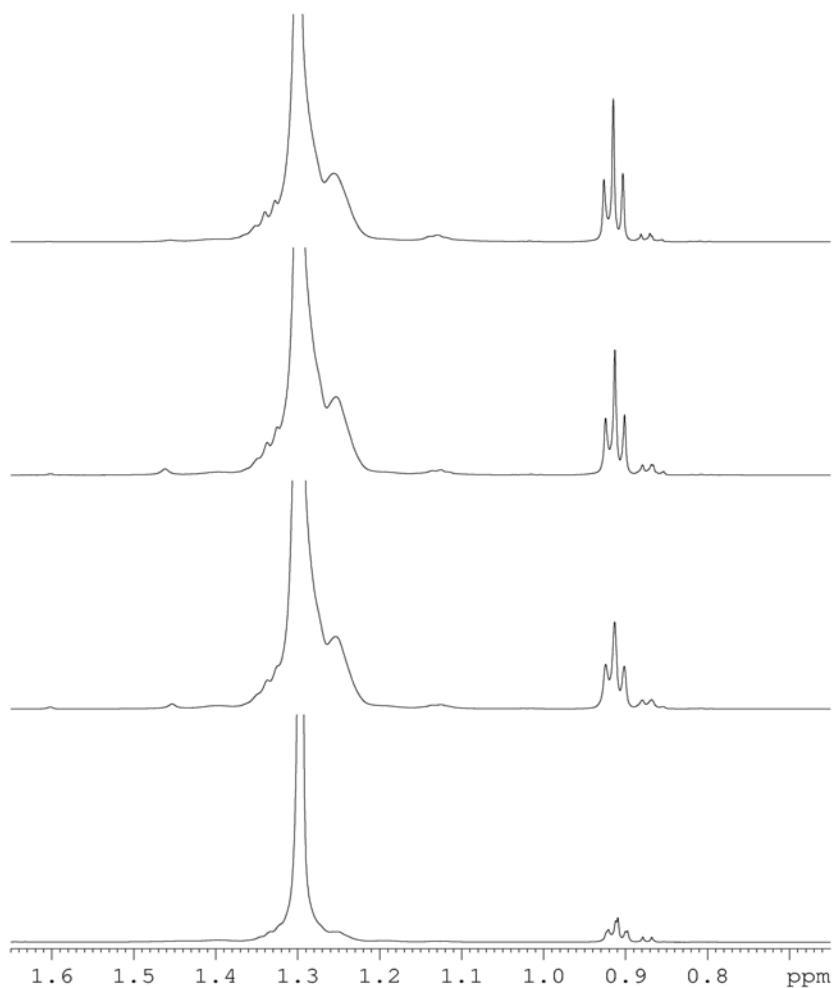


Figure 48: ^1H NMR (600 MHz, 1,1,2,2- $\text{C}_2\text{D}_2\text{Cl}_4$, 90 °C) spectra of PE-*co*-PO obtained from CCSP *via* varied ratios of **35** and **48** activated by **01** (top to bottom: Entries 5.18-5.21). Peaks at 1.30 ppm were normalized to the same height.

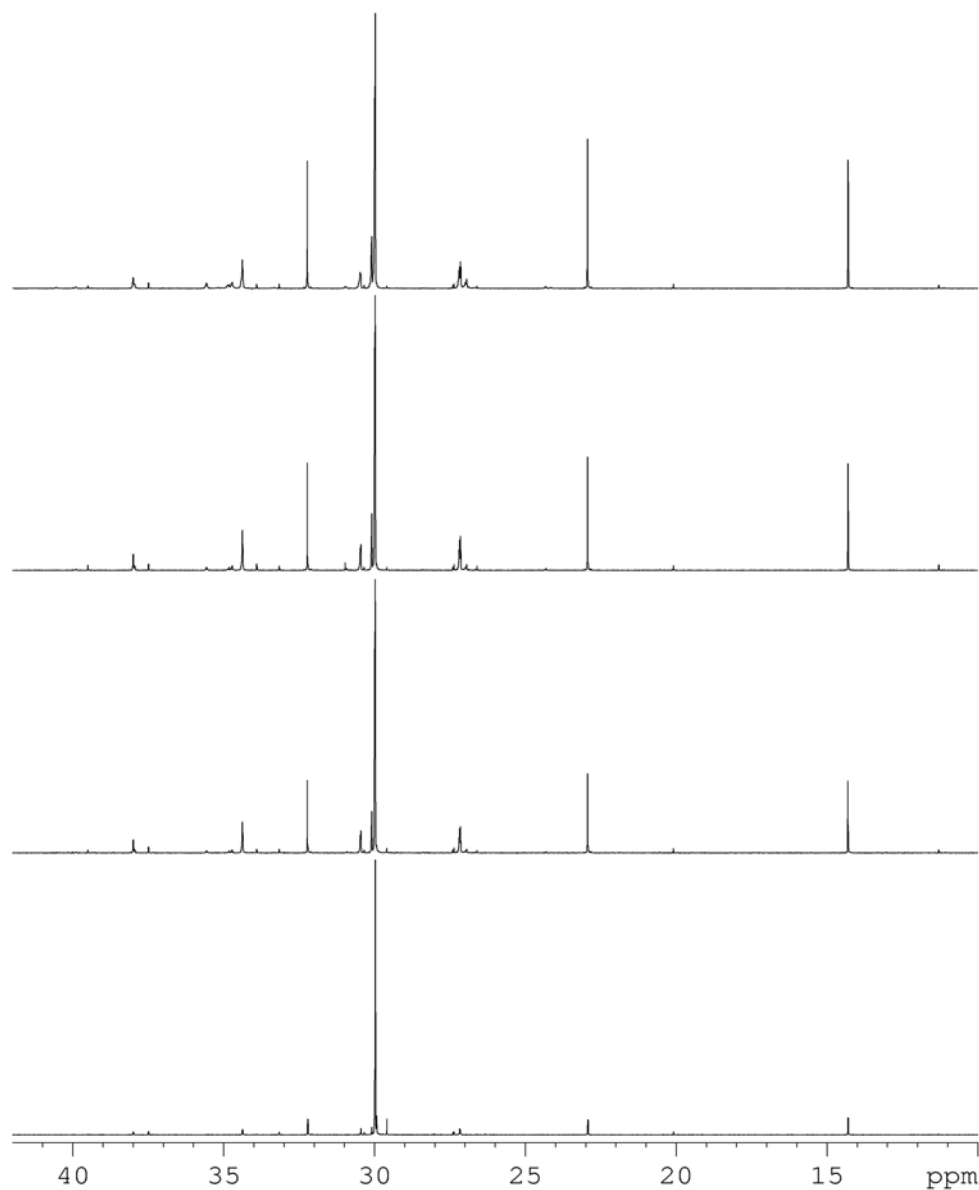


Figure 49: ^{13}C $\{^1\text{H}\}$ NMR (150 MHz, $1,1,2,2\text{-C}_2\text{D}_2\text{Cl}_4$, 90 °C) spectra of PE-co-PO obtained from CCSP via varied ratios of **35** and **48** activated by **01** (top to bottom: Entries 5.18-5.21).

5.5 CCSP Random Copolymerization in a Dual Cocatalyst System

5.5.1 CCSP copolymerization of ethene and 1-hexene with two cocatalysts

The different comonomer selectivity can be obtained not only with different precatalysts, but also with different cocatalysts. The latter provides the counterion for

the active center, thus different ion pairs (e.g. loose and tight) can be formed and might display different copolymerization behaviors. This new strategy was realized for the first time during the CCSP random copolymerization of ethene and 1-hexene *via* **35** activated by the cocatalysts **01** and **03**. Experiments were carried out in the same manner as that for the CCTP random copolymerization described in Section 5.3.1, except **03** was also dissolved in toluene together with **01**. See Table 13 for details.

Table 13: CCSP random copolymerization of ethene and 1-hexene with ZnEt_2 *via* **35** activated by different amount of **01** and **03**

Entry	01	03	Yield (g)	M_n (kDa)	PDI	co-%
	(μmol)	(μmol)				
5.22	0	20	1.02	--	--	5.1%
5.23	4	16	1.48	4.29	1.21	15.1%
5.24	10	10	1.65	3.79	1.21	25.9%
5.25	20	0	1.68	3.50	1.20	38.7%

Conditions: 20 μmol of **35**, 1.68 g (1000 eq) of 1-hexene, and 20 equivalents of ZnEt_2 were used; total volume of toluene, 40 mL; T_p , 20 °C; t_p , 30 min. Comonomer content co-% (molar percent) was determined by NMR.

The obtained copolymer samples were monomodal and had narrow polydispersity indices as shown by GPC analysis. The comonomer content was reliant on the ratio of the two cocatalysts employed. In Figures 50 and 51 we can see that the methyl group originally from 1-hexene has a triplet peak at 0.92 ppm in the ^1H NMR and a resonance at 14.3 ppm in the ^{13}C NMR. Its content increased with an increasing amount of **01** versus **03**, as we expected from the CCSP system *via* **35** activated by

two cocatalysts possessing different levels of comonomer incorporation rate. The trend here was similar to that from the dual precatalyst CCSP system, but it was realized with a new strategy. The dual cocatalyst CCSP system might give rise of some new features in the future studies.

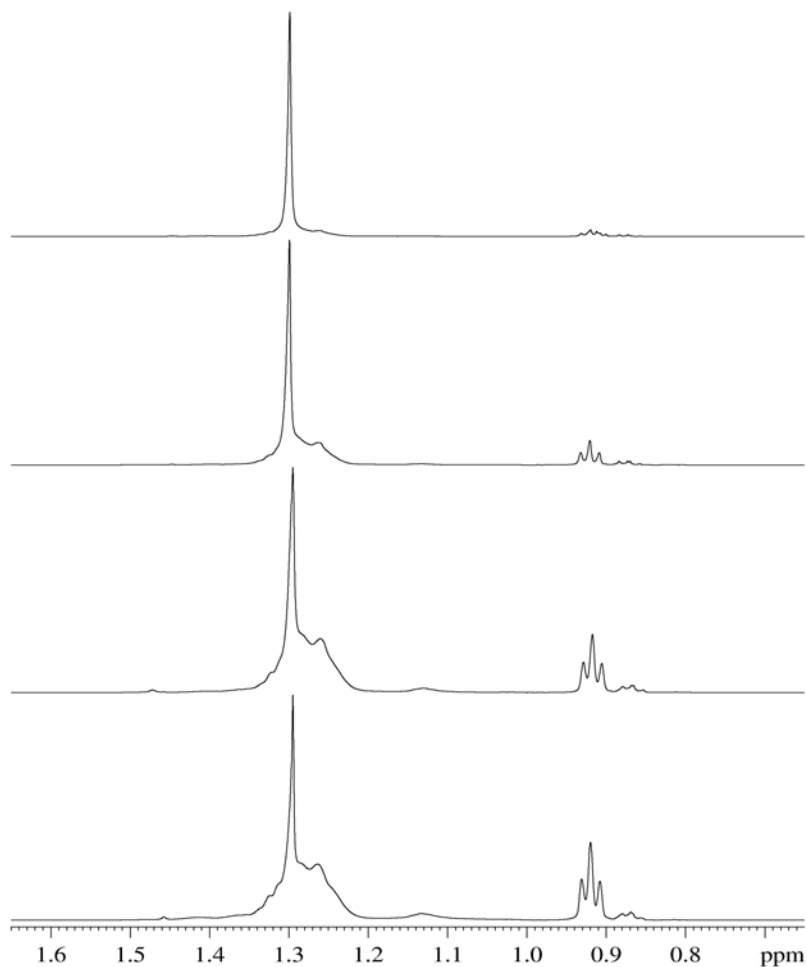


Figure 50: ^1H NMR (600 MHz, $1,1,2,2\text{-C}_2\text{D}_2\text{Cl}_4$, $90\text{ }^\circ\text{C}$) spectra of PE-co-PH obtained from CCSP via **35** activated by varied ratios of **01** and **03** (top to bottom: Entries 5.22-5.25).

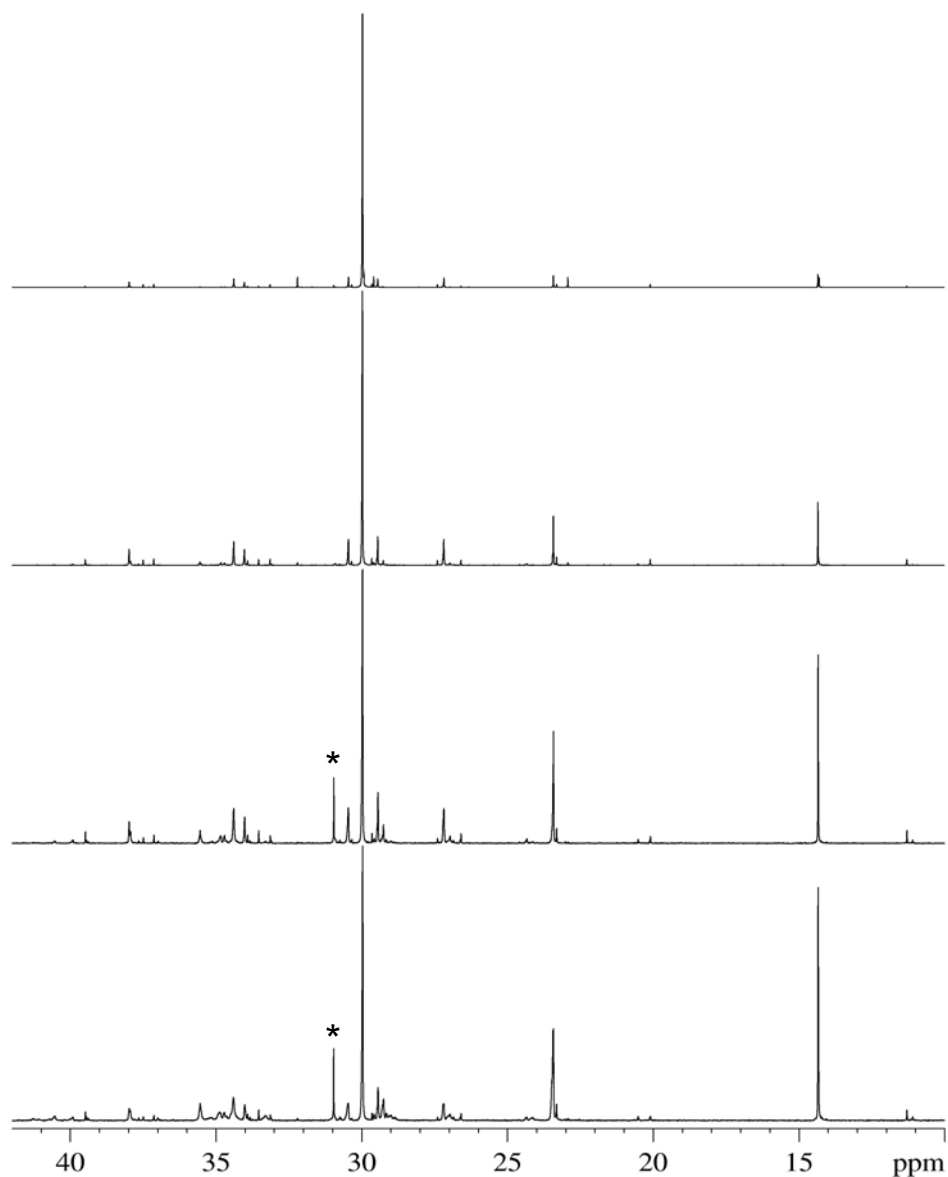


Figure 51: $^{13}\text{C} \{^1\text{H}\}$ NMR (150 MHz, $1,1,2,2\text{-C}_2\text{D}_2\text{Cl}_4$, 90 °C) spectra of PE-*co*-PH obtained from CCSP *via* **35** activated by varied ratios of **01** and **03** (top to bottom: Entries 5.22-5.25). The peak marked by * was from acetone.

5.5.2 CCSP copolymerization of ethene and 1,5-HD with dual cocatalysts

The strategy of CCSP between different ion pairs was further displayed by the random copolymerization of ethene and 1,5-hexadiene. Experiments were performed in the same manner as Entry 5.16 of Table 11 except two cocatalysts, **01** and **03**, were

used instead of only one. Experimental details are shown in Table 14. Successful adjustment of the comonomer incorporation level by different amounts of two cocatalysts can be seen from both the ^1H NMR (Figure 52) and the partial ^{13}C NMR spectra (Figure 53, peak assignments follow Figures 44 and 47).

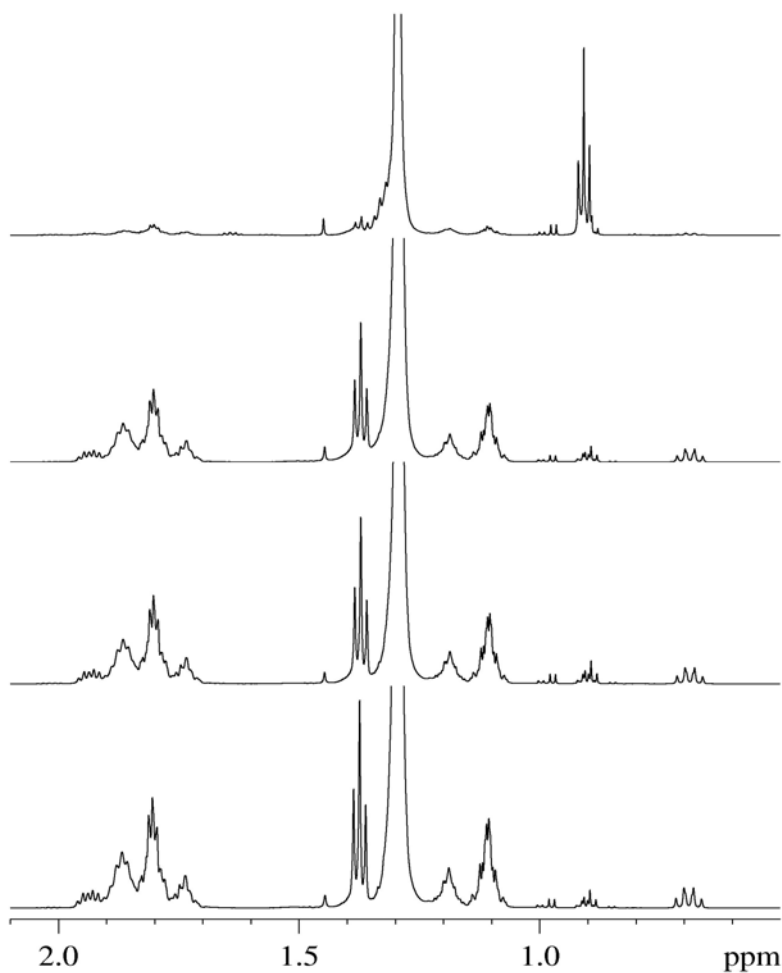


Figure 52: ^1H NMR (600 MHz, $1,1,2,2\text{-C}_2\text{D}_2\text{Cl}_4$, 90 °C) spectra of PE-*co*-PMCP obtained from CCSP *via* **35** activated by varied ratios of **01** and **03** (top to bottom: Entries 5.26-5.28 and 5.16).

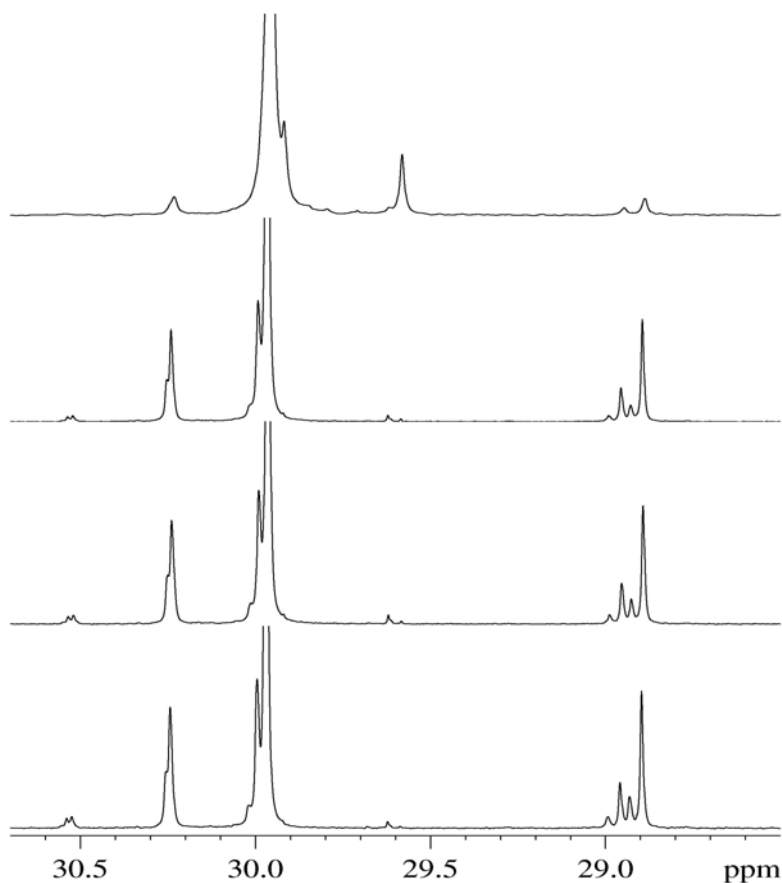


Figure 53: Partial ^{13}C $\{^1\text{H}\}$ NMR (150 MHz, 1,1,2,2- $\text{C}_2\text{D}_2\text{Cl}_4$, 90 °C) spectra of PE-*co*-PMCP obtained from CCSP via **35** activated by varied ratios of **01** and **03** (top to bottom: Entries 5.26-5.28 and 5.16).

Table 14: CCSP of ethene and 1,5-hexadiene via **35** activated by **01** and **03**

Entry	ZnEt ₂ (equiv.)	01 (μmol)	03 (μmol)	t_p	Yield (g)	M_n (kDa)	PDI	co-%
5.26	50	0	10.0	30	0.37	1.16	1.07	3.3%
5.27	20	5.0	5.0	60	2.23	9.72	1.26	12.8%
5.28	20	6.7	3.3	60	2.32	10.7	1.09	13.6%
5.16	20	10.0	0	60	2.45	14.8	1.06	14.9%

Conditions: 10 μmol of **35**, 1.23 g (1500 eq) of 1,5-HD, and 20 equivalents of ZnEt₂ were used; total volume of toluene, 40 mL; T_p , 25 °C. Comonomer content co-% (molar percent) was determined by NMR spectroscopy.

5.6 Conclusions

The living CCTP polymerization of higher α -olefins and α,ω -nonconjugated dienes was realized for the first time *via* **35**. The molecular weight of polymers obtained was adjusted by the amount of chain transfer agent employed, and the molecular weight distribution was very narrow.

The CCTP random copolymerization of higher α -olefins and 1,5-hexadiene with propene or ethene was also successfully achieved. The structures of the copolymers obtained were studied by high field ^1H and ^{13}C NMR spectroscopy. CCTP provided not only an appreciable amount of (co)polymers in an economic way, but also some new fundamental structures for further study on their physical properties.

The first example of CCSP process with different cocatalysts was also accomplished for the ethene copolymerization with 1-hexene and 1,5-hexadiene. This provided an alternative way for the CCSP process with dual precatalysts as shown by the copolymerization of ethene and 1-octene *via* **35** and **48**.

Chapter 6: Multi-stereoblock Polypropene by CCSP with ZnEt_2 between CpAm Group 4 Metal Catalysts

6.1 Background

6.1.1 Well-defined stereoblock PP *via* TLCP technique

The stereoblock structure was proposed as early as fifty years ago to explain the physical properties of polypropene produced.¹⁴¹ Currently a lot of efforts are taken to prepare stereoblock copolymers for their potential application as thermoplastic elastomers, in which the hard, crystalline segments provide conjunctions for the soft, amorphous network.^{142, 143} The semicrystalline property of thermoplastic elastomers can be obtained from polymer blends, random copolymers and block copolymers. Block copolymers have a homogeneous constitution which prevents macrophase separation in a long term, and attract much attention. Stereoblock copolymers also have the advantage of simple monomer supply during the production.

In the past two decades, with the development of single-site metallocene and post-metallocene catalysts, especially those suitable for living coordination polymerization, polyolefin based thermoplastic elastomers were rapidly developed and some commercial materials were produced from them.^{144, 145} Stereoblock polypropenes were also reported recently and some attractive properties were studied. First example of stereoblock polypropene I am going to present was made from the programmable SCTL polymerization.⁶² By turning SCTL on and off, atactic and isotactic PP blocks were obtained in sequence and several blocky structures were made successfully. Herein another new type of well-defined stereoblock PP, *iso-a-iso*

PP was prepared with isotactic PP blocks on both ends. The hard-soft-hard constitution was expected to possess high mechanical strength. Its microstructure was illustrated by ^{13}C NMR spectroscopy and compared with the multi-stereoblock PP obtained by CCSP.

Coates and coworkers reported a polypropene copolymer of isotactic and regioirregular blocks by a strategy of changing the polymerization temperature to influence the microstructure of PP.¹⁴⁶ Different from the strategy of activation level or temperature manipulation, Shiono and coworker used different solvents¹⁴⁷ or changed the monomer pressure¹⁴⁸ to make syndiotactic-atactic stereoblock polypropenes.

6.1.2 Stereoblock PP obtained through chain transfer process

Well-defined stereoblock PP was successfully achieved with the technique of living coordinative polymerization. However, all the procedures mentioned above included substantial changes of experimental conditions when switching to the next block. It also had the limitation of only one polymer chain produced by one catalytic metal center, resulting in a high price of the final product. The coordinative chain shuttling polymerization (CCSP) provided a solution to these problems, and at the same time maintained the living character.

Chien and coworkers^{149, 150}, and Brintzinger and Lieber¹¹³ independently reported the synthesis of stereoblock PP by reversible chain transfer with alkyl aluminum between two catalysts with different stereoselectivities. A similar binary metallocene system was also studied by Rytter and coworkers.¹⁵¹ Fink and Pryzbyla¹⁵² investigated an elegant strategy for generating isotactic/syndiotactic PP-block

structures through mixing correspondingly stereoselective metallocenes on carrier surfaces. However, for all these examples, there was only a small portion of stereoblock copolymer in the polymer product obtained. The predominant product was a mixture of atactic and isotactic polymer.

The oscillating system developed by Waymouth and Coates was also used to prepare thermoplastic elastomeric PP and the origin of stereoblocks was attributed to the dynamic configurations of the catalyst.¹⁵³ The study of stereoblock junctions in the PP made by this system was delivered by Busico and coworkers based on ¹³C NMR spectroscopy, which provided a reference for multi-stereoblock PP structures.¹⁵⁴⁻¹⁵⁶ Recently, low molecular weight multi-stereoblock PP ($M_n < 3$ kDa) was synthesized by a chain shuttling system with AlMe₃ employing a enantiomorphous catalyst. The obtained PP structure was confirmed by being compared with that from the enantiopure catalyst under the same conditions.¹¹⁸

Contributing to the area of CCTP, we recently reported the successful polymerization of propene using Cp*Hf(Me)₂[N(Et)C(Me)N(Et)] (**35**) as the precatalyst with a wide range of the chain transfer agent, ZnEt₂ (5-200 equivalents).⁶⁴ Herein we tested a series of monocyclopentadienyl monoamidinate group IV precatalysts (**12**, **04** and **26-28**) under CCTP conditions for the polymerization of propene, and a variety of polymer microstructures were obtained and studied.

To make a multi-stereoblock polypropene using the process of CCSP, two of the precatalysts were selected to provide the PP blocks of different stereochemistry. Control factors on the isotactic content in the final polymers were demonstrated and

discussed in the dual system, including the relative amount of the two precatalysts and equivalents of chain transfer reagent.

6.2 Stereoregular PP by CCTP via Binuclear Catalysts

By using CCTP with ZnEt_2 via **35** we produced amorphous polypropene. To make stereoblock PP, the main task is to find a catalyst which can provide crystalline PP under CCTP conditions. This is a demanding task when a site control mechanism dominates, because the chain transfer process will interrupt the continuous monomer insertion with the same configuration. Our concern was confirmed by the results of CCTP via $\text{Cp}^*\text{Zr}(\text{Me})_2[\text{N}(\text{Et})\text{C}(\text{Me})\text{N}(\text{tBu})]$ (**04**), which provided isotactic PP (*mmmm* 71%) under TLCP conditions when being activated with the cocatalyst $[\text{PhNMe}_2\text{H}][\text{B}(\text{C}_6\text{F}_5)_4]$ (**01**) in chlorobenzene.⁶² The CCTP with ZnEt_2 via **04** turned out to provide only slightly iso-rich PP with an *mm* triad content of 49% (Entry 6.01 of Table 15). Its ^{13}C NMR spectrum is shown in Figure 54.

Table 15: CCTP of propene via a series of CpAm zirconium precatalysts

Entry	Precatalyst		t_p (h)	Yield (g)	M_n (kDa)	PDI	<i>mm</i>
	Identity	(μmol)					
6.01	04	20	15	1.39	3.02	1.13	0.49
6.02	26	10	23	1.10	3.09	1.22	0.63
6.03	27	10	23	1.37	3.75	1.60	0.74
6.04	28	10	23	1.48	4.98	1.70	0.68
6.05	12	20	15	8.17	15.7	1.04	0.26

Conditions: an equal molar amount of cocatalyst **01** and 20 equivalents of ZnEt_2 relative to total Zr centers were added at $-10\text{ }^\circ\text{C}$ into a total volume of 20 mL toluene, under a constant propene pressure of 5psi.

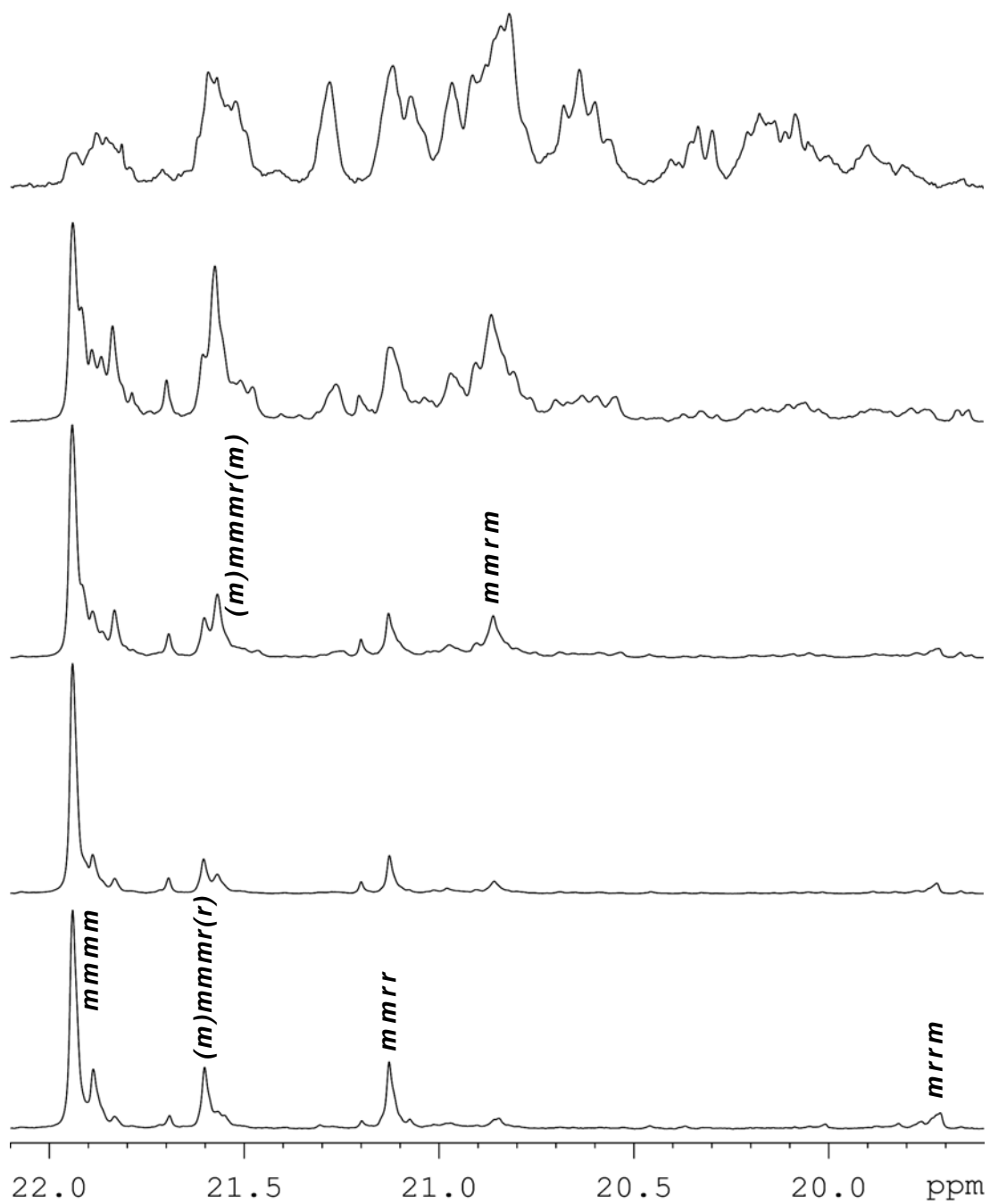


Figure 54: $^{13}\text{C} \{^1\text{H}\}$ NMR (125 MHz, $1,1,2,2\text{-C}_2\text{D}_2\text{Cl}_4$, 70 °C) spectra of methyl region of PP obtained under CCTP by five CpAm zirconium precatalysts (top to bottom: *via* **12**, **04** and **26-28**).

The results of propene CCTP *via* **04** suggested that, to obtain an isotactic structure, we might need to lower the chain transfer rate between the stereoregular catalytic species and chain transfer agent to ensure successive isotactic triads. For CpAm catalysts, another important origin of atactic components should also be considered, which is the amidinate ring-flipping. A higher isotacticity of PP would be associated with a slower ring-flipping process. Recently we developed a series of binuclear zirconium precatalysts which have a common structure of $[(\eta^5\text{-C}_5\text{Me}_5)\text{ZrMe}_2]_2[\text{N}(\text{}^t\text{Bu})\text{C}(\text{Me})\text{N}(\text{CH}_2)_x\text{NC}(\text{Me})\text{N}(\text{}^t\text{Bu})]$ (**26**, $x = 8$; **27**, $x = 6$; **28**, $x = 4$).⁸¹ Under SDTL coordination polymerization conditions, they provided more isotactic PP than the structurally related mononuclear precatalyst **04**. It's easy to imagine that under CCTP conditions, these binuclear catalysts can also provide quite isotactic PP, and the current results proved our expectation.

28 showed a relatively low stereoselectivity (Entry 6.04) due to a short linkage between two zirconium centers. This type of stereoerror resulted in a high frequency of triad *rr* as indicated by the resonances for *mmmr*, *mmrr* and *mrrm* pentads in the $^{13}\text{C} \{^1\text{H}\}$ NMR spectra (Figure 54). A similar trend was also observed in the TLCP *via* **28** (Chapter 2). PP *via* **26** (Entry 6.02) showed a high level of atactic component due to a relative fast chain transfer process with ZnEt_2 and/or rapid amidinate ring-flipping process, which was quite close to what happened when the mononuclear catalyst **04** was used. The chain transfer process produced isolated diad *r*, which can be seen by the resonances for *mmmr* and *mrrm* pentads (Figure 54).

Binuclear complex **27** has a tether length between those of **26** and **28**, and tends to provide both higher stereoselectivity and less atactic component. The PP obtained

from **27** showed small values of both triad rr and isolated diad r (Figure 54). It had an mm content of 74% (Entry 6.03) and behaved as an isotactic PP with a melting point of 101 °C measured by DSC. Thus **27** was selected as the precatalyst to provide isotactic PP blocks in the following studies.

PDI is another important index for the chain transfer process.⁶⁰ To determine whether the polydispersity matches the chain transfer rate, we can compare the PDI values of PP *via* **04** and **26-28** with the corresponding isolated diad r indicated by the pentad contents of $mmmr$ and $mrmr$ in the ¹³C NMR spectra (Figure 54). For a longer tether length ($x = 4$ for **28**, 6 for **27**, 8 for **26**, and ∞ for **04**, from Entries 6.04 to 6.01), a faster chain transfer process between zirconium and zinc was expected, a smaller value of PDI was observed (1.70, 1.60, 1.22 and 1.13, from Entries 6.04 to 6.01), and higher contents of $mmmr$ and $mrmr$ pentads were obtained.

6.3 Pure Atactic PP by CCTP via 12

Now that we have two precatalysts **35** and **27** which can provide both crystalline and amorphous polypropene under CCTP conditions, are we ready to make multi-stereoblock PP by a CCSP process? The answer from the first try was not confirmative. The ¹³C NMR spectra of PP from Entry 6.06 of Table 16 did display a stereoblock structure, but the isotactic content was fairly low (see Appendix II). This result was not a surprise when we noticed the big activity difference between **35**⁺ (6.02 g PP in 2 h, Entry 3.01 in Table 5) and **27**⁺ (1.37 g PP in 23 h, Entry 6.03 in Table 15). The less active catalyst derived from **27** only contributed a small portion to the final yield and the polymer product was mainly made from the hafnium catalyst **35**⁺. This triggered us to explore more catalysts for their CCTP polymerization

behavior, and finally the **12**⁺ was selected as a moderate catalyst to provide atactic PP component in the following CCSP process.

The highly efficient, living coordinative chain transfer polymerization of propene with ZnEt₂ was also successfully achieved using the formamidinate precatalyst Cp*Zr(Me)₂[N(Et)C(H)N(^tBu)] (**12**). It demonstrated a mild activity (8.17 g in 15 h) under CCTP conditions (Entry 6.05 in Table 15), and the polydispersity of the resulting polymer was very narrow (PDI 1.04), indicating the living character of the polymerization system. The PP obtained was purely atactic with trace amount of regioirregular units in the ¹³C {¹H} NMR spectrum (triad contents: *mm* 26%; *mr* 51% and *rr* 23%, Figure 54).

A detailed kinetic study further showed the living property of the CCTP process, see Figure 55. The experiment was carried out as followings: to a solution of **01** (32.0 mg, 40 μmol) in 40 mL toluene at -10 °C were added **12** (15.3 mg, 40 μmol) and (0.66 g, 20 equivalents) ZnEt₂ as a 15 wt% solution in toluene. The reaction flask was then pressurized to 5 psi with propene and the pressure was maintained while stirring. Aliquots were taken every 1 h over a period of 5 h and quenched with methanol. The aliquots were purified by filtration through silica gel and dried *in vacuo*. The rest of the reaction solution was then quenched with 1.0 mL of methanol after 7 h and precipitated into 800 mL of acidic methanol. The final product was collected and dried *in vacuo*. GPC results are presented in Figure 55. The molecular weight of PP increased linearly with the reaction time, at least within the period explored.

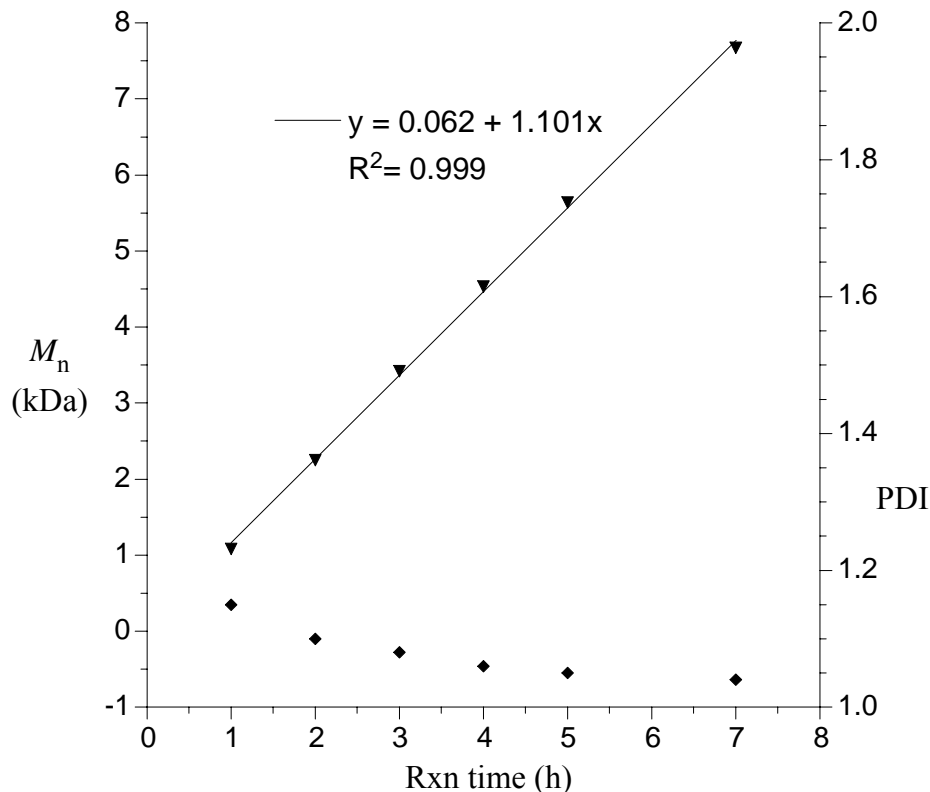


Figure 55: Kinetic study for the polymerization of propene under CCTP *via* **12**

The PDI values of PP obtained kept narrow through the whole polymerization process. However at the beginning, the polydispersity was slightly higher than 1.1 for the low molecular weight samples, then it dropped off gradually to 1.04. This could be explained by the fact that a relatively long time was needed for the chain transfer reagent to equalize all the polymer chain length. Specifically, it is easier for a lower molecular weight polymer to see the same molecular weight difference among polymer chains, which might be caused by a slow initiation step.¹⁵⁷

6.4 Coordinative Chain Shuttling Polymerization between 12 and 27

The propene polymerization rate *via* **35** was much faster than that *via* **27** and only a small content of isotactic PP blocks were obtained when they were employed for the CCSP of propene (Entry 6.06). The propene polymerization rates *via* **12** and

27 were relatively close to each other and much higher content of isotactic PP blocks were incorporated into the pure atactic PP (Entry 6.07). The CCSP polymerization of propene was carried out as following: in a Schlenk flask, to a toluene solution of cocatalyst **01** at -10 °C were added the desired precatalysts and ZnEt₂. The flask was then pressurized to 5 psi with propene and the pressure was maintained for a certain time with stirring before quenching with 1.0 mL of methanol. The toluene solution was precipitated into 600 mL of acidic methanol to isolate the polypropene. The final product was collected and dried overnight *in vacuo* before GPC and NMR analyses. Details of the amount of reagents added, polymerization time and experimental results are provided in Tables 16 and 17.

Table 16: CCSP of propene with ZnEt₂ via precatalyst **12** and **27**

Entry	12	27	ZnEt ₂	Tol	T _p	t _p	Yield	M _n	PDI	<i>mmmm</i>
	(μmol)	(μmol)	(equiv.)	(mL)	(°C)	(h)	(g)	(kDa)		
6.06	10 **	5	20	30	20	4	3.22	4.67	1.06	5.0%
6.07	10	5	20	20	-10	15	5.34	10.6	1.05	12.6%
6.08	10	5	20	20	-10	30	8.32	14.3	1.07	12.6%
6.09	10	10	20	30	-10	15	5.89	8.27	1.07	15.6%
6.10	10	10	20	30	-10	30	11.3	13.9	1.06	16.1%
6.10e	--	--	--	--	--	--	--	14.8	1.06	16.4%
6.11	10	10	20	30	25	41	1.61	2.76	1.17	21.2%
6.12	10	10	50	30	-10	18	8.48	5.38	1.06	8.8%
6.13	10	15	20	40	-10	24	12.1	12.2	1.09	20.7%
6.13e	--	--	--	--	--	--	--	12.5	1.09	20.8%

Conditions: an equal molar amount of cocatalyst **01** relative to total Zr centers was added.

, **35 was used instead of **12**.

In the ^{13}C $\{^1\text{H}\}$ NMR spectra of methyl region of the resulting PP (Figures 56 and 57, and for Entries 6.11 and 6.12 see Appendix II), the resonance of *mmmm* pentad at 21.94 ppm was obviously higher than other resonances for atactic components, which provided a direct proof of the stereoblock architecture. The polydispersity indices for all the samples obtained at -10 °C in Table 16 were very narrow (PDI 1.05-1.09), which was in accordance with a living process. The GPC curves were monomodal (Figure 58), indicating the homogeneity among polymer chains in all the PP materials.

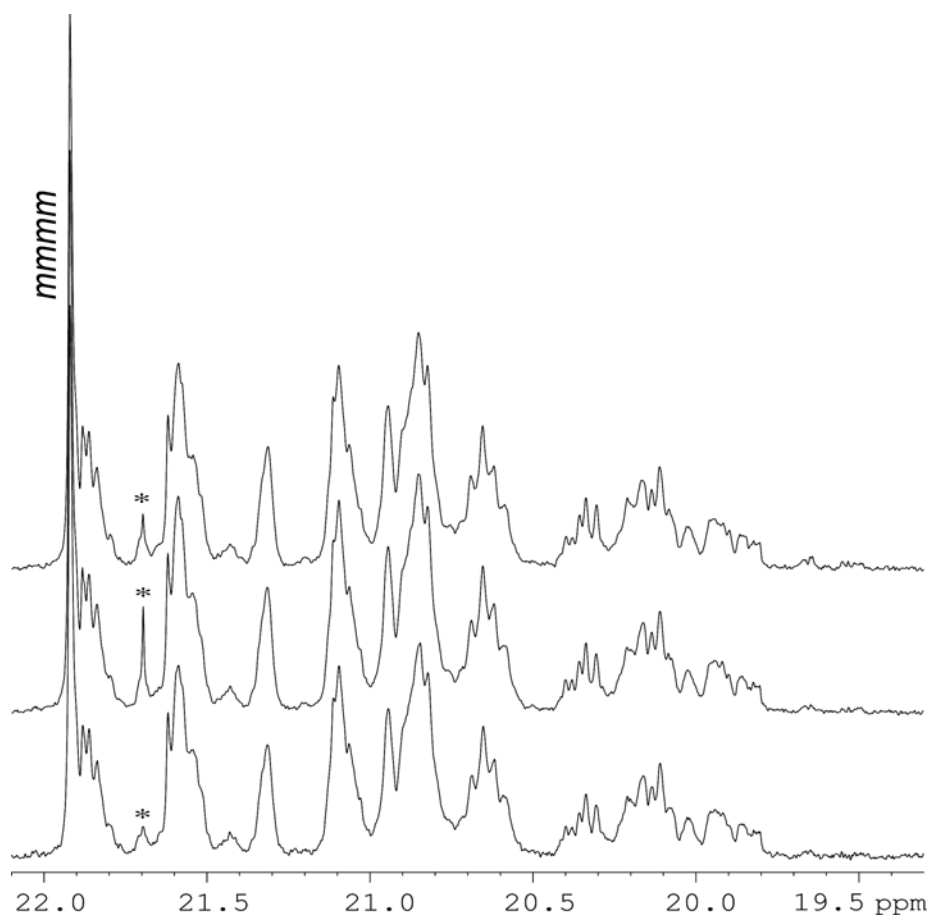


Figure 56: ^{13}C NMR (150 MHz, $1,1,2,2\text{-C}_2\text{D}_2\text{Cl}_4$, 90 °C) spectra of methyl region of multi-stereoblock PP samples from Entries 6.09 (top), 6.10 (middle), and 6.10e (bottom). Peaks marked by asterisks (*) were mainly from H,D residual isotopomers in the NMR solvent.

For different polymerization times, 15 h (Entries 6.07 and 6.09) versus 30 h (Entries 6.08 and 6.10), the polypropene obtained showed quantitatively the same microstructure (top two spectra in Figure 56). This confirmed the homogeneous property along a polymer chain in the polymer product, and ruled out the possibility of being a diblock or triblock copolymer. In addition, the homogeneous property of PP samples was further confirmed by extraction experiments. After the PP samples were extracted by diethyl ether (Entries 6.10e and 6.13e in Table 16), all the materials were recovered, and GPC and NMR analyses showed the same characterization results (bottom two spectra in Figure 56). Now we can safely reach the conclusion that monomodal multi-stereoblock polypropene was made using the CCSP system with dual precatalysts.

6.5 Modulation of Isotactic Block Content during the CCSP Process

To obtain different levels of isotactic content, different precatalyst ratios were employed for the CCSP of propene bearing the idea that more isoselective catalyst provided more isotactic blocks. The results were satisfactory, as shown by the increased isotacticity (or decreased atacticity) with more **27** relative to **12** (Figure 57). The *mmmm* pentad contents were 12.6%, 16.1% and 20.7% for the precatalyst molar ratio of 1:1, 2:1 and 3:1 respectively (Entries 6.08, 6.10 and 6.13 in Table 16).

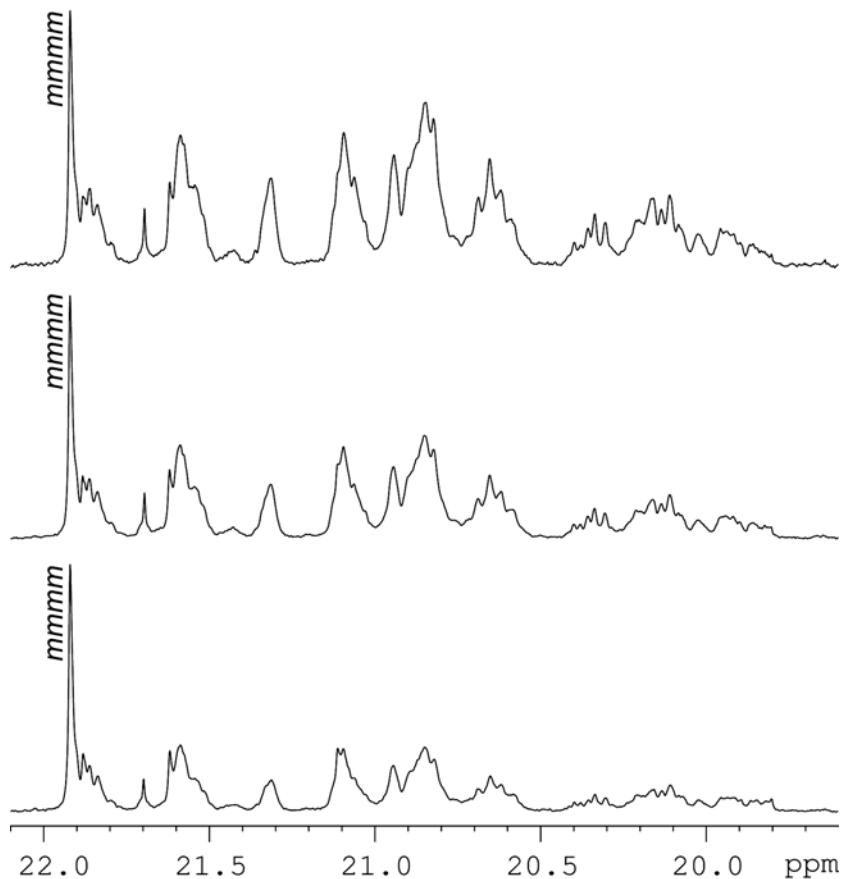


Figure 57: ^{13}C $\{^1\text{H}\}$ NMR (150 MHz, $1,1,2,2\text{-C}_2\text{D}_2\text{Cl}_4$, 90 °C) spectra of methyl region of multi-stereoblock PP obtained using different ratios of **12** and **27**, top (Entry 6.08), middle (Entry 6.10), bottom (Entry 6.13).

Another important factor influencing the isotacticity of the resulting polymer is the amount of chain transfer agent. When more ZnEt_2 was used, a polymer chain on an active species had a higher chance of being transferred, and the opportunity for continuous chain propagation on the isoselective catalyst was smaller. Such expectation was confirmed by the experimental results from Entries 6.09 and 6.12 (Table 16) and Entry 6.15 (Table 17). The *mmmm* pentad content was lowered due to an enhanced chain transfer process arising from higher concentration of ZnEt_2 . The *mmmm* values were 25.3%, 15.6% and 8.8% for 10, 20 and 50 equivalents of ZnEt_2 respectively.

In addition to the precatalyst ratio and equivalent of chain transfer agent, other factors that might change the isotacticity of PP include monomer pressure, reaction temperature, amount of solvent and concentration. Entry 6.11 was used to explore the temperature effect. The *mmmm* content was 21.2%, higher than that from Entry 6.10 of Table 16, which was probably caused by temperature influence on the catalyst activity and thermostability.

Table 17: CCSP of propene via **12** and **27** beyond homogeneity

Entry	12	27	ZnEt ₂	Tol	t _p	Yield	M _n	PDI	<i>mmmm</i>
	(μmol)	(μmol)	(equiv.)	(mL)	(h)	(g)	(kDa)		
6.14	10	5	10	20	30	7.66	27.0	1.09	18.2%
6.14e	--	--	--	--	--	--	27.8	1.09	15.5%
6.15	10	10	10	60	45	10.5	27.3	1.43	25.3%
6.15e	--	--	--	--	--	--	24.5	1.07	21.7%
6.16	10	15	10	40	30	9.56	18.9	1.27	22.5%
6.16e	--	--	--	--	--	--	17.7	1.12	21.3%
6.17	10	10	20	90	72	15.4	21.1	1.41	--
6.18	10	5	10	60	72	8.41	32.7	1.26	--

Conditions: an equal molar amount of cocatalyst **01** relative to total Zr centers was added at -10 °C, except **02** was used instead of **01** at 0 °C for Entry 6.18.

Attempts to make higher isotacticity and/or higher molecular weight of multi-stereoblock PP ended up with broader polydispersity and partial precipitation was observed during polymerization (all Entries in Table 17). Extraction experiments showed that a mixture of polymers was obtained from polymerization with a prolonged polymerization time and/or lower amount of ZnEt₂. The GPC curve of

polypropylene from Entry 6.15 revealed that there was a small amount of isotactic, ether insoluble component besides the monomodal multi-stereoblock PP of narrow PDI (Figure 58). These results can also serve as a control experiment to prove that the PP samples in Table 16 are homogeneous, for which the GPC and NMR showed the same results before and after being extracted with diethyl ether.

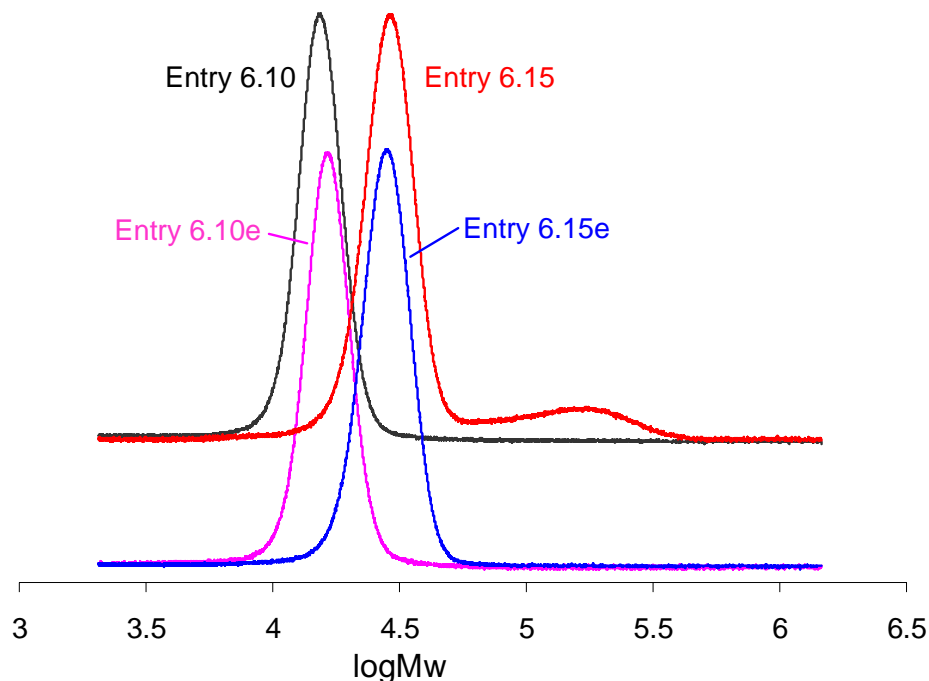


Figure 58: GPC curves for a homogenous PP sample (left) and a PP mixture (right) before (top) and after (bottom) extraction with diethyl ether

6.6 Preparation of an iso-a-iso triblock PP and microstructure comparison

By turning SDTL on and off, a diblock *a-iso* PP, a triblock *a-iso-a* PP and a tetrablock *a-iso-a-iso* PP were synthesized and well characterized.⁶² Herein, another type of well-defined stereoblock PP, *iso-a-iso* PP was obtained with hard blocks on both ends, according to the following procedures: to a solution of **04** (0.100 mmol, 39.8 mg) in 1.5 mL PhCl at -10 °C was added **01** (0.105 mmol, 84.1 mg) in another 1.5 mL PhCl. This solution was then rapidly added to a 500 mL Schlenk flask

charged with 200 mL PhCl at -10 °C, which was previously pressurized to 5 psi with propene. The flask was then repressurized and the pressure was maintained while stirring for 1.5 h before a solution of **07** (0.055 mmol, 24.2 mg) in 3 mL PhCl was added by temporarily opening the reaction flask. After another period of 38 h, a solution of **01** (0.060 mmol, 48.1 mg) in 4 mL PhCl was added before 1 mL sample solution was taken out. The rest reaction solution was stirred for 4.5 h before quenching with 1 mL of methanol. The 1 mL diblock sample and the final triblock PP solution were diluted with toluene and precipitated into acidic methanol to isolate the final product, which was then dried *in vacuo*. Yield: 14.0 g; GPC for the diblock PP, M_w 217 kDa, M_n 183 kDa, PDI 1.18; GPC for the triblock PP, M_w 251 kDa, M_n 206 kDa, PDI 1.22.

The microstructure of this *iso-a-iso* triblock PP and its *iso-a* diblock precursor were illustrated by ^{13}C NMR spectroscopy, and compared with a multi-stereoblock PP sample obtained by CCSP (Figure 59). The similarity in the ^{13}C NMR spectra of the well-defined triblock PP and the multi-stereoblock PP (bottom two spectra in Figure 59) further confirmed the microstructure of stereoblock PP obtained by CCSP process.

Based on the pentad analysis, the triblock PP has a symmetric constitution with about 12% isotactic PP on both ends (e.g. a structure of *12iso-76a-12iso*). The full characterization is currently going on including DSC calorimetry, AFM microscopy, FT-Raman and FTIR spectroscopy. Other samples of the hard-soft-hard series (such as *6iso-88a-6iso* and *18iso-64a-18iso*) are also being prepared, and these well-defined

stereoblock PP materials are going to be used to produce fibers by electrospinning from their cyclohexane/acetone solution.

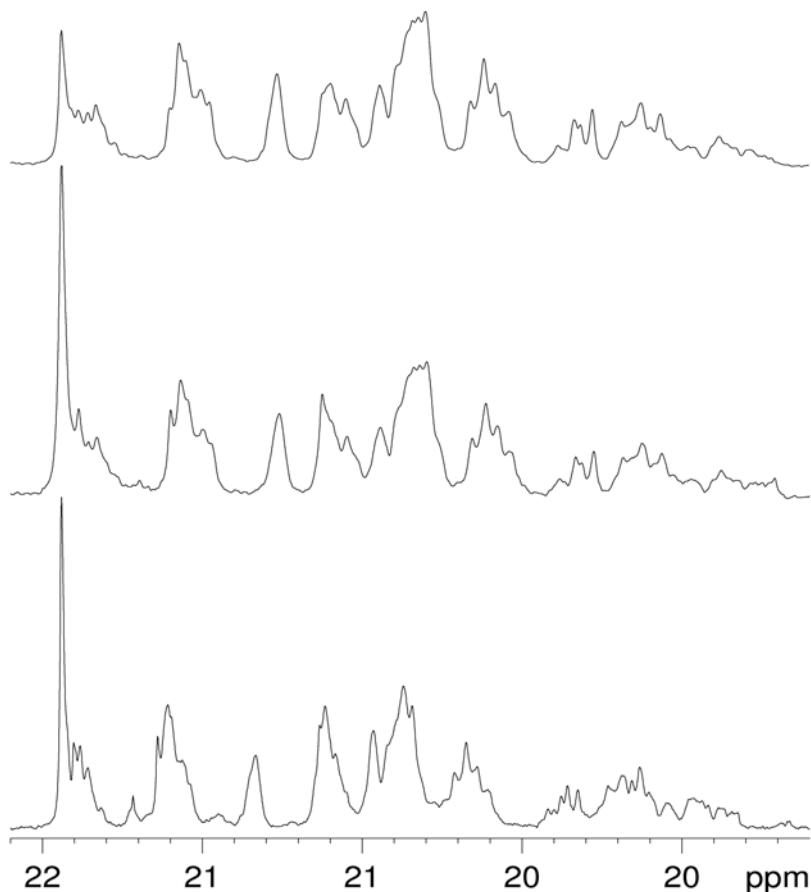


Figure 59: ^{13}C NMR (150 MHz, $1,1,2,2\text{-C}_2\text{D}_2\text{Cl}_4$, 90 °C) spectra of methyl region of a multi-stereoblock PP from Entry 6.09 (bottom), a well-defined *iso-a-iso* triblock PP (middle) and its corresponding *iso-a* diblock PP (top).

6.7 Conclusions

Coordinative chain transfer polymerization with ZnEt_2 was studied employing a series of CpAm zirconium catalysts. Efficient chain transfer happens between the chain transfer agent (ZnEt_2) and all the studied catalysts (**04**, **12** and **26-28**). The microstructure of PP materials produced was elucidated by high field ^{13}C $\{^1\text{H}\}$ NMR spectroscopy.

Multi-stereoblock polypropene of extremely narrow polydispersity (PDI = 1.05-1.09) was obtained by a process named as coordinative chain shuttling polymerization *via* two selected precatalysts **12** and **27**. To achieve an efficient CCSP system, these criteria should be considered: first, two catalysts are capable of providing polymers with different tacticity under the same degenerative chain transfer conditions; second, the chain transfer agent undergoes efficient chain transfer with the aspecific catalyst and moderate chain transfer with the stereospecific catalyst, and the transfer processes are reversible; finally, the two catalysts have comparable polymerization rates under the same conditions, especially in the binary system.

The microstructure of multi-stereoblock PP was also illustrated by ^{13}C NMR and compared with a new well-defined *iso-a-iso* triblock PP sample. The homogeneity within a polymer chain and among polymer chains was confirmed by narrow polydispersity, monomodal GPC curves, NMR spectra, and extraction experiment results. The isotactic content in the resulting polymers can be controlled by the relative ratio of two precatalysts, and/or equivalents of ZnEt_2 . More catalysts are desired to be developed for higher stereoselectivity, activity and temperature tolerance.

Chapter 7: Conclusions

The documented hafnium system with ZnEt_2 represents the first example of truly living CCTP for ethene, propene, higher α -olefins and α,ω -nonconjugated dienes. The number of growing polymer chains was quantitatively determined by the equivalents of chain transfer agent(s) added. The complete chain extension on zinc catalyzed by the hafnium catalyst (35^+) was confirmed by *in situ* NMR study observing the α -carbon bonded to zinc. The CCTP random copolymerization of ethene or propene with higher α -olefins or 1,5-hexadiene was also successfully realized. The (co)polymers obtained were characterized by GPC, DSC, GC, ^1H and ^{13}C NMR spectroscopy. The steadily available polyolefins from a small amount of transition metal catalyst provided a solution to the intrinsic problem, only one polymer chain per catalytic center, of a TLCP polymerization system, and might open a new platform for material engineering.

The living property of this CCTP system was proven by the extremely narrow polydispersity (PDI 1.03-1.10) of (co)polymers obtained and the Poisson distribution of resulting *n*-alkanes from the CCTP of ethene. The results of kinetic studies for the CCTP of ethene, propene and 1-hexene, and the quantitative end group functionalization of PE and PP by CCTP further confirmed the living character.

Several bimolecular processes were studied and found to have unique applications. During the CCSP random copolymerization, the comonomer incorporation rate can be controlled not only by dual catalysts, but also by dual cocatalysts. When two chain transfer agents were employed within one

polymerization system, we have the benefit from the desired features of both agents such as rapid and effective chain transfer, lower price and safety. The strategy of using different precatalysts to prepare monomodal multi-stereoblock polymer was also realized for the first time.

A series of binuclear complexes (**26-28**) were developed and applied to the TLCP, SDTL and CCTP polymerization of propene. Their molecular structures were fully characterized by ^1H NMR, elemental analysis and single crystal X-ray diffraction. The tacticity of PP obtained was illustrated by high field ^{13}C NMR spectroscopy and compared with that obtained *via* the corresponding mononuclear complex **04**. Under TLCP, the PP obtained by these binuclear catalysts also showed high level of isotacticity, with a slightly higher stereoerror detected when the linkage between the two zirconium centers shortens. However, under SDTL conditions, the isotacticity of resulting PP increases when the two linked zirconium centers become closer. The binuclear species are not as sensitive as the mononuclear one towards the degenerative chain transfer process.

A similar trend was observed for the binuclear catalysts under CCTP conditions. A faster chain transfer process happened when the tether length was longer, as illustrated by an increased occurrence of isolated diad *r* and a smaller PDI value. At the same time, the stereoerror characterized by the triad *rr* decreased. As an overall result, the PP *via* **27** showed the highest level of isotacticity using CCTP, and **27** was selected to make multi-stereoblock PP with **12** by a CCSP process.

The TLCP and CCTP behavior of propene polymerization *via* some other recently developed and previously reported CpAm complexes was also investigated,

such as $(\eta^5\text{-C}_5\text{Me}_5)\text{ZrMe}_2[\text{N}(\text{Et})\text{C}(\text{Me})\text{N}(\text{Et})]$ (**36**) and $(\eta^5\text{-C}_5\text{Me}_5)\text{ZrMe}_2[\text{N}(\text{Et})\text{C}(\text{H})\text{N}(\text{tBu})]$ (**12**). More CCTP systems, perhaps *via* novel catalysts, are needed to be developed in the future for better performance such as temperature resistance, oxygen and/or moisture tolerance and the ability to provide high molecular weight and stereospecific polymers.

Appendix I: Experimentals

General: All manipulations throughout this thesis were performed under an inert atmosphere of dinitrogen using either standard Schlenk techniques or a vacuum atmosphere glovebox. Dry, oxygen-free solvents were employed throughout. Diethyl ether and pentane were distilled from sodium/benzophenone (with a few milliliters of triglyme being added to the pot in the case of pentane). Toluene was distilled from sodium. Chlorobenzene and methylene chloride were distilled from calcium hydride. Benzene- d_6 and toluene- d_8 were vacuum transferred from NaK prior to use for NMR spectroscopy.

Materials: Polymer grade ethene and propene were purchased from Matheson Trigas, and passed through activated Q5 and molecular sieves (4 Å) before polymerization reactions. 1-hexene, 1-octene, 1-dodecene and 1,5-hexadiene were dried by NaK and vacuum transferred prior to use for polymerizations. Cp*Zr(Me)₂[N(Et)C(Me)N(^tBu)] (**04**) and other reported precatalysts were prepared according to the literatures. Cp*ZrCl₃, Cp*HfCl₃, [Ph₃C][B(C₆F₅)₄] (**02**) and B(C₆F₅)₃ (**03**) were obtained from Strem Chemicals while [PhNHMe₂][B(C₆F₅)₄] (**01**) was purchased from Boulder Scientific and used without further purification. ZnEt₂ was added as a 1.1M (15% wt) solution in toluene. ZnⁱPr₂ was used as a 1.0M solution in toluene.

Instrumentation: GPC analyses were performed using a Viscotek GPC system equipped with a column oven and differential refractometer both maintained at 45 °C and four columns also maintained at 45 °C. THF was used as the eluant at a flow rate of 1.0 mL/min. M_n , M_w and M_w / M_n values were obtained using a Viscotek GPC

with OmniSEC software (conventional calibration) and ten polystyrene standards (M_n = 580 Da to 3,150 kDa) (from Polymer Laboratories). DSC was performed using Q-1000 series at a heating rate of 10 °C /min, and the 2nd heating cycle was recorded. ^{13}C { ^1H } NMR spectra were recorded at 150 MHz, using 1,1,2,2-tetrachloroethane- d_2 as the solvent at 90 °C unless otherwise noted. Gas Chromatography (GC) analyses were carried out on a Shimadzu GC-9A instrument using nitrogen as the carrier.

Syn 1: Preparation of $^t\text{Bu-NH-CO-NH-(CH}_2)_8\text{-NH-CO-NH-}^t\text{Bu}$ (29)

To a solution of 4.96 g (50.0 mmol) tert-butyl isocyanate in 125 mL chloroform at 0 °C was added a solution of 3.61 g (25.0 mmol) 1,8-diaminooctane in 125 mL chloroform over 30 min. The resulting solution was stirred for 30 min before being concentrated *in vacuo* and then precipitated into 500 mL pentane. The product was isolated as a white powder *via* filtration and washed with several portions of pentane before being dried *in vacuo*. Yield: 8.51 g, 95.1 %. ^1H NMR (400 MHz, CDCl_3 , 293 K) δ 4.25 (2H, br s), 4.18 (2H, br t), 3.10 (4H, dt, $J = 6.0$, $J = 6.8$ Hz), 1.46 (4H, br p), 1.33 (18H, s), 1.30 (8H, br s).

Syn 2: Preparation of $^t\text{Bu-N=C=N-(CH}_2)_8\text{-N=C=N-}^t\text{Bu}$ (32)

To a solution of 14.8 g (56.3 mmol) triphenylphosphine in 225 mL methylene chloride under a nitrogen atmosphere and at 0 °C was added dropwise a solution of 8.99 g (56.3 mmol) bromine in 25 mL methylene chloride *via* addition funnel over 30 min. After stirring for another 15 min, 11.4 g (113 mmol) triethylamine was added dropwise into the solution over 15 min. During the next hour, 7.71 g (22.5 mmol) **29** was added in four equal portions. The solution was stirred overnight, washed with 125 mL distilled water, and the organic layer was separated and dried with anhydrous

sodium sulfate. After being concentrated *in vacuo*, the solution was slowly added into 700 mL pentane, filtered, and the volatiles were removed *in vacuo* to provide the crude product as an orange liquid, which was then vacuum distilled from calcium hydride. Yield: 4.82g, 70.0%; bp: 158 °C /0.40 Torr. ¹H NMR (400 MHz, C₆D₆, 293 K) δ 3.05 (4H, t, J = 6.8 Hz), 1.44 (4H, br p), 1.20 (18H, s), 1.26-1.16 (4H, m), 1.14-1.06 (4H, m).

Syn 3: Prep of [(η⁵-C₅Me₅)ZrMe₂]₂[N(^tBu)C(Me)N(CH₂)₈NC(Me)N(^tBu)](26)

To a solution of 0.33 g (1.0 mmol) (η⁵-C₅Me₅)ZrCl₃ in 50 mL Et₂O at -65 °C was added a solution of 3.2 mmol of MeLi in 1.9 mL of Et₂O *via* syringe over 10 min. The mixture was stirred for 3 h at -30 °C and then quenched with the addition of 0.05 mL trimethylsilylchloride *via* syringe. A solution of 0.15 g (0.50 mmol) **32** in 10 mL of Et₂O was then added *via* cannula at -30 °C over 45 min. The mixture was stirred for 1 h at -30 °C and then was allowed to warm up to room temperature overnight, after which the volatiles were removed *in vacuo*. The resulting white residue was extracted with toluene and filtered through Celite. The volatiles were removed *in vacuo* and the yellow crude product was washed with 10 mL cold pentane to provide the final product as a white powder (0.31 g, 73%). Crystals suitable for X-ray analysis were obtained by slow evaporation of a pentane solution at room temperature. Its molecular structure is shown in Figure 7. ¹H NMR (400 MHz, C₆D₆, 293 K) δ 2.97-2.90 (4H, m), 2.06 (30H, s), 1.80 (6H, s), 1.50-1.39 (4H, m), 1.35-1.27 (4H, m), 1.26-1.21 (4H, m), 1.20 (18H, s), 0.29 (12H, s). Anal. Calcd. for C₄₄H₈₂N₄Zr₂: %C 62.20, %H 9.73, %N 6.59; Found %C 61.90, %H 9.77, %N 6.59.

Syn 4: Preparation of ^tBu-NH-CO-NH-(CH₂)₆-NH-CO-NH-^tBu (30)

To a solution of 4.96 g (50.0 mmol) tert-butyl isocyanate in 125 mL chloroform at 0 °C was added a solution of 2.91 g (25.0 mmol) 1,6-diaminohexane in 125 mL chloroform over 30 min. The resulting solution was stirred for 30 min before being concentrated *in vacuo* and then precipitated into 700 mL pentane. The product was isolated as a white powder *via* filtration and washed with several portions of pentane before being dried *in vacuo*. Yield: 7.79 g, 99.1 %. ¹H NMR (400 MHz, CDCl₃, 293 K) δ 4.34 (2H, br t), 4.28 (2H, br s), 3.14 (4H, q, J = 6.4 Hz), 1.51-1.42 (4H, m), 1.36-1.31 (4H, m), 1.33 (18H, s).

Syn 5: Preparation of ^tBu-N=C=N-(CH₂)₆-N=C=N-^tBu (33)

To a solution of 14.8 g (56.3 mmol) triphenylphosphine in 225 mL methylene chloride under a nitrogen atmosphere and at 0 °C was added dropwise a solution of 8.99 g (56.3 mmol) bromine in 25 mL methylene chloride *via* addition funnel over 30 min. After stirring for an additional 15 min, 11.4 g (113 mmol) triethylamine was added dropwise into the solution over another 15 min. During the next hour, 7.08 g (22.5 mmol) **30** was added in four equal portions. The solution was stirred overnight, washed with 125 mL distilled water, and the organic layer was separated and dried with anhydrous sodium sulfate. After being concentrated *in vacuo*, the solution was slowly added into 800 mL pentane, filtered, and the volatiles were removed *in vacuo* to provide the crude product as an orange liquid, which was then vacuum distilled from calcium hydride and a colorless liquid was obtained. Yield: 4.27g, 68.2%; bp: 114 °C /0.02 Torr. ¹H NMR (400 MHz, C₆D₆, 293 K) δ 3.01 (4H, t, J = 6.8 Hz), 1.43-1.34 (4H, m), 1.20 (18H, s), 1.13-1.19 (4H, m).

Syn 6: Prep of $[(\eta^5\text{-C}_5\text{Me}_5)\text{ZrMe}_2]_2[\text{N}(\text{tBu})\text{C}(\text{Me})\text{N}(\text{CH}_2)_6\text{NC}(\text{Me})\text{N}(\text{tBu})]$ (27)

To a solution of 0.33 g (1.0 mmol) $(\eta^5\text{-C}_5\text{Me}_5)\text{ZrCl}_3$ in 50 mL Et_2O at $-65\text{ }^\circ\text{C}$ was added a solution of 3.2 mmol of MeLi in 1.8 mL of Et_2O *via* syringe over 10 min. The mixture was stirred for 3 h at $-30\text{ }^\circ\text{C}$ and then quenched with the addition of 0.05 mL trimethylsilylchloride *via* syringe. A solution of 0.14 g (0.50 mmol) **33** in 10 mL of Et_2O was then added *via* cannula at $-30\text{ }^\circ\text{C}$ over 55 min. The mixture was stirred for 1 h at $-30\text{ }^\circ\text{C}$ and then was allowed to warm up to room temperature overnight, after which the volatiles were removed *in vacuo*. The resulting white residue was extracted with toluene and filtered through Celite. The volatiles were removed *in vacuo* and the yellow crude product was washed with 10 mL cold pentane to provide the final product as a white powder (0.24 g, 58%). Crystals suitable for X-ray analysis were obtained by slow evaporation of a pentane solution at room temperature. Its molecular structure is shown in Figure 8. ^1H NMR (400 MHz, C_6D_6 , 293 K) δ 2.96-2.91 (4H, m), 2.05 (30H, s), 1.81 (6H, s), 1.50-1.40 (4H, m), 1.28-1.22 (4H, m), 1.19 (18H, s), 0.28 (12H, s). Anal. Calcd. for $\text{C}_{42}\text{H}_{78}\text{N}_4\text{Zr}_2$: %C 61.40, %H 9.57, %N 6.82; Found %C 61.69, %H 9.59, %N 6.73.

Syn 7: Preparation of $\text{tBu-NH-CO-NH-(CH}_2)_4\text{-NH-CO-NH-tBu}$ (31)

To a solution of 4.96 g (50.0 mmol) tert-butyl isocyanate in 200 mL chloroform at $0\text{ }^\circ\text{C}$ was added a solution of 2.20 g (25.0 mmol) 1,4-diaminobutane in 20 mL chloroform *via* cannula over 25 min. The resulting solution was stirred for 20 min before being concentrated *in vacuo* and then precipitated into 500 mL pentane. The product was isolated as a white powder *via* filtration and washed with several portions of pentane before being dried *in vacuo*. Yield: 6.97 g, 97.3 %. ^1H NMR (400

MHz, CDCl₃, 293 K) δ 4.60 (2H, br t), 4.37 (2H, br s), 3.16 (4H, br q), 1.54-1.48 (4H, m), 1.33 (18H, s).

Syn 8: Preparation of ^tBu-N=C=N-(CH₂)₄-N=C=N-^tBu (34)

To a solution of 16.4 g (62.5 mmol) triphenylphosphine in 250 mL methylene chloride under a nitrogen atmosphere and at 0 °C was added a solution of 10.0 g (62.5 mmol) bromine in 30 mL methylene chloride *via* addition funnel over 30 min. After stirring for an additional 15 min, 12.8 g (126 mmol) triethylamine was added dropwise into the solution over 10 min. During the next hour, 6.92 g (24.2 mmol) **31** was added in four equal portions. The solution was stirred overnight, washed with 100 mL distilled water, and the organic layer was separated and dried with anhydrous sodium sulfate. After being concentrated *in vacuo*, the solution was slowly added into 500 mL pentane, filtered, and the volatiles were removed *in vacuo* to provide the crude product as an orange liquid, which was then vacuum distilled from calcium hydride. Yield: 2.96g, 48.9%; bp: 85 °C /0.01 Torr. ¹H NMR (400 MHz, C₆D₆, 293 K) δ 2.99-2.93 (4H, m), 1.49-1.41 (4H, m), 1.18 (18H, s).¹⁵⁸

Syn 9: Prep of [(η⁵-C₅Me₅)ZrMe₂]₂[N(^tBu)C(Me)N(CH₂)₄NC(Me)N(^tBu)] (28)

To a solution of 0.66 g (2.0 mmol) (η⁵-C₅Me₅)ZrCl₃ in 100 mL Et₂O at -65 °C was added a solution of 6.2 mmol of MeLi in 3.7 mL of Et₂O *via* syringe over 10 min. The mixture was stirred for 3 h at -30 °C and then quenched with the addition of 0.1 mL trimethylsilylchloride *via* syringe. A solution of 0.25 g (1.0 mmol) **34** in 10 mL of Et₂O was then added *via* cannula at -30 °C over 35 min. The mixture was stirred for 1 h at -30 °C and then was allowed to warm up to room temperature overnight, after which the volatiles were removed *in vacuo*. The resulting white residue was

extracted with toluene and filtered through Celite. The volatiles were removed *in vacuo* and the yellow crude product was washed with several ~2 mL portions of cold pentane to provide the final product as a white powder (0.63 g, 79%). Crystals suitable for X-ray analysis were obtained by slow evaporation of a toluene solution at room temperature. Molecular structure is shown in Figure 9. ¹H NMR (400 MHz, C₆D₆, 293 K) δ 2.97-2.89 (4H, m), 2.05 (30H, s), 1.77 (6H, s), 1.39-1.32 (4H, m), 1.18 (18H, s), 0.27 (12H, s). Anal. Calcd. for C₄₀H₇₄N₄Zr₂: %C 60.55, %H 9.40, %N 7.06; Found %C 60.54, %H 9.37, %N 7.11.

Syn 10: Preparation of Et-NH-CO-NH-Et (40)

To a solution of 4.98 g (70.0 mmol) ethyl isocyanate in 100 mL chloroform at 0 °C was added a solution of 35 mL 2.0 M ethylamine solution in THF *via* cannula over 25 min. The resulting solution was stirred for 20 min before being concentrated *in vacuo* to about 20 mL, and then precipitated into 700 mL petroleum ether (38.5-54.3 °C). The product was isolated as a white powder *via* filtration and washed with pentane before being dried *in vacuo*. Yield: 7.65 g, 94.1 %. ¹H NMR (400 MHz, CDCl₃, 293 K) δ 3.22 (q, 4H, *J* = 7.2 Hz), 1.15 (t, 6H, *J* = 7.2 Hz).¹⁵⁹

Syn 11: Preparation of Et-N=C=N-Et (41)

To a solution of 42.1 g (161 mmol) triphenylphosphine in 320 mL methylene chloride under a nitrogen atmosphere and at 0 °C was added a solution of 25.7 g (161 mmol) bromine in 30 mL methylene chloride *via* addition funnel over 45 min. After stirring for an additional 15 min, 32.8 g (324 mmol) triethylamine was added dropwise into the solution over 10 min. During the next hour, 14.9 g (128 mmol) **40** was added in five equal portions. The reaction solution was stirred for another hour at

0 °C. Upon warming to room temperature, the suspension was washed with 150 mL distilled water, and the organic layer was separated and dried with anhydrous sodium sulfate. After being concentrated *in vacuo* to about 90 mL, the solution was slowly added into 900 mL pentane, filtered, and the solvents were removed using a rotary evaporator at room temperature under a pressure of 100 mmHg. The orange crude product was further purified by vacuum transfer (< 0.001 mmHg) from calcium hydride to provide the final product as a clear, colorless liquid (7.1 g, 56%). ¹H NMR (400 MHz, C₆D₆, 293 K) δ 2.94 (q, 4H, *J* = 7.2 Hz), 0.97 (t, 6H, *J* = 7.2 Hz).¹⁰³

Syn 12: Preparation of (η⁵-C₅Me₅)HfMe₂[N(Et)C(Me)N(Et)] (35)

To a solution of (η⁵-C₅Me₅)HfCl₃ (1.26 g, 3.0 mmol) in 120 mL Et₂O at -60 °C was added 5.8 mL of a solution of MeLi (1.7 M in Et₂O) *via* syringe over a period of 10 min. The mixture was allowed to warm to -10 °C over a period of 3 h whereupon any remaining MeLi was quenched with the addition of 0.30 mL Me₃SiCl at -30 °C *via* syringe. At this time, a solution of **41** (0.29 g, 3.0 mmol) in 10 mL of Et₂O was added *via* cannula at -30 °C over a period of 45 min. The mixture was then allowed to warm to -10 °C over a period of 1.5 h after which the volatiles were removed *in vacuo*. The resulting white residue was extracted with pentane and filtered through a small pad of Celite in a glass frit. The pentane filtrate was concentrated and cooled to -25 °C thereafter the final product was isolated as a white crystalline material (0.92g, yield 67%). Single crystal X-ray analysis confirmed the solid state molecular structure (Figure 16). ¹H NMR (400 MHz, C₆D₆, 293 K): δ 2.96 (q, 4H, *J* = 7.2 Hz), 2.03 (s, 15H), 1.33 (s, 3H), 0.90 (t, 6H, *J* = 7.2 Hz), 0.00 (s, 6H). Anal. Calcd. for C₁₈H₃₄N₂Hf: %C 47.31, %H 7.50, %N 6.13; Found %C 47.21, %H 7.43, %N 6.29.

Syn 13: Preparation of $(\eta^5\text{-C}_5\text{Me}_5)\text{ZrMe}_2[\text{N}(\text{Et})\text{C}(\text{Me})\text{N}(\text{Et})]$ (36)

To a solution of $(\eta^5\text{-C}_5\text{Me}_5)\text{ZrCl}_3$ (1.00 g, 3.0 mmol) in 120 mL Et_2O at $-65\text{ }^\circ\text{C}$ was added 5.9 mL of a solution of MeLi (1.6 M in Et_2O) *via* syringe over a period of 5 min. The mixture was allowed to warm to $-10\text{ }^\circ\text{C}$ over a period of 2.5 h whereupon any remaining MeLi was quenched with the addition of 0.30 mL Me_3SiCl at $-30\text{ }^\circ\text{C}$ *via* syringe. At this time, a solution of **41** (0.29 g, 3.0 mmol) in 10 mL of Et_2O was added *via* cannula at $-30\text{ }^\circ\text{C}$ over a period of 40 min. The mixture was then allowed to warm to $-10\text{ }^\circ\text{C}$ over a period of 1 h after which the volatiles were removed *in vacuo*. The resulting white residue was extracted with pentane and filtered through a small pad of Celite in a glass frit. The pentane filtrate was concentrated and cooled to $-25\text{ }^\circ\text{C}$ thereafter the final product was isolated as a white crystalline material (0.62g, yield 56%). Single crystal X-ray analysis confirmed the solid state molecular structure (Figure 16). ^1H NMR (400 MHz, C_6D_6 , 293 K): δ 2.94 (q, 4H, $J = 7.2$ Hz), 2.00 (s, 15H), 1.39 (s, 3H), 0.91 (t, 6H, $J = 7.2$ Hz), 0.19 (s, 6H). Anal. Calcd. for $\text{C}_{18}\text{H}_{34}\text{N}_2\text{Zr}$: %C 58.48, %H 9.27, %N 7.58; Found %C 58.31, %H 9.32, %N 7.63.

Syn 14: Preparation of $^i\text{Pr-NH-CO-NH-Et}$ (42)

To a solution of 4.98 g (70.0 mmol) ethyl isocyanate in 100 mL chloroform at $0\text{ }^\circ\text{C}$ was added a solution of 4.14 g (70.0 mmol) 2-aminopropane in 10 mL chloroform *via* cannula over 50 min. The resulting solution was stirred for 20 min before being concentrated *in vacuo* to about 20 mL, and then precipitated into 700 mL petroleum ether ($35\text{-}60\text{ }^\circ\text{C}$). The product was isolated as a white powder *via* filtration and washed with pentane before being dried *in vacuo*. Yield: 8.54 g, 93.7 %. ^1H NMR

(400 MHz, CDCl₃, 293 K) δ 3.86 (sept, 1H, J = 6.4 Hz), 3.20 (q, 2H, J = 7.2 Hz), 1.15 (d, 6H, J = 6.4 Hz), 1.14 (t, 3H, J = 7.2 Hz).

Syn 15: Preparation of ⁱPr-N=C=N-Et (43)

To a solution of 21.5 g (82.0 mmol) triphenylphosphine in 250 mL methylene chloride under a nitrogen atmosphere and at 0 °C was added a solution of 13.1 g (82.0 mmol) bromine in 30 mL methylene chloride *via* addition funnel over 25 min. After stirring for an additional 5 min, 16.7 g (165 mmol) triethylamine was added dropwise into the solution over 10 min. During the next hour, 8.54 g (65.6 mmol) of **42** was added in four equal portions. The reaction solution was stirred for an additional hour at 0 °C. Upon warming to room temperature, the suspension was washed with 100 mL distilled water, and the organic layer was separated and dried with anhydrous sodium sulfate. After being concentrated *in vacuo* to about 50 mL, the solution was slowly added into 800 mL pentane, filtered, and the solvents were removed using a rotary evaporator at room temperature under a pressure of 100 mmHg. The orange crude product was further purified by vacuum transfer (< 0.001 mmHg) from calcium hydride to provide the final product as a clear, colorless liquid (4.0 g, 54%). ¹H NMR (400 MHz, CDCl₃, 293 K) δ 3.55 (sept, 1H, J = 6.4 Hz), 3.22 (q, 2H, J = 7.2 Hz), 1.23 (t, 3H, J = 7.2 Hz), 1.21 (d, 6H, J = 6.4 Hz).

Syn 16: Preparation of (η^5 -C₅Me₅)ZrMe₂[N(ⁱPr)C(Me)N(Et)] (37)

To a solution of (η^5 -C₅Me₅)ZrCl₃ (1.66 g, 5.0 mmol) in 125 mL Et₂O at -40 °C was added 9.4 mL of a solution of MeLi (1.6 M in Et₂O) *via* syringe over a period of 10 min. The mixture was allowed to warm to -10 °C over a period of 2.5 h whereupon any remaining MeLi was quenched with the addition of 0.10 mL Me₃SiCl at -10 °C

via syringe. At this time, a solution of **43** (0.56 g, 5.0 mmol) in 10 mL of Et₂O was added *via* cannula at -30 °C over a period of 45 min. The mixture was then allowed to warm to -10 °C over a period of 1.5 h after which the volatiles were removed *in vacuo*. The resulting white residue was extracted with pentane and filtered through a small pad of Celite in a glass frit. The pentane filtrate was concentrated and cooled to -30 °C thereafter the final product was isolated as a white crystalline material (0.53g, yield 28%). ¹H NMR (400 MHz, C₆D₆, 293 K): δ 3.31 (sept, 1H, *J* = 6.4 Hz), 2.89 (q, 2H, *J* = 7.2 Hz), 2.00 (s, 15H), 1.46 (s, 3H), 1.05 (d, 6H, *J* = 6.4 Hz), 0.91 (t, 3H, *J* = 7.2 Hz), 0.25 (s, 6H).

Syn 17: Preparation of ^tBuCH₂-NH-CO-NH-Et (44)

To a solution of 9.45 g (133 mmol) ethyl isocyanate in 200 mL chloroform at 0 °C was added a solution of 11.6 g (133 mmol) neopentylamine in 25 mL chloroform *via* cannula over 2 h. The resulting solution was stirred for 20 min before the solvent was removed *in vacuo*. The product was obtained as a white powder. Yield: 20.1 g, 95.7 %. ¹H NMR (400 MHz, CDCl₃, 293 K) δ 4.79 (br s, 2H), 3.21 (m, 2H), 2.97 (d, 2H, *J* = 6.4 Hz), 1.13 (t, 3H, *J* = 7.2 Hz), 0.90 (s, 9H).

Syn 18: Preparation of ^tBuCH₂-N=C=N-Et (45)

To a solution of 32.8 g (125 mmol) triphenylphosphine in 250 mL methylene chloride under a nitrogen atmosphere and at 0 °C was added a solution of 20.0 g (125 mmol) bromine in 30 mL methylene chloride *via* addition funnel over 20 min. After stirring for an additional 5 min, 25.3 g (250 mmol) triethylamine was added dropwise into the solution over 5 min. During the following 1.5 h, 15.8 g (100 mmol) of **44** was added in six equal portions. The reaction solution was stirred for an additional hour at

0 °C. Upon warming to room temperature, the suspension was washed with 100 mL distilled water, and the organic layer was separated and dried with anhydrous sodium sulfate. After being concentrated *in vacuo* to about 60 mL, the solution was slowly added into 800 mL pentane, filtered, and the solvents were removed using a rotary evaporator at room temperature under a pressure of 100 mmHg. The orange crude product was further purified by vacuum transfer (< 0.001 mmHg) from calcium hydride to provide the final product as a clear, colorless liquid (7.8 g, 56%). ¹H NMR (400 MHz, C₆D₆, 293 K) δ 2.96 (q, 2H, *J* = 7.2 Hz), 2.82 (s, 2H), 0.98 (t, 3H, *J* = 7.2 Hz), 0.84 (s, 9H).

Syn 19: Preparation of (η⁵-C₅Me₅)ZrMe₂[N(CH₂^tBu)C(Me)N(Et)] (38)

To a solution of (η⁵-C₅Me₅)ZrCl₃ (1.33 g, 4.0 mmol) in 70 mL Et₂O at -60 °C was added 10 mL of a solution of MeLi (1.2 M in Et₂O) *via* syringe over a period of 25 min. The mixture was allowed to warm to -10 °C over a period of 2 h whereupon any remaining MeLi was quenched with the addition of 0.1 mL Me₃SiCl at -30 °C *via* syringe. At this time, a solution of **45** (0.56 g, 4.0 mmol) in 10 mL of Et₂O was added *via* cannula at -30 °C over a period of 10 min. The mixture was then allowed to warm to -10 °C over a period of 2 h after which the volatiles were removed *in vacuo*. The resulting white residue was extracted with pentane and filtered through a small pad of Celite in a glass frit. The pentane filtrate was concentrated and cooled to -30 °C thereafter the final product was isolated as a white crystalline material (1.0 g, yield 62%). ¹H NMR (400 MHz, C₆D₆, 293 K): δ 3.08 (s, 2H), 2.88 (q, 2H, *J* = 7.2 Hz), 1.98 (s, 15H), 1.56 (s, 3H), 0.93 (t, 3H, *J* = 7.2 Hz), 0.79 (s, 9H), 0.12 (s, 6H).

Syn 20: Preparation of $\text{CH}_3\text{CH}_2\text{C}(\text{CH}_3)_2\text{-NH-CO-NH-Et}$ (46**)**

To a solution of 3.55 g (50.0 mmol) ethyl isocyanate in 100 mL chloroform at 0 °C was added a solution of 4.36 g (50.0 mmol) tert-amylamine in 10 mL chloroform *via* cannula over 35 min. The resulting solution was stirred for 20 min before the solvent was removed *in vacuo*. The product was obtained as a white powder. Yield: 7.36 g, 93.0 %. ^1H NMR (400 MHz, CDCl_3 , 293 K) δ 4.10 (br s, 2H), 3.16 (m, 2H), 1.69 (q, 2H, $J = 7.6$ Hz), 1.27 (s, 6H), 1.11 (t, 3H, $J = 7.2$ Hz), 0.85 (t, 3H, $J = 7.6$ Hz).

Syn 21: Preparation of $\text{CH}_3\text{CH}_2\text{C}(\text{CH}_3)_2\text{-N=C=N-Et}$ (47**)**

To a solution of 13.1 g (50.0 mmol) triphenylphosphine in 250 mL methylene chloride under a nitrogen atmosphere and at 0 °C was added a solution of 8.00 g (50.0 mmol) bromine in 30 mL methylene chloride *via* addition funnel over 30 min. After stirring for an additional 5 min, 10.1 g (100 mmol) triethylamine was added dropwise into the solution over 5 min. During the next hour, 6.33 g (40.0 mmol) of **46** was added in three equal portions. The reaction solution was stirred for additional 2 h at 0 °C. Upon warming to room temperature, the suspension was washed with 100 mL distilled water, and the organic layer was separated and dried with anhydrous sodium sulfate. After being concentrated *in vacuo* to about 50 mL, the solution was slowly added into 800 mL pentane, filtered, and the solvents were removed using a rotary evaporator at room temperature under a pressure of 100 mmHg. The orange crude product was further purified by vacuum transfer (< 0.001 mmHg) from calcium hydride to provide the final product as a clear, colorless liquid (3.6 g, 64%). ^1H NMR (400 MHz, CDCl_3 , 293 K) δ 2.97 (q, 2H, $J = 7.2$ Hz), 1.39 (q, 2H, $J = 7.4$ Hz), 1.14 (s, 6H), 1.00 (t, 3H, $J = 7.2$ Hz), 0.85 (t, 3H, $J = 7.4$ Hz).

Syn 22: Preparation of $(\eta^5\text{-C}_5\text{Me}_5)\text{ZrMe}_2[\text{N}(\text{iPr})\text{C}(\text{Me})\text{N}(\text{Et})]$ (39)

To a solution of $(\eta^5\text{-C}_5\text{Me}_5)\text{ZrCl}_3$ (1.33 g, 4.0 mmol) in 70 mL Et_2O at $-60\text{ }^\circ\text{C}$ was added 10 mL of a solution of MeLi (1.2 M in Et_2O) *via* syringe over a period of 15 min. The mixture was allowed to warm to $-10\text{ }^\circ\text{C}$ over a period of 2 h whereupon any remaining MeLi was quenched with the addition of 0.10 mL Me_3SiCl at $-30\text{ }^\circ\text{C}$ *via* syringe. At this time, a solution of **47** (0.56 g, 4.0 mmol) in 10 mL of Et_2O was added *via* cannula at $-30\text{ }^\circ\text{C}$ over a period of 15 min. The mixture was then allowed to warm to $-10\text{ }^\circ\text{C}$ over a period of 2 h after which the volatiles were removed *in vacuo*. The resulting white residue was extracted with pentane and filtered through a small pad of Celite in a glass frit. The pentane filtrate was concentrated and cooled to $-30\text{ }^\circ\text{C}$ thereafter the final product was isolated as a white crystalline material (1.1 g, yield 68%). ^1H NMR (400 MHz, C_6D_6 , 293 K): δ 2.86 (q, 2H, $J = 7.2$ Hz), 2.02 (s, 15H), 1.69 (s, 3H), 1.49 (q, 2H, $J = 7.6$ Hz), 1.12 (s, 6H), 0.91 (t, 3H, $J = 7.2$ Hz), 0.80 (t, 3H, $J = 7.6$ Hz), 0.23 (s, 6H).

Syn 23: Preparation of $(1,3\text{-}^t\text{Bu}_2\text{-}\eta^5\text{-C}_5\text{H}_3)\text{ZrMe}_2[\text{N}(\text{Et})\text{C}(\text{Me})\text{N}(^t\text{Bu})]$ (48)

To a solution of $(1,3\text{-}^t\text{Bu}_2\text{-}\eta^5\text{-C}_5\text{H}_3)\text{HfCl}_3$ ^{101, 102} (1.3 g, 3.5 mmol) in 120 mL Et_2O at $-60\text{ }^\circ\text{C}$ was added 6.9 mL of a solution of MeLi (1.6 M in Et_2O) *via* syringe over a period of 15 min. The mixture was allowed to warm to $-10\text{ }^\circ\text{C}$ over a period of 2 h whereupon any remaining MeLi was quenched with the addition of 0.1 mL Me_3SiCl at $-40\text{ }^\circ\text{C}$ *via* syringe. At this time, a solution of $^t\text{Bu-N=C=N-Et}$ (0.44 g, 3.5 mmol) in 20 mL of Et_2O was added *via* a cannula at $-30\text{ }^\circ\text{C}$ over a period of 20 min. The mixture was then allowed to warm to $-10\text{ }^\circ\text{C}$ over a period of 2 h after which the

volatiles were removed *in vacuo*. The resulting white residue was extracted with pentane and filtered through a small pad of Celite in a glass frit. The pentane filtrate was concentrated and cooled to -25 °C thereafter the final product was isolated as a white crystalline material (0.98 g, yield 64%). Single crystal X-ray analysis confirmed the solid state molecular structure (Figure 17). ¹H NMR (400 MHz, C₆D₆, 293 K): δ 6.65 (t, 1H, *J* = 2.5 Hz), 6.05 (d, 2H, *J* = 2.5 Hz), 3.16 (q, 2H, *J* = 7.2 Hz), 1.66 (s, 3H), 1.30 (s, 18H), 1.15 (s, 9H), 1.03 (t, 3H, *J* = 7.2 Hz), 0.54 (s, 6H). Anal. Calcd. for C₂₃H₄₄N₂Zr: %C 62.81, %H 10.08, %N 6.37; Found %C 62.71, %H 10.15, %N 6.53.

Syn 24: Preparation of (η⁵-C₅Me₅)ZrMe₂[N(ⁱPr)C(NMe₂)N(ⁱPr)] (49)

To a solution of (η⁵-C₅Me₅)ZrCl₂[N(ⁱPr)C(NMe₂)N(ⁱPr)]¹⁰³ (0.32 g, 0.68 mmol) in 60 mL Et₂O at -65 °C was added 0.75 mL of a MeLi solution (1.9 M in Et₂O) *via* syringe over a period of 6 min. The mixture was allowed to warm to room temperature over a period of 2 h whereupon any remaining MeLi was quenched with the addition of 0.06 mL Me₃SiCl. The volatiles were removed *in vacuo*, and the resulting white residue was extracted with pentane and filtered through a thin pad of Celite in a glass frit. The pentane filtrate was concentrated and cooled to -25 °C to isolate the final product as a white crystalline material (0.11 g, yield 38%). Single crystal X-ray analysis confirmed the solid state molecular structure (Figure 17). ¹H NMR (400 MHz, C₆D₆, 293 K): δ 3.46 (sept, 2H, *J* = 7.2 Hz), 2.40 (s, 6H), 2.04 (s, 15H), 1.12 (d, 12H, *J* = 7.2 Hz), 0.37 (s, 6H).

Syn 25: Preparation of Et-N=CH-N(Et)-SiEt₃ (52)

In a 50 mL Schlenk tube were sealed 1.96 g (20.0 mmol) of N,N-diethyl carbodiimide **41**, 2.79g (24.0 mmol) of triethylsilane HSiEt₃ and 0.07 g (0.4 mmol) of palladium dichloride PdCl₂. This mixture was heated to 150 °C overnight, and then cooled to room temperature whereupon the final product was isolated by vacuum distillation as a colorless oily liquid (3.0 g, yield 71%), b.p. 46 °C at 0.2 mmHg. ¹H NMR (400 MHz, CDCl₃, 293 K): δ 7.42 (s, 1H), 3.25 (q, 2H, *J* = 6.8 Hz), 3.25 (q, 2H, *J* = 7.2 Hz), 1.12 (t, 3H, *J* = 6.8 Hz), 1.11 (t, 3H, *J* = 7.2 Hz), 0.95 (t, 9H, *J* = 8.0 Hz), 0.70 (q, 6H, *J* = 8.0 Hz).

Syn 26: Preparation of Et-N=CH-NH-Et (53)

Into 3.0 g (14 mmol) of freshly distilled **52** was added 0.54 g (17 mmol) of methanol at -25 °C. The mixture was allowed to warm to room temperature over a period of 1 h while stirring. The desired product was isolated by vacuum distillation as a colorless liquid (1.0 g, yield 74%), b.p. 28 °C at 0.6 mmHg. ^{160, 161} ¹H NMR (400 MHz, CDCl₃, 293 K): δ 7.40 (s, 1H), 3.22 (q, 4H, *J* = 7.2 Hz), 1.14 (t, 6H, *J* = 7.2 Hz).

Syn 27: Preparation of (η⁵-C₅Me₅)ZrCl₂[N(Et)C(H)N(Et)] (51)

To a solution of 0.50 g (5.0 mmol) of **53** in 50 mL of Et₂O at -30 °C was added 1.8 mL of ⁿBuLi solution (3.0 M in Et₂O) *via* a syringe within 10 min. The mixture was allowed to warm to -10 °C over a period of 2.5 h whereupon the clear solution was transferred *via* a cannula within 12 min to a Schlenk flask, into which was previously added 1.7 g (5.0 mmol) of Cp*ZrCl₃ suspended in 75 mL of Et₂O and cooled to -70 °C beforehand. The reaction mixture was then slowly warmed up to

room temperature overnight (15 h) after which volatiles were removed *in vacuo*. The resulting yellow residue was extracted with toluene and filtered through a small pad of Celite in a glass frit. The toluene filtrate was concentrated and cooled to -25 °C to isolate the final product as a yellow solid material (0.91 g, yield 46%). ¹H NMR (400 MHz, C₆D₆, 293 K): δ 7.35 (s, 1H), 3.03 (q, 4H, *J* = 7.2 Hz), 2.01 (s, 15H), 0.92 (t, 6H, *J* = 7.2 Hz).

Syn 28: Preparation of (η⁵-C₅Me₅)ZrMe₂[N(Et)C(H)N(Et)] (50)

To a solution of **51** (0.63 g, 1.6 mmol) in 60 mL Et₂O at -65°C was added 1.8 mL of a MeLi solution (1.9 M in Et₂O) *via* a syringe within 8 min. The mixture was allowed to warm to room temperature over a period of 2 h whereupon any remaining MeLi was quenched with the addition of 0.1 mL Me₃SiCl. The volatiles were removed *in vacuo*, and the resulting residue was extracted with pentane and filtered through a thin pad of Celite in a glass frit. The pentane filtrate was concentrated and cooled to -25 °C to isolate the final product as a crystalline material (0.09 g, yield 16%). Single crystal X-ray analysis confirmed the solid state molecular structure (Figure 17). ¹H NMR (400 MHz, C₆D₆, 293 K): δ 7.75 (s, 1H), 2.92 (q, 4H, *J* = 7.2 Hz), 1.98 (s, 15H), 0.93 (t, 6H, *J* = 7.2 Hz), 0.18 (s, 6H).

Appendix II: NMR spectra for selected (co)polymers

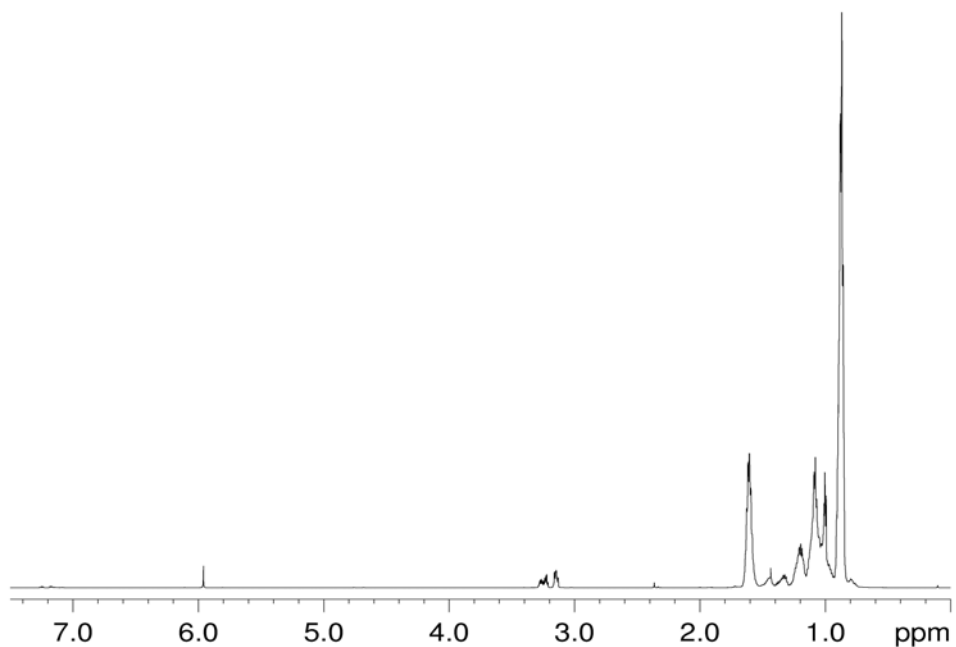


Figure 60: ¹H NMR (600 MHz, 1,1,2,2-C₂D₂Cl₄, 90 °C) spectrum of iodo-PP by CCTP via **35** (section 3.2.7)

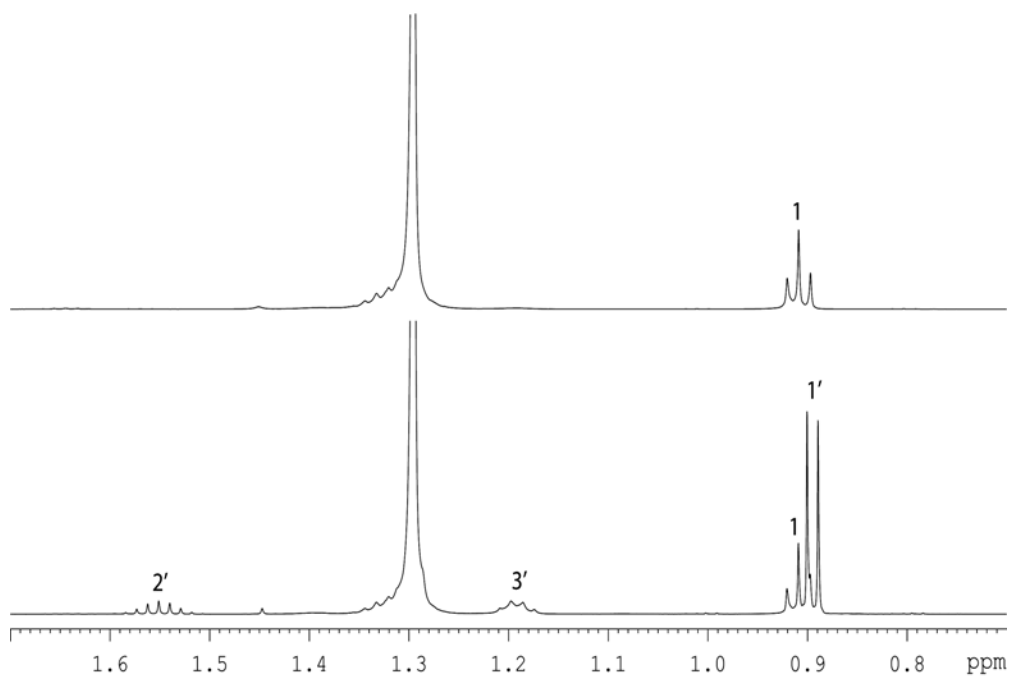


Figure 61: ¹H NMR (600 MHz, 1,1,2,2-C₂D₂Cl₄, 90 °C) spectra of isolated PE (Entry 4.05, top) and 2-methyl PE (Entry 4.06, bottom) by CCTP via **35**

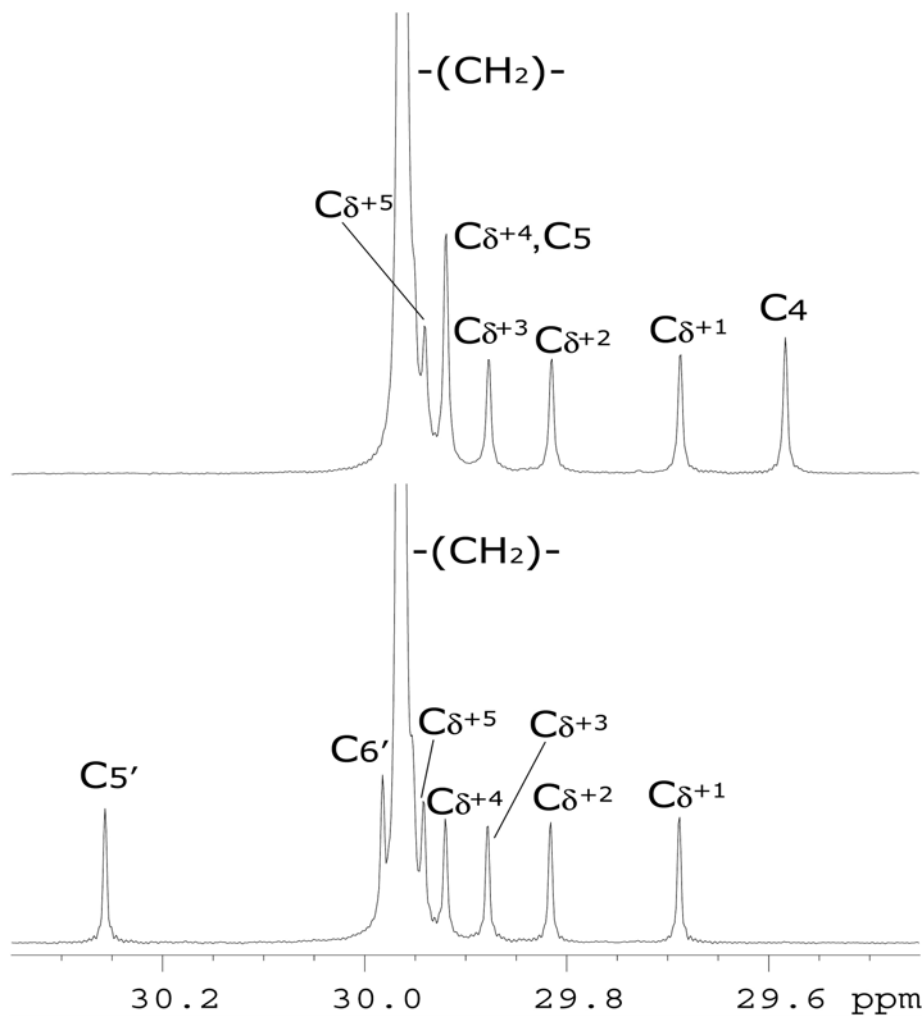


Figure 62: Partial ^{13}C $\{^1\text{H}\}$ NMR (150 MHz, 1,1,2,2- $\text{C}_2\text{D}_2\text{Cl}_4$, 90 $^\circ\text{C}$) spectra of Et-PE-I (top) and $^i\text{Pr-PE-I}$ (bottom) obtained by CCTP *via* **35** (Section 4.4)

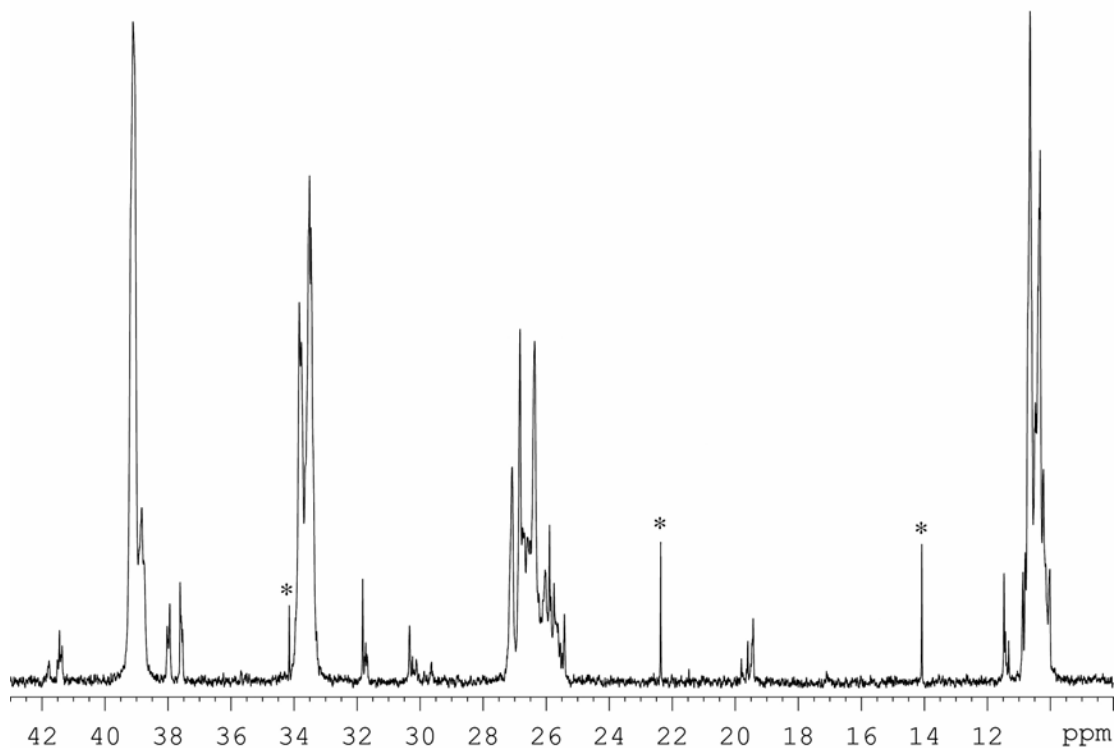


Figure 63: ^{13}C $\{^1\text{H}\}$ NMR (100 MHz, CDCl_3 , 20 $^\circ\text{C}$) spectrum of poly-1-butene from Entry 5.01 in Table 9. The three peaks marked by * are from *n*-pentane.

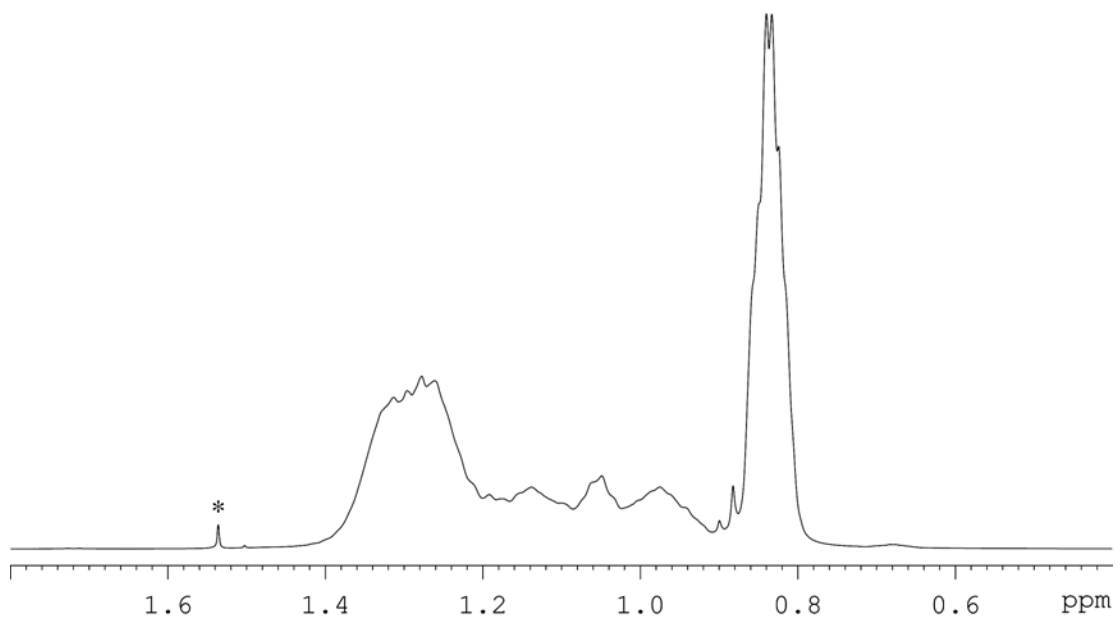


Figure 64: ^1H NMR (400 MHz, CDCl_3 , 20 $^\circ\text{C}$) spectrum of poly-1-butene from Entry 5.01 in Table 9. The peak marked by * is from water.

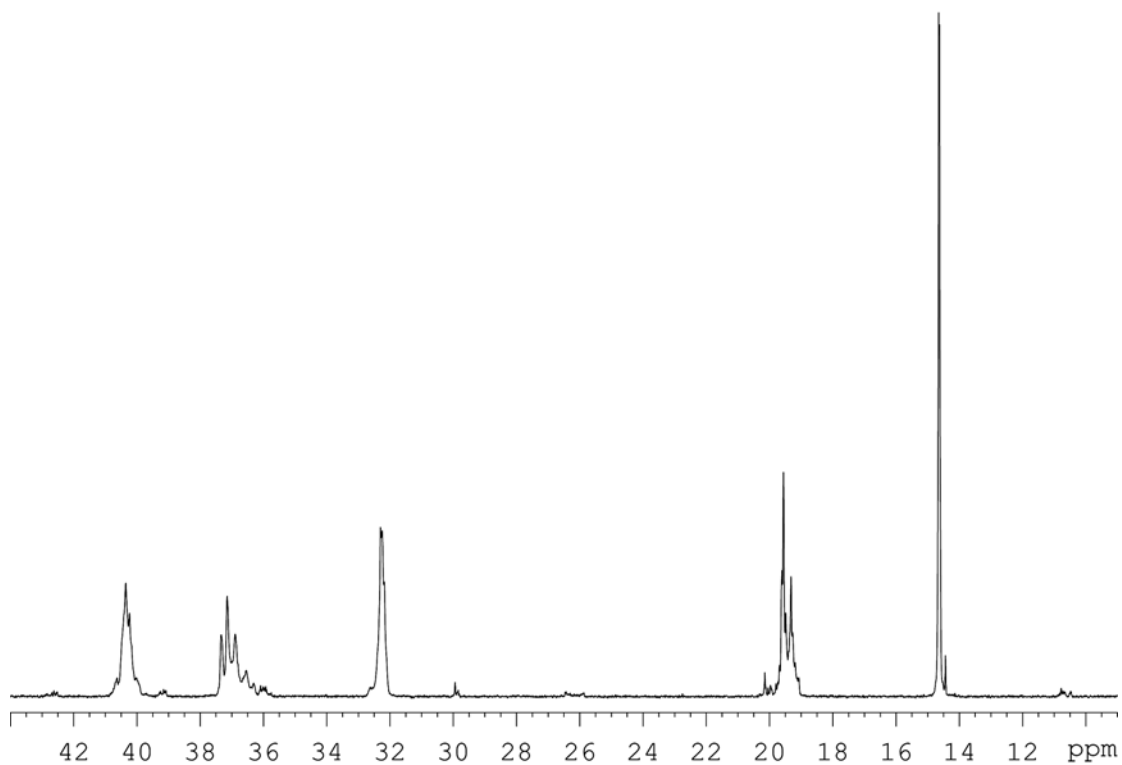


Figure 65: ^{13}C $\{^1\text{H}\}$ NMR (150 MHz, CDCl_3 , 20 °C) spectrum of poly-1-pentene from Entry 5.02 in Table 9.

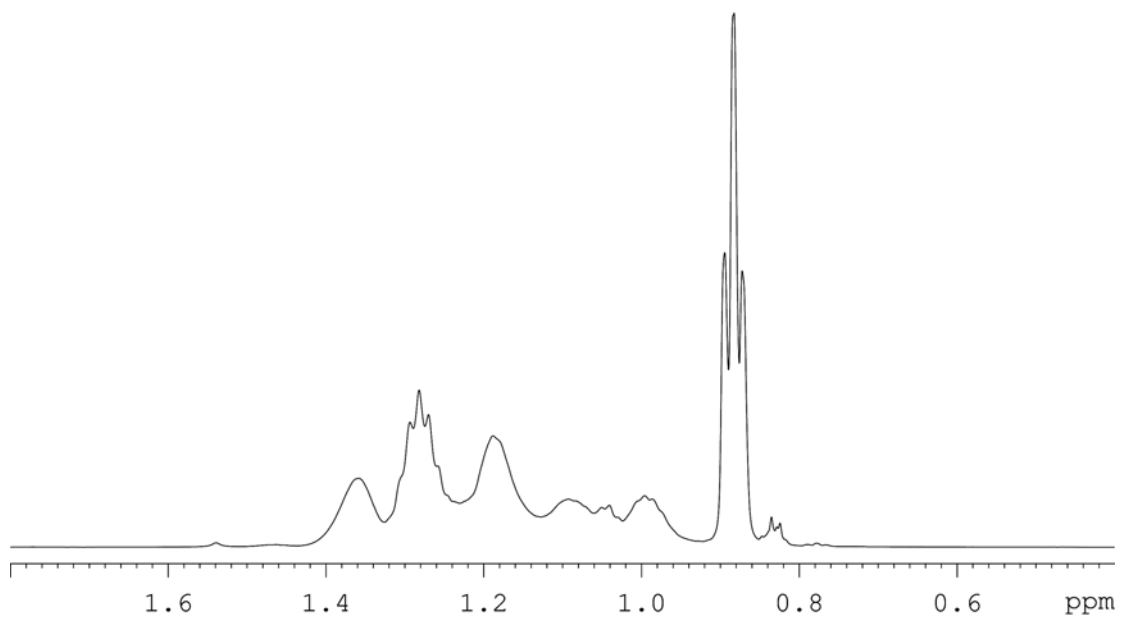


Figure 66: ^1H NMR (600 MHz, CDCl_3 , 20 °C) spectrum of poly-1-pentene from Entry 5.02 in Table 9.

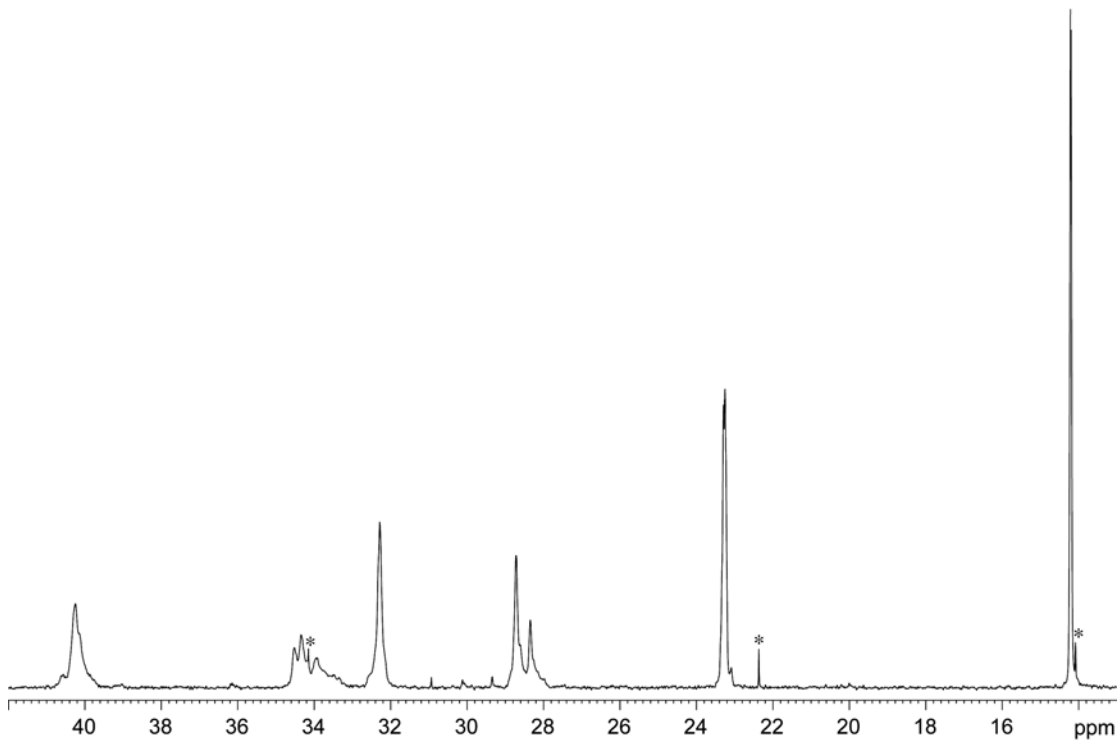


Figure 67: ^{13}C $\{^1\text{H}\}$ NMR (100 MHz, CDCl_3 , 20 $^\circ\text{C}$) spectrum of poly-1-hexene from Entry 5.03 in Table 9. The three resonances marked by asterisks (*) are from a trace amount of *n*-pentane.

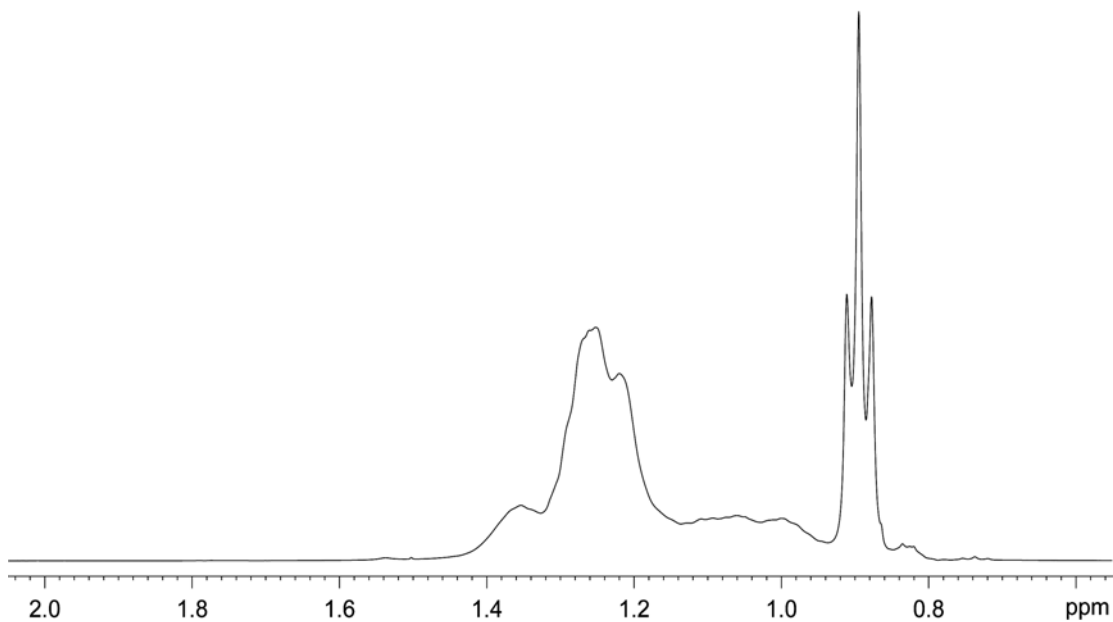


Figure 68: ^1H NMR (400 MHz, CDCl_3 , 20 $^\circ\text{C}$) spectrum of poly-1-hexene from Entry 5.03 in Table 9.

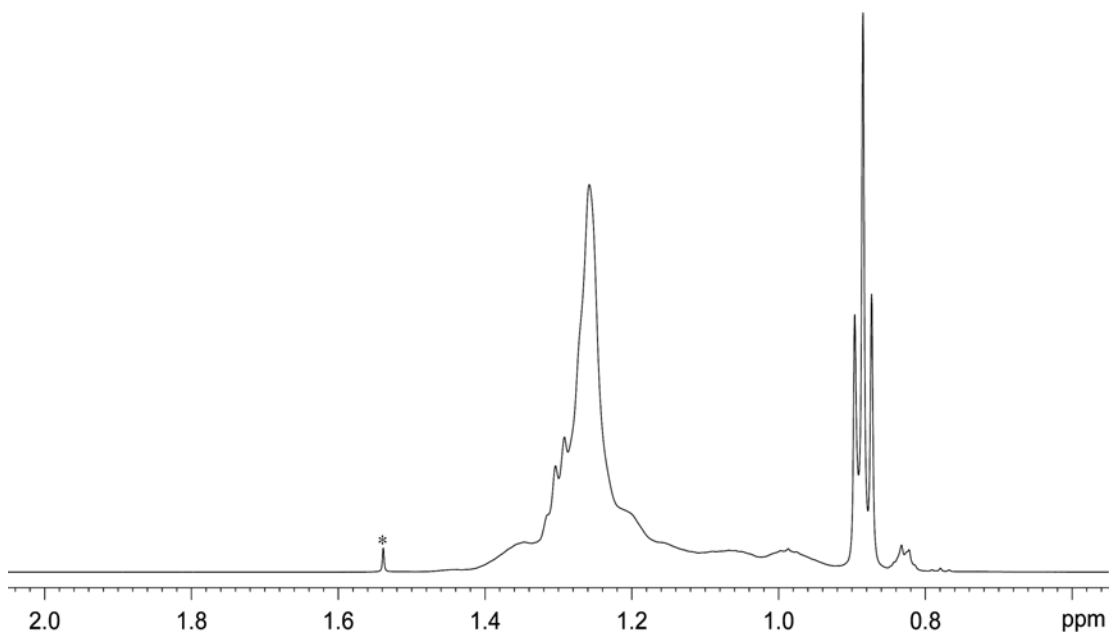


Figure 69: ¹H NMR (600 MHz, CDCl₃, 20 °C) spectrum of poly-1-octene from Entry 5.05 in Table 9. The resonance marked by an asterisk (*) is from H₂O.

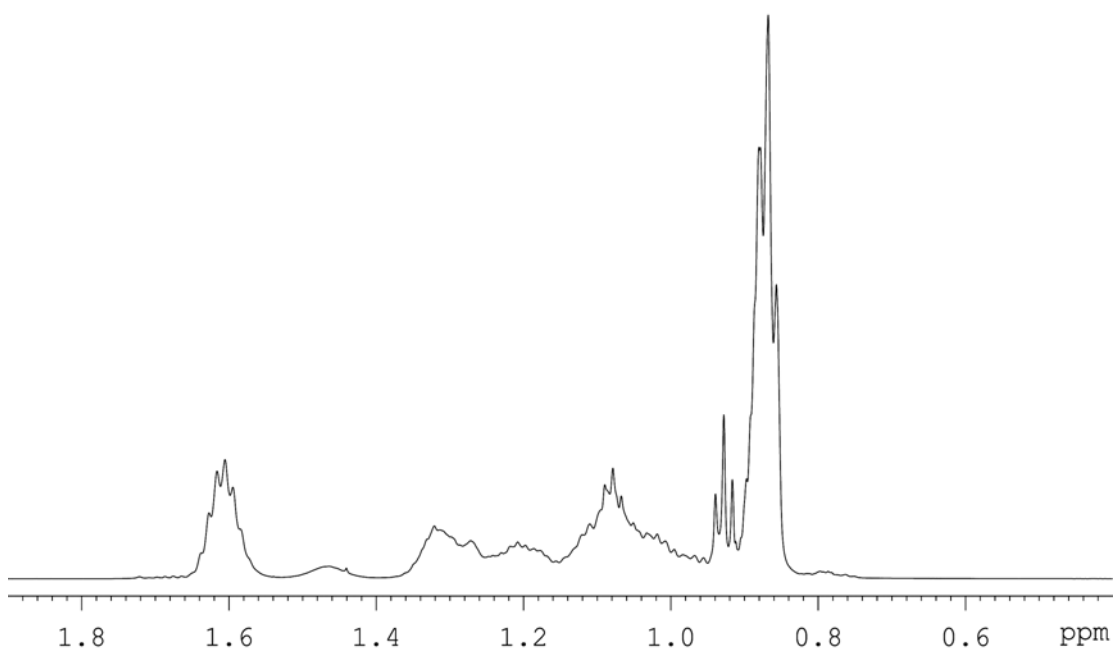


Figure 70: ¹H NMR (600 MHz, 1,1,2,2-C₂D₂Cl₄, 90 °C) spectrum of poly(propene-co-1-hexene) from Entry 5.07 in Table 10.

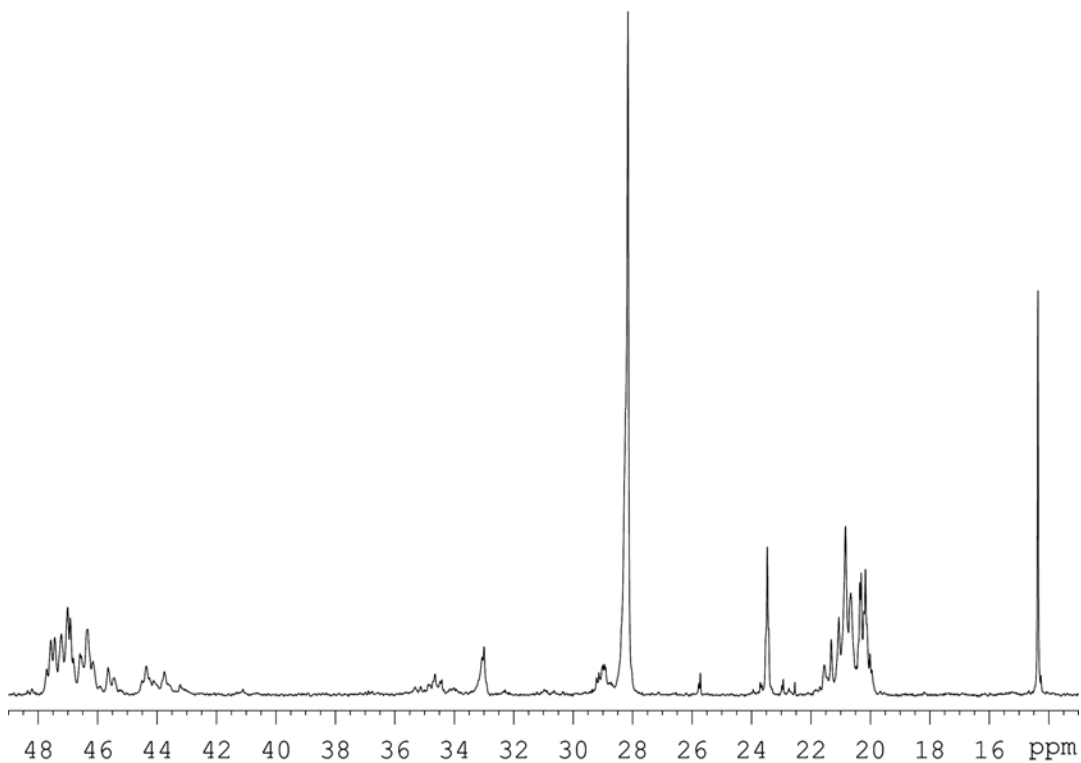


Figure 71: ^{13}C { ^1H } NMR (150 MHz, $1,1,2,2\text{-C}_2\text{D}_2\text{Cl}_4$, 90°C) spectrum of poly(propene-*co*-1-hexene) from Entry 5.07 in Table 10.

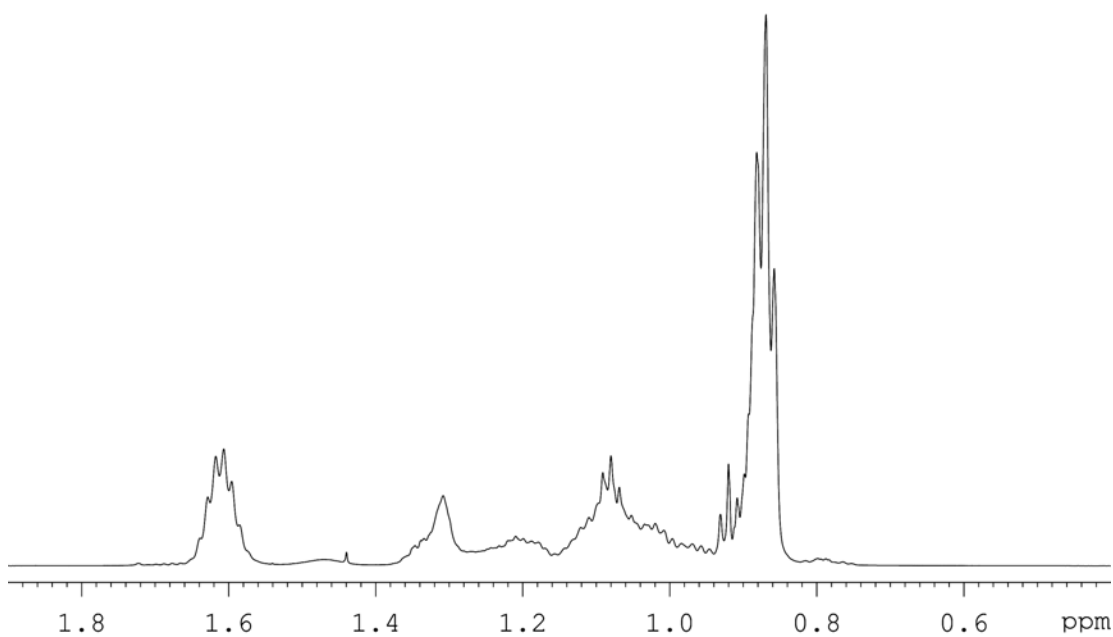


Figure 72: ^1H NMR (600 MHz, $1,1,2,2\text{-C}_2\text{D}_2\text{Cl}_4$, 90°C) spectrum of poly(propene-*co*-1-octene) from Entry 5.08 in Table 10.

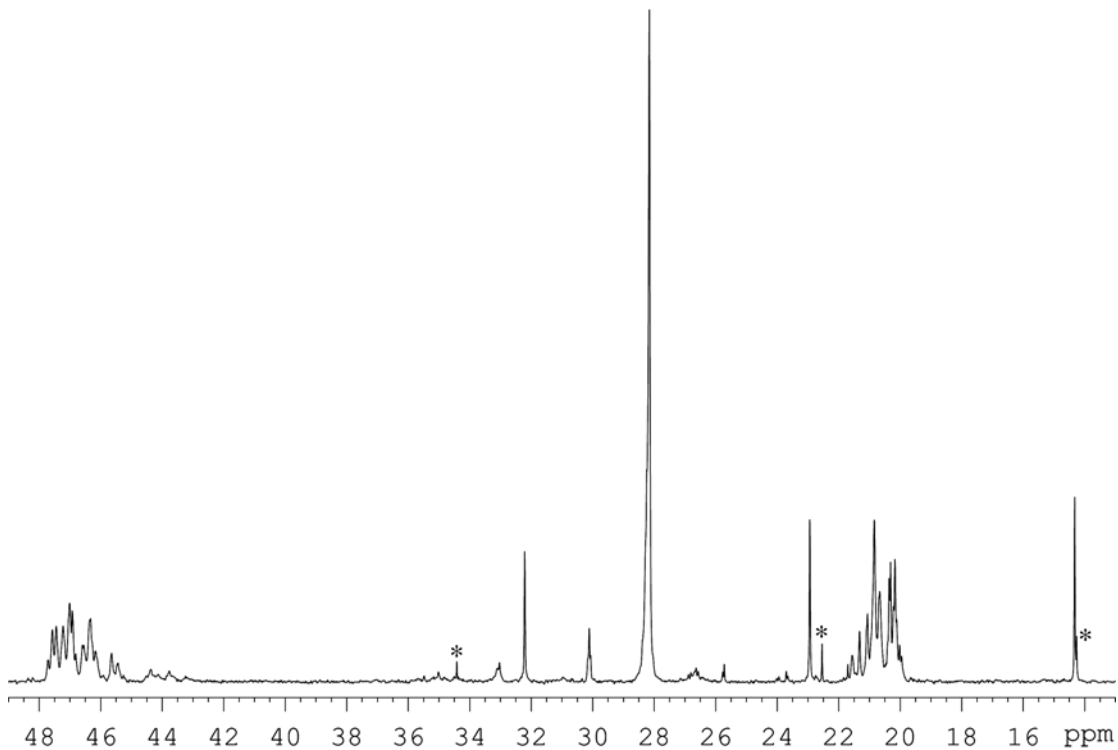


Figure 73: ^{13}C $\{^1\text{H}\}$ NMR (150 MHz, $1,1,2,2\text{-C}_2\text{D}_2\text{Cl}_4$, 90 °C) spectrum of poly(propene-*co*-1-octene) from Entry 5.08 in Table 10. Peaks marked by asterisks * are from *n*-pentane.

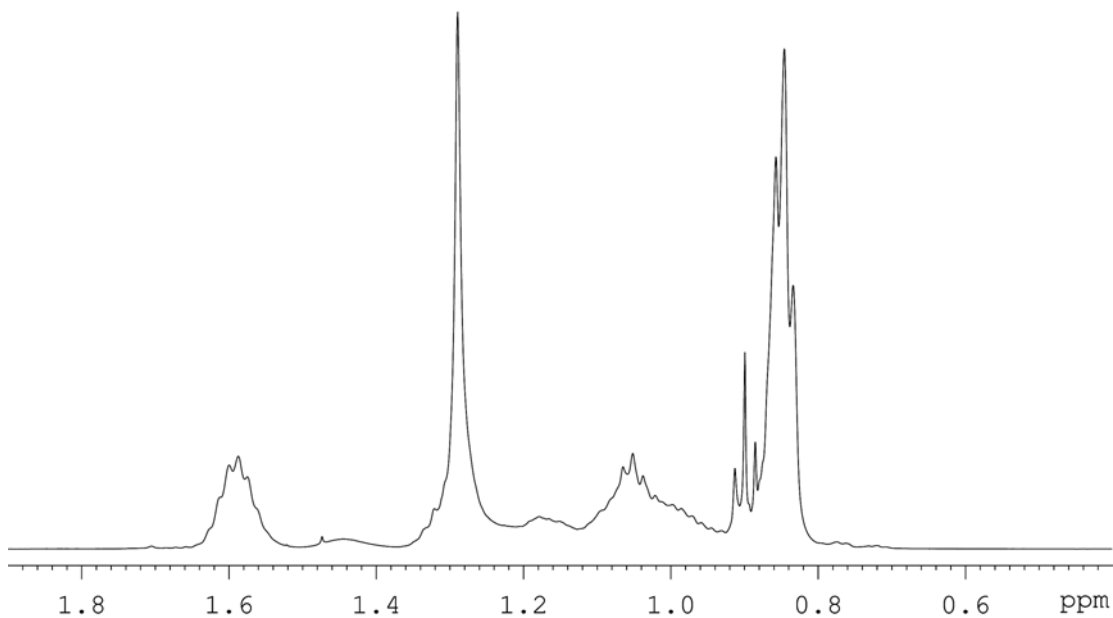


Figure 74: ^1H NMR (600 MHz, $1,1,2,2\text{-C}_2\text{D}_2\text{Cl}_4$, 90 °C) spectrum of poly(propene-*co*-1-dodecene) from Entry 5.09 in Table 10.

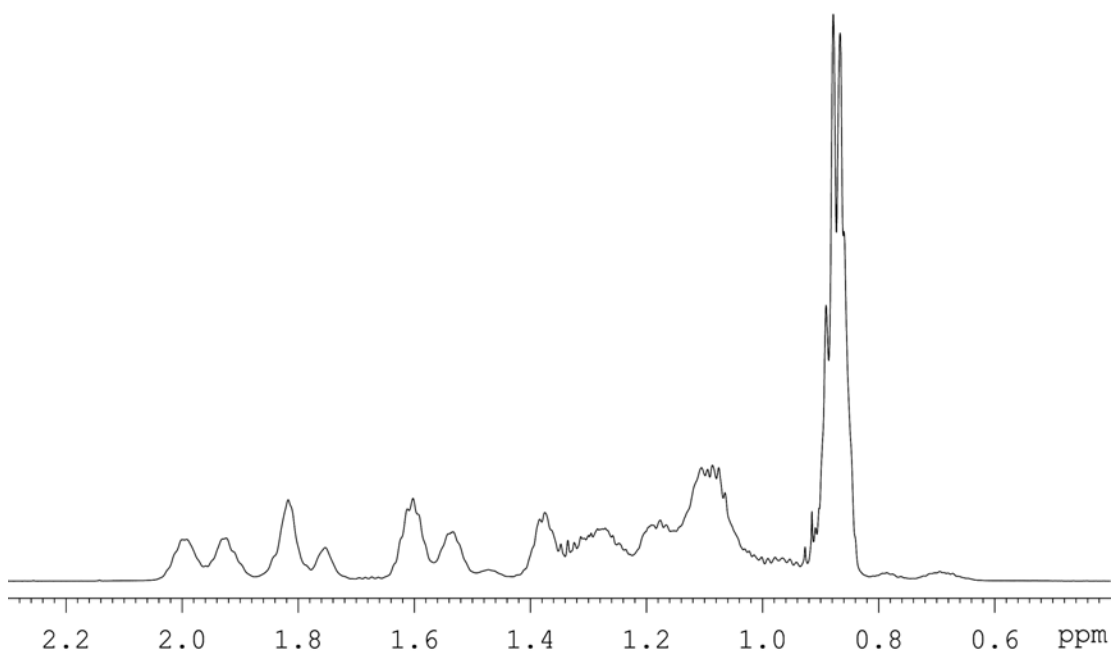


Figure 75: ^1H NMR (600 MHz, 1,1,2,2- $\text{C}_2\text{D}_2\text{Cl}_4$, 90 °C) spectrum of PP-*co*-PMCP from Entry 5.10 in Table 10.

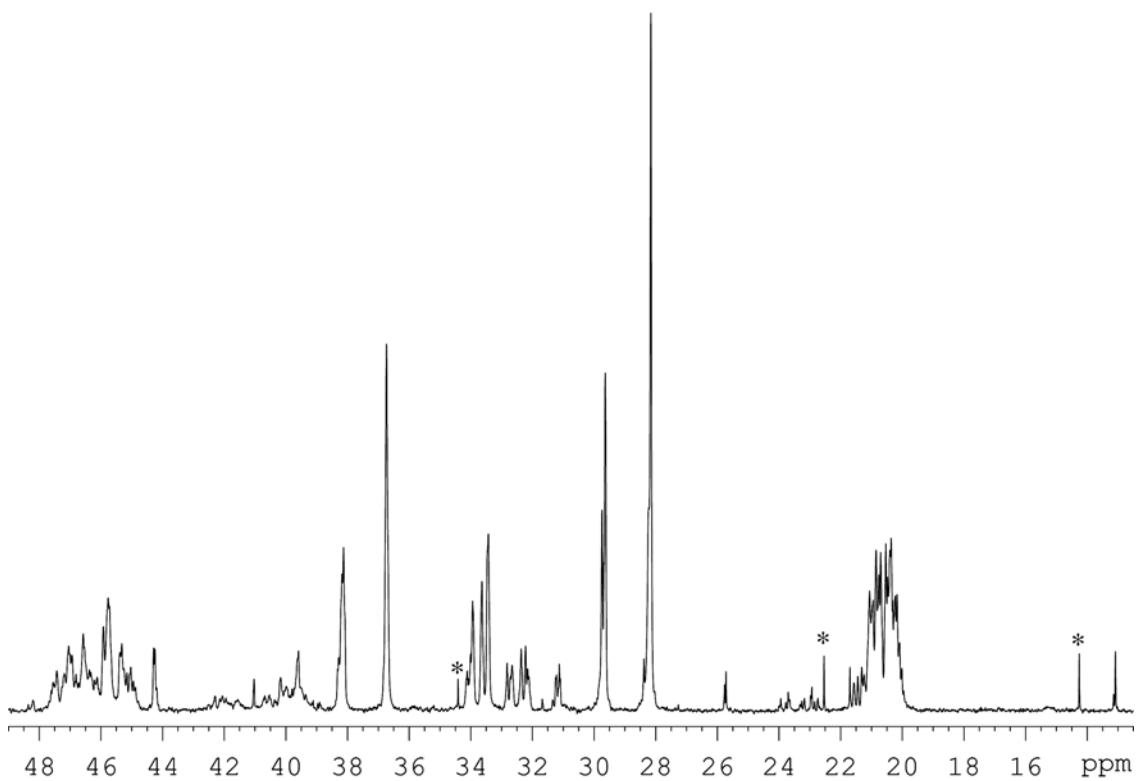


Figure 76: ^{13}C $\{^1\text{H}\}$ NMR (150 MHz, 1,1,2,2- $\text{C}_2\text{D}_2\text{Cl}_4$, 90 °C) spectrum of PP-*co*-PMCP from Entry 5.10 in Table 10. Peaks marked by * are from *n*-pentane.

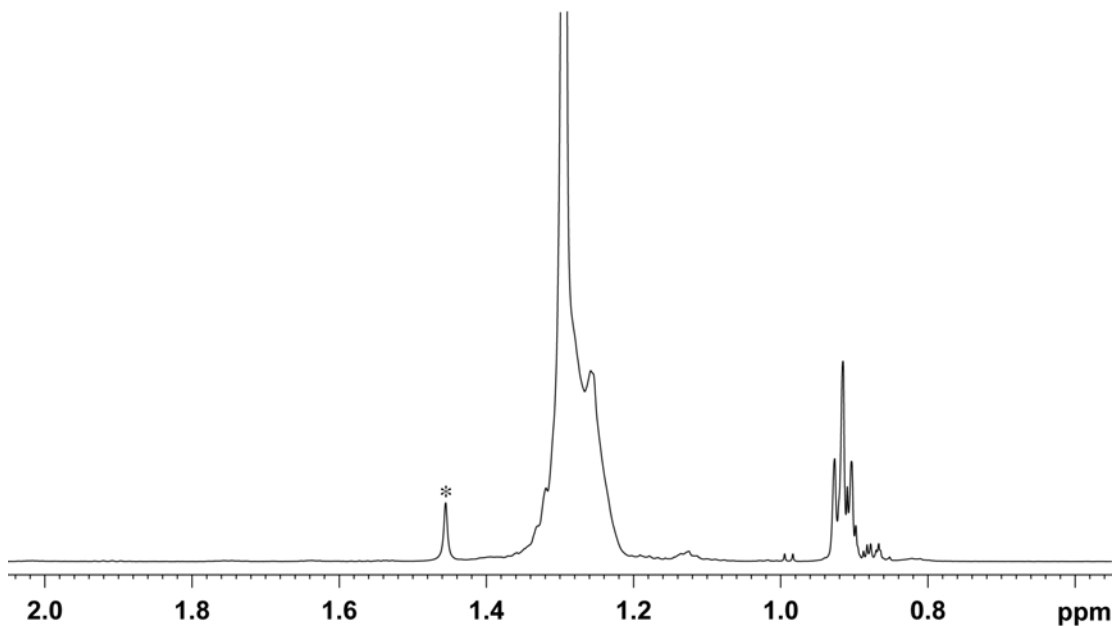


Figure 77: ¹H NMR (600 MHz, 1,1,2,2-C₂D₂Cl₄, 90 °C) spectrum of poly(ethene-co-1-hexene) from Entry 5.11 in Table 11. The resonance marked by an asterisk (*) is from H₂O.

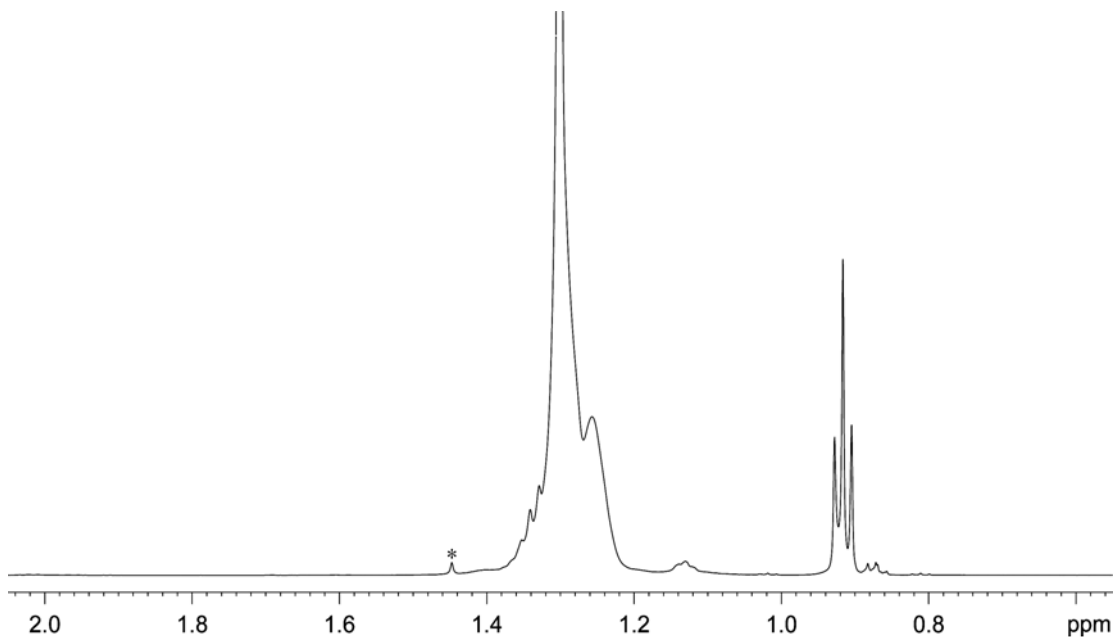


Figure 78: ¹H NMR (600 MHz, 1,1,2,2-C₂D₂Cl₄, 90 °C) spectrum of poly(ethene-co-1-octene) from Entry 5.13 in Table 11. The resonance marked by an asterisk (*) is from H₂O.

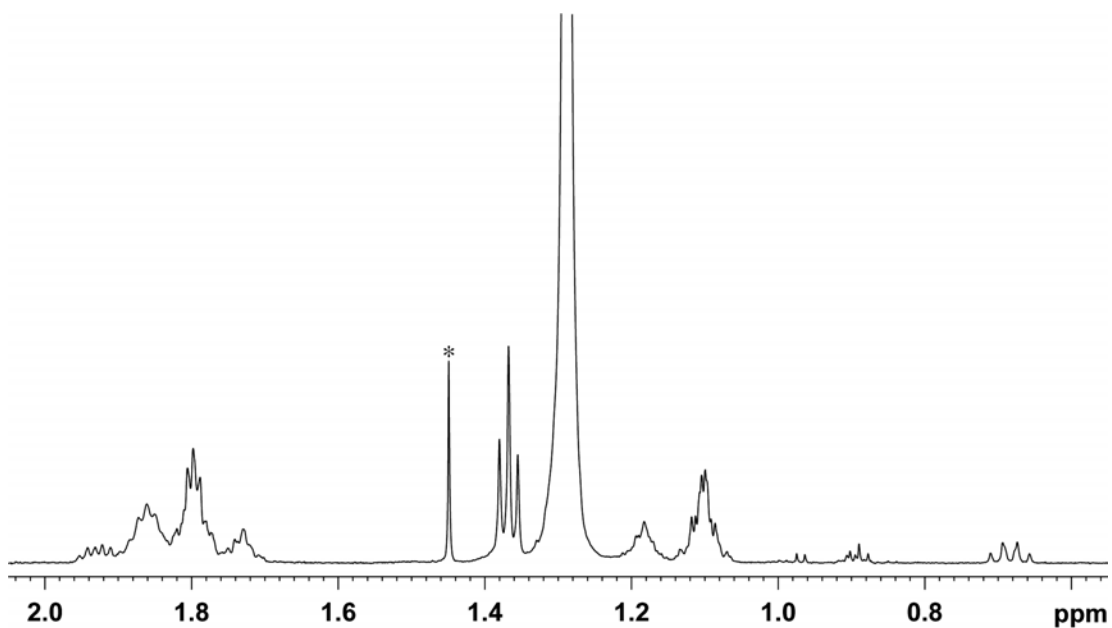


Figure 79: ^1H NMR (600 MHz, 1,1,2,2- $\text{C}_2\text{D}_2\text{Cl}_4$, 90 °C) spectrum of PE-co-PMCP from Entry 5.16 in Table 11. The resonance marked by an asterisk (*) is from water.

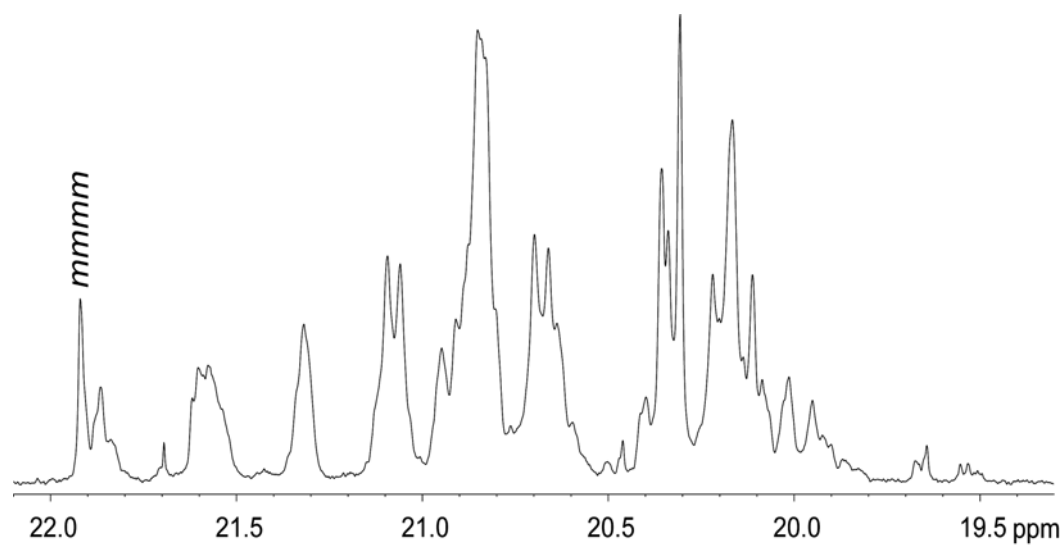


Figure 80: ^{13}C $\{^1\text{H}\}$ NMR (150 MHz, 1,1,2,2- $\text{C}_2\text{D}_2\text{Cl}_4$, 90 °C) spectra of methyl region of multi-stereoblock PP sample from Entry 6.06 of Table 16.

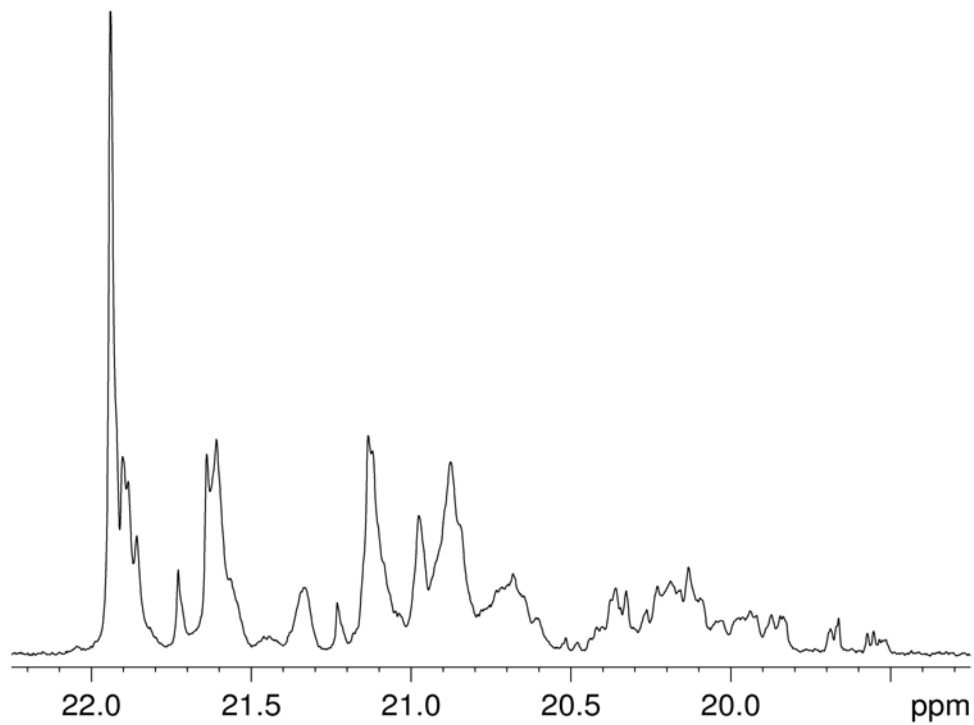


Figure 81: $^{13}\text{C} \{^1\text{H}\}$ NMR (150 MHz, $1,1,2,2\text{-C}_2\text{D}_2\text{Cl}_4$, 90 °C) spectra of methyl region of multi-stereoblock PP sample from Entry 6.11 of Table 16.

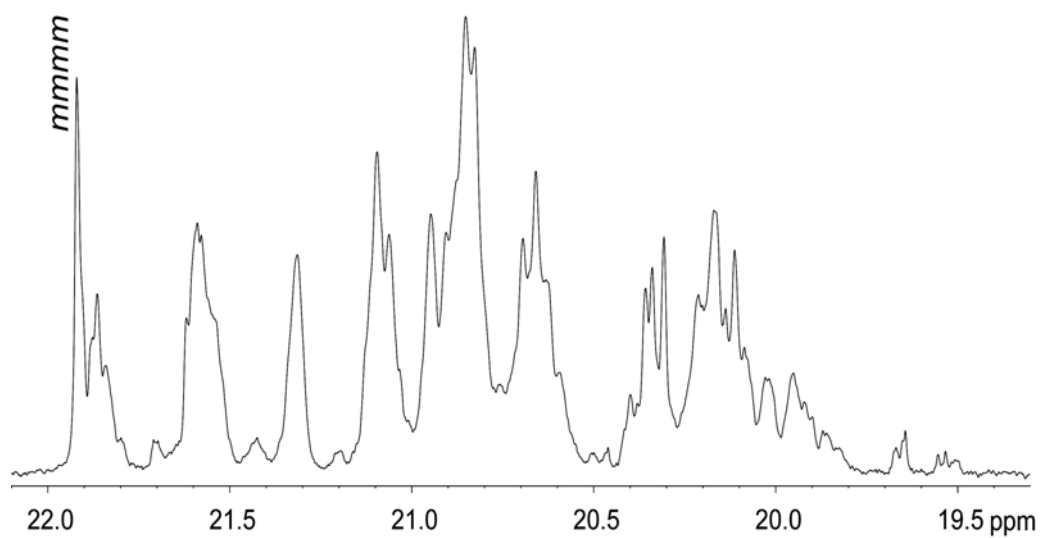


Figure 82: $^{13}\text{C} \{^1\text{H}\}$ NMR (150 MHz, $1,1,2,2\text{-C}_2\text{D}_2\text{Cl}_4$, 90 °C) spectra of methyl region of multi-stereoblock PP sample from Entry 6.12 of Table 16.

References:

1. Ziegler, K.; Holzkamp, E.; Breil, H.; Martin, H. *Angew. Chem.* **1955**, *67*, 426.
2. Natta, G.; Pino, P.; Corradini, P.; Danusso, F.; Mantica, E.; Mazzanti, G.; Moraglio, G. *J. Am. Chem. Soc.* **1955**, *77*, 1708.
3. Kashiwa, N. *Polym. J. (Tokyo, Jpn.)* **1980**, *12*, 603.
4. Chum, P. S.; Swogger, K. W. *Prog. Polym. Sci.* **2008**, *33*, 797.
5. Cossee, P. *J. Catal.* **1964**, *3*, 80.
6. Arlman, E. J.; Cossee, P. *J. Catal.* **1964**, *3*, 99.
7. Huang, J.; Rempel, G. L. *Prog. Polym. Sci.* **1995**, *20*, 459.
8. Castonguay, L. A.; Rappe, A. K. *J. Am. Chem. Soc.* **1992**, *114*, 5832.
9. Breslow, D. S.; Newburg, N. R. *J. Am. Chem. Soc.* **1957**, *79*, 5072.
10. Natta, G.; Pino, P.; Mazzanti, G.; Lanzo, R. *Chim. Ind. (Milan, Italy)* **1957**, *39*, 1032.
11. Sinn, H.; Kaminsky, W.; Vollmer, H. J.; Woldt, R. *Angew. Chem.* **1980**, *92*, 396.
12. Kaminsky, W. *Macromol. Chem. Phys.* **1996**, *197*, 3907.
13. Jordan, R. F.; Bajgur, C. S.; Willett, R.; Scott, B. *J. Am. Chem. Soc.* **1986**, *108*, 7410.
14. Chien, J. C. W.; Tsai, W. M.; Rausch, M. D. *J. Am. Chem. Soc.* **1991**, *113*, 8570.
15. Yang, X.; Stern, C. L.; Marks, T. J. *J. Am. Chem. Soc.* **1991**, *113*, 3623.
16. Scollard, J. D.; McConville, D. H. *J. Am. Chem. Soc.* **1996**, *118*, 10008.
17. Baumann, R.; Davis, W. M.; Schrock, R. R. *J. Am. Chem. Soc.* **1997**, *119*, 3830.
18. Ewen, J. A. *J. Am. Chem. Soc.* **1984**, *106*, 6355.

19. Johnson, L. K.; Killian, C. M.; Brookhart, M. *J. Am. Chem. Soc.* **1995**, *117*, 6414.
20. Gibson, V. C.; Spitzmesser, S. K. *Chem. Rev.* **2003**, *103*, 283.
21. Szwarc, M. *Nature (London, U. K.)* **1956**, *178*, 1168.
22. Baskaran, D.; Mueller, A. H. E. *Prog. Polym. Sci.* **2007**, *32*, 173.
23. Haddleton, D. M.; Muir, A. V. G.; Richards, S. N. *Plastics Engineering (New York)* **1997**, *40*, 123.
24. Smid, J.; Van Beylen, M.; Hogen-Esch, T. E. *Prog. Polym. Sci.* **2006**, *31*, 1041.
25. Yagci, Y.; Tasdelen, M. A. *Prog. Polym. Sci.* **2006**, *31*, 1133.
26. Hadjichristidis, N.; Iatrou, H.; Pitsikalis, M.; Mays, J. *Prog. Polym. Sci.* **2006**, *31*, 1068.
27. Matyjaszewski, K. *J. Phys. Org. Chem.* **1995**, *8*, 197.
28. Matyjaszewski, K.; Penczek, S. *Journal of Polymer Science, Polymer Chemistry Edition* **1974**, *12*, 1905.
29. Matyjaszewski, K.; Kubisa, P.; Penczek, S. *Journal of Polymer Science, Polymer Chemistry Edition* **1974**, *12*, 1333.
30. Goethals, E. J.; Du Prez, F. *Prog. Polym. Sci.* **2007**, *32*, 220.
31. Braunecker, W. A.; Matyjaszewski, K. *Prog. Polym. Sci.* **2007**, *32*, 93.
32. Georges, M. K.; Veregin, R. P. N.; Kazmaier, P. M.; Hamer, G. K. *Macromolecules* **1993**, *26*, 2987.
33. Hawker, C. J.; Bosman, A. W.; Harth, E. *Chem. Rev.* **2001**, *101*, 3661.
34. Wayland, B. B.; Poszmik, G.; Mukerjee, S. L.; Fryd, M. *J. Am. Chem. Soc.* **1994**, *116*, 7943.

35. Le Grogneec, E.; Claverie, J.; Poli, R. *J. Am. Chem. Soc.* **2001**, *123*, 9513.
36. Wang, J.-S.; Matyjaszewski, K. *J. Am. Chem. Soc.* **1995**, *117*, 5614.
37. Kato, M.; Kamigaito, M.; Sawamoto, M.; Higashimura, T. *Macromolecules* **1995**, *28*, 1721.
38. Chiefari, J.; Chong, Y. K.; Ercole, F.; Krstina, J.; Jeffery, J.; Le, T. P. T.; Mayadunne, R. T. A.; Meijs, G. F.; Moad, C. L.; Moad, G.; Rizzardo, E.; Thang, S. H. *Macromolecules* **1998**, *31*, 5559.
39. Lai, J. T.; Shea, R. *J. Polym. Sci., Part A: Polym. Chem.* **2006**, *44*, 4298.
40. Lowe, A. B.; McCormick, C. L. *Prog. Polym. Sci.* **2007**, *32*, 283.
41. Bielawski, C. W.; Grubbs, R. H. *Prog. Polym. Sci.* **2007**, *32*, 1.
42. Yokozawa, T.; Yokoyama, A. *Prog. Polym. Sci.* **2007**, *32*, 147.
43. Penczek, S.; Cypryk, M.; Duda, A.; Kubisa, P.; Slomkowski, S. *Prog. Polym. Sci.* **2007**, *32*, 247.
44. Domski, G. J.; Rose, J. M.; Coates, G. W.; Bolig, A. D.; Brookhart, M. *Prog. Polym. Sci.* **2007**, *32*, 30.
45. Doi, Y.; Ueki, S.; Keii, T. *Macromolecules* **1979**, *12*, 814.
46. Scollard, J. D.; McConville, D. H.; Payne, N. C.; Vittal, J. J. *Macromolecules* **1996**, *29*, 5241.
47. Mehrkhodavandi, P.; Schrock, R. R. *J. Am. Chem. Soc.* **2001**, *123*, 10746.
48. Matsui, S.; Tohi, Y.; Mitani, M.; Saito, J.; Makio, H.; Tanaka, H.; Nitabaru, M.; Nakano, T.; Fujita, T. *Chem. Lett.* **1999**, 1065.
49. Matsui, S.; Mitani, M.; Saito, J.; Tohi, Y.; Makio, H.; Tanaka, H.; Fujita, T. *Chem. Lett.* **1999**, 1263.

50. Tian, J.; Hustad, P. D.; Coates, G. W. *J. Am. Chem. Soc.* **2001**, *123*, 5134.
51. Jayaratne, K. C.; Sita, L. R. *J. Am. Chem. Soc.* **2000**, *122*, 958.
52. Keaton, R. J.; Jayaratne, K. C.; Fettinger, J. C.; Sita, L. R. *J. Am. Chem. Soc.* **2000**, *122*, 12909.
53. Hagihara, H.; Shiono, T.; Ikeda, T. *Macromolecules* **1998**, *31*, 3184.
54. Hasan, T.; Ioku, A.; Nishii, K.; Shiono, T.; Ikeda, T. *Macromolecules* **2001**, *34*, 3142.
55. Tshuva, E. Y.; Goldberg, I.; Kol, M. *J. Am. Chem. Soc.* **2000**, *122*, 10706.
56. Tshuva, E. Y.; Goldberg, I.; Kol, M.; Goldschmidt, Z. *Inorg. Chem. Commun.* **2000**, *3*, 611.
57. Jayaratne, K. C.; Keaton, R. J.; Henningsen, D. A.; Sita, L. R. *J. Am. Chem. Soc.* **2000**, *122*, 10490.
58. Zhang, Y.; Sita, L. R. *Chem. Commun.* **2003**, 2358.
59. Zhang, Y.; Keaton, R. J.; Sita, L. R. *J. Am. Chem. Soc.* **2003**, *125*, 9062.
60. Mueller, A. H. E.; Zhuang, R.; Yan, D.; Litvinenko, G. *Macromolecules* **1995**, *28*, 4326.
61. Jayaratne, K. C.; Sita, L. R. *J. Am. Chem. Soc.* **2001**, *123*, 10754.
62. Harney, M. B.; Zhang, Y.; Sita, L. R. *Angew. Chem., Int. Ed.* **2006**, *45*, 2400.
63. Zhang, Y.; Sita, L. R. *J. Am. Chem. Soc.* **2004**, *126*, 7776.
64. Zhang, W.; Sita, L. R. *J. Am. Chem. Soc.* **2008**, *130*, 442.
65. Zhang, W.; Wei, J.; Sita, L. R. *Macromolecules* **2008**, *41*, 7829.
66. Westerhausen, M.; Guckel, C.; Haberer, T.; Vogt, M.; Warchhold, M.; Noth, H. *Organometallics* **2001**, *20*, 893.

67. Kempe, R. *Chem.--Eur. J.* **2007**, *13*, 2764.
68. Britovsek, G. J. P.; Cohen, S. A.; Gibson, V. C.; Maddox, P. J.; Van Meurs, M. *Angew. Chem., Int. Ed.* **2002**, *41*, 489.
69. Britovsek, G. J. P.; Cohen, S. A.; Gibson, V. C.; van Meurs, M. *J. Am. Chem. Soc.* **2004**, *126*, 10701.
70. Van Meurs, M.; Britovsek, G. J. P.; Gibson, V. C.; Cohen, S. A. *J. Am. Chem. Soc.* **2005**, *127*, 9913.
71. Kretschmer, W. P.; Meetsma, A.; Hessen, B.; Schmalz, T.; Qayyum, S.; Kempe, R. *Chem.--Eur. J.* **2006**, *12*, 8969.
72. Pelletier, J.-F.; Mortreux, A.; Olonde, X.; Bujadoux, K. *Angew. Chem., Int. Ed. Engl.* **1996**, *35*, 1854.
73. Bazan, G. C.; Rogers, J. S.; Fang, C. C. *Organometallics* **2001**, *20*, 2059.
74. Ganesan, M.; Gabbaie, F. P. *Organometallics* **2004**, *23*, 4608.
75. Mani, G.; Gabbai, F. P. *Angew. Chem., Int. Ed.* **2004**, *43*, 2263.
76. Arriola, D. J.; Carnahan, E. M.; Hustad, P. D.; Kuhlman, R. L.; Wenzel, T. T. *Science* **2006**, *312*, 714.
77. Kissounko, D. A.; Fettinger, J. C.; Sita, L. R. *Inorg. Chim. Acta* **2003**, *345*, 121.
78. Zhang, Y.; Reeder, E. K.; Keaton, R. J.; Sita, L. R. *Organometallics* **2004**, *23*, 3512.
79. Keaton, R. J.; Jayaratne, K. C.; Henningsen, D. A.; Koterwas, L. A.; Sita, L. R. *J. Am. Chem. Soc.* **2001**, *123*, 6197.
80. Harney, M. B.; Keaton, R. J.; Fettinger, J. C.; Sita, L. R. *J. Am. Chem. Soc.* **2006**, *128*, 3420.

81. Zhang, W.; Sita, L. R. *Adv. Synth. Catal.* **2008**, *350*, 439.
82. Busico, V.; Cipullo, R. *Prog. Polym. Sci.* **2001**, *26*, 443.
83. Harney, M. B.; Zhang, Y.; Sita, L. R. *Angew. Chem., Int. Ed.* **2006**, *45*, 6140.
84. Beck, S.; Prosenc, M.-H.; Brintzinger, H.-H.; Goretzki, R.; Herfert, N.; Fink, G. *J. Mol. Catal. A: Chem.* **1996**, *111*, 67.
85. Li, L.; Metz, M. V.; Marks, T. J.; Liable-Sands, L.; Rheingold, A. L. *Polym. Prepr.* **2000**, *41*, 1912.
86. Li, H.; Stern, C. L.; Marks, T. J. *Macromolecules* **2005**, *38*, 9015.
87. Li, L.; Metz, M. V.; Li, H.; Chen, M.-C.; Marks, T. J.; Liable-Sands, L.; Rheingold, A. L. *J. Am. Chem. Soc.* **2002**, *124*, 12725.
88. Wang, J.; Li, H.; Guo, N.; Li, L.; Stern, C. L.; Marks, T. J. *Organometallics* **2004**, *23*, 5112.
89. Guo, N.; Li, L.; Marks, T. J. *J. Am. Chem. Soc.* **2004**, *126*, 6542.
90. Guo, N.; Stern, C. L.; Marks, T. J. *J. Am. Chem. Soc.* **2008**, *130*, 2246.
91. Noh, S. K.; Kim, J.; Jung, J.; Ra, C. S.; Lee, D.-H.; Lee, H. B.; Lee, S. W.; Huh, W. S. *J. Organomet. Chem.* **1999**, *580*, 90.
92. Noh, S. K.; Kim, S.; Yang, Y.; Lyoo, W. S.; Lee, D. *Eur. Polym. J.* **2003**, *40*, 227.
93. Noh, S. K.; Lee, J.; Lee, D. *J. Organomet. Chem.* **2003**, *667*, 53.
94. Noh, S. K.; Yang, Y.; Lyoo, W. S. *J. Appl. Polym. Sci.* **2003**, *90*, 2469.
95. Spaleck, W.; Kuber, F.; Bachmann, B.; Fritze, C.; Winter, A. *J. Mol. Catal. A: Chem.* **1998**, *128*, 279.

96. Ushioda, T.; Green, M. L. H.; Haggitt, J.; Yan, X. *J. Organomet. Chem.* **1996**, *518*, 155.
97. Ban, H. T.; Uozumi, T.; Soga, K. *J. Polym. Sci., Part A: Polym. Chem.* **1998**, *36*, 2269.
98. Sierra, J. C.; Hueerlaender, D.; Hill, M.; Kehr, G.; Erker, G.; Froehlich, R. *Chem.--Eur. J.* **2003**, *9*, 3618.
99. Kuwabara, J.; Takeuchi, D.; Osakada, K. *Organometallics* **2005**, *24*, 2705.
100. Shibayama, K.; Seidel, S. W.; Novak, B. M. *Macromolecules* **1997**, *30*, 3159.
101. Amor, J. I.; Cuenca, T.; Galakhov, M.; Royo, P. *J. Organomet. Chem.* **1995**, *497*, 127.
102. Amor, J. I.; Cuenca, T.; Galakhov, M.; Gomez-Sal, P.; Manzanero, A.; Royo, P. *J. Organomet. Chem.* **1997**, *535*, 155.
103. Hirotsu, M.; Fontaine, P. P.; Zavalij, P. Y.; Sita, L. R. *J. Am. Chem. Soc.* **2007**, *129*, 12690.
104. Kissounko, D. A.; Zhang, Y.; Harney, M. B.; Sita, L. R. *Adv. Synth. Catal.* **2005**, *347*, 426.
105. Busico, V.; Cipullo, R.; Chadwick, J. C.; Modder, J. F.; Sudmeijer, O. *Macromolecules* **1994**, *27*, 7538.
106. Cheng, H. N. *Polymer Bulletin (Berlin, Germany)* **1985**, *14*, 347.
107. Ziegler, K. *Angew. Chem.* **1952**, *64*, 323.
108. Resconi, L.; Piemontesi, F.; Franciscono, G.; Abis, L.; Fiorani, T. *J. Am. Chem. Soc.* **1992**, *114*, 1025.

109. Barsties, E.; Schaible, S.; Prosenc, M.-H.; Rief, U.; Roell, W.; Weyand, O.; Dorer, B.; Brintzinger, H.-H. *J. Organomet. Chem.* **1996**, *520*, 63.
110. Naga, N.; Mizunuma, K. *Polymer* **1998**, *39*, 5059.
111. Leino, R.; Luttikhedde, H. J. G.; Lehmus, P.; Wilen, C.-E.; Sjoeholm, R.; Lehtonen, A.; Seppaelae, J. V.; Naesman, J. H. *Macromolecules* **1997**, *30*, 3477.
112. Kim, I.; Choi, C.-S. *J. Polym. Sci., Part A: Polym. Chem.* **1999**, *37*, 1523.
113. Lieber, S.; Brintzinger, H.-H. *Macromolecules* **2000**, *33*, 9192.
114. Lahelin, M.; Kokko, E.; Lehmus, P.; Pitkaenen, P.; Loefgren, B.; Seppaelae, J. *Macromol. Chem. Phys.* **2003**, *204*, 1323.
115. Kukral, J.; Lehmus, P.; Klinga, M.; Leskela, M.; Rieger, B. *Eur. J. Inorg. Chem.* **2002**, 1349.
116. Hild, S.; Cobzaru, C.; Troll, C.; Rieger, B. *Macromol. Chem. Phys.* **2006**, *207*, 665.
117. Cai, Z.; Shigemasa, M.; Nakayama, Y.; Shiono, T. *Macromolecules* **2006**, *39*, 6321.
118. Alfano, F.; Boone, H. W.; Busico, V.; Cipullo, R.; Stevens, J. C. *Macromolecules* **2007**, *40*, 7736.
119. Kurosawa, H.; Shiono, T.; Soga, K. *Macromol. Chem. Phys.* **1994**, *195*, 3303.
120. Shiono, T.; Kurosawa, H.; Soga, K. *Macromolecules* **1994**, *27*, 2635.
121. Shiono, T.; Kurosawa, H.; Soga, K. *Macromolecules* **1995**, *28*, 437.
122. Chenal, T.; Olonde, X.; Pelletier, J.-F.; Bujadoux, K.; Mortreux, A. *Polymer* **2007**, *48*, 1844.

123. Ring, J. O.; Thomann, R.; Muelhaupt, R.; Raquez, J.-M.; Degee, P.; Dubois, P. *Macromol. Chem. Phys.* **2007**, *208*, 896.
124. Klement, I.; Lutjens, H.; Knochel, P. *Tetrahedron* **1997**, *53*, 9135.
125. Jeon, S.-J.; Li, H.; Garcia, C.; LaRochelle, L. K.; Walsh, P. J. *J. Org. Chem.* **2005**, *70*, 448.
126. Jeon, S.-J.; Li, H.; Walsh, P. J. *J. Am. Chem. Soc.* **2005**, *127*, 16416.
127. Rozema, M. J.; Sidduri, A.; Knochel, P. *J. Org. Chem.* **1992**, *57*, 1956.
128. Scollard, J. D.; McConville, D. H.; Vittal, J. J.; Payne, N. C. *J. Mol. Catal. A: Chem.* **1998**, *128*, 201.
129. Byun, D.-J.; Shin, D.-K.; Kim, S. Y. *Polym. Bull. (Berlin)* **1999**, *42*, 301.
130. Mogstad, A. L.; Waymouth, R. M. *Macromolecules* **1992**, *25*, 2282.
131. Po, R.; Cardi, N.; Abis, L. *Polymer* **1998**, *39*, 959.
132. Song, F.; Cannon, R. D.; Bochmann, M. *Chem. Commun.* **2004**, 542.
133. Kim, I.; Zhou, J.-M.; Chung, H. *J. Polym. Sci., Part A: Polym. Chem.* **2000**, *38*, 1687.
134. Resconi, L.; Waymouth, R. M. *J. Am. Chem. Soc.* **1990**, *112*, 4953.
135. Coates, G. W.; Waymouth, R. M. *J. Am. Chem. Soc.* **1991**, *113*, 6270.
136. Coates, G. W.; Waymouth, R. M. *J. Am. Chem. Soc.* **1993**, *115*, 91.
137. Graef, S. M.; Wahner, U. M.; Van Reenen, A. J.; Brull, R.; Sanderson, R. D.; Pasch, H. *J. Polym. Sci., Part A: Polym. Chem.* **2001**, *40*, 128.
138. Van Reenen, A. J.; Brull, R.; Wahner, U. M.; Raubenheimer, H. G.; Sanderson, R. D.; Pasch, H. *J. Polym. Sci., Part A: Polym. Chem.* **2000**, *38*, 4110.
139. Seger, M. R.; Maciel, G. E. *Anal. Chem.* **2004**, *76*, 5734.

140. Zintl, M.; Rieger, B. *Angew. Chem., Int. Ed.* **2007**, *46*, 333.
141. Natta, G. *Journal of Polymer Science* **1959**, *34*, 531.
142. Muller, G.; Rieger, B. *Prog. Polym. Sci.* **2002**, *27*, 815.
143. Rajan, G. S.; Vu, Y. T.; Mark, J. E.; Myers, C. L. *Eur. Polym. J.* **2003**, *40*, 63.
144. Ewen, J. A.; Jones, R. L.; Elder, M. J.; Camurati, I.; Pritzkow, H. *Macromol. Chem. Phys.* **2004**, *205*, 302.
145. Edson, J. B.; Wang, Z.; Kramer, E. J.; Coates, G. W. *J. Am. Chem. Soc.* **2008**, *130*, 4968.
146. Hotta, A.; Cochran, E.; Ruokolainen, J.; Khanna, V.; Fredrickson, G. H.; Kramer, E. J.; Shin, Y.-W.; Shimizu, F.; Cherian, A. E.; Hustad, P. D.; Rose, J. M.; Coates, G. W. *Proc. Natl. Acad. Sci. U. S. A.* **2006**, *103*, 15327.
147. Nishii, K.; Shiono, T.; Ikeda, T. *Macromol. Rapid Commun.* **2004**, *25*, 1029.
148. Cai, Z.; Nakayama, Y.; Shiono, T. *Macromolecules* **2008**, *41*, 6596.
149. Chien, J. C. W.; Iwamoto, Y.; Rausch, M. D. *J. Polym. Sci., Part A: Polym. Chem.* **1999**, *37*, 2439.
150. Chien, J. C. W.; Iwamoto, Y.; Rausch, M. D.; Wedler, W.; Winter, H. H. *Macromolecules* **1997**, *30*, 3447.
151. Tynys, A.; Eilertsen, J. L.; Seppala, J. V.; Rytter, E. *J. Polym. Sci., Part A: Polym. Chem.* **2007**, *45*, 1364.
152. Przybyla, C.; Fink, G. *Acta Polym.* **1999**, *50*, 77.
153. Coates, G. W.; Waymouth, R. M. *Science (Washington, D. C.)* **1995**, *267*, 217.
154. Busico, V.; Cipullo, R.; Segre, A. L.; Talarico, G.; Vacatello, M.; Castelli, V. V. *A. Macromolecules* **2001**, *34*, 8412.

155. Busico, V.; Cipullo, R.; Kretschmer, W. P.; Talarico, G.; Vacatello, M.; Van Axel Castelli, V. *Angew. Chem., Int. Ed.* **2002**, *41*, 505.
156. Busico, V.; Castelli, V. V. A.; Aprea, P.; Cipullo, R.; Segre, A.; Talarico, G.; Vacatello, M. *J. Am. Chem. Soc.* **2003**, *125*, 5451.
157. Hustad, P. D.; Kuhlman, R. L.; Carnahan, E. M.; Wenzel, T. T.; Arriola, D. J. *Macromolecules* **2008**, *41*, 4081.
158. Babcock, J. R.; Incarvito, C.; Rheingold, A. L.; Fettingner, J. C.; Sita, L. R. *Organometallics* **1999**, *18*, 5729.
159. Pallucca, E.; Degani, J.; Serri, A. M.; Fochi, R.; Gazzetto, S.; Fenoglio, C.; Ornati, C.; Migliaccio, M.; Cadamuro, S.; Carvoli, G. **2003**, EP 1334965.
160. Jentsch, W.; Seefelder, M. *Chem. Ber.* **1965**, *98*, 1342.
161. Komatsu, M.; Nishikaze, N.; Sakamoto, M.; Ohshiro, Y.; Agawa, T. *J. Org. Chem.* **1974**, *39*, 3198.